



The
University
Of
Sheffield.

**Stem Cell Therapies For Sensorineural Hearing Loss: Understanding
The Role Of Glial Cells**

By:

Ali Sameer Mallick

A thesis submitted for the degree of
Doctor of Philosophy

The University of Sheffield
Faculty of Science
Department of Biomedical Science

September 2017.

ACKNOWLEDGEMENTS

I would like to start off by thanking Almighty God for facilitating a fantastic opportunity for me to pursue research in an exciting area of biomedical science, which may revolutionise the way in which we treat patients afflicted with sensorineural hearing loss. I also thank Him for helping me to remain firm and resolute during the peaks and troughs of my PhD journey.

The work that I have presented within this thesis would not have been possible without the expert guidance of my supervisor, Professor Marcelo Rivolta. His advice, critique and mentorship over these past few years has helped me immensely in developing my scientific thinking, which I hope to carry with me for the rest of my career. After every single meeting I had with him, I always left his office feeling a few inches taller.

I would also like to extend my gratitude to my clinical-academic mentor, Professor Gerry O'Donoghue, for presenting me with the inspiring opportunities to experience cutting-edge research in prestigious laboratories across the UK and abroad, and also to the training programme director for ENT surgery in the East Midlands, Mr. Mark Johnston, who took care of all the logistics for me to take time out of my surgical training to pursue this PhD. I also am thankful to the consultant body of the ENT department at the Leicester Royal Infirmary, in particular Ms. Marianne Elloy and Mr. Peter Conboy, who have been incredibly forthcoming in facilitating my transition back into clinical practice by tailoring my training needs

to bring me back up to speed, whilst giving me sufficient space to finalise my thesis write-up.

A particular mention must be made to the entire Rivolta laboratory, who have helped me during the course of my studies. I would like to thank in particular Dr Leila Abbas, for sharing her immense knowledge and expertise of *in vivo* surgery and experimentation methods with me, and also for being my companion in trying out new genres of chili sauce with nachos; Dr Daniela Cacciabue for teaching me the basics of cryostat use and for the hours of laughs she provided me to cheer me up during the lows; Dr Darrell Barrott and Dr Sarah Jacob for teaching me all there is to know about stem cell culture *in vitro* and enduring my incessant questioning in the early days (and all the amusement with the cockney banter); Dr Paul Gokhale for his help with the InCell Analyser; Oscar Solis, who tolerated sitting next to me in the office, and to Mr. Matthew Farr, who as a fellow clinical-academic became my good friend with whom I could discuss the unique challenges of undertaking a lab-based PhD study whilst simultaneously learning the craft of ENT surgery.

A special thanks also goes to my close friend, Muhammad Nizami, who always provided me with numerous moments of clarity whenever I began to lose focus. I feel truly blessed to have such an amazing individual as a friend, and his catchphrase 'Man up cuz!' continues to echo within me to this day!

I am indebted to my parents for everything they have done for me. Throughout their lives, they have made numerous sacrifices to ensure that myself and my

siblings attained a world-class education, and their continual support of my academic endeavors has been immensely helpful. Despite my father's fight with bowel cancer during my PhD, he was there to listen to me when I needed him, and my mother's continual thoughts and prayers have most certainly helped me get over the line. Every success I attain today is because of their hard work in my formative years.

I have perhaps left the most important person in my PhD till last, my amazing wife Bushra. She has been by my side throughout this journey, and has put up with my stresses, mood-swings and erratic working hours. Often weeks would go by before we were able to spend quality time together, particularly towards the end, yet she never complained and always offered me words of encouragement. She always believed in my ability to complete this work, even during the times when I doubted it myself. As clichéd as it sounds, you most certainly have been my rock. I love you with all my heart.

I dedicate this thesis to my two boys, Ibrahim and Danial, and I hope they live their lives exhibiting three key characteristics a PhD student needs; **Perseverance, hard-work and Dedication!**

ABSTRACT

Previous work from the Rivolta laboratory has demonstrated that stem cells can be used to restore auditory function in animal models of sensorineural hearing loss. Transplanted otic neural progenitors are likely to be reliant on glial cells for their long term survival. Thus, the purpose of this work was threefold: firstly, to ascertain whether otic neural progenitors (ONPs) are capable of producing glia de novo during *in vitro* differentiation; secondly, to assess how ONPs interact with glial cells in an *in vitro* co-culture system, and finally, to assess the changes that our deafness inducing protocol induces within the cochlear glial environment *in vivo*.

ONPs were subjected to neuronal and glial driving conditions, and in both instances a significant upregulation of neuronal markers was observed, with hardly any upregulation of glial markers in either condition, suggesting that ONPs may be fate restricted to a neuronal lineage. When ONPs were co-cultured with cochlear Schwann cells, they extended longer neurites when compared to cells grown in isolation, and also obtained directional cues from adjacent Schwann cell networks. Astrocytes in culture underwent reactive changes and were inhibitory to neurite outgrowth from cells.

The Ouabain protocol presented here caused a significant decrease in the expression of peripheral glial markers in mice and gerbils *in vivo*. An upregulation of central glial markers was observed at the glial transitional zone of the auditory nerve suggesting that central glia undergo reactive changes in response to

Ouabain injury. The feasibility of the mouse as model for intra-modiolar transplantation of otic neural progenitors was also demonstrated. Future work should focus on further understanding the pathophysiology of glial cells within the cochlea in order to further the cause of cochlear nerve regeneration.

CONTENTS

Acknowledgements
Abstract
Figures
Tables
Abbreviations

CHAPTER 1

Introduction

1.1 Anatomy of the Human Auditory System	3
1.1.2 Brief Overview of Cochlear Physiology	6
1.2 Hearing Impairment and its Association with Cognitive Impairment	9
1.2.1 Classification of Hearing Impairment	10
1.2.2 Age Related Sensorineural Hearing Impairment	11
1.2.3 Congenital Hearing Impairment	14
1.2.4 Ototoxicity	16
1.2.5 Noise Induced Hearing Loss	18
1.2.6 Auditory Neuropathy	20
1.3 Treatment Strategies for Sensorineural Hearing Loss	23
1.3.1 Hearing Aids	23
1.3.2 Cochlear Implants	24
1.3.3 Auditory Brainstem Implants	28
1.4 Biological Approaches to Treating Sensorineural Hearing Loss	29
1.4.1 Gene Therapy	30
1.4.2 Regenerative Medicine	33
1.4.3 Neurotrophin Therapy	35
1.4.4 Stem Cell therapies – An Introduction	37
1.4.5 Cochlear Stem Cell Therapies	38
1.4.6 Generating Hair Cell-Like Cells From Stem Cells	40
1.4.7 Generating Otic Neural Progenitors From Stem Cells	42
1.5 Glial Cells of the Auditory System, and the Glial Transitional Zone	46
1.6 Aims and Objectives	51

CHAPTER 2

Methods

2.1 Routine In-Vitro Stem Cell Culture	53
Methods	
2.1.1 Derivation of Mouse Embryonic Feeders- Dissection and Initial Culture	53
2.1.2 Derivation of Mouse Embryonic Feeders – Inactivation	54
2.1.3 Culture and Maintenance of Human Embryonic Stem Cells	55
2.2 In Vitro Stem Cell Differentiation	57
Methods	
2.2.1 Generation of Otic Neural Progenitors from Human Embryonic Stem Cells	57
2.2.2 Maintenance of Otic Neural Progenitor Cultures	59
2.2.3 Neuralisation of Otic Neural Progenitors	60
2.2.4 Glial Differentiation of Otic Neural Progenitors	62
2.3 Primary Cell Culture Methods	63
2.3.1 Dissection and Preparation of Schwann Cell Cultures from Gerbil Cochlea	63
2.3.2 Co-culture of Spiral Ganglion Schwann Cells with Otic Neural Progenitors	66
2.3.3 Dissection and Preparation of Gerbil Cortical Astrocyte Cultures	67
2.3.4 Co-culture of Cortical Astrocytes with Otic Neural Progenitors	69
2.3.5 Examining the Effect of Neuralising Medium on Astrocytes Immediately After Passaging	70
2.4 In Vivo Experimentation	70
2.4.1 Measurement of Evoked Auditory Brainstem Response	71
2.4.2 Gerbil Ouabain Surgical Technique	74
2.4.3 Dissection of Temporal Bones for Fixation	76
2.4.4 Processing of Temporal Bones for Cryosectioning	76
2.4.5 Preparation of Glass Slides for Cryosectioning	77
2.4.6 Cryosectioning of Tissue	78
2.5 Immunocytochemistry	78
2.5.1 Immunocytochemistry	78
2.5.2 Immunohistochemistry	79

2.5.3 Image Analysis	83
2.6 Polymerase Chain Reaction Analysis	86
2.6.1 Extraction of RNA	86
2.6.2 Processing of RNA for cDNA Synthesis	86
2.6.3 PCR Primers	87
2.6.4 PCR Conditions	88
2.6.5 Gel Electrophoresis of PCR Products	89
2.7 Statistical Analysis	90

CHAPTER 3

Do hESC-Derived Otic Neural Progenitors Produce Glia?

3.1 Introduction	91
3.1.1 The Otic Placode and Neurogenesis	92
3.1.2 The Neural Differentiation Protocol	95
3.1.3 Schwann Cell Development	97
3.1.4 Cochlear Glial Cells – Development and Function	101
3.1.5 Objectives of this Chapter	105
3.2 Results	106
3.2.1 Co-expression of S100 with B-Tubulin but not GFAP in Early Passage ONPs	106
3.2.2 Lack of S100 and GFAP Expression in Late Passage ONPs	115
3.2.3 S100 Expression Correlates with Neuronal Markers as Opposed to Glial Markers in Shef-1 Otic Neural Progenitors	125
3.2.4 Neuralisation of Shef-3.2 Otic Neural Progenitors	130
3.2.5 Otic Neural Progenitors Do Not Produce Significant Amounts of Glia in Glial-Driving Conditions	140
3.3 Discussion	152
3.3.1 Late Passage ONPs Lose the Ability to Differentiate into Neurons	152
3.3.2 S100 as a Neuronal Marker	155
3.3.3 Otic Neural Progenitors Do Not Appear to Produce Significant Populations of Glia	156

CHAPTER 4

The Interaction Between Otic Neural Progenitors and Glia In Vitro

4.1 Introduction	160
4.1.1 Early Interactions Between Axons and Schwann Cells	160
4.1.2 Radial Sorting	161
4.1.3 The Role of Notch Signaling	162
4.1.4 The Role of Neuregulin Signaling	162
4.1.5 Schwann Cell-Neuronal Co-culture systems	163
4.1.6 Central Glial Development	165
4.1.7 The Role of Astrocytes in the Central Nervous System	168
4.1.8 Reactive Astrocytes and In Vitro Co-Culture Models of Reactive Gliosis	168
4.1.9 Aims and Objectives	171
4.2 Results	173
4.2.1 The Effect of Neuralising Medium on Schwann Cells	173
4.2.2 Schwann Cells Promote and Direct the Growth of Neurites From Otic Neural Progenitors In Vitro	179
4.2.3 Neuralising Medium Induces a Reactive Phenotype in Cultured Cortical Astrocytes	188
4.2.4 Astrocytes Appear to Adopt a Neuronal Morphology in Neuralising Medium Immediately After Passaging	195
4.2.5 Astrocytes Are Inhibitory to Growth of Neurites from Otic Neural Progenitors in vitro	199
4.3 Discussion	207
4.3.1 The Plasticity of Schwann Cells In Vitro	207
4.3.2 Schwann Cells are Supportive of Neurite Growth from Otic Neural Progenitors	209
4.3.3 Astrocytes Adopt A reactive Phenotype in Neuralising Conditions	211
4.3.4 Astrocytes Are Inhibitory to Neurite Outgrowth from Otic Neural Progenitors	214

CHAPTER 5

The Glial Compartment In The Ouabain Model Of Auditory Neuropathy And Cell Transplantation In The Murine Cochlea

5.1 Introduction	217
5.1.1 Disruption of Peripheral Glia on Auditory Function	217
5.1.2 Cochlear Supporting Cells – A Specialised Type of Glia?	220
5.1.3 Disruptions to Central Glia Within the Auditory System	221
5.1.4 Methods of Cochlear Stem Cell Delivery – Scala Tympani Approach	224
5.1.5 Methods of Cochlear Stem Cell Delivery – Intraneural Approach	225
5.1.6 Aims and Objectives	227
5.2 Results	229
5.2.1 Surgical Access To The Murine Cochlea For Drug Delivery and Stem Cell Transplantation	229
5.2.2 Effect of Ouabain on Spiral Ganglia Within Mice and Gerbils	239
5.2.3 Effect of Ouabain on Peripheral Glia Of The Auditory System In Gerbils And Mice	249
5.2.4 Effect Of Ouabain On Central Glia of The Auditory Nerve in Mice and Gerbils	258
5.2.5 Transplantation of Otic Neural Progenitors into the Murine Cochlea	264
5.3 Discussion	271
5.3.1 Ouabain Administration in the Mouse	271
5.3.2 Ouabain Administration Causes a Loss of Peripheral Glial Cells in Murine and Gerbil Cochleae	272
5.3.3 Ouabain Administration Causes and Upregulation of GFAP in the Central Segment of the Auditory Nerve	275
5.3.4 Changes in Glia Following Ouabain Injury – A supportive Environment for Neural Regeneration?	276
5.3.5 Transplantation of Otic Neural Progenitors within the Murine Cochlea	277

CHAPTER 6

Conclusions and Further Implications

6.1 Introduction	279
6.2 The Potency of Otic Neural Progenitors to Produce Glia	281
6.3 The Permissive Effect of Schwann Cells Versus the Inhibitory Effect of Reactive Astrocytes on Otic Neural Progenitors In Vitro	284
6.4 Implications of Glial Responses to Ouabain For Stem Cell Transplantation	286
6.5 Summary	289
References	290

Figure	Description	Page
1.1	Cartoon showing anatomy of the human ear	5
1.2	Cartoon showing cross section of the cochlea	6
1.3	Cartoon showing cross section of the Organ of Corti and its relationship with Spiral Ganglia	8
2.1	Cartoon showing method of measuring neurite angle	84
3.1	Diagram showing stepwise differentiation protocol of human embryonic stem cells to otic neural progenitors	96
3.1a	Diagram illustrating the development of Schwann Cells	100
3.2	Brightfield microscopy images showing the morphological changes that take place from when Shef-1 otic neural progenitors are maintained in OSCFM to when they are placed in neuralising conditions	109
3.3	Representative images showing B-Tubulin and S100 immunolabelling in early passage otic neural progenitors grown in control conditions in OSCFM	110
3.4	Representative images showing B-Tubulin and GFAP immunolabelling in early passage otic neural progenitors grown in control conditions in OSCFM	110
3.5	Representative images showing immunolabelling in early passage otic neural progenitors with B-Tubulin and GFAP at day 6 and day 12 of neuralisation	111
3.6	Representative images showing immunolabelling in early passage otic neural progenitors with B-Tubulin and S100 at day 6 and day 12 of neuralisation	112
3.7	Representative images showing immunolabelling in early passage otic neural progenitors with S100 and GFAP at day 6 and day 12 of neuralisation	113
3.8	Mean percentage expression of mature glial markers S100 and GFAP, alongside mean percentage expression of B-Tubulin in early passage otic neural progenitors.	114
3.9	Representative images showing immunolabelling in late passage otic neural progenitors with B-Tubulin and GFAP in control conditions in OSCFM	117
3.10	Representative images showing immunolabelling in late passage otic neural progenitors with B-Tubulin and S100 in control conditions in OSCFM	117
3.11	Representative images showing immunolabelling in late passage otic neural progenitors with B-Tubulin and S100 at day 6 and day 12 of neuralisation	118
3.12	Representative images showing immunolabelling in late passage otic neural progenitors with B-Tubulin and GFAP at day 6 and day 12 of neuralisation. Panel B shows S100 and GFAP	119
3.13	Mean percentage expression of mature glial markers S100 and GFAP, alongside mean percentage expression of B-Tubulin in late passage otic neural progenitors	120

3.14	Representative images showing immunolabelling in early passage otic neural progenitors with B-Tubulin and S100 In OSCFM and day 12 of neuralisation	124
3.15	Representative images showing immunolabelling in early passage otic neural progenitors with B-Tubulin and NF200 In OSCFM and day 12 of neuralisation	125
3.16	Representative images showing immunolabelling in early passage otic neural progenitors with S100 and P0 at day 12 of neuralisation	126
3.17	Representative images showing immunolabelling in early passage otic neural progenitors with S100 and SOX10 at day 12 of neuralisation	126
3.18a	Mean percentage expression of S100 alongside mean percentage expression of the glial markers GFAP, SOX10 and P0 in early passage otic neural progenitors	127
3.18b	Mean percentage expression of S100 alongside mean percentage expression of the neuronal markers B-Tubulin and NF200.	127
3.19a	Mean percentage co-expression of markers, showing B-Tubulin with NF200, B-Tubulin with S100, S100 with P0 and S100 with SOX10 in early passage otic neural progenitors	128
3.19b	Mean percentage co-expression showing B-Tubulin with NF200, B-Tubulin with S100, S100 with P0 and S100 with SOX10	128
3.20	PCR gels from neural differentiation of early vs late passage Shef-1 ONPs showing representative gels for the genes RPLPO, SOX10, P75 and Brn3a	129
3.21	Brightfield microscopy images showing the morphological changes that take place from when Shef-3.2 otic neural progenitors are maintained in OSCFM to when they are placed in neuralising conditions	132
3.22	Representative images showing immunolabelling in early passage Shef-3.2 otic neural progenitors with B-Tubulin and S100.	133
3.23	Representative images showing immunolabelling in early passage Shef-3.2 otic neural progenitors with B-Tubulin and NF200	134
3.24	Representative images showing immunolabelling in Shef-3.2 otic neural progenitors with intermediate glial markers. Panel A shows S100 and SOX10 and panel B shows S100 with P0.	135
3.25	Mean percentage expression of S100 with neuronal markers B-Tubulin and NF200 in early passage Shef-3.2 Batch A otic neural progenitors	136
3.26	Mean percentage expression of S100 with neuronal markers NF200 and B-Tubulin in early passage Shef-3.2 Batch B otic neural progenitors	136
3.27	Mean percentage expression of S100 with Glial markers GFAP, SOX10 and P0 and NF200 in early passage Shef-3.2 Batch A otic neural progenitors	137

3.28	Mean percentage expression of S100 with Glial markers GFAP, SOX10 and P0 and NF200 in early passage Shef-3.2 Batch B otic neural progenitors	137
3.29	Mean percentage co-expression of B-Tubulin with NF200, B-Tubulin with S100, S100 with SOX10 and S100 with P0 in early passage Shef-3.2 otic neural progenitors Batch A	138
3.30	Mean percentage co-expression of B-Tubulin with NF200, B-Tubulin with S100, S100 with SOX10 and S100 with P0 in early passage Shef-3.2 otic neural progenitors Batch B	138
3.31	Mean percentage co-expression of B-Tubulin with NF200, B-Tubulin with S100, S100 with SOX10 and S100 with P0 in early passage Shef-3.2 otic neural progenitors Batch A	139
3.32	Mean percentage co-expression of B-Tubulin with NF200, B-Tubulin with S100, S100 with SOX10 and S100 with P0 in early passage Shef-3.2 otic neural progenitors Batch B	139
3.33	Representative images showing immunolabelling in early passage Shef-1 otic neural progenitors with B-Tubulin and NF200 in Glial Conditions	144
3.34	Representative images showing immunolabelling in early passage Shef-1 otic neural progenitors with S100 and GFAP in Glial conditions	145
3.35	Representative images showing immunolabelling in late passage Shef-1 otic neural progenitors in control conditions and at the culmination of the glial protocol.	146
3.36	Mean percentage expression of B-Tubulin, NF200, S100 and GFAP in early passage Shef-1 otic neural progenitors in Glial conditions	147
3.37	Mean percentage expression of B-Tubulin, NF200, S100 and GFAP in late passage Shef-1 otic neural progenitors in Glial Conditions	147
3.38	Representative images showing immunolabelling in early passage Shef-1 otic neural progenitors with B-Tubulin and NF200 in Glial conditions grown on Gelatin or Laminin/Polyornithine	148
3.39	Representative images showing immunolabelling in early passage Shef-1 otic neural progenitors with B-Tubulin and S100 in Glial conditions grown on Gelatin or Laminin/Polyornithine	149
3.40	Representative images showing immunolabelling in early passage Shef-1 otic neural progenitors with S100+P0 and S100+SOX10 in Glial conditions grown on Gelatin or Laminin/Polyornithine	150
3.41	Mean percentage co-expression of B-Tubulin with NF200, B-Tubulin with S100, S100 with SOX10 and S100 with P0 in early passage Shef-1 otic neural progenitors in glial conditions	151
4.1	Representative images showing immunolabelling in cochlear Schwann cell cultures.	175

4.2	Mean percentage expression of Schwann cell markers S100 and SOX10, alongside mean percentage expression of B-Tubulin and NF200 in Schwann cell cultures in Schwann cell culture medium versus neuralising medium	176
4.3	Mean percentage of cells co-expressing Schwann cell markers S100 with SOX10, alongside mean percentage co-expression of neuronal markers B-Tubulin and NF200 in Schwann cell culture medium versus neuralising medium	177
4.4	Representative images showing immunolabelling from cochlear Schwann cell cultures for neuronal markers B-Tubulin and NF200, showing the difference in expression between cells in Schwann cell medium and neuralising medium	178
4.5	Representative images showing immunolabelling from otic neural progenitors co-cultured with cochlear Schwann cells <i>in vitro</i>	182
4.6	Histogram and showing distribution of neurite lengths of early Shef-1 otic neural progenitors grown in co-culture with Schwann cells	183
4.7	Histogram showing a comparison of mean of neurite lengths from all experiments involving co-cultures of Shef-1 otic neural progenitors	184
4.8	Histogram showing distribution of neurite lengths of early H14 NOP/SOX2 otic neural progenitors grown in co-culture with Schwann cells	185
4.9	Histogram showing a comparison of mean of neurite lengths from all experiments involving co-cultures of H14 NOP/SOX2 otic neural progenitors	186
4.10	Histograms showing frequency distribution data of neurite angle minus Schwann cell angle in Schwann cell co-cultures with either Shef-1 or H14 NOP/SOX2 Otic neural progenitors.	187
4.11	Representative images showing immunolabelling of cortical astrocytes in Astrocyte medium.	191
4.12	Representative images showing immunolabelling of cortical astrocytes in Neuralising medium.	191
4.13	Representative images showing immunolabelling of cortical astrocytes examining expression of GFAP and B-Tubulin in astrocyte medium and neuralising medium	192
4.14	Mean percentage expression of GFAP and S100, alongside mean percentage expression of B-Tubulin within Astrocytes in Astrocyte culture medium versus neuralising medium.	193
4.15	Comparison of the mean fluorescence density of GFAP signal/cell in astrocytes within astrocyte medium versus neuralising medium, as measured on the Incell Analyser	194
4.16	Representative images showing immunolabelling of cortical astrocytes examining expression of GFAP and B-Tubulin in astrocyte medium and neuralising medium	197

4.17	Representative images showing immunolabelling of cortical astrocytes examining expression of GFAP and B-Tubulin in astrocyte medium and neuralising medium	198
4.18	Representative images showing immunolabelling from Shef-1 otic neural progenitors co-cultured with cortical astrocytes <i>in vitro</i>	202
4.19	Histogram showing distribution of neurite lengths of early Shef-1 otic neural progenitors grown in co-culture with Astrocytes	203
4.20	Histogram and showing mean neurite lengths of early Shef-1 otic neural progenitors grown in co-culture with Astrocytes	204
4.21	Representative images showing co-culture of Shef-3.2 Otic neural progenitors with Astrocytes	205
4.22	Graph showing percentage of human mitochondrial positive cells growing on top of GFAP positive astrocytes	206
5.1	Site of Post aural Incision in mouse	230
5.2	Division of subcutaneous fat to expose sternocleidomastoid	231
5.3	Identification of Greater Auricular Nerve	232
5.3a	Division of Sternocleidomastoid	233
5.4	Identification of facial nerve	234
5.5	Freeing of digastric muscle	234
5.6	Position of drill for Bullostomy	236
5.7	Exposure of Round Window	236
5.8	Modiolusostomy	238
5.9	Representative images showing immunolabelling from murine cochlear sections for B-Tubulin and MYO 7A	241
5.10	Graph showing average counts for TUJ1 positive spiral ganglia in mice from the apical, mid and basal turns of the cochlea in left ears treated with ouabain versus counts from the right, untreated ear	242
5.11	Representative images showing immunolabelling from gerbil cochlear sections for B-Tubulin	233
5.12	Graph showing average counts for TUJ1 positive spiral ganglia in gerbils from the apical, mid and basal turns of the cochlea in left ears treated with ouabain versus counts from the right, untreated ear	244
5.13	Plot of difference between wave ii positive peak and wave iii negative peak at various Sound Pressure Levels (dB) in the mouse.	245
5.14	Change in ABR threshold before and after Ouabain administration in the mouse	246

5.15	Plot of difference between wave ii positive peak and wave iii negative peak at various Sound Pressure Levels (dB) in the gerbil	247
5.16	Change in ABR threshold before and after Ouabain administration in the gerbil	248
5.17	Representative images showing immunolabelling from murine cochlear sections for SOX10 in Rosenthal's canal	251
5.18	Graph showing average counts for SOX10 positive cells in mice from the apical, mid and basal turns of the cochlea in left ears treated with ouabain versus counts from the right, untreated ear	252
5.19	Representative images showing immunolabelling from gerbil cochlear sections for SOX10 in Rosenthal's canal	253
5.20	Graph showing average counts for SOX10 positive cells in gerbils from the apical, mid and basal turns of the cochlea in left ears treated with ouabain versus counts from the right, untreated ear	254
5.21	Representative images showing immunolabelling from mouse cochlear sections for P0	255
5.22	Representative images showing immunolabelling from gerbil cochlear sections for P0	256
5.23	Brightfield images of H and E staining from a mouse cochleae showing the left ear treated with Ouabain and the right ear which was the control untreated ear	257
5.24	Image showing the mask used by the Incell analyser to measure the intensity of glial fibres within the central portion of the auditory nerve	259
5.25	Representative images showing immunolabelling from mouse cochlear sections of the central portion of the auditory nerve for GFAP	260
5.26	Graphs showing mean fluorescence density of the GFAP signal from glial fibres in the central portion of the auditory nerve from individual mice	261
5.27	Representative images showing immunolabelling from Gerbil cochlear sections of the central portion of the auditory nerve for GFAP	262
5.28	Graphs showing mean fluorescence density of the GFAP signal from glial fibres in the central portion of the auditory nerve from individual gerbil	263
5.29	Micrographs of sections showing presence of beads within the Modiolus, as depicted by arrows.	267
5.30	Representative images showing immunolabelling cochlear sections of cochleae from M28 transplanted with H14 NOP/SOX2 cells	268
5.31	Representative images showing immunolabelling from mouse cochlear sections of cochleae transplanted with H14 NOP/SOX2 cells	269

Table	Description	Page
2.1	Table of Antibodies used for Immunocytochemistry	81
2.2	Primer Conditions	88
3.1	Proposed developmental timeline of peripheral glial cells in human fetal cochlea	104
5.1	Summary of transplantation experiments in the mouse	270

Abbreviation	Full Version
AMP	Adenosine Monophosphate
ANOVA	Analysis of Variance
Arg-8	Acetylornithine aminotransferase
Atoh1	Atonal homolog 1
ATP	Adenosine Triphosphate
BDNF	Brain Derived Neurotrophic Factor
bFGF	Basic Fibroblast Growth Factor
BMP3	Bone Morphogenic Protein 3
BRN 3C	Brain-specific homeobox/POU domain protein 3C
c-myc	Avian myeloblastosis virus oncogene cellular homolog
CNS	Central Nervous System
CO ₂	Carbon Dioxide
CTNF	Ciliary Neurotrophic Factor
Cx26	Connexin-26
DAPI	4',6-diamidino-2-phenylindole
DMEM	Dulbecco's Modified Eagle Medium
DNA	Deoxyribonucleic Acid
EDTA	Ethylenediaminetetraacetic acid
EGF	Epidermal Growth Factor
EPHA4	Ephrin type-A receptor 4
EYA	Eyes-absent homolog
FBS	Fetal Bovine Serum
FGF 10	Fibroblast Growth Factor 10
FGF3	Fibroblast Growth Factor 3
FOXP1	Forkhead Box 1
GATA3	GATA binding protein 3
GFAP	Glial Fibrillary Acidic Protein
GFP	Green Fluorescent Protein
GJB2	Gap Junction Beta-2 Protein
GJB2	Gap Junction Beta-2
HBSS	Hank's Balanced Salt Solution
hES medium	Human Embryonic Stem Cell Medium
hESC	Human Embryonic Stem Cell
IGF	Insulin Growth Factor
K	Potassium
kHz	Kilohertz
KLF4	Kruppel-like Factor 4
LMX1A	LIM Homeobox Transcription Factor 1 alpha
MATH1	
MEM	Minimum Essential Medium
MMP	Matrix Metalloproteinase
MYO 7A	Myosin 7A
N-CAM	Neuronal Cell Adhesion Molecule
Na	Sodium
NF200	Neurofilament-200
NFIA	Nuclear Factor 1 A-type
NG2	Neuron-Glial Antigen 2
NRG1	Neuregulin-1
NT-3	Neurtrophin-3
OCT3/4	Octamer-Binding Transcription factor ³ / ₄
OEP	Otic Epithelial Progenitor

OLIG	Oligodendrocyte transcription Factor
ONPs	Otic Neural Progenitors
OSFCM	Otic Stem Cell Full Medium
OTOF	Otoferlin
P0	Myelin Protein Zero
PAX	Paired Box Gene
PBS	Phosphate Buffered Saline
PBST	Phosphate Buffered Saline+Trigene
PCR	Polymerase Chain Reaction
PCTZ	Peripheral-Central Transition Zone
PMP22	Peripheral Myelin Protein 22
RNA	Ribonucleic Acid
S100	S100 Protein
SAMP8 mouse	Senescence Accelerated Prone-8 mouse
SCP	Schwann Cell Precursor
SGN	Spiral Ganglion Neurons
Shh	Sonic Hedgehog
SIX	SIX Homeobox
SLC17A8	Solute Carrier Family 17 member 8
SOD2	Superoxide Dismutase 2
SOX10	Sex determining Region Y-related HMG-box-10
SOX2	Sex determining Region Y-Box2
SVZ	Subventricular Zone
TBX1	T-Box 1
TGF	Tumour Growth Factor
TUJ1	Neuron Specific Type III Beta-Tubulin
UK	United Kingdom

THIS PAGE HAS BEEN LEFT INTENTIONALLY BLANK



“I must confess that I lead a miserable life. For almost two years, I have ceased to attend any social functions, just because I find it impossible to say to people, 'I am deaf.' If I had any other profession, I might be able to cope with my infirmity; but in my profession, it is a terrible handicap.”

Ludwig Van Beethoven

CHAPTER 1: INTRODUCTION

1.1 Anatomy of The Human Auditory System

The sense of hearing is one of five special senses, and is concerned with our ability to perceive sound. At its most fundamental level, the auditory system allows us to detect dangers in our surrounding environment, and its binaural nature enables us to assess the directionality of any such dangers to our survival. Furthermore, it plays a quintessential role in our ability to communicate with others; from early childhood it is our auditory system that provides us with the ability to learn spoken language, and it is through listening to the thoughts of others and expressing our own that we are able to form intimate relationships with one another and express complex ideas. A subsidiary result of having an auditory system is the ability for us to listen to sounds that bring us pleasure, whether this be a piece of classical music or a melodious recital of some poetry.

The auditory system can be divided into its peripheral and central components. The peripheral auditory system consists of all the anatomical structures of the ear that are concerned with conveying sounds from the outside world to the brainstem, whilst the central part of the system is concerned with the structures transmitting and processing this information from the brainstem to the auditory cortex.

The peripheral auditory system can be considered within its three anatomical divisions; the *outer ear*; the *middle ear* and the *inner ear*. The outer ear consists

of a cartilaginous projection known as the *pinna*, which has the principle function of funneling sound energy towards the opening of the auditory system, the *external auditory meatus*. This meatus opens into the *external auditory canal*, the outer two-thirds of which are cartilaginous, whilst the inner third is made up of bone. As the canal is roughly 2.5 cm in length, it is broadly resonant at a frequency of 4 kHz. As a result, sound waves in the vicinity of the 4 kHz frequency benefit from this property, which accounts for the increased sensitivity of the human ear to sounds in this frequency range (Fuchs, 2010).

The tympanic membrane is found at the medial end of the canal to which are attached the 3 ossicles of the ear: the *malleus*, *incus* and *stapes*. These structures are found within the *middle ear cavity*, and their principle function is to conduct the energy from a sound wave towards the inner ear.

The footplate of the stapes attaches to the oval window of the cochlea; the structure within the *inner ear* which converts sound energy into a neural impulse. Given that one of the central themes of this thesis revolves around the regeneration of the neural elements within the cochlea, the basic physiology of the cochlea will briefly be considered.

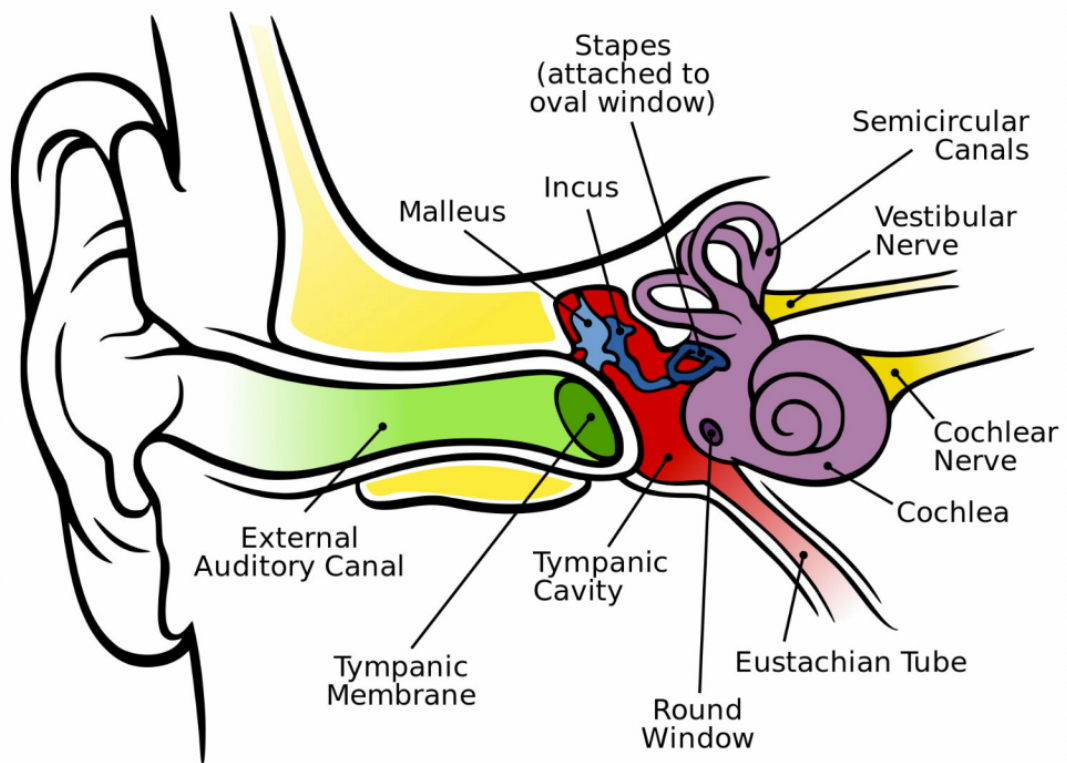


Fig 1.1. Cartoon showing the anatomy of the human ear through the coronal plane. Image taken from worksheet world (<http://comprar-en-internet.net>)

1.1.2 Brief Overview Of Cochlear Physiology

The cochlea consists of three fluid filled compartments; the *scala tympani*, the *scala media* (or *cochlear duct*) and the *scala vestibuli* (Slepecky, 1996). The *scala vestibuli* and *scala tympani* are in continuum with one another and are filled with perilymph. The *scala media*, as the name suggests, resides in the centre of the cochlea, and contains endolymph (LeMasurier and Gillespie, 2005). These intracochlear fluids have differing ionic compositions; perilymph has a high sodium and low potassium content (much like extracellular fluid), whilst endolymph contains high potassium and low sodium content. The resulting high endocochlear potential, along with the high endolymphatic potassium concentration helps to drive the mechanotransduction and the amplification of the wave as it travels through the cochlea (Pickles, 2008).

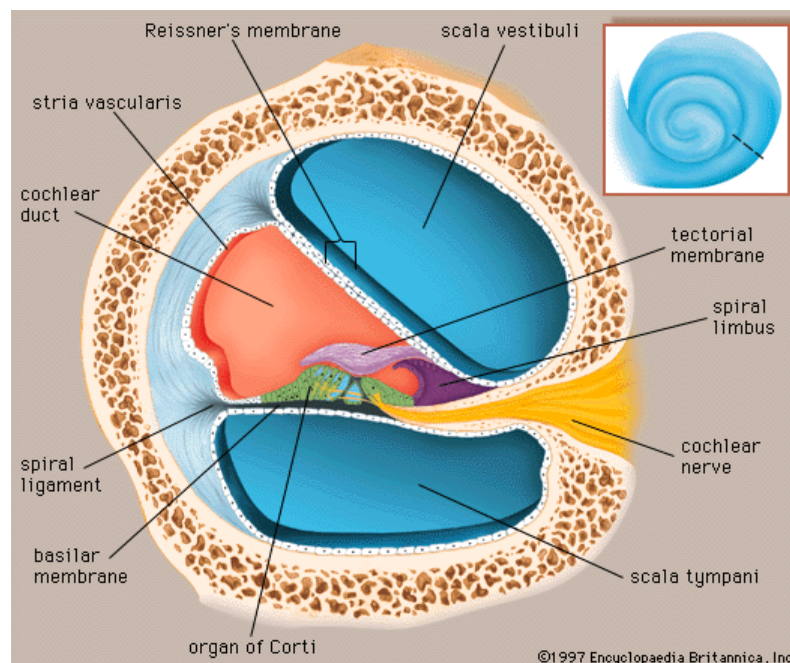


Fig 1.2. Cartoon showing cross section of the cochlea. Image taken from Encyclopedia Britannica online (<http://www.britannica.com>)

As a sound wave hits the stapes footplate at the oval window, a pressure difference is created between the scala tympani and the other cochlear compartments, resulting the basement membrane of the cochlea to vibrate. Sitting on the basement membrane within the scala media is the *Organ of Corti*, which consists of *outer hair cells*, *inner hair cells*, *supporting cells* and the *tectorial membrane*. As the basilar membrane vibrates, shearing forces act on the tectorial membrane, which attenuates displacement of the stereocilia of the outer hair cells. The stereocilia of inner hair cells are not securely attached to the tectorial membrane, however they are displaced by friction against the endolymph of the scala media (Robles and Ruggero, 2001). The displacement of stereocilia results in the opening of cation channels, and in conjunction with the endocochlear potential, a receptor potential is produced (Howard et al., 1988, Hudspeth, 2001). Once these receptor potentials cross a threshold, an action potential is generated within the auditory nerve fibres synapsing with the hair cells.

The cells bodies of peripheral auditory nerve fibres form the *spiral ganglia* of the cochlea, and thus peripheral auditory nerve fibres are often referred to as *spiral ganglion neurons (SGNs)*. Of the two types of SGNs, Type I SGNs are the most in number, which are myelinated fibres synapsing with inner hair cells. Type 2 SGNs are fewer in number that are thin and unmyelinated fibres, forming connections with the outer hair cells (Barclay et al., 2011).

Much of our understanding of intra-cochlear mechanics comes from the pioneering work of Georg Békésy. The focus of his study revolved around the nature of the travelling wave within the cochlea, and the effect it had on cochlear

structures. He showed that the cochlea seems to undertake a Fourier analysis of complex sound waves, and thus different frequencies are mapped in a longitudinal fashion along the cochlea. As the wave travels through the cochlea, its amplitude peaks and then decays; high frequency waves tend to peak near the base of the cochlea, whereas lower frequency waves peak towards the apex (Von Bekesy, 1960). It was from this work that we have subsequently come to learn that the cochlea is *tonotopically* arranged, where the structures at the base of cochlea are optimised for processing high frequency sounds and those towards the apex process low frequency sounds.

Given the precise and intricate nature of the anatomy and physiology of the auditory system, it should be apparent that even the smallest of pathological insults could have dramatic effects in auditory function.

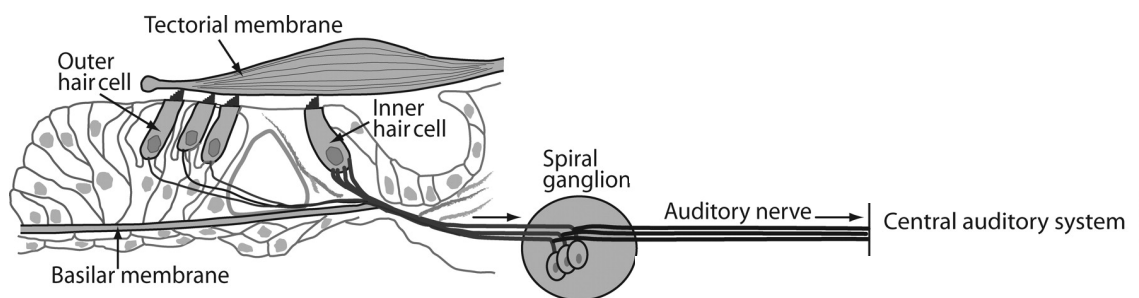


Fig 1.3. Cartoon showing cross the Organ of Corti, and its relationship with Spiral Ganglion Neurons. Image adapted from Zhang et al., 2011.

1.2 Hearing Impairment and its Association with Cognitive Impairment

Hearing impairment is an extremely significant public health issue. It has been estimated that almost 11 million people in Britain suffer with some form of hearing impairment, and projected figures suggest that this could rise to as much as 15.6 million by the year 2035 (Action On Hearing Loss 2015).

Furthermore, evidence has emerged through a number of prospective clinical studies that there is a link between hearing impairments and adult-onset dementia (Lin et al., 2011, Lin et al., 2013, Gurgel et al., 2014). There are two proposed hypotheses to try and explain this link. The first is that hearing impairment and cognitive decline occur as a result of common neurodegenerative processes affecting both the auditory system and centres of higher function in the brain (Baltes and Lindenberger, 1997, Lindenberger and Baltes, 1994), whilst others suggest that long term hearing impairment has a causal effect on cognitive decline, whether this be through social isolation and depression that hearing loss can cause, or a more direct effect as a result of decreased auditory stimulation (Lin et al., 2013).

Estimates suggest that there are 850,000 people in the UK suffering with dementia (Alzheimers Society, 2015), and when one takes into account their complex healthcare needs along with their dependency on social services, the demands such patients place upon the health service become apparent. Thus, there is interest in the idea that treatment of hearing impairments may slow cognitive decline in the elderly, and possibly even prevent it altogether. A study

by Dawes and colleagues tested the impact of hearing aid usage on cognitive performance in a sample of over 500,000 adults in the UK between the ages of 40 and 69. Their results indicated that adults who used hearing aids had better cognitive outcomes than those who didn't, adding weight to the idea that cognitive decline may occur as a result of diminished auditory input. Furthermore, they found no significant association between hearing aid usage and depression, but they did identify increased social isolation amongst hearing aid users due to the difficulties faced by wearing aids in social settings with a high level of background noise, such as bars and restaurants (Dawes et al., 2015). Thus, whilst the problem of social isolation is perhaps reflective of the limitations of current hearing aid technology, the improved cognitive performance amongst hearing aid users is an interesting finding, placing greater emphasis on recognising and treating hearing impairments in a prompt manner, and making the endeavor of improving the treatment modalities to treat hearing loss even more pertinent.

1.2.1 Classification of Hearing Impairment

Hearing impairments are generally considered to be *conductive*, *sensorineural* or *mixed*, where hearing impairments have both conductive and sensorineural elements. Conductive hearing loss occurs as a result of pathology affecting structures of the outer ear and middle ear cavity, and can be caused by things as trivial as foreign bodies in the external auditory canal and cerumen impaction, to more complex disease processes such as cholesteatoma formation and otosclerosis. Within the paediatric population, conductive hearing impairments are by far the most common, due to the high prevalence of Eustachian tube

dysfunction in children, which causes negative pressure within the middle ear. This is the primary causative factor of otitis media with effusion or *glue ear*, and chronic otitis media, with or without cholesteatoma.

Sensorineural hearing loss occurs as a result of pathology affecting the inner ear and central auditory pathways, and is the most prevalent form of hearing impairment within the adult population. Given that the interest in stem cell therapies for deafness lies primarily in their potential to ameliorate sensorineural hearing loss, the aetiology and pathophysiological mechanisms of these impairments will be considered in further detail.

1.2.2 Age-Related Sensorineural Hearing Impairment

Age-related hearing loss is a progressive, bilateral sensorineural hearing loss occurring in mid- to late- adulthood (Baguley, 2008). Typically, age-related sensorineural hearing impairment is associated with a hearing deficit particularly affecting higher frequencies.

In an attempt to understand the pathophysiology of age-related sensorineural impairment, Schuknecht initially classified age-related changes in the cochlea causing hearing loss into 4 types, based on his studies of temporal bones and audiograms from elderly patients (Schuknecht, 1964):

- 1) Sensory – characterized by a loss of hair cells in the Organ of Corti at the basal end of the cochlea, resulting in a high frequency sensorineural hearing loss.
- 2) Neural – Loss of neurons within the cochlear nerve, which causes a fall in speech discrimination scores with stable pure tone audiometry.
- 3) Metabolic – caused by atrophy of the stria vascularis, which causes elevated thresholds at all frequencies. The stria vascularis consists of ion pumps and transport proteins that are involved in maintaining the ionic composition of the intracochlear fluids, and thus maintaining the endocochlear potential.
- 4) Mechanical – Thought to be caused by increased stiffness of the basement membrane of the cochlea.

While Schuknecht's classification provides a logical approach to understand the mechanisms underlying age-related hearing loss, there are of course limitations. Firstly, its focus is solely on the peripheral auditory system, and seems to overlook the changes that occur within the neuronal circuitry of the central auditory pathways, such as a reduction in the number of neurons and synapses alongside alternations in the neurochemical make-up of cells at the level of the cochlear nucleus and auditory cortex. Secondly, there are many instances where the audiogram picture is vague, in which age-related hearing loss may be attributed to an overlap of the 4 mechanisms described above, or indeed, may be indeterminate. Thus, the correlation between findings at audiometry and histopathological analysis are perhaps not quite as clear as suggested by Schuknecht.

Studies from mice have suggested that reactive oxygen species and mitochondrial dysfunction play a causal role in the development of age-related hearing loss. The SAMP8 mouse strain is a useful mouse model that undergoes accelerated ageing, enabling the study of impact of ageing on biological processes. These mice are known to suffer with premature age-related changes in the cochlea which occur as a result of oxidative stress and changes in levels of anti-oxidant enzymes, triggering apoptotic pathways (Menardo et al., 2012). Whilst this alone may shed light on the underlying molecular mechanisms of age-related hearing loss, one may question whether an accelerated ageing mouse is an adequate model for the normal ageing process that mammals undergo. The oxidative stress theory is given further weight by work on the CBA/J mouse, a strain often used in auditory research, as it doesn't suffer with premature hearing loss unlike other common strains such as C57/BL6 and BALB/c. It has been shown that the aged cochlea of CBA/J mice has increased markers of oxidative stress such as lipid peroxidation and glutathionylation, whilst antioxidant protection from free radical scavengers such as mitochondrial apoptosis inducing factor and enzymes inactivating superoxides such as SOD2 were significantly diminished (Jiang et al., 2007). Furthermore, Han and Someya have reviewed a number a mouse models that have specific mutations in mitochondrial DNA resulting in increased oxidative stress, and subsequently causing age-related hearing loss (Han and Someya, 2013). Thus, there is a reasonable amount of evidence to suggest that oxidative stress plays a significant role in the development of age-related hearing loss, which not only is significant in the context of otoprotection, but is also relevant in the field of cochlear regeneration,

and the effect that oxygen free-radicals might have on the long term survival of exogenous cells transplanted into the aged mammalian cochlea.

1.2.3 Congenital Hearing Impairment

Congenital hearing impairments affect around 1 in every 500 births and of these, roughly half can be attributed to a genetic abnormality of some sort (Morton and Nance, 2006). Congenital hearing impairments can be classified as either *syndromic* where hearing impairment is part of a wider condition with multiple anomalies affecting an individual, or *non-syndromic* in which the genetic abnormality is isolated to the inner ear. In non-syndromic sensorineural hearing loss, an autosomal recessive pattern of inheritance occurs in 77-93% of cases and tends to be prelingual, whereas autosomal dominant patterns occur in 10-20% of cases and tend to be postlingual (Duman and Tekin, 2012).

The most frequent genetic abnormality that has been identified in non-syndromic sensorineural hearing loss is in the gene GJB2, encoding the gap junction protein connexin-26 (Kelsell et al., 1997). Gap junctions within the cochlea play an essential role in potassium homeostasis within the cochlea, and maintenance of the endocochlear potential (Wangemann, 2002). However, although mutations in other genes coding for gap junction proteins have been discovered, GJB2 remains to be the most common.

Of other genetic abnormalities affecting the cochlea include mutations in genes coding for tight junctions such as Claudin 14 (Wilcox et al., 2001), and genes

involved in cellular organisation within the cochlea, such as MYO7A. Mutations in MYO7A can lead to either autosomal dominant sensorineural hearing loss or autosomal recessive sensorineural loss. Furthermore, a large number of mutations in the MYO7A gene have been associated with Usher Syndrome Type I; a syndrome which causes bilateral, profound sensorineural hearing loss with vestibular hypofunction, and retinitis pigmentosa (Liu et al., 1997, Weil et al., 1997).

Genetic abnormalities have also been identified to interfere with neuronal transmission. The protein Otoferlin is a key component involved in neurotransmitter release at the ribbon synapse of the inner hair cell (Roux et al., 2006). Mutations in the OTOF gene result in a profound autosomal recessive sensorineural loss, which is accompanied by auditory neuropathy; in which otoacoustic emissions are present despite poor auditory brainstem responses (Rodriguez-Ballesteros et al., 2008).

Most recently, our knowledge of the genetic mutations causing deafness has been greatly enhanced by large scale studies on mice. In a collaborative effort as part of the International Mouse Phenotyping Consortium, hearing loss screening was performed in 3006 mouse knockout strains. In total, they found 67 candidate hearing loss genes, of which 52 were not known of before. This will of course further our understanding of the genetic basis of deafness, and will no doubt be of use when translating such understanding to humans with a genetic impairment causing deafness (Bowl et al., 2017).

1.2.4 Ototoxicity

Ototoxicity is defined as chemical injury to the labyrinth occurring as a result of pharmacotherapy (O'Leary, 2008). The most well-known pharmacological agents for inducing ototoxic damage to the cochlea are aminoglycoside antibiotics and the platinum based chemotherapeutic agents such as cisplatin.

Alongside being ototoxic, aminoglycosides can also cause nephrotoxic damage, however this is usually reversible (Hock and Anderson, 1995), unlike their ototoxic effects which tend to be permanent (Greenwood, 1959). Some aminoglycosides have preponderance to being more vestibulotoxic, such as gentamycin; a property that makes gentamycin a useful treatment for Meniere's disease as an agent capable of inducing a *medical labyrinthectomy*. Others, such as kanamycin and neomycin tend to be more cochleotoxic (Rizzi and Hirose, 2007, Matz, 1993).

After systemic administration, aminoglycosides enter into the cochlea through the stria vascularis (Wang and Steyger, 2009). Once in the cochlear fluids, it has been proposed that aminoglycosides are taken up by hair cells either by endocytosis (Hashino and Shero, 1995), or through the mechanotransducer channel located on the tip of the hair cell (Marcotti et al., 2005). Once in the hair cell, aminoglycosides combine with iron salts, promoting the formation of reactive oxygen species as the iron salts catalyse oxidative reactions (Priuska and Schacht, 1995).

Traditionally it has been suggested that following ototoxic damage to the cochlear hair cells, a gradual secondary degeneration takes place of the spiral ganglion neurons. However, in a study by Dodson, it was demonstrated that guinea pig cochlea that were perfused with aminoglycosides experienced a concomitant loss of hair cells and spiral ganglion as soon as 4 hours post initial exposure, suggesting that aminoglycosides may induce primary cell death in spiral ganglion neurons (Dodson, 1997).

Although aminoglycosides continue to be used in clinical practice as effective antimicrobial agents, with the growing worldwide problem of antibiotic resistance and the global push to identify newer generations of antibiotics, it is hoped that aminoglycosides may eventually be phased out and thus negating the clinical significance of this form of ototoxic damage.

The chemotherapeutic agent cisplatin is also known for its ototoxic effects. Similar to aminoglycosides, cisplatin enters the cochlear fluids via the stria vascularis and is taken up by the hair cells, resulting in toxic accumulation of reactive oxygen species, by inhibiting antioxidant enzymes such as glutathione-S-transferase, glutathione peroxidase and superoxide dismutase (Khyriam and Prasad, 2002, Sadzuka et al., 1992).

Other medications that are known to be ototoxic include loop diuretics (Ikeda et al., 1997), salicylates and quinine (Jung et al., 1993).

1.2.5 Noise-Induced Hearing Loss

Noise-induced hearing loss occurs as a result of prolonged exposure to loud sounds, and it often occurs amongst those whose occupation entails working in loud environments; thus employers have a duty to provide protection for employees who may be frequently be exposed to loud sounds. Prevention is a far better strategy than cure, and stricter employment legislation has meant that over the last decade, the number of people affected with noise-induced hearing loss decreased in the UK, from 68 per 100,000 people employed to 48 per 100,000 UK employees (Health&SafetyExec., 2015). Nevertheless, despite the best of efforts from employers, individuals within certain lines of work will always be vulnerable to loud noise exposure, such as military personnel.

Historically, it was thought that noise-induced hearing loss was caused by direct mechanical damage to the structures of the auditory epithelium (Spoendlin, 1971, Hunter-Duvar and Bredberg, 1974, Hamernik and Henderson, 1974), with some suggesting that loud noise might cause an increase in metabolic activity within the cochlea, resulting in increased free-radical formation by mitochondria (Lim and Melnick, 1971). Later, work by Yamane and colleagues showed an increase in free-radical formation in the guinea pig following prolonged loud noise exposure (Yamane et al., 1995), whilst Ohlemiller later showed similar effects in the mouse (Ohlemiller et al., 1999). Henderson later reviewed the mechanisms of noise-induced hearing loss, caused by increased free radical formation, which induces apoptosis in the cellular structures comprising the Organ of Corti, and also disruption of hair cell synapses with spiral ganglion neurons (Henderson et

al., 2006). Noise exposure not only affects hair cells, but can also affect the glial cells in the cochlea. Tagoe and colleagues have shown that acoustic overexposure can cause elongation of the nodes of Ranvier within the auditory nerve, hampering conduction velocities of action potentials (Tagoe et al., 2014).

With greater knowledge of the mechanisms underlying noise-induced hearing loss, it is anticipated that otoprotective strategies will become more sophisticated, with the advent of antioxidant therapy as a preventative measure. N-Acetylcysteine has provoked some interest as a potential compound to prevent noise-induced hearing loss following encouraging results in *in vivo* experiments (Fetoni et al., 2009, Kopke et al., 2000, Duan et al., 2004), however a randomized control trial of N-acetylcysteine administration in patients undergoing stapes surgery, who can suffer noise-induced hearing loss from high frequency sounds generated from drilling, found no significant improvement in hearing thresholds within the treatment group (Bagger-Sjoback et al., 2015); a reminder that successes seen on studies in *in vivo* models of disease do not necessarily always translate into clinical practice.

1.2.6 Auditory Neuropathy

In 1996 Starr and colleagues published a study comprising of 10 patients with sensorineural hearing impairment, most of whom had particularly difficulty with speech discrimination, particularly in the presence of background noise. These patients had severely abnormal wave I complexes in their auditory brainstem responses with present otoacoustic emissions, suggesting that these patients had a particularly problem with their cochlear nerve function, despite normal hair cell function. All these patients had evidence of a wider peripheral neuropathy; three of the patients suffered with Charcot-Marie-Tooth disease whilst the remaining had subtle evidence of peripheral neuropathy present on nerve conduction studies. Thus, the term *auditory neuropathy* was coined to describe this pattern of hearing impairment (Starr et al., 1996). This brought about a paradigm shift in our understanding of sensorineural hearing loss; much of the work in elucidating the mechanisms of sensorineural hearing loss focused on the pathophysiology of outer hair cell loss and maintenance of ionic composition of cochlear fluids and the endocochlear potential. Neuronal degeneration was traditionally thought to occur as a consequence of hair cell loss, which have been suggested to provide trophic support to the spiral ganglion neurons of the auditory nerve. Starr's observations illustrated that neuronal degeneration does not necessarily have to be a secondary event, but can be the principle cause of an inner ear lesion.

Auditory neuropathies can be considered on the basis of the site where the lesion is impairing neural conduction (Moser and Starr, 2016). *Pre-synaptic* auditory

neuropathies describe a situation where inner hair cell function is impaired with preserved outer hair cell function; thus these patients would fit the criteria of having normal otoacoustic emissions. Selective inner hair cell loss is nevertheless unusual, but has been reported to occur in premature infants. In a study of neonatal intensive care patients comparing objective hearing tests with findings on autopsy, three out of 15 patients exhibited selective inner hair cell loss (Amatuzzi et al., 2001). Isolated inner hair cell loss has also been reported in another temporal bone study of a preterm infant (Slack et al., 1986), however as of yet there aren't any reports of such a pattern of loss occurring in the adult.

Synaptic auditory neuropathy can be used to describe hearing deficits occurring as a result of impaired synaptic transmission. As mentioned earlier, homozygous mutations in the OTOF gene result in impaired release of glutamate release (Roux et al., 2006), and mutations in SLC17A8 results in dysfunction of the transporter VGLUT3; the transport protein employed by hair cells to load synaptic vesicles with glutamate, which has been described in a large family of Czech descent (Thirlwall et al., 2003).

Post-synaptic auditory neuropathies consist of disorders affecting the fibres of the auditory nerve. Kuwaja et al have shown that dendrites can swell and retract from their synaptic connections in response to exposure to loud noises (Kujawa and Liberman, 2009), and a reduction in auditory nerve terminals has been proposed as a contributory factor in age related hearing loss (Chen et al., 2006). These effects have been described as 'hidden hearing loss', as they tend to

produce perceptual difficulties in apparently normal hearing individuals clinically (Plack et al., 2014).

Post-synaptic disorders of the nerve can also occur further downstream. Axonal degeneration of the auditory nerve has been noted as a late complication in patients suffering with Friedrich's Ataxia (Rance et al., 2010), whilst myelinopathies such as Charcot-Marie-Tooth disease can result in demyelination of the auditory nerve and prolonged neural conduction (Rance et al., 2012). Aplasia or hypoplasia of the auditory nerve is a congenital malformation that can occur in children who have a physiologically normal cochlea (Buchman et al., 2006). Hyperbilirubinaemia can affect up to 84% of late pre-term and term infants in the first week of life (Bhutani et al., 2013), and the auditory nerve is particularly vulnerable to excessive levels of bilirubin; in fact the auditory nerve can be susceptible to damage even if bilirubin levels are slightly raised (Smith et al., 2004). Bilirubin results in increased oxidative stress within the auditory nerve, resulting in decreased neuronal proliferation, a decrease in the size of spiral ganglia (Brito et al., 2008) and impaired transmission at glutamergic synapses (Haustein et al., 2010). Thus, children who suffer with hyperbilirubinaemia early in their life are more susceptible to auditory neuropathy, and more than 50% of children who receive a diagnosis of auditory neuropathy have a preceding history of hyperbilirubinaemia (Rance, 2005).

Auditory neuropathies can be a vexing problem to treat. For those on the milder end of the scale who have perceptual difficulties, gross amplification of sound will provide them with little benefit, and can potentially make the situation worse for

them by amplifying background noise to intolerable levels. For others on the more severe end of the spectrum, treatment strategies such as cochlear implants will also be less effective; as it is thought that successful outcomes with implants are partly reliant on the presence of a healthy auditory nerve. Treatment strategies for sensorineural hearing loss, and their limitations will now be considered in further detail.

1.3 Treatment Strategies for Sensorineural Hearing Loss

Sensorineural hearing loss has traditionally been a troublesome condition to treat. The mainstay of treatment for many years centered on the use of analogue hearing aids. Today, the treatment still centres around the use of prosthetic devices, such as hearing aids, cochlear implants and brainstem implants.

1.3.1 Hearing Aids

In essence, hearing aids work as body worn sound amplifiers. A microphone is situated in the device, which picks up sound and subsequently turns it into an electrical signal that is then fed back into the ear. Over the last decade hearing aid technology has improved with the advent of digital technology, replacing the analogue variety. With sophisticated signal processing mechanisms built into newer digital hearing aids reducing feedback and digitally enhancing speech, coupled with longer battery life and more aesthetic behind the ear moulds, one would expect improved compliance from patients with the newer devices.

However, this is not the case, as hearing aid compliance remains unsatisfactory (McCormack and Fortnum, 2013). Reasons for this include low patient satisfaction with sound quality from hearing aids particularly in noisy environments (Cohen-Mansfield and Taylor, 2004); patients finding them uncomfortable to wear (Chien and Lin, 2012); experience difficulties with care and maintenance of hearing aids (Brooks, 1985); the continue to experience problems with devices such as feedback and whistling (Chien and Lin, 2012) and concerns with the appearance of hearing aids remain (Bertoli et al., 2009). Given that hearing aids continue to be the mainstay of treatment for sensorineural hearing loss, the numerous limitations of hearing aids resulting in poor patient compliance illustrates the urgent need for better treatments for this condition.

1.3.2 Cochlear Implants

It would not be an over exaggeration to say that cochlear implants have been one of the greatest technological developments of modern medicine. They have revolutionised the way in which sensorineural hearing loss is treated, particularly for those individuals who suffer with a clinically profound sensorineural hearing deficit; a patient group who prior to the advent of implants, gained minimal benefit from traditional hearing aids. Cochlear implants are essentially a *bionic ear*; a device that converts sound waves into an electrical impulse that directly stimulates the neural elements within the cochlea.

The idea of stimulating the hearing apparatus with an electrical current is something that has intrigued scientists for centuries. The Italian physicist

Alessandro Volta famously tried to stimulate his own ear with electrical currents, in which he describes hearing a sound resembling a thick boiling soup, most probably due to the damage inflicted by the current as opposed to successfully stimulating his hearing apparatus (Volta, 1800). However, the French pair Djournon and Eyries are widely accredited as the team who first used an electrical device to stimulate the stump of the auditory nerve, in a patient who had undergone radical mastoid surgery for cholesteatoma – suggesting in their report that a similar device might be used to electrically stimulate the cochlea (Djournon and Eyries, 1957). This idea was then furthered by House and Doyle in Los Angeles, who were the pioneers of the cochlear implant, having undertaken the first successful implant of a patient in 1961 (Doyle et al., 1963).

Early devices were single channel implants, however greater understanding of how electrical impulses stimulate the auditory nerve, courtesy of extensive work in the field by Michael Merzenich, paved the way for multichannel implants which would provide improved frequency resolution to implant users (Merzenich et al., 1973, Merzenich et al., 1974). The eminent Australian otologist, Graham Clark was also interested in the concept of multi-channel implants, and later implanted the first multi-channel implant in 1978, giving patients improved discrimination of sound as compared to the single-channel predecessors (Clark et al., 1979).

Modern cochlear implants consist of a sound processor that is worn behind the ear, which digitises captured sound. This is then transmitted to the coil of the implant on the outside of the head, which is in magnetic contact with the implant. The implant converts the digital code into electrical impulses, which then

stimulate the cochlea via an intracochlear electrode. In this way, the cochlear implant completely bypasses the natural hearing apparatus and directly stimulates the spiral ganglia of the auditory nerve.

With improvements in implant technology and developments in surgical technique, the candidacy for cochlear implants has increased dramatically. Whereas implants were initially only offered unilaterally, studies have now shown the benefits of performing bilateral cochlear implantation, with improved perception of speech and hearing with background noise (Venail et al., 2008). Whilst in adults it appears that timing of sequential implantation doesn't appear to be a significant factor in affecting outcomes (Reeder et al., 2014), timing appears to be a more important variable in paediatric cochlear implantation. Children who have bilateral implantation performed simultaneously tend to perform better than those who are implanted sequentially (Lammers et al., 2014)

Cochlear implants are also being increasingly considered as a therapeutic measure in single-sided deafness. Traditionally these patients have been treated with either a contralateral routing of sound device, or a bone-anchored hearing aid; on the premise that through bone conduction, sounds from the affected side could be transmitted towards the functioning cochlea. The principle difficulty that these patients experience is with sound localization, and studies are beginning to suggest that sound localization outcomes for patient with single sided deafness treated with cochlear implants are significantly better than those with bone anchored hearing aids (Nawaz et al., 2014).

Cochlear implants were traditionally inserted in patients who had profound hearing loss. As the surgical insertion of the electrode can be a traumatic insult to the delicate structures of the cochlea, only those with the severest of hearing deficits were considered as candidates, for whom the damage of intracochlear structures would be of little significance. However, there has been a significant move to implement hearing preservation strategies within the realm of cochlear implantation, as even patients with clinically profound hearing loss tend to have an element of residual hearing. Thus, preserving this alongside a cochlear implant has been shown to improve speech comprehension, sound localization and hearing in challenging environments (Gifford et al., 2013). Improvements in electrode design and development of 'soft surgery' have paved the way for this development (Miranda et al., 2014).

Despite the success of the cochlear implant as a neural prosthesis, a fundamental limitation of the device has been the variability in outcomes for patients treated with it; a factor that has continued to persist despite advances in sound processor technologies (Ganek et al., 2012). There are many possible causes to explain this, such as variables in the auditory periphery, which receive the stimulus from the implant, to issues in the central processing of the auditory input. Moreover, music perception and hearing in complex environments continues to be problem for implant users (Limb and Roy, 2014).

1.3.3 Auditory Brainstem Implants

Aside from the limitations of cochlear implants mentioned above, they are also generally unsuitable for patients who have severe pathology of the auditory nerve. For patients who have a significant lesion between the cochlea and the cochlear nucleus as the principle cause of their hearing impairment, a brainstem implant may be an appropriate treatment strategy by directly stimulating the cochlear nucleus. The first brainstem implant was undertaken at the House Ear Institute in 1979 in a patient following acoustic neuroma removal (Eisenberg et al., 1987), and much like cochlear implants, auditory brainstem implants too have since evolved from single channel to multi-channel devices .

The principle indication for auditory brainstem implants are for those patients who suffer with neurofibromatosis type II, who have a preponderance to develop bilateral vestibular schwannomas. However, the compressive nature of these tumours at the cerebellopontine angle results in oedema and fibrosis at the level of the cochlear nucleus, which may limit the efficacy from implantation (Colletti et al., 2004).

Auditory brainstem implants may also be considered in patients who have an ossified cochlea; a possible complication of meningitis, and also one of the more deleterious effects of severe otosclerosis. As access to the cochlea may be severely impaired, a brainstem implant may offer these patients some restoration of auditory input, and they may have better outcomes than patients with neurofibromatosis type II, as the cochlear nucleus would have been spared of

any significant pathology (Colletti et al., 2004). Furthermore, patients with congenital malformations affecting the inner ear, such as labyrinthine aplasia and cochlear nerve aplasia may also be candidates for a brainstem implant (Sennaroglu et al., 2009).

Results with auditory brainstem implants haven't been quite as encouraging as with the cochlear implant, and variability in outcomes appears to be even more of an issue with these patients, with some patients not receiving any auditory sensations whatsoever. This illustrates the difficulties in treating sensorineural hearing loss where the auditory nerve is the principle site of pathology.

1.4 Biological Approaches to Treating Sensorineural Hearing Loss

Despite the significant advances that have been made in prostheses used in the treatment of sensorineural hearing loss, it is clear that each of them has limitations in the quest to recreate the experience of natural hearing for the user. However with exciting developments in fields such as genetics, regenerative medicine and nanotechnology, a path is being paved for the tantalising prospect of combining cell and molecular biology alongside prosthetic devices to overcome these limitations. From using the cochlear implant as a sophisticated drug delivery device to the combination of stem cell therapies with implants, a number of strategies have yielded encouraging results in the laboratory, which may well be translated into the clinic in the very near future.

1.4.1 Gene Therapy

With a much deeper understanding of genetic mutations that can give rise to sensorineural hearing loss, gene therapy has been an important line of enquiry in the search for improved therapies.

The development of gene therapies hinges upon the development of an effective carrier for genetic material. Within the context of the ear, vital characteristics of such a carrier include the ability to target specific cell types with an efficient transduction profile, whilst the carrier vehicle itself should not induce intracochlear inflammation and ototoxicity. Strategies for delivery include nanoparticles and inactivated viruses. Non-viral gene delivery systems have the advantage that they can be tested for toxic effects through *ex-vivo* experimentation and modified accordingly. However, their limitations lie in the ability to induce effective genetic transduction. Hyperbranched polylysine nanoparticles have been shown to efficiently internalize into the Organ of Corti and spiral ganglion cells, and induced a higher transfection efficiency than Lipofectamine in primary culture (Zhang et al., 2011). More Recently, Arg-8 conjugated nanoparticles have been demonstrated as a potential nanocarrier of genetic material with a high level of nuclear delivery in both organotypic cultures of the cochlear epithelium and *in vivo* (Yoon et al., 2015). However, it remains to be seen whether these delivery vehicles can effectively deposit genetic material to induce a therapeutic response.

Viral vectors have the advantage of being a far more effective genetic carrier system than synthetic nanoparticles. A range of viral vectors have been tested for intracochlear delivery of genetic material such as adeno-associated virus, adenovirus and lentivirus, which have been reviewed by Akil and Lustig (Lustig and Akil, 2012). From all the viral candidates for gene delivery, it appears that the adeno-associated virus is the one that exhibits the best potential, as it transduces host cells very efficiently without causing ototoxicity or inflammation.

As mentioned previously, mutations in the *GJB2* gene which codes for connexin-26 have been identified as the most common cause of hereditary non-syndromic hearing loss. Crispino et al. provided initial strong evidence that genetic transfer of *GJB2* can restore the gap junctions, which play a crucial role in maintaining intracochlear potassium homeostasis through genetic delivery with bovine adeno-associated virus into organotypic cultures from deaf *Cx26Sox10cre* mice (Crispino et al., 2011). Yu et al. built upon these interesting findings, and showed that *in vivo* delivery of *GJB2* with the adeno-associated virus resulted in widespread expression of connexin-26 in the supporting cell network, although they fell short of illustrating function recovery of hearing (Yu et al., 2014).

The gene *Atoh 1* has also been viewed as a therapeutic target for hair cell restoration, and its absence results in a loss of hair cells and the supporting cell network (Pan et al., 2011). Intracochlear delivery of *Atoh 1* has been shown to induce supporting cells to change phenotype and transform into ectopic hair cells, which were labeled as immature hair cells due to their lack of proteins found in mature hair cells such as prestin and oculomodulin (Kawamoto et al., 2003).

Crucially, it appears that efficacy of such a therapy is dependent upon the severity of the introcochlear lesion; *Atoh 1* delivery has been shown to yield functional recovery of hearing shortly after deafening (Izumikawa et al., 2005), but Atkinson et al. have shown that in severe lesions, despite a significant increase in the number of cells expressing hair cell markers, there appears to be a lack of functional recovery even if the gene was delivered shortly after the initial insult (Atkinson et al., 2014). Interestingly, their study also showed there was no significant increase in synaptic ribbons post treatment either; which might suggest that witnessing therapeutic benefits with gene therapy in severe lesions of the cochlea might require a combination of genes not only to induce hair cell formation, but also to treat the resulting synaptopathy.

There is currently much excitement around the CRISPR/Cas9 technique for gene editing. The groundbreaking work from Jennifer Doudna's laboratory illustrated the sequence-specific DNA cleavage by the crRNA (CRISPR RNA):tracrRNA (Trans-activating CrRNA)-Cas9 complex, and that by changing the target specific sequence of crRNA they could redirect DNA cleavage to any sequence of interest (Jinek et al., 2014). This technique has greatly simplified the challenging task of precisely editing the genome, and holds great promise in translating as a potential therapy for numerous genetic diseases, as well as implications in cancer biology. Within the context of the ear, Zuris and colleagues have shown that a complex formed between the Cas9 protein and nucleic acid gRNA can be delivered to inner hair cells *in vivo*, being able to successfully edit the genome by silencing the GFP signal in *Atoh1*-GFP transgenic mice (Zuris et al., 2015). This obviously has implications as a potential therapy in conditions

such as Usher's syndrome where such techniques would be useful in correcting the dominant MYO7A mutation.

However, there are numerous ethical issues that surround the use of genome editing which may well act as a significant barrier in the translational of this powerful laboratory based technique into a therapeutic measure.

1.4.2 Regenerative Medicine

The other biological approach to treating sensorineural hearing loss is through regenerative medicine, and in this regard, the cochlea is a particularly interesting organ within which to study the science of regeneration. A number of animal species have the ability to replace damaged hair cells, including amphibians, fish and birds (Corwin, 1985, Corwin and Cotanche, 1988, Ryals and Rubel, 1988). Mammals, however, do not have the capacity to regenerate the sensory structures of the peripheral auditory system and although hopes of stimulating regeneration were raised following reports of a stem cell niche persisting in the vestibular system of adult mice, the adult cochlea unfortunately does not seem to harbour a similar population of cells beyond the postnatal period (Li et al., 2003b).

However, stem cells are only part of the story when considering an appropriate regenerative strategy. In the central nervous system for example, regeneration remains a challenging task despite the presence of neural stem cell niches, as

the principle problem appears to be neuroinflammatory responses to injury that hinder resident stem cells to undertake repair. Thus, in order to have an effective strategy for regeneration, 3 key ingredients are necessary:

- 1) An availability of a stem cell population which can repair and replace the damaged tissues
- 2) An understanding of inflammatory responses to injury, and the impact they have in facilitating or inhibiting repair
- 3) Knowledge of tissue biology within the organ of interest; how the tissue is organised and the interactions between the various cell types within the tissue, which help it to undertake its physiological function.

Thus, the cochlea presents itself as a particularly challenging organ within which to promote regeneration; the complex organisation of the structures within the cochlea, the apparent absence of a stem cell niche and its delicate nature making it susceptible to inflammation with even the smallest of disturbances present significant hurdles in the quest to find the ideal regenerative strategy.

1.4.3 Neurotrophin Therapy

Within the paradigm discussed above when considering regenerative strategies, it is widely thought that neurotrophic support to the spiral ganglion neurons within the cochlea is provided by hair cells, although more recently this idea has been contested with the notion that the principle source of neurotrophic support for spiral ganglia comes from the supporting cells (Zilberstein et al., 2012, Abbas and Rivolta, 2015). In any case, given that most ototoxic insults cause damage to both hair cells and supporting cells, a secondary degeneration of spiral ganglion neurons is often observed as their trophic support is diminished. A number of studies have demonstrated that delivery of exogenous neurotrophins into the cochlea can rescue spiral ganglion neurons from degeneration (Gillespie et al., 2003, Leake et al., 2011, Leake et al., 2013, Landry et al., 2011). However, a number of fundamental questions require answering prior to translating this therapy clinically, including the optimal duration of neurotrophin therapy and the subsequent development of an appropriate drug delivery strategy. For example, the study by Gillespie looked at the application Brain derived neurotrophic factor (BDNF) into the deafened guinea pig cochlea with an osmotic pump, and found that BDNF prevented the degeneration of spiral ganglion neurons, however upon cessation of treatment, there was accelerated decline in spiral ganglion survival, suggesting that the hair cells most probably provide neurotrophic support to the cochlea (Gillespie et al., 2003). However, Agterberg and colleagues performed a similar study in the guinea pig and found that spiral ganglion densities remained the same as that in control animals 2 weeks after cessation of treatment. In their study however, animals underwent cochlear implantation alongside neurotrophin

therapy, although the animals did not undergo any cochlear implant stimulation protocols and implantation was undertaken purely to assess whether the surviving spiral ganglion cells were amenable to electrical stimulation, as assessed by recording electronically evoked auditory brainstem responses (Agterberg et al., 2009). Explaining this discrepancy, it is possible that the measuring of eABRs was inducing a trophic effect on the spiral ganglion neurons through electronic stimulation from the implant, as has also been observed by Shepherd et al. (Shepherd et al., 2005), although their study only found enhanced survival in the basal turn of the cochlea, whereas Agterber's study found enhanced survival throughout the cochlea. A definitive answer to the question of SGN survival following neurotrophin therapy is extremely important if they are to be translated into the clinic; if, as Agterberg's data suggest, spiral ganglia can indeed survive after a finite period of neurotrophin therapy, then combining this with existing cochlear implant technologies could lead to improving the health of the damaged neural elements within the cochlea, resulting in improved outcomes for patients.

Drug delivery strategies are also an important issue to consider for neurotrophin therapies. Most experimental studies have been undertaken with osmotic pumps, which cannot be used clinically due to the unacceptable risk they pose for infection. A range of biomaterials have been tried, including polypyrrole coatings (Richardson et al., 2009) and hydrogels loaded with neurotrophins (Rejali et al., 2007), which could release neurotrophins into the intracochlear environment alongside a cochlear implant. However, acquiring the optimal release profile over the period of treatment remains the fundamental challenge when developing

controlled release biomaterials for intracochlear drug delivery. Furthermore, the long term effects of neurotrophin therapy would also need to be assessed thoroughly before translation is considered.

1.4.4 Stem Cell Therapies – An Introduction

The key features of a pluripotent stem cell include the ability to differentiate into representative cells of the three embryological germinal layers; namely the ectoderm, mesoderm and endoderm, whilst simultaneously having the capability to self-replicate, thus maintaining their 'stemness' in successive generations of cells.

Human embryonic stem cells (hESCs) are a classic example of truly pluripotent stem cells. They are derived from the inner cell mass of the blastocyst, and are capable of being cultured *in vitro*. They have proved to be an extremely valuable tool not only in generating differentiated cells arising from the germinal layers which may be translated into clinical therapies, but also provide an opportunity to further understand the cellular and molecular mechanisms underlying human development, as much of our current understanding of development comes from mouse and zebrafish studies, due to the difficulties in accessing human fetal material. Furthermore, they present an opportunity to model disease and test novel therapies on human-derived cells.

Mammalian adults also possess stem cell niches residing within various organ systems, which too are capable of self-renewing, but have their fate restricted to the cell types of the organ system they reside within. Haematopoietic stem cells are an example of such stem cells, which are capable of producing various types of blood cell throughout mammalian life.

A significant advancement in the field of stem cell biology is the ability to reprogramme differentiated cells to behave like pluripotent stem cells. In Takahashi's landmark work (Takahashi and Yamanaka, 2006, Takahashi et al., 2007), it was shown that forced expression of the genes SOX2, OCT3/4, C-MYC and KLF4 led to differentiated cells to behave like pluripotent stem cells in their morphological appearance, proliferation and gene expression. Moreover, these cells are capable of producing representative cells of the three germ layers. These *induced pluripotent stem cells* have the advantage that they avert the ethical dilemmas posed by human embryonic stem cells, in addition to the fact that they open up the possibility of patient specific stem cell therapies.

1.4.5 Cochlear Stem Cell Therapies

A population of stem cells has been described to exist within the mammalian inner ear. Li and colleagues initially demonstrated the presence of a stem cell niche within the vestibular system of the adult mouse, capable of forming representative cells of the three germinal layers. They also reported that a subset of these cells was capable of differentiating into hair cell-like cells (Li et al., 2003a). Later, Oshima and colleagues isolated sphere forming stem cells from

the cochlear and vestibular tissues of mice of various ages, from day 1 to 4 months of age. They found that during the first three weeks of life, cells from the spiral ganglia, the Organ of Corti and the stria vascularis contain a population of sphere-forming cells capable of self-renewal, however during the second and third weeks these populations greatly diminished in number. In contrast, stem cells in the vestibular system tended to persist for longer, remaining present up until 4 months of age (Oshima et al., 2007a). It has thus been postulated on this basis, that the mammalian cochlea quickly loses the ability to self-renew in the early postnatal period. However, more recently it has been demonstrated that the adult mouse auditory nerve contains neural stem/progenitor cells within a SOX2 positive population of glial cells associated with the nerve, the production of which can be stimulated by acute neuronal injury (Lang et al., 2015). Moreover, work from Chow and colleagues suggests that expression of the intermediate filament protein nestin (a marker suggestive of cells with stem cell characteristics) is present in various regions of the cochlea during development, including the Organ of Corti and Spiral Ganglia, however this generally diminishes into adulthood, persisting in a region of the spiral ganglia below the hair cells and also within the Dieter's cells of the cochlear apex. Their data suggests that the nestin positive Dieter's cells in the apex of the adult cochlea are unlikely to represent stem cells, however the nestin positive population in the spiral ganglion exhibited some stem cell characteristics (Chow et al., 2016). Combining these findings with the work of Lang, it seems that the auditory nerve may indeed have a population of stem cells persisting in the adult mammalian cochlea, which may be able to repair damaged neural elements within the inner ear. Future work should examine the biology of these populations further; in particular understanding the

mechanisms that might be preventing these cells from differentiating and repairing damaged nerve fibres in the pathological ear, and how these might be modulated for therapeutic benefit.

1.4.6 Generating hair cell-like cells from stem cells

Alongside attempts to identify an endogenous stem cell niche within the inner ear, a considerable amount of effort has been made to explore the possibility of exogenous stem cells being introduced into the cochlea afflicted with pathology to repair its delicate structures and restore function. Li et al. initially described a protocol to generate inner ear progenitors from murine embryonic stem cells by culturing them in serum free media supplemented with EGF, IGF and bFGF, based on the role these molecules play during development of the inner ear. They found that differentiated cells appeared to express markers associated with the sensory epithelium of the inner ear, namely MATH1, MYO7A and BRN 3C (Li et al., 2003b). Oshima and colleagues later reported a protocol for generating hair cells from mouse embryonic stem cells and induced pluripotent stem cells through an embryoid body process, culturing them in serum free media containing, bFGF, FGF3 and FGF10, which have been shown to be the principle growth factors in inducing otic specification in development. When progenitors were co-cultured with utricle stromal cells inactivated with mitomycin C, they generated hair cell-like cells that co-expressed ATOH1 and MYO7A, and also found hair bundles on scanning electron microscopy of cells (Oshima et al., 2010). Generation of sensory epithelium from mouse embryonic stem cells employing three dimensional culture methods have also been described, which

may be a promising tool for *in vitro* drug screening of medications that might have ototoxic effects on hair cells (Koehler et al., 2013).

Whilst work on murine stem cells is useful, therapeutic potential can only be realised through translation of these protocols to cells of a human source. Chen et al initially described techniques for the isolation of human fetal auditory stem cells, and hair cell differentiation using EGF and Retinoic Acid (Chen et al., 2009). They later showed that this protocol could equally be applied to inner ear hair cell progenitors derived from human embryonic stem cells to produce functional hair cell-like cells (Chen et al., 2012). Others have also shown the potential for hair cell-like cells to be generated from stem cells originating from a human source (Ronaghi et al., 2014, Kil et al., 2016, Ohnishi et al., 2015).

The prospect of using hair cell-like cells derived from stem cells as a therapy for deafness is an extremely challenging task. Specifically, surgical access to the scala media and directing the cells to their precise position within the Organ of Corti is the main technical barrier to translation, whilst getting cells to survive in the unique endolymphatic potassium-rich environment is yet another aspect that requires consideration.

1.4.7 Generating otic neural progenitors from stem cells

Another potential application of stem cell therapies to the cochlea may be through the generation and transplantation of neural progenitors into the cochlea. Primarily, such a therapy may be useful in conjunction with a cochlear implant; the theory being that by improving the health of the neural elements within the cochlea might lead to better outcomes for patients who have undergone a significant degree of Wallerian degeneration of the auditory nerve fibres. Whilst attempting to ameliorate this situation may yield some benefit in improving outcomes with a cochlear implant, it is likely that the notion of improving patient outcomes is multifactorial. In a study of temporal bones from 15 implanted patients, it was found that there was no correlation between speech recognition scores and spiral ganglion counts from those patients (Khan et al., 2005). Although it can be argued that this is quite a small study to draw any robust conclusions, similar findings have also been reported from other histopathological studies of implanted patients (Fayad et al., 1991, Nadol et al., 2001). This obviously brings into question the exact significance of the peripheral auditory system in improving patient outcomes, and whether our efforts in improving results following cochlear implantation might be better directed towards understanding the mechanisms of central plasticity of the auditory pathway. The best course of action would obviously be to try and improve the health of the peripheral auditory system given the knowledge we have of the importance that the ribbon synapse plays in encoding temporal information about sound (Heil and Peterson, 2016, Moser and Starr, 2016), alongside furthering our knowledge of the remodelling that takes place in the cochlear nucleus and auditory cortex.

Therefore, by adopting such a 'two pronged' approach to the problem of improving patient outcomes, we are more likely to be successful in our endeavour of recreating the natural hearing experience for implanted patients.

Another potential application of neural progenitors into cochlea would be in auditory neuropathy, in particular those patients who have hypogenesis or agenesis of the cochlear nerve. In such patients, transplantation of progenitors in theory could help to re-establish connections between the cochlear nucleus and the Organ of Corti, thus presenting a wholly biological therapy for a particular type of sensorineural hearing loss.

It is important that neural progenitors derived *in vitro* have truly otic characteristics, given the importance that nerve fibres play in encoding sound. Shi and colleagues successfully demonstrated that culturing sensory progenitors derived from human embryonic stem cells with BMP4 gave rise to peripherin positive neurons. There was also increased expression of markers such as GATA3 and Neurogenin1 (Shi et al., 2007).

Alongside generating hair cell-like cells, Chen and colleagues have shown that they can generate functional auditory neurons derived from human fetal auditory stem cells. They cultured the cells in serum free medium supplemented with Sonic Hedgehog, with the neurotrophins BDNF and NT-3 added into the system on the third day of culture, and Sonic Hedgehog withdrawn on the 5th day. The neurons generated from this protocol shared electrophysiological properties of mammalian auditory nerve fibres. These neurons also expressed classical

neuronal markers such as TUJ1 and NF200, alongside expressing Brn3a, suggesting that these were sensory neurons (Chen et al., 2009). This work was also replicated with human embryonic stem cells, which were first fate restricted into an otic lineage, and then subsequently differentiated to generate spiral ganglion-like neurons (Chen et al., 2012). Similar work has also been undertaken with induced pluripotent stem cells (Gunewardene et al., 2014), as well as with human bone marrow mesenchymal stem cells (Boddy et al., 2012). The replication of this work in cells that can easily be derived from a human source without the ethical barriers raises the therapeutic potential of otic neural progenitors as a potential treatment for sensorineural hearing loss.

There have been numerous studies that have been undertaken to examine the effects of transplanting stem cells into the denervated cochlea. Comparison of studies is somewhat challenging, given the variation between studies. Variables include the species used, the method used to induce the intracochlear lesion, the source of stem cells and their stage of differentiation, and the surgical route of cell delivery. However, looking at the studies as a whole some conclusions can be drawn; firstly, it appears that transplanting cells which have been fate restricted into a neural phenotype is an important factor in order to re-establish connections between the Organ of Corti and the cochlear nucleus. Secondly, it seems the most notable successes in transplantation have occurred when the cells have been delivered directly into the modiolus. Corrales and colleagues showed that neurites grew out from cells transplanted into the modiolus through the spiral lamina and into the Organ of Corti, however they did not manage to exhibit functional recovery (Corrales et al., 2006). The Rivolta laboratory were the

first team to robustly illustrate that functional recovery of hearing can be achieved through stem cell transplantation (Chen et al., 2012). In their study, gerbils were deafened with $\text{Na}^+/\text{K}^+/\text{ATPase}$ inhibitor Ouabain, which damages Type I spiral ganglion fibres, whilst keeping the Type II fibres and hair cells intact; thus making this a model of auditory neuropathy. Cells were injected into the base of the auditory nerve through what can be described as a 'modiolusostomy', and transplanted animals were kept alive for a maximum of ten weeks. Their study showed that cells formed an ectopic ganglion within the nerve, which projected fibres peripherally towards the Organ of Corti, and centrally towards the cochlear nucleus. Remarkably, the group also exhibited functional recovery through a range of frequencies. This was a particularly intriguing finding; given that the cells were mainly located in the base of the nerve, one would expect that any functional recovery would be restricted to the higher frequencies of sound. One possible explanation of this finding is that alongside re-establishing neuronal connections, the cells secreted trophic actors that rescued damaged resident spiral ganglion neurons. In a recent study, olfactory epithelium neural stem cells were infused into rats afflicted with noise-induced hearing loss and functional recovery was again illustrated by this research group, and they illustrated that the cells secreted Nerve Growth Factor and Neurtrophin-3, which most likely resulted in the rescue of neurons (Xu et al., 2016).

The prospect of functionally restoring hearing in the pathological cochlea is extremely exciting, however a number of issues need to be addressed prior to this therapy making its way into the clinic. Surgical access to the modiolus is extremely challenging, and achieving this in a manner that is atraumatic to the

cochlea requires immense skill and precision. Furthermore, questions need to be answered about the long-term survival of the cells within the cochlea. One way of doing this would be to conduct a range of long-term studies in various species. However, alongside this, we must try and elucidate how the cells engraft and interact with resident cells within the host auditory system; specifically, the glial cells of the auditory nerve. Given that the focus of this thesis is on understanding how Otic Neural Progenitors interact with glia, and the changes that take place in the glial environment *in vivo* following administration of Ouabain, the glial cells of the mammalian auditory system will now be considered.

1.5 Glial cells of the auditory system, and the glial transitional zone

The principle goal of any stem cell therapy for regeneration of the auditory nerve is to restore a functional neuronal connection between the Organ of Corti and the cochlear nucleus residing in the brainstem. Although Chen et al did illustrate this to some extent (Chen et al., 2012), part of the reason for their partial restoration of auditory function may lie in the incomplete re-establishment of this connection. Thus, by further acquainting ourselves with the glial cells of the auditory system, the changes they undergo in response to pathology and the mechanisms through which differentiated stem cells interact with them may yield further insight into developing a more robust re-connection of the peripheral auditory system with the central pathways.

Historically, glia were thought to be little more than cells that held neural tissue together; indeed the term 'glia' is derived from the Greek word for glue, as a

reflection of this view. Whilst the term continues to be used today, we now know that glial cells are much more complex and sophisticated than previously thought. For example, it is well established that glia play a role in conductance of action potentials through nerve fibres via the process of myelination, and they also play an important role in synaptic uptake of neurotransmitters.

Within the central nervous system two principle glial cell types exists; *Oligodendrocytes* which are the chief myelinating cells of nerve fibres in this part of the nervous system (Li et al., 2016), and *astrocytes*. Astrocytes play numerous roles within the CNS, from formation of the blood brain barrier (Attwell et al., 2010) to the maintenance of synaptic contacts (Clarke and Barres, 2013). The central nervous system also contain *microglia*, although these are macrophage like cells that arise from monocytes (Kim and Cho, 2016).

Within the peripheral nervous system, Schwann cells are the glial cell type that one encounters. Schwann cells are either myelinating or non-myelinating. Myelinating cells, as their name suggests, manufacture and ensheath nerve fibres in the peripheral nervous system with myelin, whilst non-myelinating Schwann cells play a role which is not too dissimilar to that of astrocytes which is that of synaptic regulation and homeostasis (Jessen, 2004).

Glial cells also undergo changes in response to neuronal injury. Within the central nervous system, astrocytes respond to trauma, ischaemia and inflammation by changing into a 'reactive' phenotype, whereby the astrocytes undergo morphological and physiological changes (Sofroniew and Vinters, 2010).

Traditionally it has been thought that reactive astrocytes form scarring in the CNS that presents a harsh regenerative environment, which prevents survival of oligodendrocyte precursor cells and their ability to differentiate into a mature phenotype and remyelinate damaged axons. They also prevent axons from re-establishing connections with one another (Wang et al., 2011). However, in many respects, the reactive changes that astrocytes undergo might be considered to be a double-edged sword, as they do also provide some benefit; in particular, containing areas of neuronal injury and preventing the spread of neurotoxins to surrounding CNS tissue (Fitch and Silver, 1997), and also acting as a trophic source to neighbouring tissue to promote its survival (do Carmo Cunha et al., 2007).

Within the peripheral nervous system the situation is somewhat different; in response to cut or crush injuries to peripheral nerves, Schwann cells behave as mediators that can facilitate neuronal repair. It was previously believed that this was achieved through Schwann cells de-differentiating into a more immature phenotype, re-entering the cell cycle and manufacturing an environment that would facilitate repair through the secretion of cell adhesion molecules and trophic factors (Jessen, 2004). However, it now seems to be the case that rather than de-differentiating into an immature phenotype, Schwann cells transdifferentiate into a 'repair' Schwann cell, which is phenotypically unique from the immature cell type, expressing genetic markers that are not seen in immature Schwann cells (Jessen and Mirsky, 2016).

The peripheral and central nervous systems interface with one another at a transition zone; an area that is often identified by a sudden change in the glial cell type associated with the nerve. Peripherally the neural fibres associate with Schwann cells, and centrally with astrocytes and oligodendrocytes. Thus a distinct and impressive boundary is formed, which is extremely relevant within the context of neural regeneration.

The nature of the transitional zone varies with the typology of the nerve. For example, in some of the earlier studies of the transitional zone it was identified that central glial tissue extended further peripherally in sensory nerves than it did in motor nerves, and the zone was usually dome shaped (Skinner, 1931). Later work confirmed these findings, but also showed that this difference in the transitional zone between sensory and motor nerves was restricted to cranial nerves when they were considered as one group, and in spinal nerves beyond a particular level. In fact there appeared to be a gradient in the length of the central glial extension, which appeared to increase in a rostrocaudal direction (Tarlov, 1937a, Tarlov, 1937b).

Fraher studied the glial transitional zones in the rat in some considerable detail, and found that within the cochlear nerve, the central glial tissue extends quite a considerable distance proximally, extending close to the lateral wall of the modiolus. He also reported that the cochlear nerve is unique, as it does not contain any nerve trunk that is solely made up of peripheral nervous tissue (Fraher, 1992); an observation that has also been noted in the cat (Berthold and Carlstedt, 1977) and the mouse (Hu, 2013). Furthermore, the majority of its length

is composed entirely of tissue arising from the central tissue, with only the facial nerve sharing this feature in the rat (Fraher, 1992).

Thus for otic neural progenitors that are transplanted into the cochlear modiolus, there are two distinct glial environments that they must interact with; the Schwann cells peripherally, and the more numerous astrocytes and oligodendrocytes centrally. This interaction will be of paramount importance in determining the long-term survival of transplanted progenitor cells. Furthermore it is important to understand how glial cells within the cochlea react in response to pathological insults; much of our knowledge of the changes in Schwann cell biology following injury comes from work on somatic peripheral nerves, whilst studies on tissue from the brain and spinal cord have furthered our understanding of the pathological changes that occur in central glia. If we apply the general principles of the changes these cell types undergo in response to pathology in the cochlea, then one would assume that otic neural progenitors would find a favourable environment to engraft in the peripheral portion of the auditory nerve and would readily extend neurites towards the Organ of Corti, but would struggle to cross the transitional zone, where neurites would have to overcome an apparently harsh environment of reactive glial cells in order to connect with the cochlear nucleus. However, given the many unique features the cochlea possesses as a sensory organ, it is quite possible that cochlear glial cells behave in a different manner to what is observed in other systems.

1.6 Aims and objectives

It is therefore evident that amidst the numerous strategies that have been employed to restore normal cochlear function in the pathological inner ear, stem cell transplantation has witnessed some of the most encouraging successes, and the application of otic neural progenitors alongside cochlear implants and in auditory neuropathy is an intriguing prospect. However, prior to translation of this therapy into the clinical a number of questions remain to be answered, in particular the long-term effects that transplanted cells may have on the host cochlea. An aspect of this is understanding how transplanted cells interact with the host glial cells of the auditory system, which will be a fundamental factor for cell therapies to provide benefit to patients for the duration of their lifetime. Moreover, it will be important to ascertain the effect that pathological glial cells might have on the ability of otic neural progenitors to differentiate and extend neurites.

In light of this, there are a number of broad aims that this project will attempt to fulfil:

- 1) Ascertain whether otic neural progenitors produce their own glial cells as they undergo differentiation *in vitro*. If otic neural progenitors do not produce their own glia during differentiation, this will imply that they are likely to be wholly reliant on the glial cells in the host environment.
- 2) Assess the interaction between otic neural progenitors with glial cell types of the central and peripheral nervous system *in vitro*. Not only will this allow for interaction to be quantified, but developing these techniques will yield

useful assays through which the interaction between the cell types might be modulated

- 3) Describe the changes that occur in the peripheral glia and in the transitional zone following Ouabain injury *in vivo*. Given that much of the experience of the laboratory where this work will be undertaken is with the gerbil species, this work will examine the changes that take place in the auditory glial cells of the mouse, and compare these with the gerbil model.
- 4) Develop surgical techniques to access the modiolus of the mouse for transplantation of otic neural progenitors. Surgery on the mouse is complex, however developing these techniques would open up potential access to a plethora of mouse models of human disease, which will be vital in the translational pathway of stem cell therapies for deafness from the bench to the bedside.

CHAPTER 2: METHODS

2.1 Routine In-Vitro Stem Cell Culture Methods

2.1.1 Derivation of Mouse Embryonic Feeders – Dissection and Initial Culture

Stem cells were cultured and maintained on mouse embryonic feeders. Pregnant females (E13.5) of the MF-1 or CD-1 mouse strain were cervically dislocated under Schedule one. A laparotomy incision was subsequently performed on the fresh cadaver, and the uterine horns were identified and dissected out of the lower abdominal cavity into a petri-dish. The embryonic sac was then identified, and embryos were removed. Embryos were then decapitated and their internal organs removed. The remaining carcasses were then washed thrice in Calcium/Magnesium free PBS (GIBCO) and were then subsequently minced with scalpel blades.

The minced tissue was then placed into a 15ml tube and was dissociated enzymatically with 2ml 0.25% trypsin:EDTA for 30 mins at 37 degrees celcius, and the enzymatic reaction stopped by then adding DMEM+20%FBS (GIBCO). The resulting suspension was then repetitively aspirated vigorously to further break up the tissue. Large fragments of tissue were allowed to settle, and the overlying supernatant was then transferred to a T75 flask (NUNC) and a further 15ml of DMEM+20%FBS was added to this. Flasks were then kept overnight at 37 degrees celcius in 10% CO₂. The following day, the overlying medium with cellular debris was removed and replaced with fresh medium and cultures were

allowed to bulk up to confluency. Once confluency was achieved, stocks of cells were cryopreserved in liquid nitrogen for later use.

2.1.2 Derivation of Mouse Embryonic Feeders – Inactivation

Cells derived from primary culture were passaged and bulked up; typically, cells can be split 1:3. Cells generally weren't used past passage 4-5, as they usually senesce past this point.

To use cells as feeders for human embryonic stem cell culture, the cells were inactivated with Mitomycin C (Sigma) that was prepared at a concentration of 10µg/ml in DMEM+20%FCS, which was then passed through a 0.2µM sterile filter (Millipore). The existing medium from the cells was then removed, and replaced with the medium supplemented with mitomycin, and incubated for 2 hours at 37 degrees Celcius in 10% CO₂.

The cells were then washed thrice with sterile PBS, and then lifted with Trypsin:EDTA at 37 degrees Celcius for a period of 5 minutes (4ml per T75 flask). The enzymatic reaction was stopped by adding 9ml DMEM+10%FBS, and the cell solution was transferred into 50ml tubes for centrifugation at 200g for 5 minutes.

Following this, cells were resuspended in DMEM+10%FBS and counted with an automated cell counter (BIORAD). Given that we typically culture human embryonic stem cells in T12.5 flasks, feeders were seeded at 300,000 cells per

flask pre-coated with Embryomax 0.1% Gelatin solution (MILLIPORE) 2 hours prior to use, or frozen down at 3,000,000 cells per cryovial at this point for later use (each vial being suitable for 10 flasks).

Mouse embryonic feeders were used 24 hours after seeding, and were kept at 37 degrees Celsius in 10% CO₂. Cells were used within a week.

2.1.3 Culture and Maintenance of Human Embryonic Stem Cells.

The cell lines used in this work were the *Shf-1*, *Shf-3.2* and *H14 NOP-SOX2* reporter line. The following section describes the general method used in the maintenance of these cells.

Cells were cultured in T12.5 flasks containing inactivated mouse embryonic feeders prepared as described above. The constituents of the Human Embryonic Stem Cell (hES) medium were as follows:

- 80% Knockout DMEM (GIBCO)
- 20% Knockout Serum (GIBCO)
- 1% Non-essential Amino Acid Solution (Stock Conc. 100X MEM non-essential amino acid solution, GIBCO)
- 1mM L-glutamine (0.146g in 10ml PBS, GIBCO)
- 0.1mM β -mercaptoethanol (Stock Conc. 14.3M, Sigma)
- 4ng/ml human bFGF (Stock Conc. 2 μ g/ml in PBS (w/o calcium and magnesium) with 0.1% BSA, GIBCO)

The medium was prepared to these final concentrations and then sterile filtered through a 0.2µm cellulose acetate filtering unit, ready for use. Cells were monitored and fed 2ml of medium on a daily basis. Cells were generally left alone, but if any areas of excessive differentiation emerged, these were scrapped off with a 1ml fine tip Pasteur pipette under microscopic guidance.

Once cells reached confluency, the culture medium bathing the cells was replaced with 1ml of 1mg/ml collagenase type IV solution (GIBCO), and cells were placed at 37 degrees Celsius. Cells were monitored every minute, checking for the point at which the edges of the colonies started to roll and lift away (usually between 6 to 12 minutes after application of collagenase). The collagenase was then discarded, and replaced with fresh hES medium. Under microscopic guidance, colonies treated with collagenase could now be easily isolated and removed from the culture system and into the overlying medium. The medium containing the colonies was then removed, and placed into a fresh T12.5 flask containing feeders.

2.2 In Vitro Stem Cell Differentiation Methods

The Rivolta lab employs a 2-stage differentiation process to generate otic progenitors from human embryonic stem cells. In the first step, human embryonic stem cells are differentiated to produce otic neural progenitors and otic epithelial progenitors. These can then be isolated manually to yield a predominant culture of the cell type of interest. Given the focus of this project, otic neural progenitors were the only cell type that were manually purified. In the second phase, otic neural progenitors were further differentiated to form spiral ganglion-like cells. The methods underpinning these differentiation phases will now be described in further detail.

2.2.1 Generation of Otic Neural Progenitors from Human Embryonic Stem Cells.

The day preceding differentiation, T12.5 flasks were coated with mouse Laminin-I (CULTREX). Laminin was used at a concentration of 2.5 μ g/cm², thus for each T12.5 flask used, 125 μ g of laminin was dissolved in ice-cold sterile PBS. Coated flasks were then placed at 37 degrees Celsius overnight, to allow for polymerization.

Prior to differentiation, stem cell colonies were again assessed for areas of excessive differentiation, which were removed using a fine Pasteur pipette under microscopic guidance. Following this, cells were then washed twice with sterile Hank's Balanced Salt Solution, and 0.025% Trypsin:EDTA was applied to the cells for 5 minutes (or until cells had fully lifted) at 37 degrees Celsius. Cells were

then transferred into a 15ml tube, and 0.5mg/ml of Soybean Trypsin Inhibitor solution (GIBCO) was then added to halt the trypsinisation process. This was then centrifuged at 1000rpm for five minutes, and the supernatant discarded. Cells were then resuspended in 1ml of 'base' medium (DFNB) for differentiation experiments, and three 10 μ l samples were placed into the automated cell counter and averaged, to give an estimation of cell number. For the purposes of generating otic neural progenitors, cells were seeded into the laminin coated flasks at a density of 4,000 cells per cm², and cultured in 'phase 1 medium'.

The DFNB 'base' medium was prepared as follows:

- 500ml DMEM (GIBCO)
- 500ml F12 (GIBCO)
- 5ml N2 (100X GIBCO)
- 10ml B27 (50X GIBCO)

Phase 1 medium was prepared as follows:

- DFNB (as above)
- FGF 3 (50ng/ml, R&D systems)
- FGF10 (50ng/ml, R&D systems)

Cells were inspected every 2 days and phase 1 medium was refreshed at the same time. Otic neural progenitors start to emerge between day 3-4, and are morphologically distinct from the other population of cells produced, otic epithelial progenitors. Otic neural progenitors were manually isolated on the basis of morphology, as cells not possessing the characteristic morphology of otic neural

progenitors were scraped away with a fine Pasteur pipette under microscopic guidance, leaving the otic neural progenitors behind. The total duration of phase 1 differentiation was 12 days, at which point large colonies of otic neural progenitors were apparent, with few contaminating cells in the culture system.

2.2.2 Maintenance of Otic Neural Progenitor Cultures

At the end of phase 1, otic neural progenitor colonies were bulked up by placing them in Otic Stem Cell Full Medium (OSCFM), which constitutes as follows:

- DFNB (as described above)
- bFGF (20ng/ml R&D systems)
- IGF (50ng/ml R&D systems)
- EGF (20ng/ml R&D systems)

Once colonies had become confluent, cultures of otic neural progenitors were passaged by trypsinising with 0.00625% Trypsin:EDTA. The purpose for such a gentle trypsinisation stem was to negate the neutralising effect of a harsh trypsin treatment. The trypsinisation step lasted a maximum of 5 minutes at 37 degrees Celsius, and the reaction was terminated by adding 0.5mg/ml Soybean Trypsin Inhibitor solution. Cells were then spun at 1000rpm for 5 minutes, and then resuspended in fresh OSCFM. Cells were then seeded into T12.5 flasks, precoated with Embryomax 0.1% Gelatin solution (2 hours prior to passaging). Cells were continually passaged in this state, or frozen down for later use.

2.2.3 Neuralisation of Otic Neural Progenitors

For neuralisation of ONPs, culture vessels were pre-coated with Embryomax 0.1% Gelatin solution 2 hours prior to differentiation. Cells were washed with Hanks Balanced Salt Solution, and then 1ml of 1X Trypsin (stock 10X, SIGMA) was applied to the cells. Cells were monitored at room temperature, as cells detached extremely quickly. The trypsinisation process was terminated by adding 1ml of Soybean Trypsin Inhibitor, and the solution transferred to a 15ml tube. A further 1.5ml of DMEM was used to rinse the flask, which was then also added to the tube. Cells were then centrifuged at 1000rpm for 5 minutes and resuspended in 1ml of DFNB for counting using the automated cell counter as previously described. Cells were then seeded into culture vessels at 4000 cells/cm², in 'phase 2 neuralising medium', consisting of the following recipes at the stipulated time points:

Day 1-3

- DFNB
- bFGF (20ng/ml)
- Shh-C24II (500ng/ml, R&D systems)

Day 4-5

- DFNB
- bFGF (20ng/ml)
- Shh-C24II (500ng/ml)
- BDNF (10ng/ml, R&D systems)
- NT-3 (10ng/ml, R&D systems)

Day 6 onwards

- DFNB
- bFGF (20ng/ml)
- BDNF (10ng/ml)
- NT-3 (10ng/ml)

Cells were fed and monitored every alternate day, and were either fixed 12 days' post plating for immunocytochemistry, or RNA extraction.

2.2.4 Glial Differentiation of Otic Neural Progenitors

Attempts were also made to differentiate otic neural progenitors to produce glial-like cells. This protocol was adapted from that of Lee et al (Lee et al., 2007), who generated neural crest stem cells from human embryonic stem cells, and differentiated these to form glial-like cells.

Experiments for glial differentiation were conducted on two types of substrate. The first was Embryomax 0.1% gelatin, which was used to coat 24-well plates 2 hours prior to differentiation as previously described. The second was Polyornithine/Laminin. In this scenario, culture vessels were precoated with Polyornithine at a concentration of 15µg/ml (Sigma) for half an hour at 37 degrees. This was then removed and mouse laminin-1 (CULTREX) was applied at a concentration of 1µg/ml overnight at 37 degrees celcius.

Otic neural progenitors were rinsed with Hank's Balanced Salt Solution, and then trypsinised with 0.00625% trypsin:EDTA for a maximum of 5 minutes at 37 degrees Celsius. Once lifted, the trypsinisation process was terminated by adding 0.5mg/ml Soybean Trypsin Inhibitor. Cells were then centrifuged at 1000rpm for 5 minutes, and then resuspended in 1ml of DFNB for counting. Cells were then seeded onto the precoated culture vessels at a density of 4000 cells/cm², in glial differentiation medium, which consisted of the following:

- DFNB
- CTNF (10ng/ml, R&D systems)
- Neuregulin (20ng/ml, R&D systems)
- bFGF (10ng/ml, R&D systems)
- dibutyryl cyclic-AMP (1mM, TOCRIS)

Cells were monitored and underwent medium replenishment every 2 days, and differentiation was terminated at day 12 post-plating, at which point cells were fixed for immunocytochemistry.

2.3 Primary Cell Culture Methods

2.3.1 Dissection and Preparation of Schwann Cell Cultures from Gerbil Cochlea.

Dissection methods were adapted for the gerbil from those described previously in Prof Robert Shepherd's laboratory describing the dissection from rat pups (Richardson et al., 2009).

On the day prior to setting up cultures, 24 well plates were pre-coated with poly-ornithine at 0.5mg/ml (SIGMA) and incubated at 4 degrees Celsius overnight. On the day of harvesting primary tissue, this was removed and then washed with sterile PBS and mouse laminin-1 was applied (CULTREX) at 0.01mg/ml and incubated at 37 degrees Celsius for 2 hours.

A litter of P5 gerbil pups was obtained. This appears to be the best time to use gerbil pups, as the bone of the cochlea is of a favorable consistency to remove and expose the endocochlear structures. Before the point, the bone is extremely soft whilst afterward the bone begins to calcify, and in both situations dissections can become quite traumatic to the structures of interest.

Pups were euthanized and decapitated under Schedule 1 procedures, and the heads of the pups were taken away for further dissection.

All dissection was conducted outside a designated laminar flow hood, however despite this no trouble was experienced with infection. Seventy per-cent ethanol was applied to the pup heads, and a longitudinal incision was made in the midline of the head with a size 11 scalpel blade, to the level of the underlying bony cranium. The skin was then removed away from the bone. A horizontal incision was then made behind the orbital sockets, and all the structures anterior to this were discarded.

With a pair of Vanna's scissors, the head was carefully divided into half, and the brain tissue from each half was scooped out. Each half will now contain the temporal bones, and they were placed in ice-cold DMEM until all the pup heads had been processed in this manner.

Halves containing the temporal bones were then placed into a petri dish one at a time containing fresh DMEM. The temporal bone can be easily identified as a 'figure of 8' structure in the centre, which can be carefully isolated using fine

forceps. The bony capsule of the cochlea is removed away from the labyrinth, and the bone is then peeled away carefully to reveal the cochlea.

The spiral ribbon-like stria vascularis and Organ of Corti should be apparent, and these can be removed by unwinding them away, leaving behind the modiolus, containing spiral ganglia. This is then placed into a petri dish containing DMEM on ice. The process is completed until all temporal bones needed have been processed (1 modiolus for 2 wells of a 24 well plate).

An enzymatic dissociation solution containing 0.1% Collagenase IV and 0.1% Trypsin was prepared, and all the modioli were placed into this and incubated at 37 degrees Celsius for 30 mins. FBS was added to terminate this step. The cells were then mechanically triturated, and then solution centrifuged at 1000rpm for 5 mins.

The supernatant was discarded, and cells were resuspended in 'Schwann Cell Medium' which was prepared as follows:

- MEM D-Valine (BIOSERA)
- 1% N2 (50X stock)
- 1% Penicillin/Streptomycin (50X stock, GIBCO)
- 10% FBS

The purpose for using MEM D-Valine is on the basis of Schwann cell culture protocols described by the Haycock laboratory (Kaewkhaw et al., 2012), as this

medium suppresses the proliferation of fibroblasts. The absence of neurotrophins in the media also suppresses the proliferation of neurons.

Cells were cultured and maintained in this manner, and co-culture experiments with otic neural progenitors were undertaken at day 4-5 post plating.

2.3.2 Co-culture of Spiral Ganglion Schwann Cells with Otic Neural Progenitors

Co-cultures were performed either with otic neural progenitors derived from the Shef-1 cell line, or the H14 NOP-SOX2 reporter line. A T12.5 flask of cells of otic neural progenitors was prepared as previously described, and maintained in OSCFM. On the day of setting up the experiment, Otic neural progenitors were trypsinised and handled, using exactly the same procedures as described in section 2.2.3.

The medium was removed from the 24-well plate containing Schwann Cells, and otic neural progenitors in Day 1-3 neuralising medium were added to the Schwann Cells. For controls, Otic neural progenitors were grown alone on the laminin/polyornithine substrate. Also, given that the entire co-culture system was in neuralising medium, the effects of this change in medium were also assessed and controlled for, by culturing Schwann cells also either in Schwann cell medium, or Day 1-3 neuralising medium. Cells were fixed at day 3 post plating for immunocytochemistry.

2.3.3 Dissection and Preparation of Gerbil Cortical Astrocyte Cultures

Dissection protocols and maintenance of cortical astrocyte cultures were adapted for the gerbil from those described by Schildge et al (Schildge et al., 2013). Stocks of astrocyte cultures were established from pups ranging from E28 (just prior to pregnant female littering) to a maximum age of P7.

Pups were decapitated under Schedule 1 procedures. A midline incision was made with a size 11 scalpel blade and the skin peeled away to reveal the cranium. With Vanna's scissors, the cranium was carefully cut in the midline. Then on each side, a small horizontal cut was made into the bone, one behind the eyes and another in the region of the cerebellum. These cuts should result in the formation of bony flaps on either side that were rotated outwards to expose the brain, which was then scooped out carefully. Brains from the pups were placed in dishes containing sterile ice cold HBSS.

Brains were processed one at a time, in a dish containing fresh HBSS under a stereomicroscope. First, the olfactory bulbs and the cerebellum were discarded. To isolate the cortices, fine forceps were used to incise in the midline. The cortices have a plate like structure, which can then be gently teased away from the rest of the brain, which should be discarded.

The cortices are covered with meninges, apparent by the meningeal blood vessels running within them. By switching to high magnification, the cling-film like meninges were carefully peeled away, to avoid contamination from meningeal

fibroblasts in our cultures. The cortices were then transferred into another dish containing ice-cold HBSS.

The cortices were then cut into small pieces and placed into a 50ml tube, with 25ml of 0.25% trypsin in HBSS for enzymatic dissociation at 37 degrees celcius. Tissue was agitated by manually shaking every 5 minutes to aid this process. The tube was then centrifuged for 5 minutes at 1000rpm. Then, the supernatant was decanted, and astrocyte medium was then added to the tube, and the tissue fragments vigorously pipetted to break it up further mechanically. The suspension was then transferred into a T75 flask, which had been precoated with 50µg/ml of Poly-L-lysine for 1 hour at 37 degrees Celsius. Astrocyte medium consists of the following:

- DMEM
- 10%FBS
- 1% Penicillin/Streptomycin

Medium was changed every 2 to 3 days. Cells became fully confluent after 7 to 8 days, which would contain a mixed culture of astrocytes, microglia and oligodendrocyte precursor cells. Cells were initially placed on an orbital shaker at 180rpm for half an hour to remove microglia. The medium was replaced, and the flask put back on the orbital shaker at 300rpm for a further 6 hours to remove the oligodendrocyte precursor cells. The remaining lawn of astrocytes was then rinsed with HBSS, and 0.05% Trypsin:EDTA was added to detach cells at 37 degrees Celcius for 5 minutes. An equal volume of culture medium was then

added to terminate the reaction, and the solution centrifuged at 1000rpm for 5 minutes. Cells were then split equally between 2 T75 flasks, which were not pre-coated, as astrocytes grow well on plastic. Medium was changed again every 2 to 3 days. Once cells reached confluence, they were ready to use for co-culture experiments, and they could also be continually passaged, bulked up and frozen down for later use.

2.3.4 Co-culture of Cortical Astrocytes with Otic Neural Progenitors.

Co-culture experiments were undertaken on uncoated 6-well plates. Confluent astrocytes were initially handled in exactly the same way as for routine passaging from a T75 flask, as described in section 2.3.3. Following centrifugation, cells were re-suspended in 1ml of astrocyte medium and counted using the automated cell counter. Cells were plated at 10,000 cells/cm² and allowed to settle for 48 hours.

Otic Neural Progenitors derived from Shef-1, Shef-3.2 and H14 NOP-SOX2 were used for co-culture experiments. Otic neural progenitors were passaged and maintained in OSCFM. On the day of setting up the co-culture, Otic neural progenitors were trypsinised and handled, using exactly the same procedures as described in section 2.2.3. After being centrifuged, cells were resuspended in 1ml DFNB and counted using the automated cell counter. Cells were seeded onto the plates containing astrocytes, and were fed neuralising medium as previously described. To control for the effect of changing medium, some astrocytes were grown alone either in astrocyte medium or neuralising medium. ONPs in co-

culture were compared to those grown alone on a gelatin substrate. Cultures were continued for 6 days, at which point cells were fixed for immunocytochemistry.

2.3.4 Examining the effect of Neuralising Medium on Astrocytes immediately after passaging

To examine the effect of neuralising medium on astrocytes further, some astrocytes were put into neuralising medium immediately after passaging. Astrocytes were passaged and seeded onto 6 well plates as described above. They were seeded into the wells at 10,000 cells/cm² in neuralising conditions. Some astrocytes were grown in astrocyte medium, to allow for comparison. Cells were fixed 6 days' post plating for immunocytochemistry.

2.4 In Vivo Experimentation

All animal procedures had been reviewed successfully by the University of Sheffield Ethical Review Committee and were carried out under a Home Office Project License.

To ascertain the changes that occur in peripheral and central glia *in vivo*, we used the gerbil (*Meriones Unguiculatus*) and the mouse (*Mus Musculus*). The purpose for using two species was to compare the reaction of glia in response to a

pharmacologically induced neuronal lesion between the two. For the mouse in particular, it presented an opportunity to develop the surgical techniques for accessing the murine cochlea, and to optimize the Ouabian deafness protocol the Rivolta lab have previously used in the gerbil for the mouse. Moreover, establishing surgical methods lead to the further step of transplanting cells into the murine cochlea through a modiolusostomy, which is yet to be described in the current literature. All the in vivo techniques will be described here except for the techniques involving murine surgery, which will be discussed in detail in Chapter 5.

2.4.1 Measurement of Evoked Auditory Brainstem Response

A designated room was used for conducting auditory brainstem responses in mice and gerbils. Both species underwent baseline testing prior to any surgical procedures, and then were tested again one-week post-surgery before being sacrificed under schedule 1 procedures (overdose with Pentobarbital followed by cervical dislocation). Gerbils were typically tested immediately before surgery, however mice were tested 4-5 days before surgery, to reduce the anaesthetic load they experienced.

Animals were anaesthetized with injectable anaesthetic agents. For the gerbil, a cocktail of ketamine (Ketaset, 100mg/ml) and xylazine (Rompun 20mg/ml) was used. The cocktail was made up 100µl at a time in the following proportions:

- Ketamine at a volume of 60µl
- Xylazine at a volume of 40µl

Gerbils were then administered 1µl/g of bodyweight via intraperitoneal injection, and a top-up of 0.5µl/g of bodyweight was given if necessary.

For mice, a cocktail of ketamine (Ketaset 100mg/ml) and medetomidine (Domitor 1mg/ml) was used. The cocktail recipe was derived from the one used in Karen Steel's laboratory (Ingham et al., 2011):

- 100µl Ketamine
- 100µl Medetomidine
- 800µl NaCl

This was then given at a volume of 100µl for every 10g of bodyweight, via intraperitoneal injection, and should provide stable anaesthesia for the entire duration of the ABR procedure. With mice, a reversal anaesthetic agent was used to aid recovery. Atipamezole (Antisedan 5mg/ml) was given at a volume of 1µl/g of bodyweight.

ABR recordings were undertaken using the System 3 digital signal processing hardware and software (TUCKER DAVIS TECHNOLOGIES (TDT)). A closed-field set-up was used for measuring ABRs, allowing for accurate testing of hearing from each individual ear. A sound stimulus was presented to the animal using 2 real-time processors (RP2.1) which was then attenuated by a

programmable attenuator (PA-5) to control sound levels, which was then delivered to the ear via a closed-field magnetic speaker (CF-1). A thin 10cm plastic pipe was connected to the speaker, which was positioned to the external auditory canal of the animal. Forceps can be used to manipulate the cartilaginous external auditory meatus to aid positioning of the tube.

To collect recordings, 27 gauge subdermal electrodes were used (ROCHESTER ELECTRO-MEDICAL). The negative electrode was placed at the vertex of the head, and the recording channel 1 electrode on the jaw. The earth electrode was placed in a paramidline position at the posterior end of the animal. The electrodes were connected to an impedance headstage (RA4LI) and a medusa preamplifier (RA4PA), prior to being processed at a medusa base station signal processor (RA16). Clicks were presented at a rate of 20/second, from 110dB SPL to 0dB SPL. For finer resolution, tone frequency thresholds were also measured, with 50ms tone pips presented at a range of frequencies from 4kHz, 8kHz, 16kHz and 32kHz. For clicks, average response was calculated from 500 click presentations, and 300 presentations for tone thresholds. The amplitude between the wave II positive peak and wave III negative peak was then measured, and thresholds were determined by comparing this value at each sound level with the average background noise level.

2.4.2 Gerbil Ouabain Surgical Technique.

All surgical instruments were autoclaved prior to the surgical procedure. A 5 mM solution of Ouabain (SIGMA) was pre-prepared and aliquoted in 5 μ l aliquots and stored at 4 degrees Celsius for up to 3 weeks.

Gerbils aged between 3-6 months were brought into the operating suite in a heavily sedated state following the baseline ABR procedure, and were placed onto an anaesthetic circuit. Anaesthesia was maintained with Isoflourane (Isoflo, ABBOTT) administered via a vapouriser (BARRATT). The left post aural region was shaved, and cleaned meticulously with Betadine. The skin behind the ear was injected subdermally with 0.25% Bupivacaine (Marcaine, ASTRA-ZENICA). A post-auricular incision was made using a size 11 scalpel blade. It is important to make a good-sized incision for satisfactory exposure of the underlying structures.

The subcutaneous fat and the post-auricular musculature was separated gently using fine forceps. This seems to be the most satisfactory method for this step, as it minimizes any bleeding and results in minimal trauma to the underlying tissue, which will aid in post-operative healing and minimize post-operative pain experienced by the animal. The bulla of the gerbil should then come into view.

The bulla is composed of a thin sheet of bone, which is divided into three distinct regions by bony septations. A bullostomy was performed by using a scalpel to chip away the bone of the middle region. It is extremely important that all three

regions have been identified prior to performing this step. By performing a bullostomy in this region, the stapedial artery should come into view, which can then be followed to the opening of the round window. At this juncture, the operating table is tilted in order to get a good view of the round window niche.

The Ouabain was prepared for delivery, and 5µl of 5mM Ouabain was drawn up into a nanofil syringe (WPI). Accuracy is extremely important, as Ouabain is toxic and can cause unnecessary damage to surrounding structures if misapplied. For precise delivery, Ouabain was administered one drop at a time; by exposing the drop and balancing it on the needle, and then placing the drop onto the round window. Replacing the Ouabain with fresh amount every 10 minutes appears to be unnecessary, and a satisfactory level of deafness was achieved with one application of Ouabain, left on for 45 minutes.

Once this time period had elapsed, the Ouabain was wicked off the round window with cotton wool, and a ball of subcutaneous fat was cut away and applied to the bullostomy site, which was secured through the application of Vetbond (3M). The wound was then closed in 2 layers with 4-0 Vicryl on a cutting needle (ETHILON).

Gerbils were then taken off the anaesthetic circuit, and allowed to recover in a warm recovery box to prevent post-operative hypothermia. Once awake, animals were given a dose of Meloxicam (Metacam, BOEHRINGER INGLEHEIM) for further analgesia, and animals were monitored for three days, in particular checking for symptoms of vestibular dysfunction including head tilt, circling and

turning. Gerbils were sacrificed 1-week post-surgery, and their cochleae were harvested and fixed for further analysis.

2.4.3 Dissection of Temporal Bones for Fixation.

At the end of procedure, animals were sacrificed using Schedule 1 methods (overdose with Pentobarbital followed by cervical dislocation) and decapitated following this. The skin was dissected off the skull, and with coarse forceps and scissors the Axis and Atlas vertebrae were removed. At the posterior end of the skull, two vertical paramidline cuts were made into the bony cranium, and the resulting shard of bone was then removed, to expose the brain which was scooped out. With the brain out of the way, the inferior portion of the skull could now be cut confidently without damaging the temporal bone. A horizontal cut was made behind the eyes, to divide the skull into halves, containing the temporal bones. Each half was placed into 4% paraformaldehyde for 24 hours to fixate the bones.

2.4.4 Processing of Temporal Bones for Cryosectioning.

After fixation, cochleae were decalcified in 0.5M EDTA. Cochleae were assessed until they were soft (typically 3-4 days), and excess bone was then trimmed away. Temporal bones were then placed into a sucrose solution gradient (Sucrose from SIGMA) starting at 7.5%, followed by 15% and finally at 30%, remaining at least a day in each concentration. Cochleae were then placed into embedding

compound (cryo-m-bed, BRIGHT) and kept at 4 degrees Celsius until ready for cryoembedding.

For embedding, cochleae were placed into 22mm X 22mm peel-a-way truncated molds (TAAB) and embedding compound was poured into them. Under microscopic guidance, cochleae were positioned longitudinally, which would produce mid-modiolar sections of the cochlea. The molds were then dipped into a box containing dry ice bathed in isopentane, until the embedding compound froze in entirety. Molds were then double wrapped in foil, and stored at -80 degrees Celsius until required for cryosectioning.

2.4.5 Preparation of Glass Slides for Cryosectioning

For preparation of slides to collect tissue sections, 76X26mm glass slides (ACADEMY SCIENCE) were placed into staining racks and washed thoroughly under running water with washing up detergent. A gelatin solution was then prepared by dissolving 2 grams of gelatin (FLUKA) in 400ml of distilled water, which was then placed into a microwave on full power for 3 minutes. The solution was stirred well, and to it 0.2 grams of chromium(iii) potassium sulphate dodecahydrate (SIGMA) was added. The slides were then fully immersed into this solution for 30 seconds, and then placed into an oven at 40 degrees Celsius overnight to bake. Slides were stored at 4 degrees Celsius until ready for use.

2.4.6 Cryosectioning of Tissue

Molds were separated open and tissue blocks were mounted onto a metal chuck using embedding compound and placed onto the quick-freeze area of the cryostat (BRIGHT OTF series). This was then placed on the microtome, and sequential sections were collected onto the prepared glass slides at a thickness of 12µm, using a stainless steel disposable microtome blade (PFM MEDICAL). Sections were stored at -20 degrees Celsius, until required for immunolabelling.

2.5 Immunocytochemistry

2.5.1 Immunocytochemistry

At given time points within an experiment, immunolabelling was used to determine protein expression within cells. Cells were initially washed with PBS, and then fixed with 4% paraformaldehyde for 15 minutes. Then, the paraformaldehyde was washed off by three washes with 0.1% TritonX-100 (PBST) in PBS, each wash lasting 5 minutes, which also permeabilised the cell membranes. To limit non-specific binding of antibodies, binding sites were blocked with a 5% donkey serum (SIGMA) solution in PBST for an hour, after which cells again underwent three washes with PBST. Primary antibodies were then applied to the cells, diluted to their working concentrations in the 5% donkey serum solution. The cells were then either incubated overnight at 4 degrees Celsius, or incubated at room temperature for two hours.

Cells were then washed thrice with PBST, and secondary antibodies diluted 5% donkey serum were applied to the cells for an hour at room temperature and kept in the dark. Working in dim lighting for here on, cells were again washed thrice with PBST, following which DAPI was applied to the cells to mark out cell nuclei. Cells were then stored with a good volume of PBS overlying them, and culture vessels were wrapped in foil and stored at 4 degrees Celsius for image processing.

2.5.2 Immunohistochemistry

Tissue for immunohistochemistry was prepared as described in sections 2.4.3-2.4.6. Slides were then placed on trays and dried at room temperature for 45 minutes. A wax pen (VECTOR LABS) was then used to draw around sections, to prevent antibody cocktails mixing with one another from adjacent sections.

A short re-fixing step with 4% paraformaldehyde was firstly undertaken for 2 minutes, and this along with the drying step helped to prevent sections being lifted off the slides during the numerous washing steps. Sections were then washed thrice with PBST with a 5-minute duration per wash, and the 5% donkey serum was applied to block non-specific antibody binding sites. After a further 3 washes with PBST, primary antibody cocktails diluted in 5% donkey serum were applied to the sections, and baked either at room temperature for 2 hours, or overnight at 4 degrees Celsius. Three washes with PBST ensued, after which secondary

antibodies diluted in 5% donkey serum were applied to sections, which were kept for an hour at room temperature in the dark.

Secondary antibodies were washed off with three PBST washes and then DAPI was applied to mark out nuclei. This was washed off with PBS and mounting medium was applied sparingly to the sections (Vectashield, VECTOR LABS). Glass coverslips were then placed on the slides, and they were sealed with nail varnish. Slides were stored wrapped in foil at 4 degrees Celsius for image processing.

Antibody	Manufacturer Product Code	Host Species	Working Conc.
BETA-3-TUBULIN (TUJ1)	Biolegend 801202	Mouse	1:100
MYO 7A	Gift From Christine Petit	Rabbit Polyclonal	1:100
NEUROFILAMENT-200	Sigma N4142	Rabbit Polyclonal	1:100
MYELIN PROTEIN ZERO (P0)	Millipore ABN363	Rabbit Polyclonal	1:100
SOX10	Santa Cruz Sc-17342	Goat Polyclonal	1:75
S100	Sigma S2657	Mouse Monoclonal	1:200
S100	Sigma S2644	Mouse Monoclonal	1:200
GFAP	Abcam ab7260	Rabbit Polyclonal	1:500
HUMAN MITOCHONDRIAL ANTIBODY	Novus NBP2-3920	Mouse	1:100
ANTI-GFP	Torrey Pines Biolabs, TP401	Rabbit Polyclonal	1:120
PAX2	Abcam 38738	Rabbit Polyclonal	1:100
SOX2	Millipore Ab5603	Rabbit Polyclonal	1:100

Antibody	Manufacturer Product Code	Host Species	Working Conc.
Alexa 568 anti-goat	Life Technologies A11057	Donkey Polyclonal	1:250
Alexa 488 anti-goat	Life Technologies A11055	Donkey Polyclonal	1:250
Alexa 568 anti-mouse	Life Technologies A10037	Donkey Polyclonal	1:250
Alexa 488 anti-mouse	Life Technologies A10042	Donkey Polyclonal	1:250
Alexa 568 anti-rabbit	Life Technologies A10042	Donkey Polyclonal	1:250
Alexa 488 anti-rabbit	Life Technologies A21206	Donkey Polyclonal	1:250

Table 2.1. Table of antibodies used for immunochemistry

2.5.3 Image Analysis

Images were taken on the EVOS FL Cell Imaging System (LIFE TECHNOLOGIES). Cells were counted manually, and were done so whilst sitting at the microscope from 5-10 randomly selected fields. Cells were compared against cells that had only been stained with the secondary antibodies, and a cell was deemed to be positive if staining was brighter than that observed in the control.

For neurite analysis in co-culture experiments, cells were photographed on the EVOS microscope, and images were analysed using Image J software. A neurite was identified with co-staining of human mitochondrial antibody with Neurofilament-200. The total number of such neurites were then measured using the software from 8-10 randomly selected fields, and the neurite lengths were compared to the lengths of neurites when ONPs were cultured alone.

Neurite orientation was also assessed as shown in the figure below. A straight vertical line was drawn, and the angle of deviation of the neurite from this line was assessed. The angle of deviation from the vertical was also measured of the adjacent S100 positive cells, and the difference between the two angles was then calculated. This was done for all the neurites in 5 random fields.

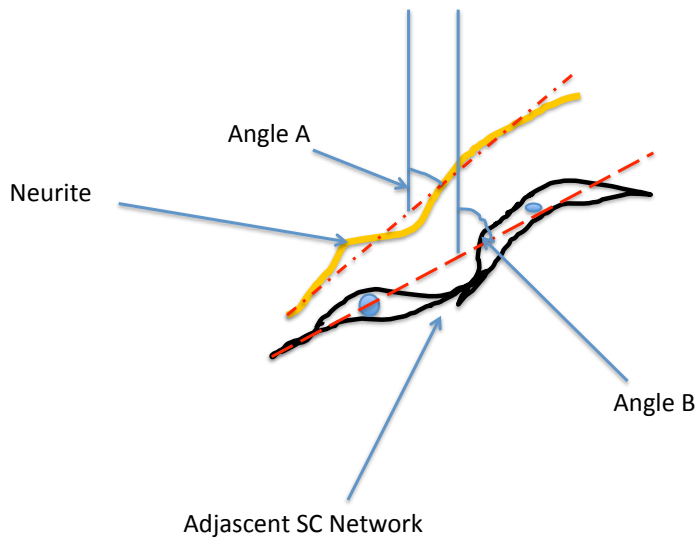


Fig 2.1. Cartoon showing method of measuring neurite angle

Fluorescence intensity of GFAP expression in astrocytes was measured by scanning 6-well plates in the In Cell Analyser 1000 Platform (GE HEALTHCARE). Images were processed using the accompanying Developer Toolbox software, and through using tools such as segmentation and sieving, a mask for the cells was created, allowing the software was able to recognize the astrocyte cells with accuracy, and calculate the fluorescence intensity of the GFAP signal within them.

For counting of cells in cochlear sections, pictures of sections were taken either with the EVOS microscope or the Olympus BX60 Microscope with the Retiga R series camera (Q IMAGING) attached to it, and viewed on the accompanying Ocular software (Q IMAGING). Pictures were then analysed using Image J software, and cells within the apical, mid and basal turns were counted from 5 mid-modiolar sections, which were at least 36µm apart from one another to prevent cells being counted twice. The area of the Rosenthal's canal was then measured, allowing for a calculation of cells per mm².

The GFAP signal intensity within the central portion of the auditory nerve was also examined using the In Cell Analyser. Sections were scanned and pictures were processed on the Developer Toolbox software. By using segmentation and sieving features within the software, a mask was created which was able to isolate GFAP positive astrocytic fibres within this region. The software was then able to analyse the fluorescence intensity of each fibre within the central portion of the auditory nerve.

2.6 Polymerase Chain Reaction Analysis

2.6.1 Extraction of RNA

For extraction of RNA from cells, the RNeasy Micro Kit (QIAGEN) was used, as per the manufacturers protocol. At various time points within the experiment, cells were initially washed with PBS, and cell lysis was undertaken using the RLT buffer. A cell scraper was used to ensure all material was lifted. This was stored at -80 degrees Celsius for further processing at a convenient time.

RLT buffer containing the lysed material was precipitated through 70% molecular grade ethanol, and the solution was then passed through the manufacturers Micro columns, which bound the RNA and facilitated the washing phases of the protocol. A digestion phase of genomic DNA was undertaken using DNase I (QIAGEN), and the RNA was eluted from the column using molecular grade water. To determine the yield of RNA, 1µl of the sample was placed onto the Nanodrop 1000 platform. Following quantification, RNA was stored at -80 degrees Celsius for later processing.

2.6.2 Processing of RNA for cDNA synthesis

For the manufacture of complimentary DNA, 1µg of RNA was used. 1µl of oligo-dt (PROMEGA) was added to RNA samples to give a total volume of 12µl, which was then incubated at 65 degrees Celsius for five minutes. After this, the following were added to each sample, in sequence:

- 4µl First Strand Buffer (LIFE TECHNOLOGIES)
- 1µl dithiothreitol (DTT) (LIFE TECHNOLOGIES)
- 1µl RNasin plus RNase Inhibitor (PROMEGA)
- 1µl of 100mM dNTPs (BIOLINE)
- 0.5µl of RNase free water
- 0.5µl Superscript III reverse transcriptase enzyme (LIFE TECHNOLOGIES)

The resulting solution was then incubated at 50 degrees Celsius for 90 minutes, and then heat inactivated at 70 degrees Celsius, for 15 minutes. The samples were then stored at -20 degrees Celsius for PCR analysis.

2.6.3 PCR Primers

Primers used for this work were obtained from publications that had previously demonstrated their success. The primers were then checked using the Primer BLAST software (NCBI), as a second check to ensure their suitability. Primers were diluted in molecular grade water to a final concentration of 100mM and stored at -20 degrees Celsius. cDNA from SOX10, P75 expressing neural crest stem cells was obtained from James Hackland, and was used for primer testing, and also as controls in PCR reactions.

Gene	Primer Sequence	Annealing Temperature	No. Cycles	Amplicon Length
SOX10	F:ACC GCA CAC CTT GGG ACA CG R: CAA CGC CCA CCT CCT CGG AC	58	40	81
P75	F:ACG GCT ACT ACC AGG ATG AG R:TGG CCT CGT CGG AAT ACG TG	58	40	144
BRN 3A	F:CGT ACC ACA CGA TGA ACA GG R:AGG AGA TGT GGT CCA GCA GA	57	40	
RPLPO	F:GAA GGC TGT GGT GCT GAT GG R:CGG GAT ATG AGG CAG CAG TT	58	40	103

Table 2.2. Primer conditions for PCR Primers.

2.6.4 PCR Conditions

PCR reactions were performed in 10 μ l aliquots, with each aliquot containing the following:

- 5.75 μ l molecular grade water
- 2 μ l Green GoTaq Flexi Buffer (PROMEGA)
- 0.8 μ l Magnesium Chloride (PROMEGA)
- 0.2 μ l dNTPs
- 0.1 μ l Forward Primer
- 0.1 μ l Reverse Primer
- 1 μ l cDNA
- 0.05 μ l GoTaq Flexi DNA Polymerase (PROMEGA)

PCR reactions were undertaken using a thermocycler (Mastercycler, EPPENDORF), with an initial denaturation step at 94 degrees Celsius for 15 seconds, followed by annealing temperature for 30 seconds, and finally extension at 72 degrees Celsius for 1 minute. A final extension phase was at 72 degrees Celsius for 10 minutes.

2.6.5 Gel Electrophoresis of PCR Products

To analyse products, gel electrophoresis was undertaken. The gel was made using the following recipe:

- 80ml 1XTBE
- 0.8g 1% Agarose (SIGMA)
- 1.4g low melting point agarose (FISHER SCIENTIFIC)
- 2µl Ethidium Bromide (FISHER SCIENTIFIC)

The solution was dissolved by heating carefully in a microwave until clear. The gel was then poured into an electrophoresis tray, and a gel comb placed in situ to mark out wells to house the PCR products. Once the gel was set, products were loaded into the wells, with the outermost well loaded with a 100bp ladder (BIOLABS). Electrophoresis was then undertaken at 100 volts for 45 minutes to 1 hour. The gel was then placed into a UV transilluminator, and pictures were analysed using the GeneSnap (INGENIUS) version 6.04 software (SYNGENE).

2.7 Statistical Analysis

All statistics were undertaken using Prism Graphpad software. For cell counts, percentage gene expression was calculated by comparing positive cells with DAPI positive nuclei. Means in each condition were then calculated, and compared with one another using a one-way ANOVA test, with Bonferroni's multiple comparison applied after this.

For comparison of neurite lengths in co-culture, mean neurite lengths were calculated for ONPs in co-culture and ONPs cultured alone, and comparison of means was undertaken using an unpaired t-test.

For fluorescence intensity of GFAP expression *in vitro* and post Ouabain treatment *in vivo* a frequency distribution histogram was first plotted, showing a positive skew to the values. Thus, the Mann-Whitney test was used to compare means of fluorescence intensity.

CHAPTER 3: DO hESC-DERIVED OTIC NEURAL PROGENITORS PRODUCE GLIA?

3.1 Introduction

Previous work in the Rivolta lab has demonstrated the efficacy of human embryonic stem cells in treating sensorineural hearing loss within an animal model of auditory neuropathy. Not only are cells able to engraft and extend neurite projections both peripherally and centrally within the auditory nerve, but they also are capable of restoring auditory function. Despite the extremely encouraging nature of such findings, a number of fundamental questions remain, specifically surrounding the long-term survival and efficacy of transplanted cells. Within an *in vivo* paradigm, neurons are closely associated with glial cells, which play a fundamental role in the proper function and maintenance of neurons. Thus, an important question to initially answer would be whether otic neural progenitors derived from human embryonic stem cells produce a population of glial-like cells alongside neuron-like cells. If otic neural progenitors do indeed form a population of glial-like cells during differentiation, this would suggest that they are less likely to be predominantly reliant on the glial cells of the host cochlea for long-term support, which may be damaged as a result of pathology.

3.1.1 *The Otic Placode and Neurogenesis*

The complex sensory organs concerned with the special senses of vision, olfaction, audition and balance are all derived from thickened discs of ectoderm known as placodes, which are in close proximity to the anterior neural plate. Although there are separate placodes for each of these sensory modalities it is now widely believed that the placodes are all derived from a common area of ectoderm, coined as the '*pre-placodal region*' (Streit, 2004, Baker and Bronner-Fraser, 2001). This area can be identified by the expression of markers such as SIX1, SIX4 and EYA2 (Litsiou et al., 2005, McLarren et al., 2003), following Bmp, WNT and FGF signaling from the underlying mesoderm and neural plate.

FGF signaling plays an important role in the induction of the otic placode from the pre-placodal domain. In fact, it has been suggested all of the developing placodal precursors initially have characteristics of the lens placode, and through FGF signaling acting in a restrictive manner, precursors of the remaining placodes are specified (Bailey et al., 2006). Moreover, FGF signaling has been demonstrated to play a key role in otic placodal induction. When chunks of embryonic head tissue containing presumptive otic placodal ectoderm were cultured in the presence of an FGF inhibitor, there was a dramatic decrease in PAX2 and EPHA4 expression within the otic ectoderm. The same study also suggested that ectoderm needs to adopt a pre-placodal phenotype in order to adequately respond to signaling that results in the formation of the placodes (Martin and Groves, 2006).

Once the placode forms, it soon invaginates to form the otic pit, and eventually delaminates completely to become the otic vesicle, which will go on to form all the intricate structures of the inner ear. Prior to complete invagination of the otic pit, it is patterned along its antero-posterior axis; the anterior portion of the pit contains the otic neurosensory progenitors, whilst the progenitors forming the non-neurosensory structures of the inner ear are located posteriorly. These regions can be distinguished by their molecular signature; EYA1, SOX2 and SIX1 (Kiernan et al., 2005, Zheng et al., 2003, Xu et al., 1999) are expressed in the anterior region and an absence of these genes can indeed cause neurosensory defects within the inner ear, whilst the posterior region can be identified by expression of TBX1 and LMX1a (Xu et al., 2007, Koo et al., 2009). This patterning occurs under the influence of a temporospatial gradient of Retinoic Acid from the notochord and mesenchyme. Prolonged exposure of Retinoic Acid in the posterior regions results in fate restriction to the non-neural structures of the inner ear (Bok et al., 2011), whilst anteriorly, low levels of Retinoic Acid help in fate-restricting this region towards the neurosensory inner ear progenitors (Delacroix and Malgrange, 2015). The release of sonic hedgehog from the notochord is also an important contributory factor in affirming the fate restriction of the ventral portion of the otocyst into a neurosensory domain, from which the cochleovestibular ganglion subsequently develops (Brown and Epstein, 2011).

The neurosensory domain gives rise to both vestibular and cochlear neurons, and generally the neurons of the vestibular system tend to form prior to cochlear neurons (Bell et al., 2008). They both form from distinct neural progenitors; vestibular neurons are generated from a population of cells expressing

neurogenin-1, whereas cochlear neurons are generated from a parent progenitor population expressing GATA3 (Lawoko-Kerali et al., 2004). GATA3 continues to be expressed during the latter part of spiral ganglion neuron development, which suggests it probably plays a role far greater than merely specification of neural progenitors within the otocyst to a cochlear phenotype. It has been shown that a suppressed expression of GATA3 can cause aberrant neurite outgrowth (Appler et al., 2013) and disrupts the organized wiring of the cochlea that is seen in normal development (Duncan and Fritzsche, 2013), indicating that alongside playing the role of specification of cochlear neural progenitors, it also facilitates neurite organisation.

Spiral ganglion neurons are heavily reliant on a supply of neurotrophins for their long-term survival. Developing cochlear neurons express the tyrosine kinase B and tyrosine kinase C receptors, indicating that they are capable of responding to neurotrophic stimuli during their developmental phase (Farinas et al., 2001). A temporospatial gradient exists for each neurotrophic factor within the developing cochlea; BDNF expression progresses in an apex-base fashion (Schechterson and Bothwell, 1994), whilst NT-3 runs in the opposing direction, from base-apex (Pujol R, 1998). Within the mature cochlea, neurotrophin supply is sustained by the cochlear support cells and hair cells, alongside the Schwann cells of the peripheral auditory system (Delacroix and Malgrange, 2015).

3.1.2 The Neural Differentiation Protocol

The neuralisation protocol employed within the Rivolta lab is a 2-step differentiation process, which is based upon some of the principles stages of otic development described above. The protocol is essentially a 2 step process; the first step 'induces' a placodal-like phenotype in human embryonic stem cells, and the second step facilitates the differentiation of placodal-like cells into spiral ganglion neuron-like cells.

Alongside playing a key role in otic development, FGF signaling has also shown to be sufficient for otic placodal induction (Martin and Groves, 2006). Following these findings in murine otic development that FGF3 and FGF10 induce the otic placode, the laboratory has successfully shown that culturing human embryonic stem cells with these FGF ligands in a predefined medium induces a placodal-like phenotype, with an upregulation of classic placodal markers such as SOX2, PAX2, PAX8 and FOXG1 (Chen et al., 2009).

Once otic neural progenitors have been isolated on the basis of their morphology, they are initially cultured in a chemically defined medium containing sonic hedgehog, to mimic the ventralisation of neurosensory progenitors that takes place within the otocyst. Neurotrophins are then added into the system, to allow for the sustained development and survival of the developing spiral ganglion-like neurons. At the end of the protocol cells express neuronal markers such as beta-3-tubulin, neurofilament 200 and BRN3A (Chen et al., 2009). The methodological details of the protocol are discussed in Chapter 2.

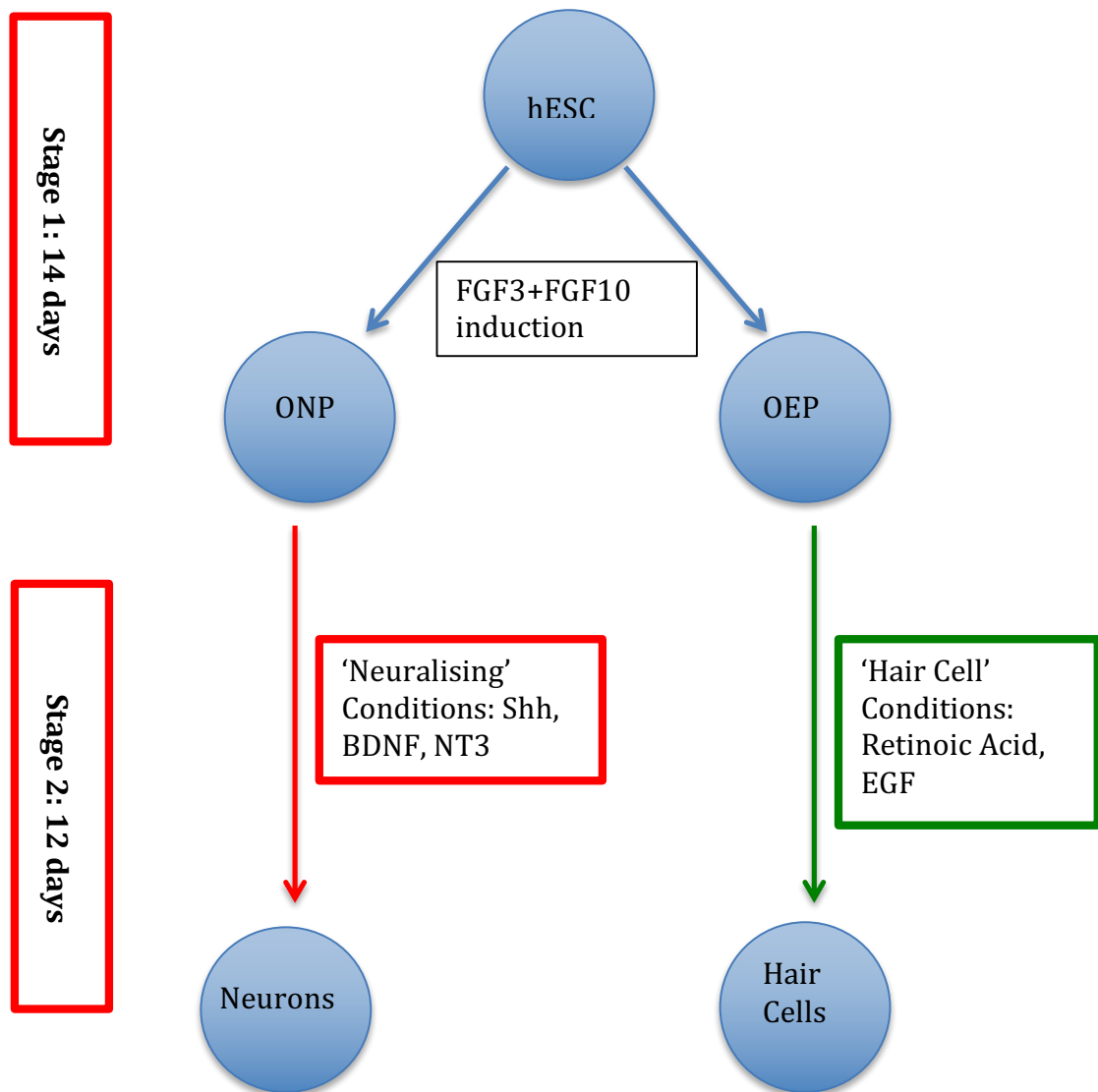


Fig 3.1 – Diagram illustrating the stepwise differentiation protocol of human embryonic stem cells (hESC) to otic neural progenitors (ONP) and otic epithelial progenitors (OEP), and the subsequent differentiation of these cells into neuronal-like cells and hair cell-like cells

3.1.3. Schwann Cell Development.

Glial cells in the peripheral nervous system consist of satellite cells in peripheral ganglia, and myelinating and non-myelinating Schwann cells enveloping axons. Developmentally, these cells originate from the neural crest and fate-restriction of neural crest stem cells towards a glial lineage happens early in embryonic development. Schwann cell development can be considered as a three step process (Jessen and Mirsky, 2005):

- 1) The specification of a neural crest cell into a Schwann Cell Precursor (SCP)
- 2) Maturation of SCPs into immature Schwann Cells and
- 3) development of mature myelinating and non-myelinating Schwann cells from the immature state.

There is an element of plasticity in this cascade; for example, it has previously been suggested that myelinating and non-myelinating Schwann cells may revert to the immature Schwann cell-like state in response to neuronal injury (Jessen and Mirsky, 2005), although more recent evidence suggests that rather than de-differentiating, Schwann cells transdifferentiate into a 'repair cell' phenotype in response to injury (Arthur-Farraj et al., 2012). Moreover, with the discovery of markers expressed by cells at each stage of development, it is possible to characterize Schwann cells during stages of development. For example, SCPs can be distinguished from neural crest cells by their expression of markers such

as P0 and PMP22, whilst immature Schwann cells can be differentiated from SCPs by their expression of late glial markers such as S100 and GFAP. The transcription factor SOX10, a classic neural crest marker, is known to be one of the main factors required for gliogenesis from the neural crest, and is expressed throughout the glial development pathway. Its importance is exemplified by the inactivation of SOX10 in mice, where Schwann cell precursors are lacking, but neuronal development seems to be initially unimpaired (Britsch et al., 2001).

Within the central nervous system, it seems that there is a sequential pathway in which neural progenitors initially form neurons, and then switch to form their associated glia (Doetsch, 2003, Gotz, 2003). Similar assertions have been made about the peripheral nervous system. Shah et al have shown that neuregulin acts as an inhibitory factor in neural differentiation of neural crest stem cells, but promotes differentiation into glial phenotypes (Shah et al., 1994). Notch signaling has also been shown to influence gliogenesis in a similar manner (Morrison et al., 2000). Whilst such *in vitro* studies do add considerable strength to the notion that there is a temporal switch from neurogenesis to gliogenesis in the development of the peripheral nervous system, conclusive *in vivo* data proving this point is yet to be demonstrated.

Schwann cell precursors derived from the neural crest closely associate with axons early in development. In mice, they are seen on day 12-13 in association with spinal nerves, whereas in the rat they are seen on day 13-14. Despite this early association, SCPs are not required for early growth and guidance of axons (Grim et al., 1992, Riethmacher et al., 1997, Woldeyesus et al., 1999). However,

SCPs seem to play an important role in providing trophic support to developing axons. In mouse mutants devoid of SCPs, early embryonic neurons eventually die, suggesting that SCPs are required to support developing neurons as they grow. Furthermore, this study also implies that SCPs play a role in facilitating normal fasciculation of axons (Garratt et al., 2000).

The relationship between SCPs and axons might be described as a symbiotic one; both are reliant upon one another for survival. SCPs are reliant upon neuregulin-1(NRG1) produced by axons, illustrated for example by the observation that SCPs begin to populate axons at the time when they start producing it (Marchionni et al., 1993, Loeb et al., 1999, Longart et al., 2004) and that SCP can be rescued following neuronal damage by exogenous administration of NRG1 (Winseck et al., 2002). Furthermore, SCP numbers are significantly reduced in genetically altered mice where NRG1 signaling has been manipulated, or in which the tyrosine kinase receptors ErbB2 or ErbB3 (which bind NRG1) have been inactivated.

In addition to playing a key role in promoting survival of SCPs, NRG1 may also facilitate the differentiation of SCPs into immature Schwann cells. For example, when E14 SCPs are cultured in vitro and supplemented with NRG1 for 4 days, they become phenotypically similar to E18 Schwann cells, in that they develop autocrine survival pathways involving Insulin-like Growth Factors, Neurotrophin-3 and Platelet Derived Growth Factors, which are a classic characteristic of Schwann cells that differentiate them from SCPs (Dong et al., 1995, Jessen and Mirsky, 1999).

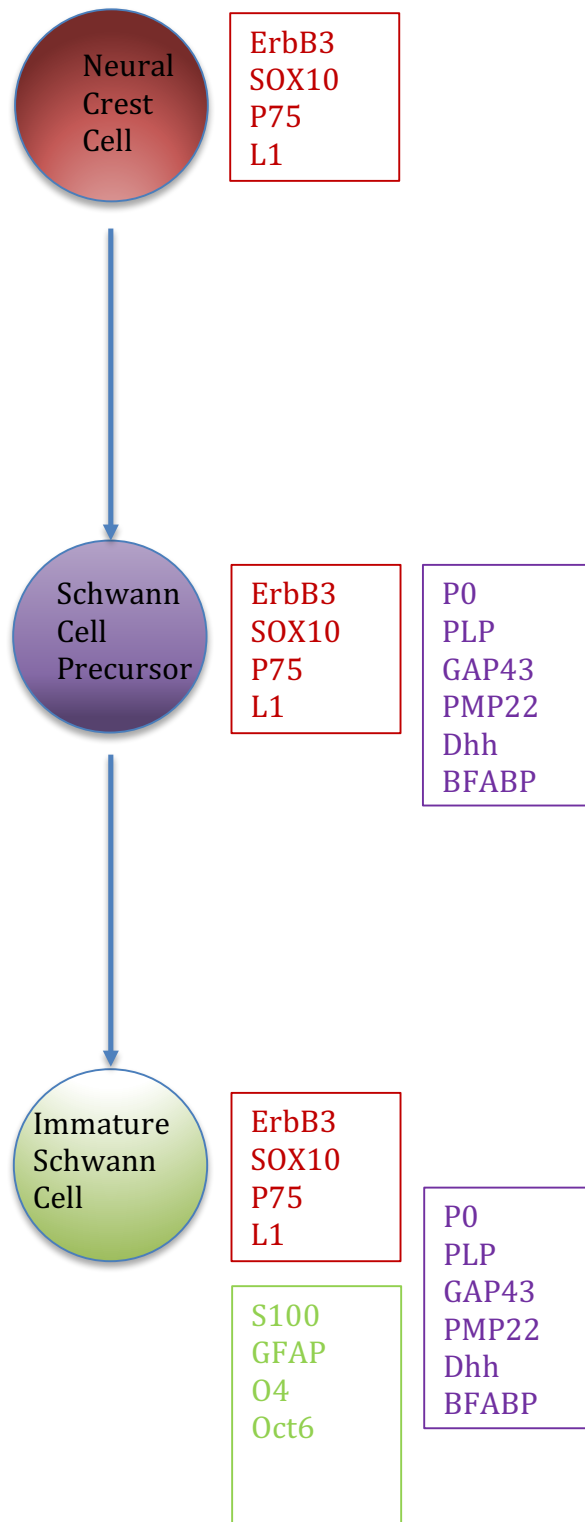


Fig 3.1a – Diagram illustrating the development of Schwann cells from neural crest cells. Markers in the red boxes are expressed throughout the development pathway. Markers in the purple boxes are expressed in Schwann cell precursors, whilst markers in the green box are expressed in immature Schwann cells. Adapted from Jessen and Mirsky (2005).

One of the key functions of Schwann cells is to facilitate the myelination of peripheral axons. In a process known as 'radial sorting', immature Schwann cells establish a 1:1 relationship with large diameter axons, which then go on to myelinate the axons they are associated with (Jessen and Mirsky, 2005, Woodhoo and Sommer, 2008). Smaller diameter axons remain unmyelinated and are associated with non-myelinating Schwann cells.

3.1.4 Cochlear Glial Cells – Development and Function

One of the seemingly unique characteristics of the cochleovestibular nerve is its exclusive placode origin; whereas most other sensory cranial nerves have dual origins, namely the sensory placodes and the neural crest (D'Amico-Martel and Noden, 1983). This notion has been contested by Freyer et al. (Freyer et al., 2011) who suggested that the neural crest may provide neurons during cochlear nerve development. However, more recent work examining cochlear glial development in the human embryo is in agreement with the general consensus that SGNs and Peripheral Glial Cells have distinct embryological origins of the otic placode and neural crest respectively (Locher et al., 2014).

The peripheral glial cells of the cochlear nerve originate from the neural crest at the level of rhombomere 4 (D'Amico-Martel and Noden, 1983), and increasing evidence suggests that the neural-glial relationship is established early through interactions between SCPs and neural progenitor cells, and is important in the development of the cochlear nerve. When ErbB2 signaling is disrupted in the mouse, cochlear nerve development is impaired (Corfas et al., 2004). In particular, neural growth decreased and misdirected (Morris et al., 2006). This is

in agreement with the rest of the peripheral nervous system, where ErbB2 null mice have poorly fasciculated peripheral nerves with disordered terminal neurites (Morris et al., 1999, Woldeyesus et al., 1999). Whilst these findings would suggest that interactions between SCP and neural progenitors are key for cochlear nerve development, the observation that the cochlear nerve develops normally in mouse embryos lacking SOX10 suggest otherwise (Breuskin et al., 2010). Although Sandell and colleagues try to explain this discrepancy by suggesting that glial progenitors are absent after E10.5 in SOX10 mutant mice and thus the critical interactions between SCPs and neural progenitors occur extremely early in development (Sandell et al., 2014), this notion is at odds with the assertion that SCPs are not required for early growth and guidance of peripheral neurons, but play a significant role later in development (Grim et al., 1992). Moreover, the reports of cochlear neurons developing normally in the absence of SOX10 raises questions about the role of SOX10 in otic development, given that SOX10 is also widely expressed in the otic placode. In an attempt to reconcile this conundrum, Mao and colleagues used Wnt1-cre to conditionally delete SOX10 from the neural crest, whilst sparing SOX10 expression in the placode. This resulted in a loss of Schwann cells in the developing ear with abnormal migration of spiral ganglia, and aberrant neurite projections that bypass the Organ of Corti (Mao et al., 2014), in a similar fashion to what was reported in ErbB2 mutant mice (Morris et al., 2006). Hence, on balance, the evidence suggests that interactions between SCPs and neural progenitors are vital for the proper development of the cochlear nerve.

Much of our knowledge regarding cochlear development stems from studies conducted in mouse and zebrafish models. Locher and colleagues have been the first group to describe the development and migration of glial cells within the human fetal cochlea (Locher et al., 2014). The earliest specimens they were able to obtain at week 9 demonstrated an abundance of S100 expression, indicating that glial cells had most probably already become immature Schwann cells at this stage of development. In particular, their findings that Schwann cells expressing P75 closely associate with developing spiral ganglia as they extend neurites suggests that they may be providing guidance cues as illustrated in other mammalian systems, however more conclusive evidence is required to prove this assertion (Locher et al., 2014).

Ray and colleagues conducted a detailed morphometric study of auditory nerve development in the human, and reported that myelination in the central fibres of the auditory nerve start occurring at week 20 (Ray et al., 2005), whereas myelination of the peripheral processes seems to occur later at week 24 (Lavigne-Rebillard and Pujol, 1988).

Despite the paucity of literature pertaining specifically to the development of peripheral glial cells in the human cochlea, a crude timeline of development can be constructed on the basis of current knowledge, as illustrated in the following table:

TIME (GESTATIONAL WEEK)	DEVELOPMENTAL STAGE OF PERIPHERAL GLIAL CELLS
W4-9	Invagination of the otic vesicle. (Lim et al., 2016) Maturation of SOX10+ neural crest derived Schwann cell precursors to immature Schwann cells (Locher et al., 2014)
W9-19	Association of immature Schwann Cells with developing spiral ganglia. Possible role in neurite guidance and pruning of fibres (Locher et al 2014).
W20	Myelination of central cochlear nerve fibres (Ray et al., 2005)
W24	Myelination of peripheral cochlear nerve fibres (Lavigne-Rebillard and Pujol, 1988)

Table 3.1 – Proposed developmental timeline of peripheral glial cells in the Human fetal cochlea.

3.1.5 Objectives of this Chapter

The neuralisation protocol employed within this work is based upon the sequence of events leading to the development of neurosensory progenitors within the otocyst *in utero*. Given this to be the case, one may hypothesise that just like the *in utero* cells they model, otic neural progenitors derived from the FGF phase of the neuralisation protocol should not yield significant populations of glial cells. There are two reasons for the importance of trying to answer this question:

- 1) Much of the work on this differentiation protocol in proving the placodal identity of progenitors derived from the FGF phase of the protocol has centred on the expression of classic placodal markers such as PAX2 and SOX2. If otic neural progenitors are unable to make glial cells, this would indicate that the placodal-like cells produced from this protocol are also phenotypically similar to the neurosensory progenitors of the cochlea, which equally do not form glial cells.
- 2) If otic neural progenitors do not possess the plasticity to produce glial cells, this would suggest that when transplanted *in vivo*, they would be completely reliant on the host glial environment for their long-term survival. This would have implications, particularly in scenarios where the glial environment had been severely disrupted as a result of a pathological insult.

3.2 Results

3.2.1 Co-expression of S100 with β -Tubulin but not GFAP in Early Passage ONPs

The first step in ascertaining whether otic neural progenitors were capable of producing glia was to place them into the neuralising conditions, and through immunocytochemistry, assess for the presence of glia with the classic glial markers GFAP and S100.

Shf-1 cells were initially placed into the phase one differentiation protocol and purified manually to isolate otic neural progenitor colonies, which were then expanded to confluence in OSCFM. Following expansion, cells underwent routine cell culture procedures in OSCFM as described in Chapter 2.

For neuralisation, early passage otic neural progenitors (either P3 or P1+2) were placed into the neuralising phase of the differentiation protocol, and maintained as per the neuralisation protocol (See Chapter 2 for further details). They were fixed for immunocytochemistry mid-way through the neuralisation protocol at day 6, and at the end of the protocol at day 12. Expression of markers in neuralised cells was compared to cells that had been kept in OSCFM and fixed at day 3. Of note, all cells were lifted with 1X Trypsin, before being placed into their respective culture media.

The criteria for ascertaining the presence of glia was to assess for co-expression of GFAP and S100, which are both expressed in Schwann cells. B-Tubulin was used as a neuronal marker, to help distinguish between neuronal cells and any population of cells co-expressing the glial markers.

Cells that were in OSCFM exhibited some neuronal morphology (Fig 3.2), and widely expressed B-Tubulin, which is likely to be as a result of the harsh trypsinisation step that these cells underwent, as previous work within the Rivolta Laboratory has illustrated that trypsinisation has a neuralising effect upon otic neural progenitors (Trachoo, 2010). There was also some widespread expression of S100, which co-localised with B-Tubulin, however there was little expression of GFAP in this condition (Figs 3.3 and 3.4).

In cells that underwent neuralisation, there was widespread B-tubulin expression at both day 6 and day 12, which had convincing neuronal morphology with the extension of projections from cell bodies. Interestingly, there was also strong expression of S100 that appeared to co-localise with B-Tubulin (Fig 3.6), however there weren't any populations of cells that co-expressed S100 and GFAP (Fig 3.7). When compared to cells on OSCFM, there wasn't any significant increase in the percentage of cells expressing B-tubulin, but there was a significant increase in the percentage of cells expressing S100 at day 6 and day 12 of the neuralisation protocol when compared to cells in OSCFM (Fig 3.8).

The results from these experiments therefore suggest that early passage ONPs do not yield significant populations of immature glial-like cells. The widespread

expression of S100 was somewhat unexpected, and there are two potential explanations for this finding. The first would be that neuronal differentiation gives rise to populations of glia that are in a precursor state at the end of the neuralising protocol, and thus are not expressing GFAP, but may well express markers suggesting a Schwann cell precursor phenotype, such as P0 and SOX10. Alternatively, the co-expression S100 with B-Tubulin in cells that have a convincing neuronal morphology might suggest that within this particular paradigm, S100 may well be behaving as a neuronal marker, which has also been reported in human spiral ganglion development (Pechriggl et al., 2015).

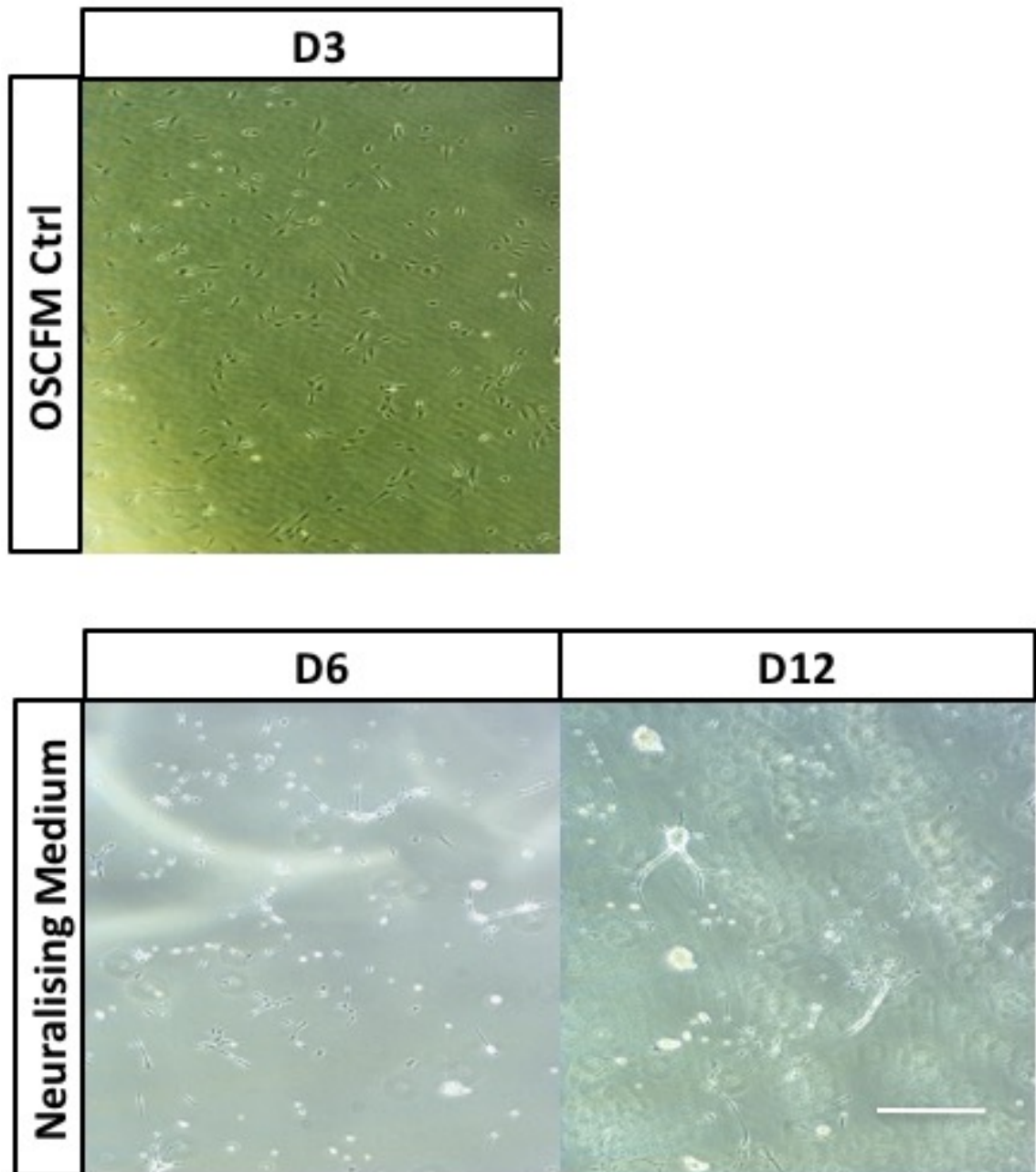


Fig 3.2 – Brightfield microscopy images showing the morphological changes that take place from when Shef-1 otic neural progenitors are maintained in OSCFM to when they are placed in neuralising conditions. Cells in OSCFM were trypsinised with 1X trypsin, and thus some of the cells did possess neuronal morphology. Scale bar represents 200µm

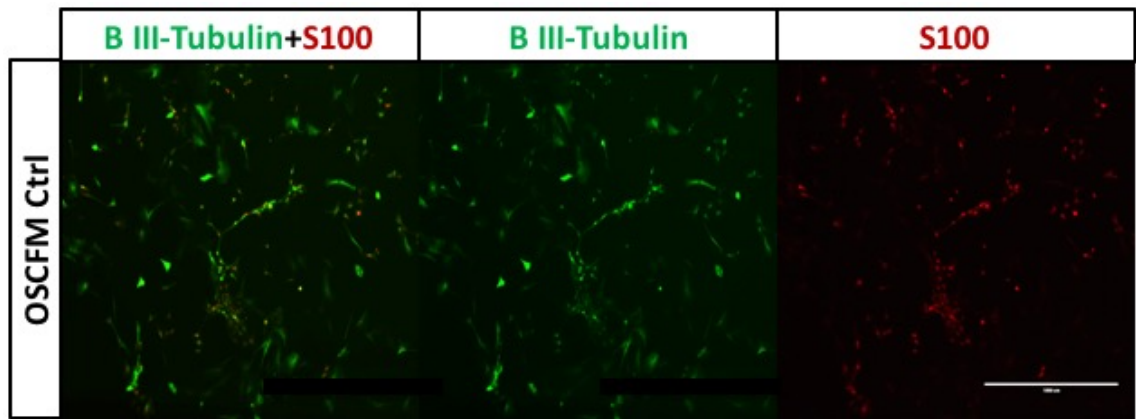


Fig 3.3 – Representative images showing immunolabelling in early passage otic neural progenitors grown in control conditions in OSCFM. B-Tubulin has been stained in green and S100 has been stained in red. Cells were fixed at day 3. Scale bar represents 1000µm

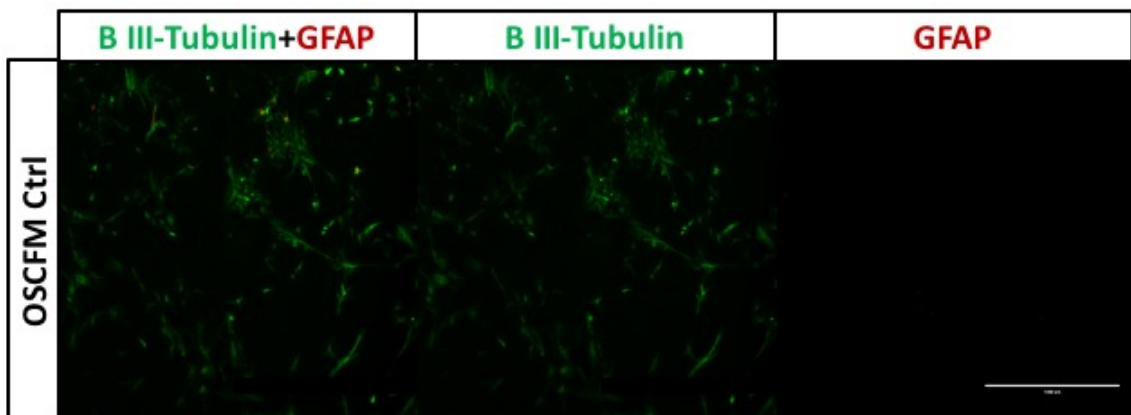


Fig 3.4 – Representative images showing immunolabelling in early passage otic neural progenitors grown in control conditions in OSCFM. B-Tubulin has been stained in green and GFAP has been stained in red. Cells were fixed at day 3. Scale bar represents 1000µm

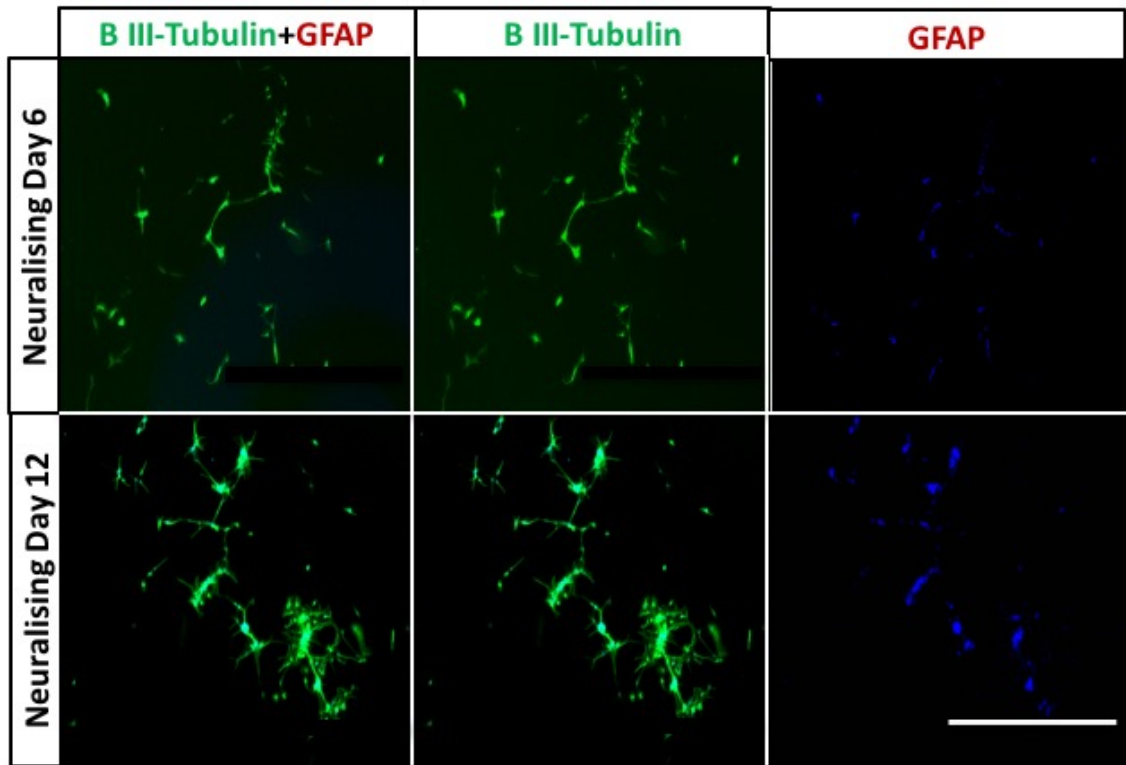


Fig 3.5 – Representative images showing immunolabelling in early passage otic neural progenitors with B-Tubulin (green) and GFAP (red). Cells were in neuralising conditions and fixed at day 6 and at day 12. Nuclei were counterstained with DAPI. Scale bar represents 1000 μ m

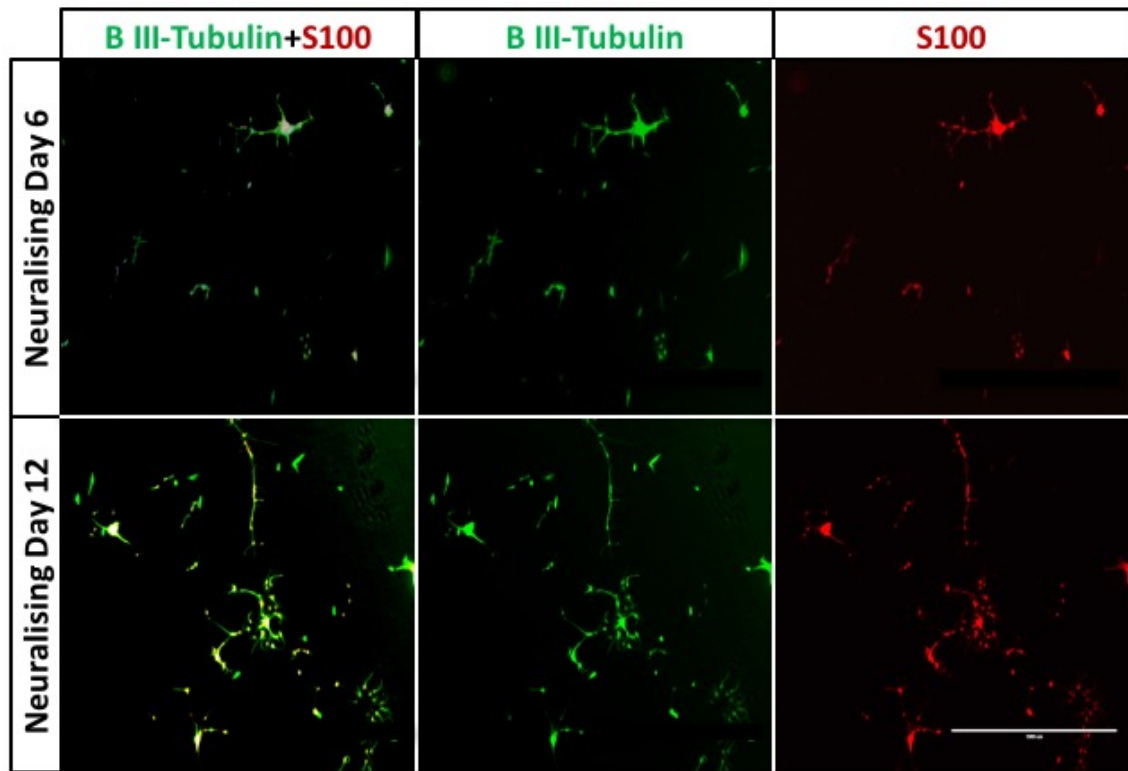


Fig 3.6 – Representative images showing immunolabelling in early passage otic neural progenitors with B-Tubulin (green) and S100 (red). Cells were in neuralising conditions and fixed at day 6 and at day 12. Scale bar represents 1000 μ m

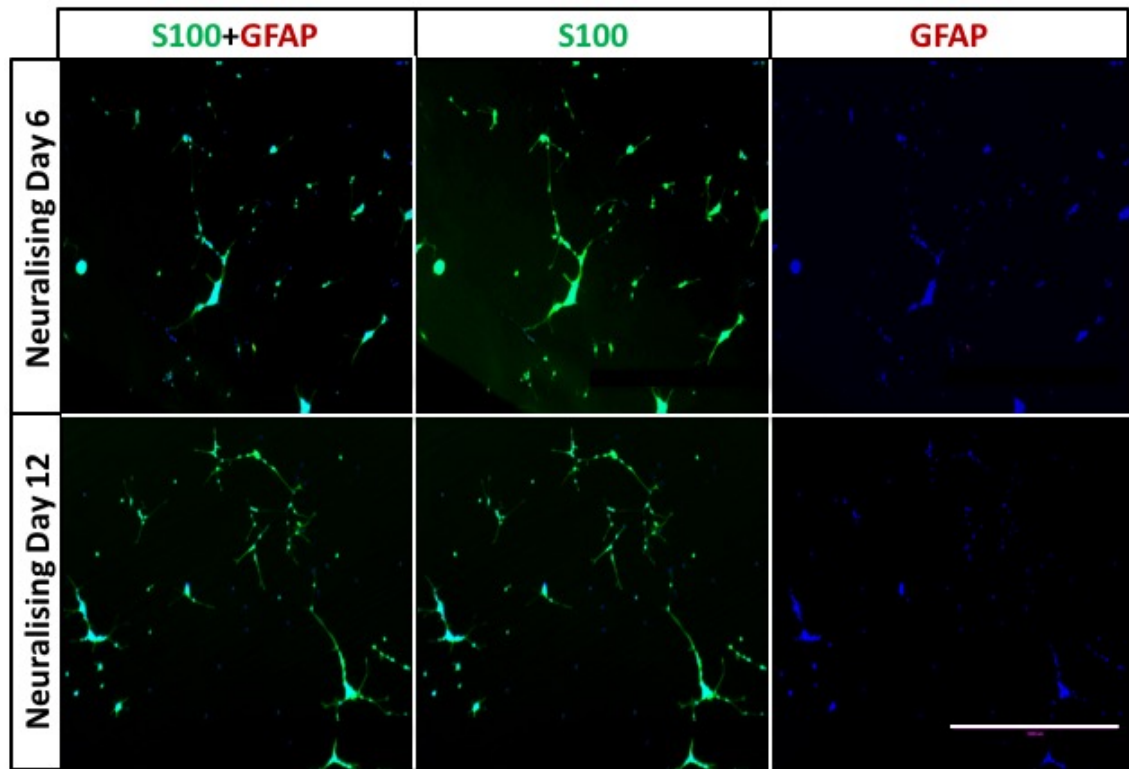


Fig 3.7 – Representative images showing immunolabelling in early passage otic neural progenitors with S100 (green) and GFAP (red). Cells were in neuralising conditions and fixed at day 6 and at day 12. Nuclei were counterstained with DAPI. Scale bar represents 1000µm

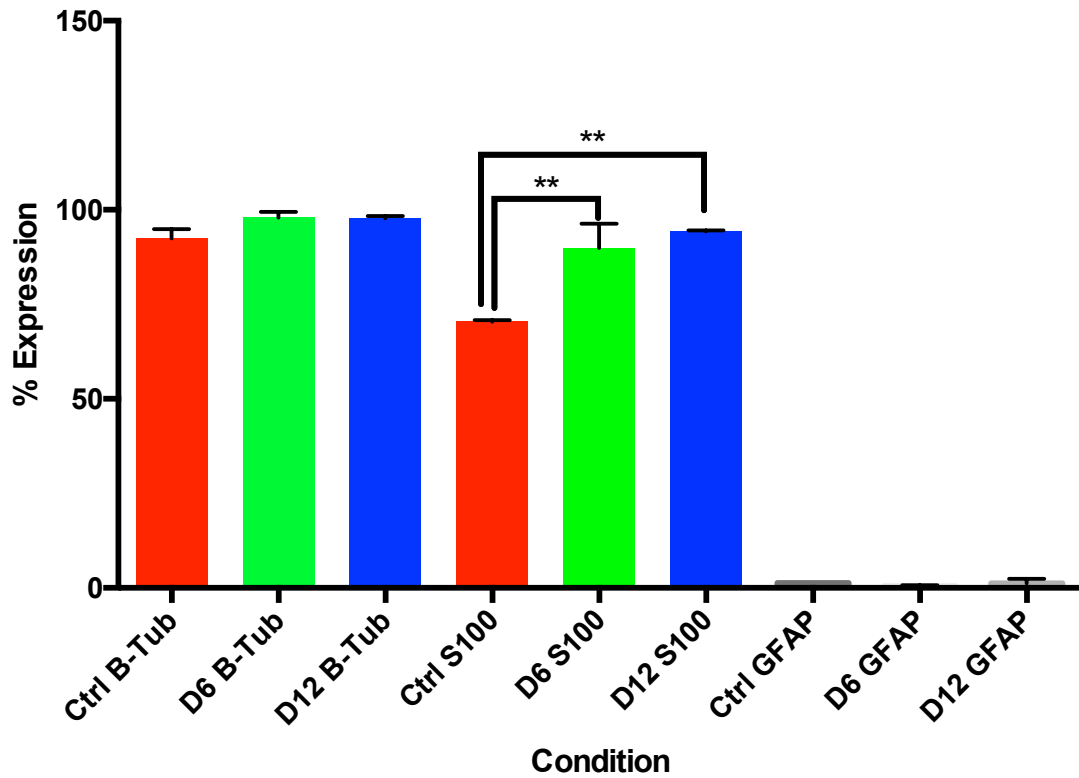


Fig 3.8 - Mean percentage expression of mature glial markers S100 and GFAP, alongside mean percentage expression of B-Tubulin in early passage otic neural progenitors (P3, P1+2). Percentage expression was calculated against total cells staining with DAPI. Error bars denote standard error from mean. Statistical significance was determined using a one-way ANOVA, with Tukey's comparison of means performed post-test. **P<0.01. (n=2)

3.2.2 Lack of S100 and GFAP Expression in late passage ONPs

Given the apparent lack of immature glia in early passage otic neural progenitors, a subsequent question to answer was whether a similar effect is observed in later passage cells. The rationale for this lies in observations of neural rosettes isolated from hESC cultures, in that those obtained from earlier phases of differentiation possess a greater differentiating potential, whereas the effects of continual expansion of these cells *in vitro* eventually results in the cells possessing a gliogenic bias (Zhang, 2006, Elkabetz et al., 2008). Thus, we wanted to ascertain whether the effect of expansion in OSCFM results in the cells attaining a similar bias towards a glial phenotype.

Otic neural progenitors were kept in OSCFM and were passaged and maintained as previously described in chapter 2. Late passage otic neural progenitors (either P7 or P1+6) underwent trypsinisation with 1X trypsin, and were then placed into neuralising conditions. As with experiments on earlier passage otic neural progenitors, cells were fixed midway through the protocol at day 6, and at day 12. Control cells were placed back into OSCFM after trypsinisation, and were fixed at day 3.

As before, B-Tubulin immunostaining was used as a marker to identify cells with a neuronal phenotype, and co-expression of S100 with GFAP was used to distinguish immature glia.

Although there continued to be widespread B-Tubulin expression, the cells lacked their characteristic neuronal morphology in all conditions. Furthermore, S100 expression was also greatly diminished in all conditions; whilst in earlier passage cells, there appeared to be widespread co-expression of B-Tubulin with S100 (Fig 3.6), observations in later passage cells show that B-Tubulin expression persists, whilst S100 expression does not (Fig 3.11). As with earlier passage cells, there is hardly any co-expression of GFAP with S100 (Fig 3.12). Upon analyzing cell counts for each marker, there wasn't any significant difference between cells in control and neutralising conditions for expression of the markers B-Tubulin, S100 and GFAP (Fig 3.13).

These results suggest that later passage otic neural progenitors do not produce glial-like cells, as indicated by the lack of S100 and GFAP co-expressing cells (Fig 3.12, Panel B). Interestingly, although B-Tubulin expression continues to be widespread, there was an apparent lack of neuronal morphology. This raises questions over the specificity of B-Tubulin as a neuronal marker; if S100 is indeed acting as a neuronal marker, then the loss of S100 co-expression with B-Tubulin coupled with the loss of neuronal morphology suggests that with continual passaging, the cells undergo a phenotypic change where they no longer are capable of producing neurons.

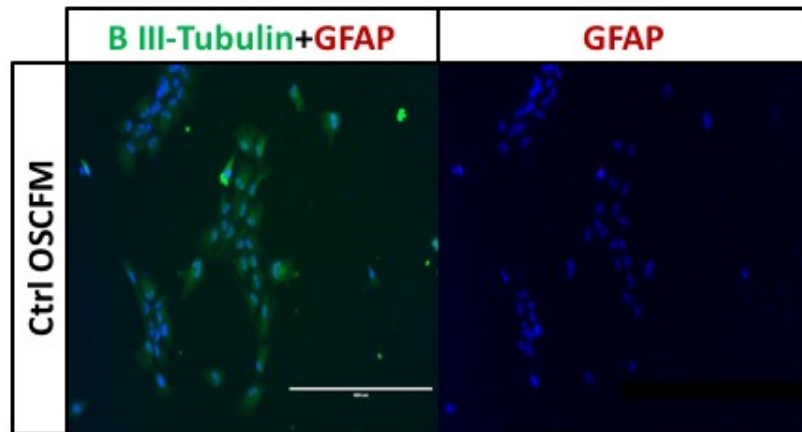


Fig 3.9 – Representative images showing immunolabelling in late passage otic neural progenitors with B-Tubulin (green) and GFAP (red). Nuclei were counterstained with DAPI. Cells were in control conditions and fixed at day 3. Scale bar represents 400µm.

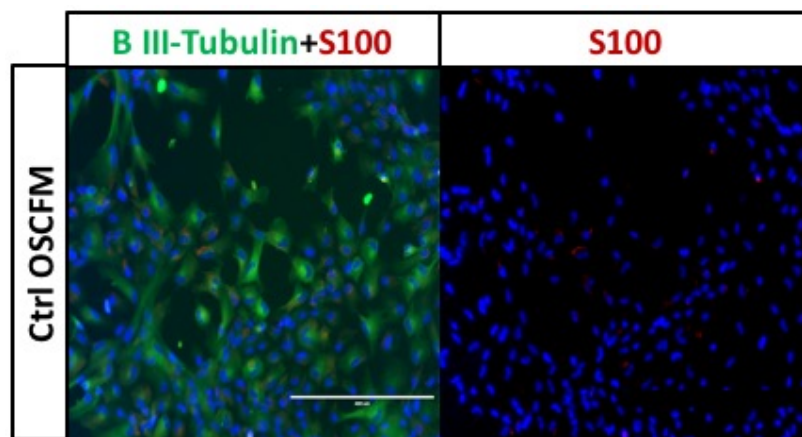


Fig 3.10 – Representative images showing immunolabelling in late passage otic neural progenitors with B-Tubulin (green) and S100 (red). Nuclei were counterstained with DAPI. Cells were in control conditions and fixed at day 3. Scale bar represents 400µm.

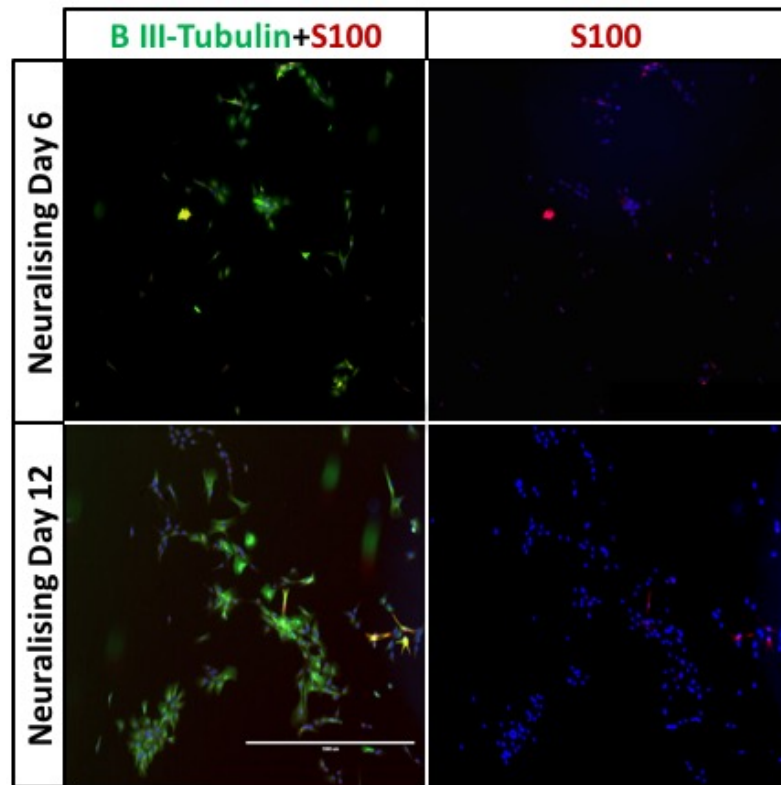


Fig 3.11 – Representative images showing immunolabelling in late passage otic neural progenitors with B-Tubulin (green) and S100 (red). Nuclei were counterstained with DAPI. Cells were in neuralising conditions and fixed at day 6 and day 12. Scale bar represents 1000 μ m.

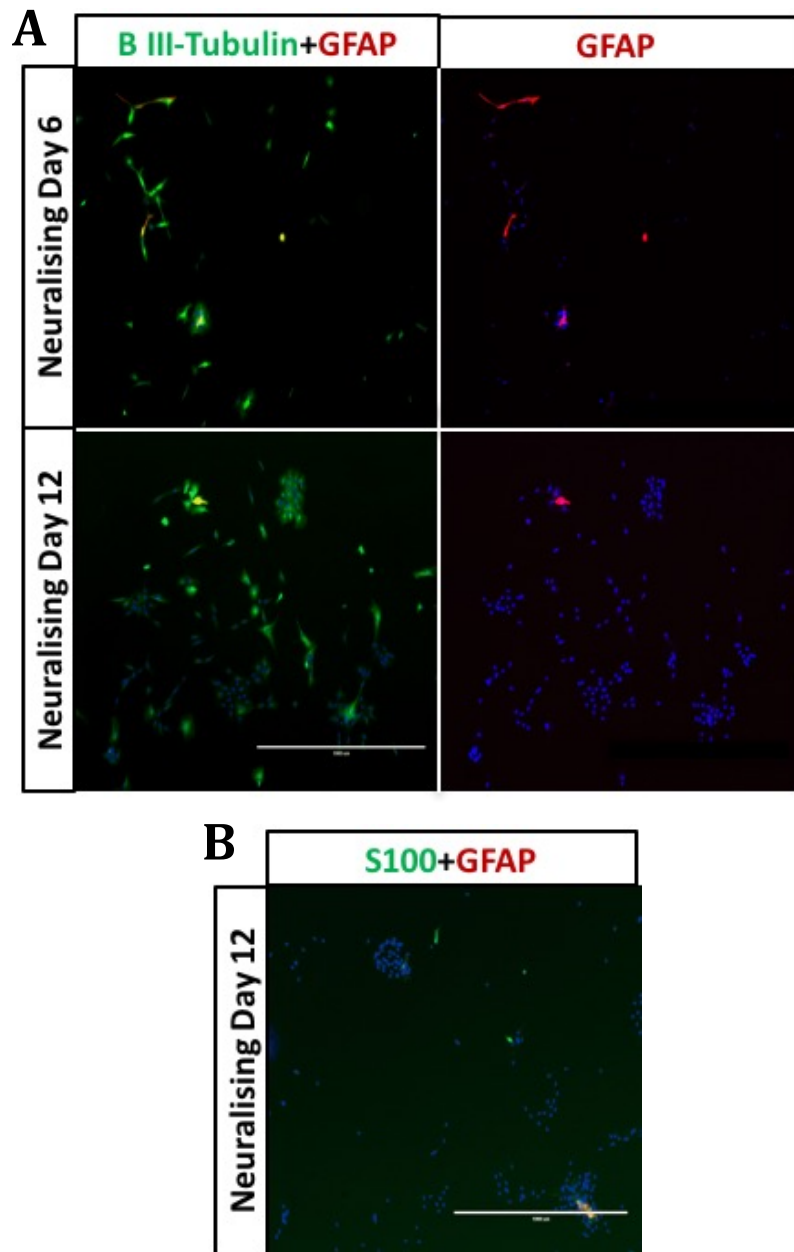


Fig 3.12 – Representative images showing immunolabelling in late passage otic neural progenitors. Panel A shows B-Tubulin (green) and GFAP (red). Panel B shows S100 (green) with GFAP (red) Nuclei were counterstained with DAPI. Cells were in neuralising conditions and fixed either at day 6 and day 12.. Scale bars represent 1000µm.

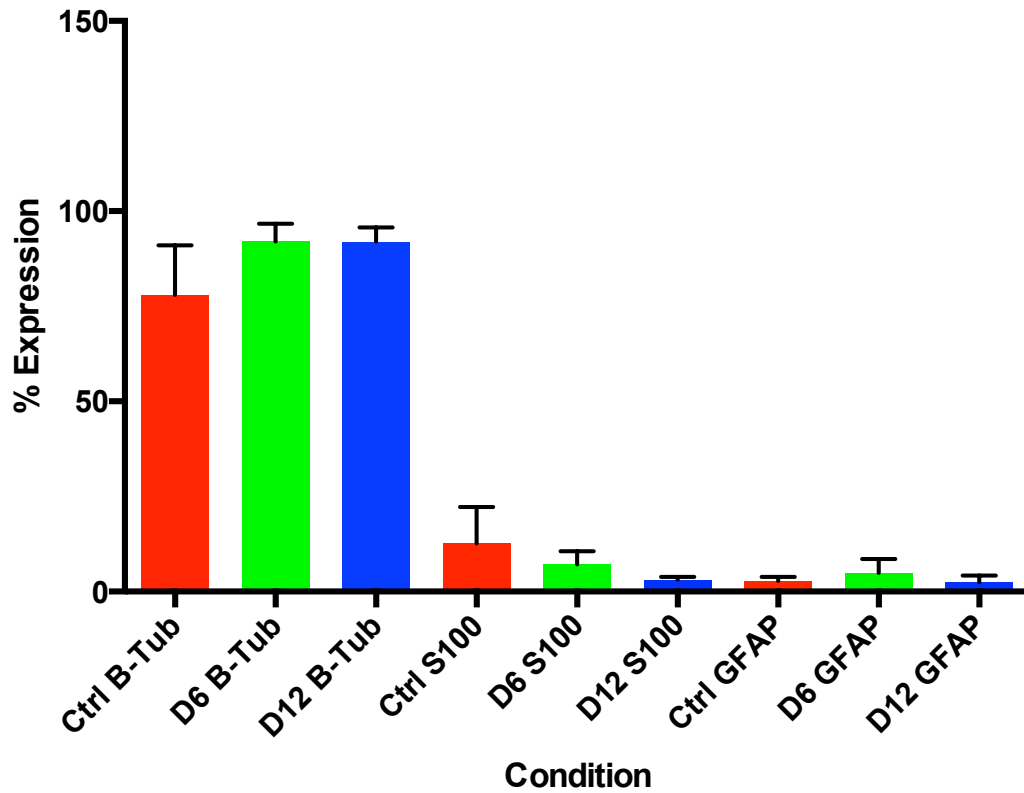


Fig 3.13 – Mean percentage expression of mature glial markers S100 and GFAP, alongside mean percentage expression of B-Tubulin in late passage otic neural progenitors (P7, P1+6). Percentage expression was calculated against total cells staining with DAPI. Error bars denote standard error from mean. Statistical significance was determined using a one-way ANOVA, with Tukey’s comparison of means performed post-test. No significance was detected in any of comparisons.

3.2.3 S100 expression correlates with neuronal markers as opposed to glial markers in Shaf-1 otic neural progenitors.

One of the possible conclusions drawn from findings in early passage otic neural progenitors was that S100 appears to be co-expressed with B-Tubulin in cells that appear to possess neuronal morphology. However, given that B-Tubulin doesn't seem to be a specific neuronal marker and with the relative absence of GFAP expression in cells, an alternative explanation for the increase in S100 expression could be that it represents populations of peripheral glial-like cells in a transitional state between the precursor stage and the immature phenotype.

In order to further explain the upregulation of S100 seen when otic neural progenitors were placed in neuralising conditions, cells were trypsinised with 1X and placed into neuralising conditions and fixed at the middle of the differentiation protocol, and at its end. Given that treatment with 1X trypsin is known to have a neuralising effect on otic neural progenitors, control cells were treated with 0.00625% trypsin:EDTA and cultured in OSCFM to negate this effect and were fixed at day 3.

B-Tubulin and NF200 were used as neuronal markers, and co-expression of these markers in cells was used as the criteria to distinguish cells with a neuronal phenotype. S100 was used alongside the intermediate Schwann cell marker P0 and SOX10, which are expressed throughout the Schwann cell development pathway. Co-expression of S100 with P0 and SOX10 was used as the criteria to distinguish peripheral glial-like cells.

Results showed that as seen previously, B-tubulin appears to be widely expressed in both control conditions and in cells that underwent differentiation in the neuralising protocol (Figs 3.14 and 3.15), and whilst there was a slight increase in the percentage of cells expressing B-Tubulin in neuralising conditions when compared to controls, Figs. 3.18 and 3.19 show that this increase was not statistically significant. Furthermore, in control conditions there was little expression of NF200, however in neuralising conditions, the percentage of cells expressing NF200 dramatically increased alongside the percentage of cells co-expressing B-Tubulin and NF200, which was statistically significant when compared to controls (Fig 3.15 and 3.18b). The pattern of S100 expression resembled that of NF200; with a similar increase in neuralising conditions when compared to cells in control conditions, which was also statistically significant (Fig 3.14 and 3.18a). These experiments confirmed the observations seen previously of S100 being co-expressed with B-tubulin in neuralising conditions, and the increase in the percentage of cells co-expressing these markers in neuralising conditions was statistically significant when compared to controls (Figs. 3.19a and 3.19b).

In contrast, there appeared to be hardly any cells expressing P0 and SOX10 (Figs. 3.16 and 3.17), and subsequently no sizeable populations of cells co-expressing S100 with either of these markers were identified, suggesting that otic neural progenitors do not seem to be producing glial-like cells when placed in neuralising conditions (Figs 3.19a and 3.19b).

Results from PCR also seemed to agree with the findings from immunocytochemistry, with no SOX10 expression detected in any of the conditions, with the neural marker BRN3A manifesting at the end of the neuralisation protocol (Fig. 3.20).

The evidence from these experiments adds further strength to the conclusion that within this particular system, S100 appears to be behaving as a neuronal marker, given that its pattern of expression increases in manner similar to that of NF200, in cells that possess neuronal morphology.

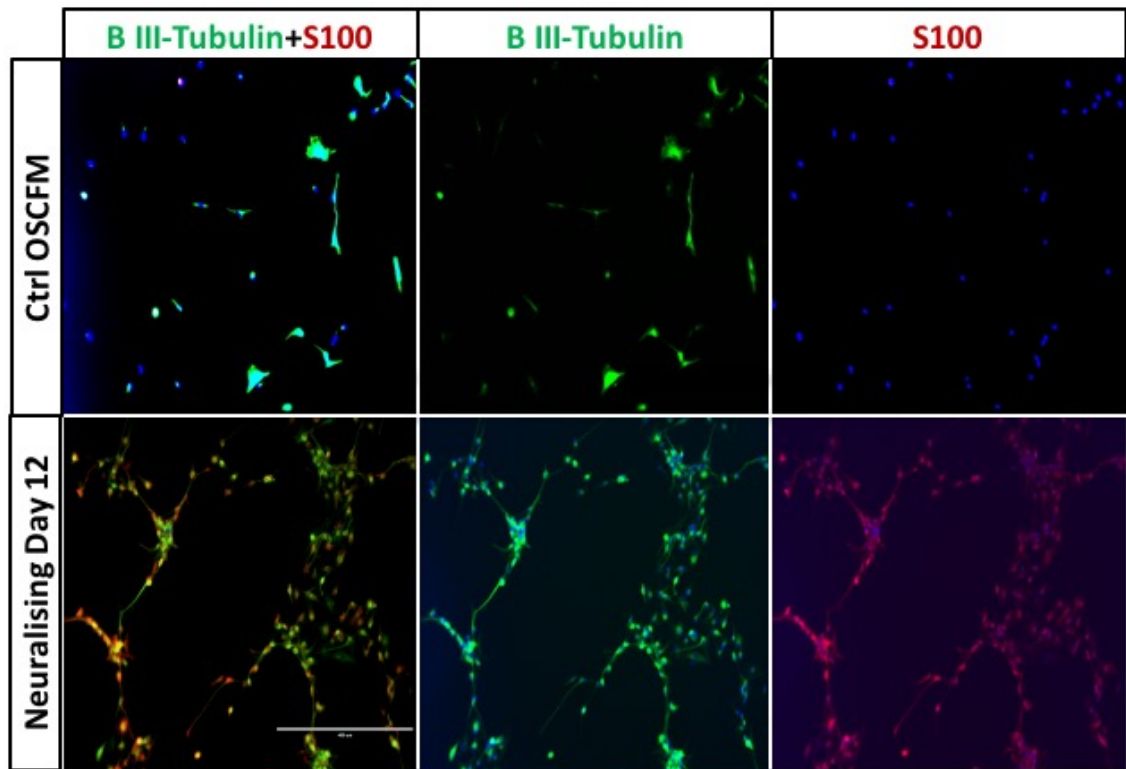


Fig 3.14– Representative images showing immunolabelling in early passage otic neural progenitors with B-Tubulin (green) and S100 (red). Nuclei were counterstained with DAPI. Images are of cells in control conditions and at day 12 of neuralisation. Scale bars represent 400 μ m

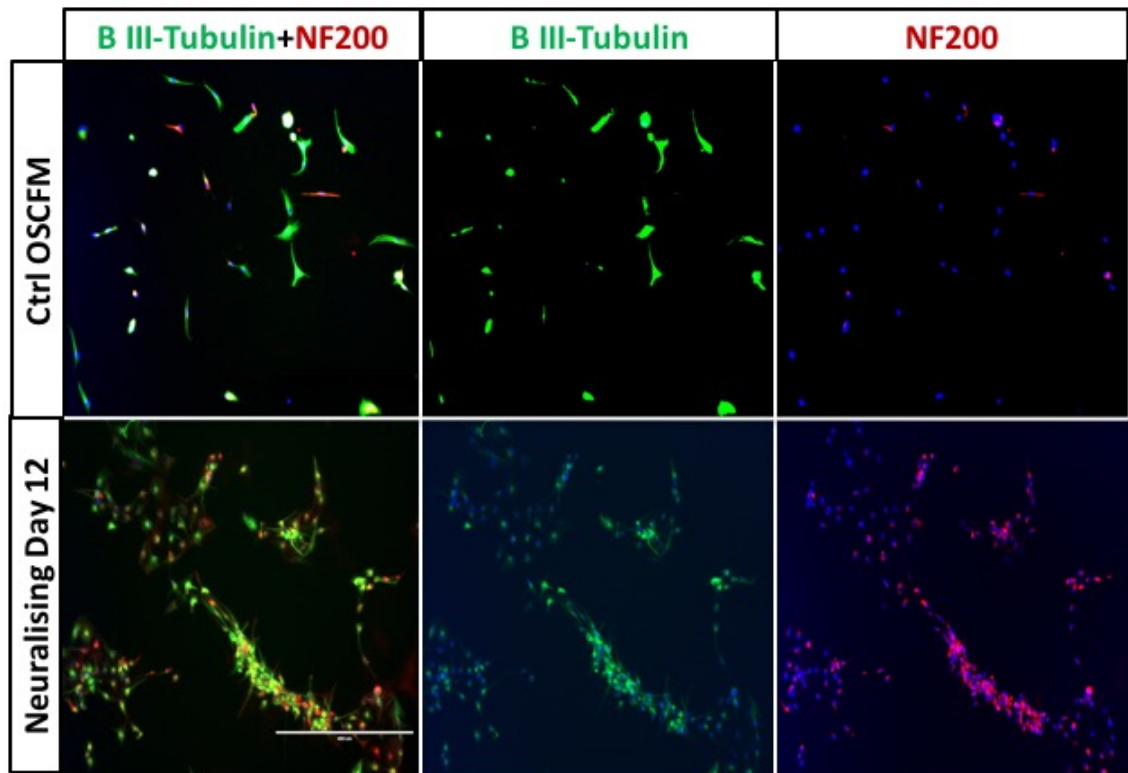


Fig 3.15- Representative images showing immunolabelling in early passage otic neural progenitors with B-Tubulin (green) and NF200 (red). Nuclei were counterstained with DAPI. Images are of cells in control conditions and at day 12 of neuralisation. Scale bars represent 400 μ m

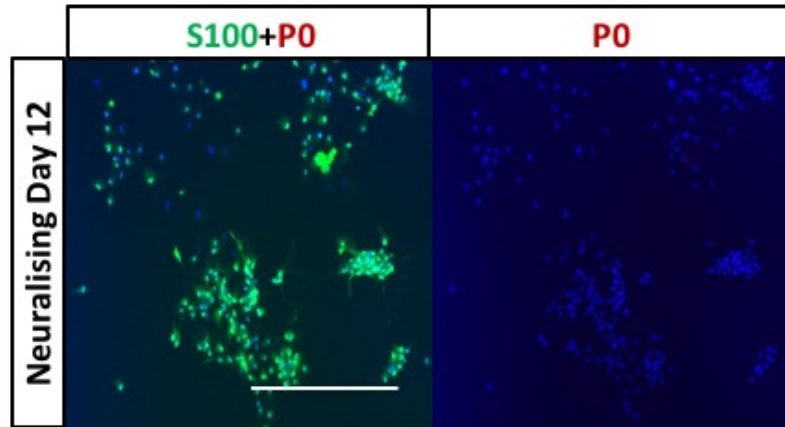


Fig 3.16 – Representative images showing immunolabelling in early passage otic neural progenitors with S100 (green) and P0 (red). Nuclei were counterstained with DAPI. Cells were in neuralising conditions and fixed at day 12. Scale bar represents 400 μ m.

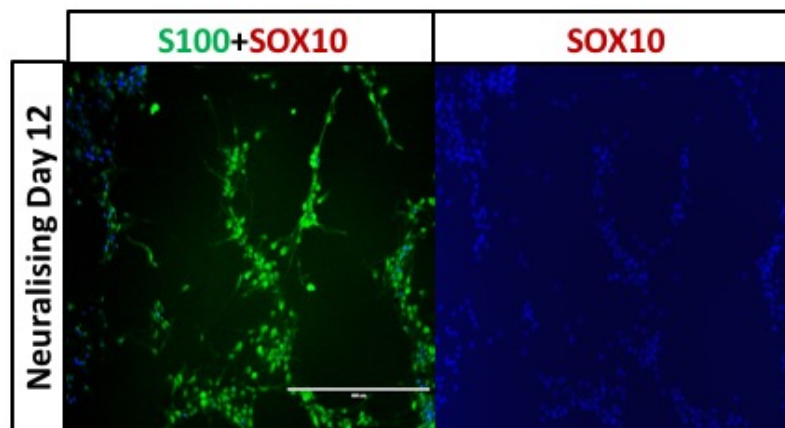


Fig 3.17 – Representative images showing immunolabelling in early passage otic neural progenitors with S100 (green) and SOX10 (red). Nuclei were counterstained with DAPI. Cells were in neuralising conditions and fixed at day 12. Scale bar represents 400 μ m.

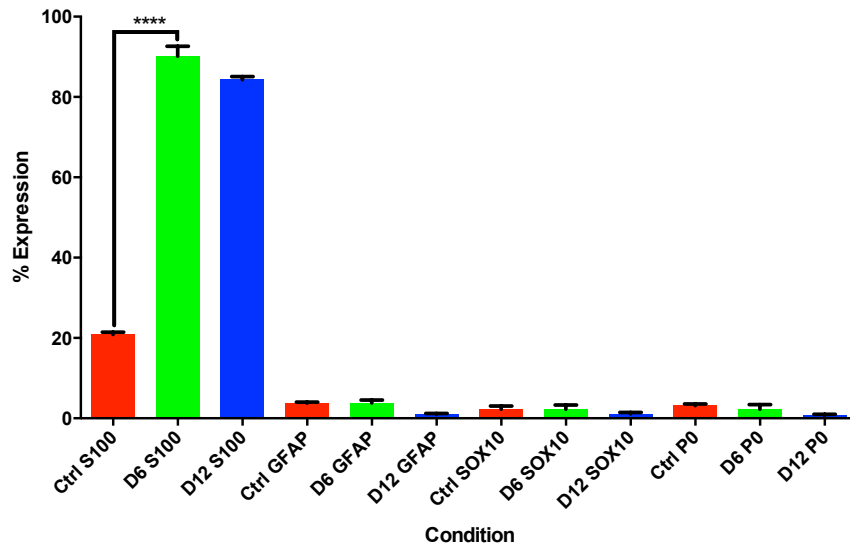
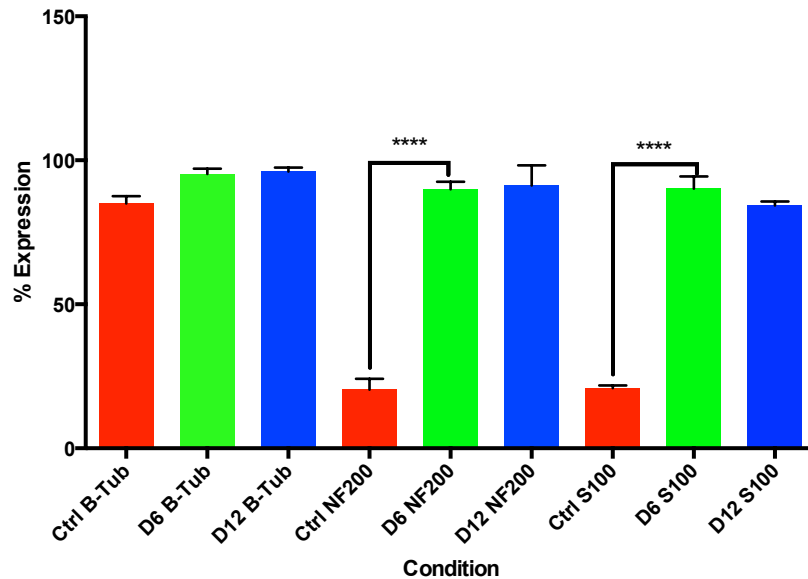
A**B**

Fig 3.18a – Mean percentage expression of S100 alongside mean percentage expression of the glial markers GFAP, SOX10 and P0 in early passage otic neural progenitors (P1+1+1). **Fig 3.18b** shows mean percentage expression of S100 alongside mean percentage expression of the neuronal markers B-Tubulin and NF200. Percentage expression was calculated against total cells staining with DAPI. Error bars denote standard error from mean. Statistical significance was determined using a one-way ANOVA, with Tukey’s comparison of means performed post-test. **** $P < 0.0001$ ($n=3$)

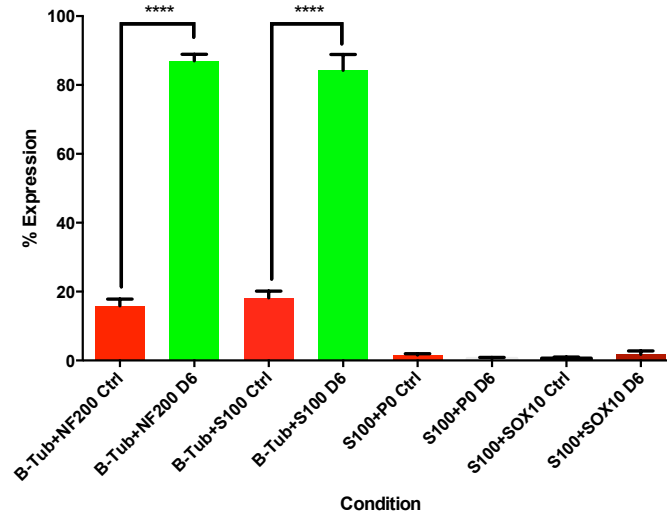
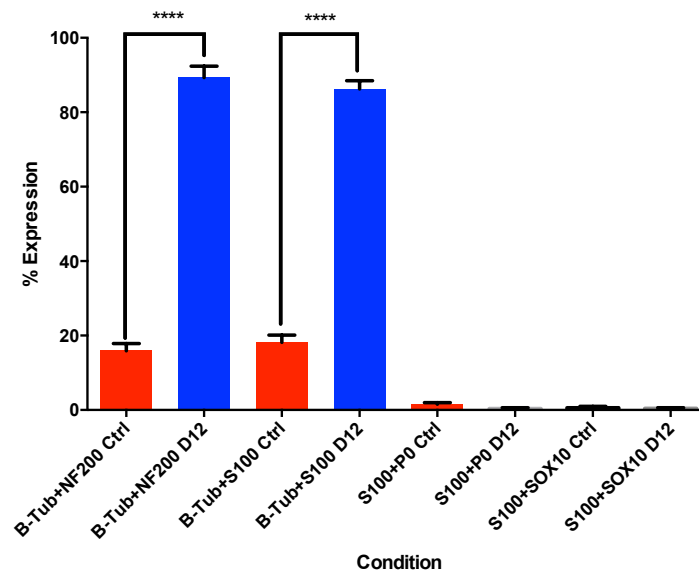
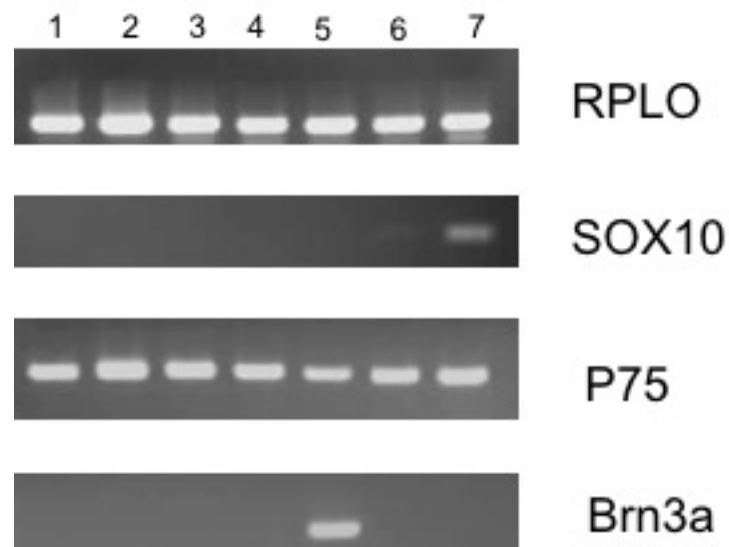
A**B**

Fig 3.19a – Mean percentage co-expression of markers, showing B-Tubulin with NF200, B-Tubulin with S100, S100 with P0 and S100 with SOX10 in early passage otic neural progenitors (P1+1+1) comparing controls in OSCFM with cells at day 6 in the neuralisation protocol. **Fig 3.19b** shows mean percentage co-expression showing B-Tubulin with NF200, B-Tubulin with S100, S100 with P0 and S100 with SOX10 comparing controls in OSCFM with cells fixed at day 12 in the neuralisation protocol. Percentage expression was calculated against total cells staining with DAPI. Error bars denote standard error from mean. Statistical significance was determined using a one-way ANOVA, with Tukey’s comparison of means performed post-test. ****P<0.0001. (n=3)



Lane 1: ONP Ctrl P1+2
 Lane 2: ONP Ctrl P7
 Lane 3: Neural D6 P1+2
 Lane 4: Neural D6 P7
 Lane 5: Neural D12 P1+2
 Lane 6: Neural D12 P7
 Lane 7: SOX10+ve Neural Crest Stem Cells

Fig 3.20 PCR gels from neural differentiation of early vs late passage Shef-1 ONPs showing representative gels for the genes RPLPO, SOX10, P75 and Brn3a (n=3)

3.2.4 Neuralisation of Shef-3.2 Otic Neural Progenitors

The Shef-3.2 cell line was derived from the Shef-3 line, and has been used by other laboratories within the Centre for Stem Cell Biology at the University of Sheffield. Otic neural progenitors derived from this line were placed into the neuralisation protocol, in order to ascertain the gliogenic potential of this line in comparison to Shef-1 derived otic neural progenitors

Shef-3.2 cells from two separate attempts at differentiation were used for these experiments, and were kindly donated by Ben Allen (referred to as Batch A) and Matthew Farr (referred to as Batch B). Early passage ONPs (P1+1 or P2) from each of these differentiations were placed into neuralising conditions. Initial microscopic evaluation of the cells suggested that when Shef-3.2 ONPs were placed into neuralising conditions, they lacked the classic neuronal morphology that was observed in early Shef-1 ONPs. Cells were fixed for immunocytochemistry at day 6 and day 12, whilst control cells in OSCFM were fixed at day 3.

The widespread B-Tubulin expression previously seen in Shef-1 cells was again witnessed in Shef-3.2 cells, however the percentage expression of NF200 and S100 was lower in Shef-3.2 cells (Fig 3.25 and 3.26) than in Shef-1 cells (Fig 3.18b), suggesting that the Shef 3.2 cell line is perhaps not as efficient in producing neuronal-like cells as the Shef-1 line. There was some variation between both of the batches in their ability to differentiate into neuronal-like cells; in batch A, there was some statistically significant upregulation of NF200 and

S100 (Fig 3.25), whilst in Batch B, no statistically significant upregulation of these markers was observed (Fig 3.26).

Given the observation of a reduced neurogenic potential with the Shef 3.2 line, we might have expected the cells to possess a stronger gliogenic potential. However, as was observed with the Shef-1 ONPs, there was hardly any expression of the markers P0 and SOX10, suggesting that whilst these cells are not efficient producers of neuron-like cells, neither do they produce any significant quantities of glial-like cells either (Figs 3.24, 3.27 and 3.28).

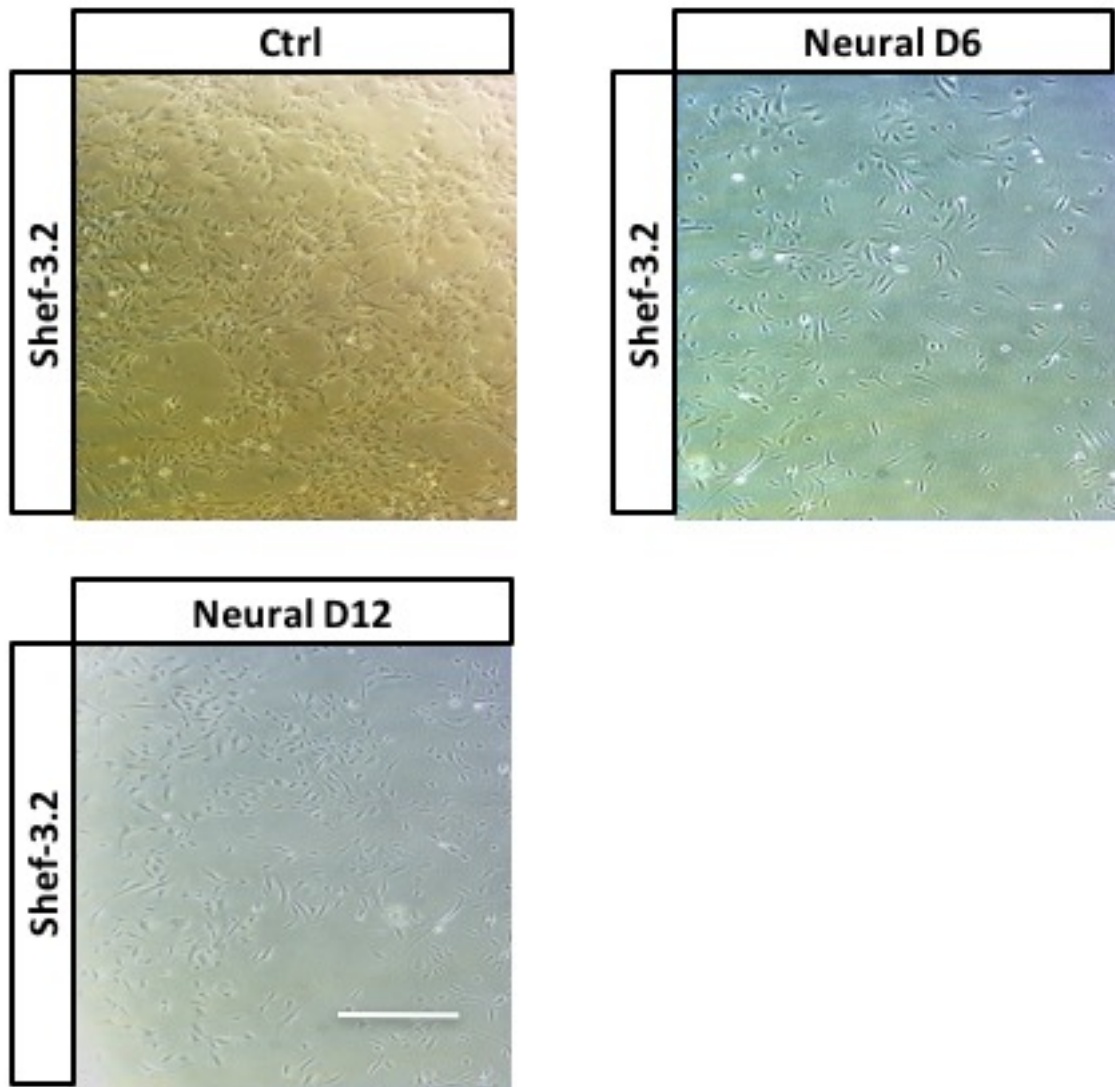


Fig 3.21 – Brightfield microscopy images showing the morphological changes that take place from when Shef-3.2 otic neural progenitors are maintained in OSCFM to when they are placed in neuralising conditions. Scale bars represent 200 μ m

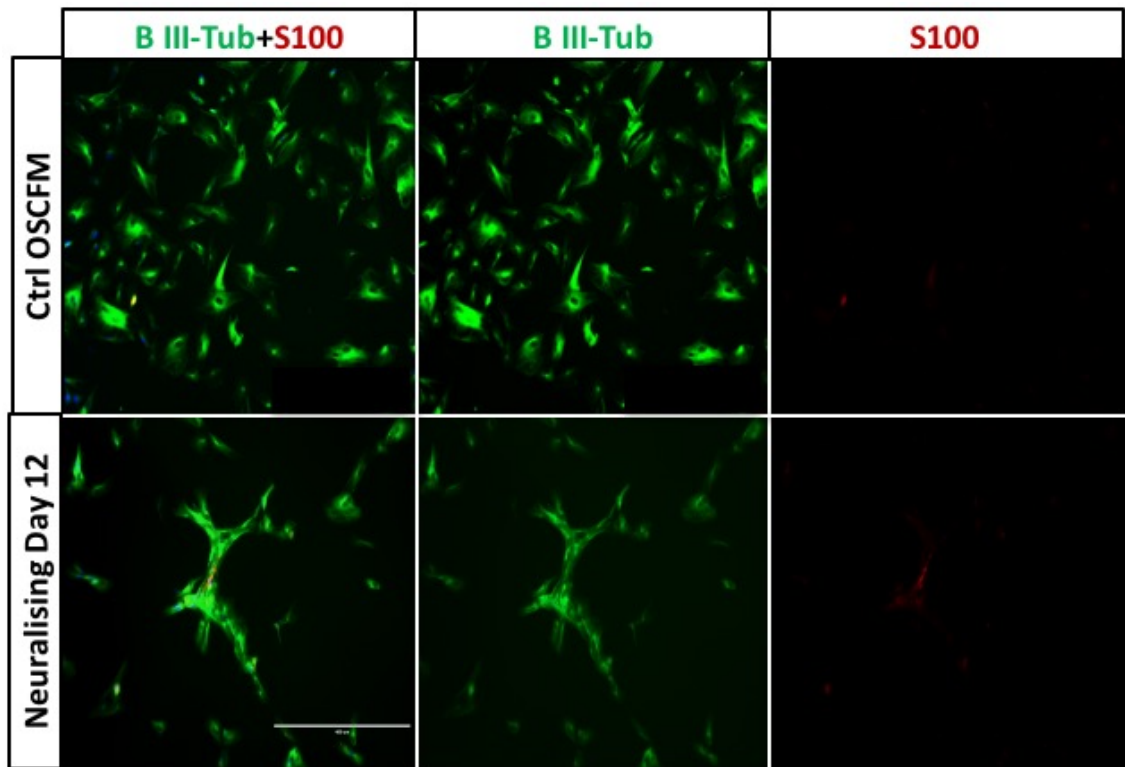


Fig 3.22- Representative images showing immunolabelling in early passage otic neural progenitors with B-Tubulin (green) and S100 (red). Images are of cells in control conditions and at day 12 of neuralisation. Scale bars represent 400 μ m

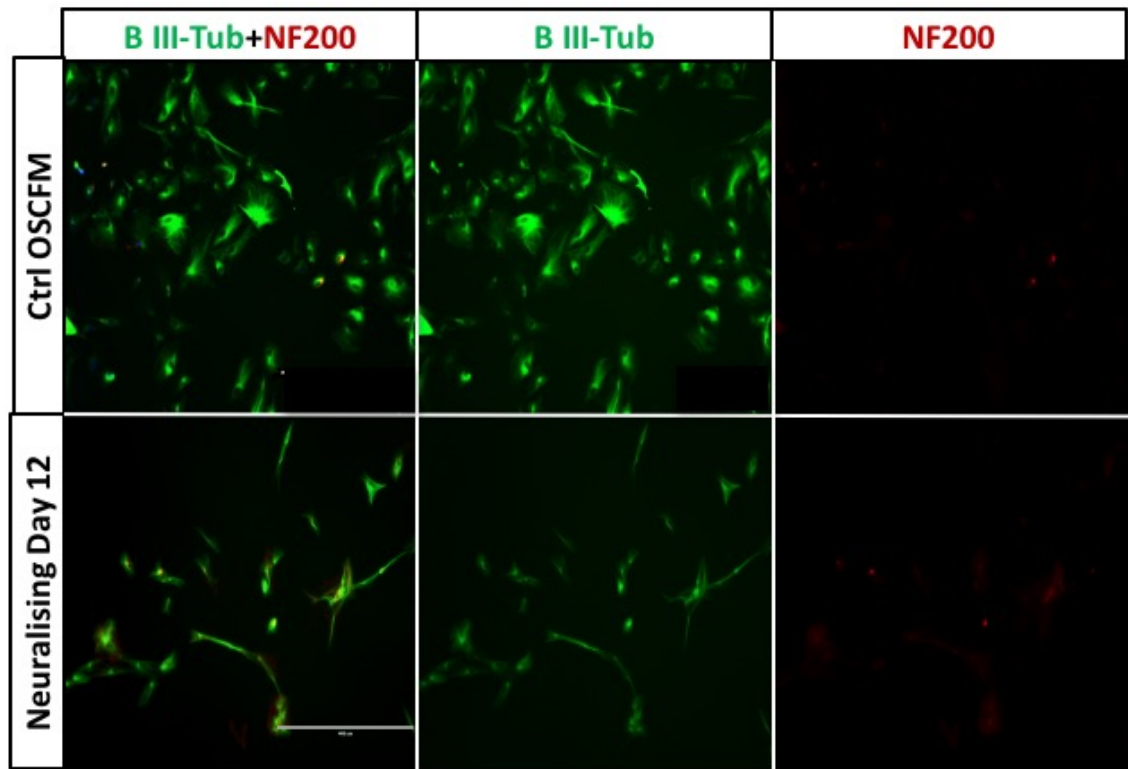


Fig 3.23– Representative images showing immunolabelling in early passage otic neural progenitors with B-Tubulin (green) and NF200 (red). Nuclei were counterstained with DAPI. Images are of cells in control conditions and at day 12 of neuralisation. Scale bars represent 200 μ m

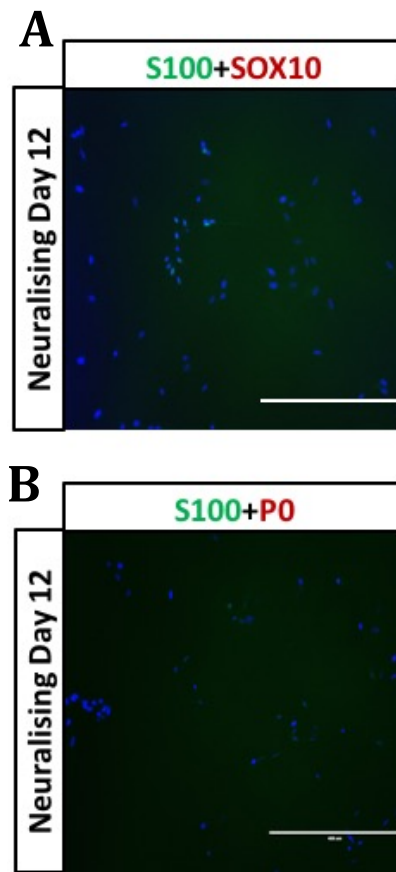


Fig 3.24 – Representative images showing immunolabelling in Shef-3.2 otic neural progenitors with intermediate glial markers. Panel A shows S100 (green) and SOX10 (red) and panel B shows S100 (green) with P0 (red). Nuclei were counterstained with DAPI. Cells were in neuralising conditions and fixed at day 12. Scale bars represent 1000 μ m.

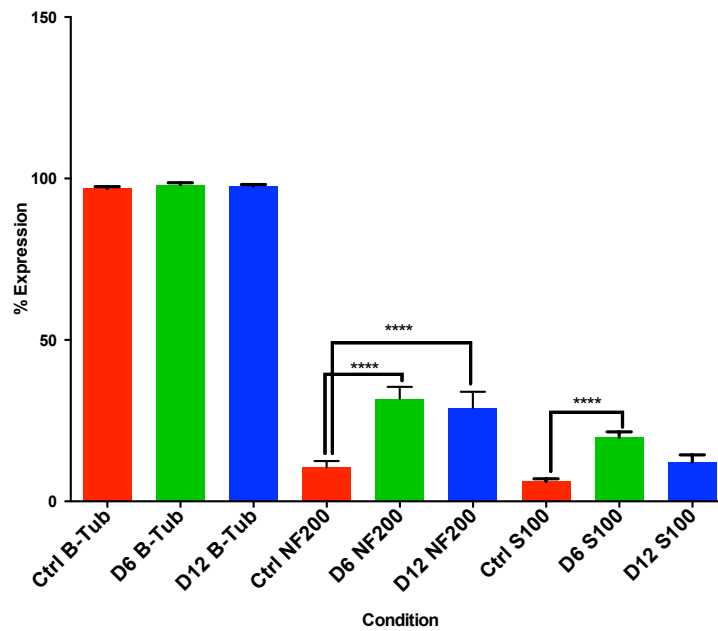


Fig 3.25 – Mean percentage expression of S100 with neuronal markers B-Tubulin and NF200 in early passage Shef-3.2 otic neural progenitors (P1+1). Statistical significance was determined using one-way ANOVA, with Tukey’s comparison of means post-test. Percentage expression was calculated against total cells staining with DAPI. Error bars denote standard error from mean ****P<0.0001, n=1 (*Batch A*)

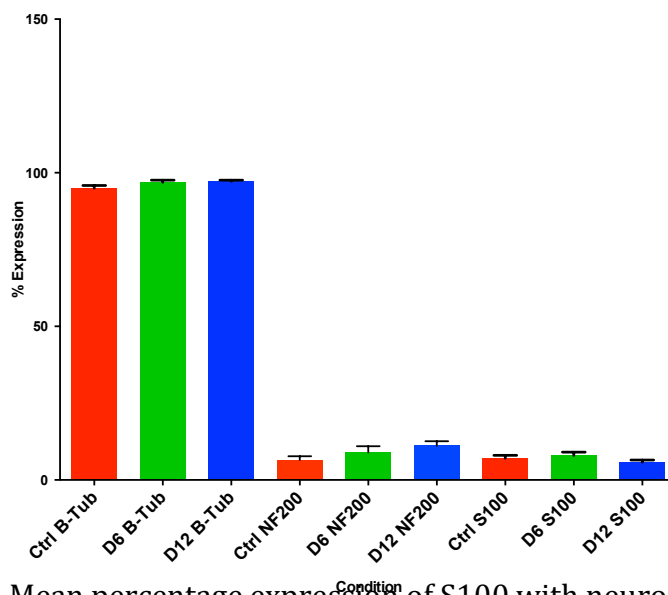


Fig 3.26 – Mean percentage expression of S100 with neuronal markers NF200 and B-Tubulin in early passage Shef-3.2 otic neural progenitors (P2). Statistical significance was determined using one-way ANOVA, with Tukey’s comparison of means post-test. Percentage expression was calculated against total cells staining with DAPI. Error bars denote standard error from mean. No significant difference between means was observed. n=1 (*Batch B*)

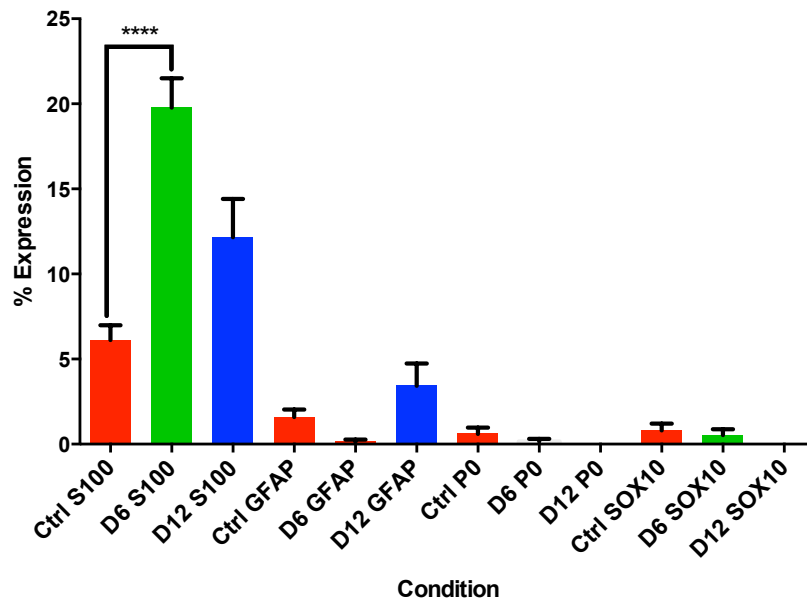


Fig 3.27 – Mean percentage expression of S100 with glial markers GFAP, SOX10 and P0 in early passage Shef-3.2 otic neural progenitors (P1+1). Statistical significance was determined using one-way ANOVA, with Tukey’s comparison of means post-test. Percentage expression was calculated against total cells staining with DAPI. Error bars denote standard error from mean. ****P<0.0001, n=1 (*Batch A*)

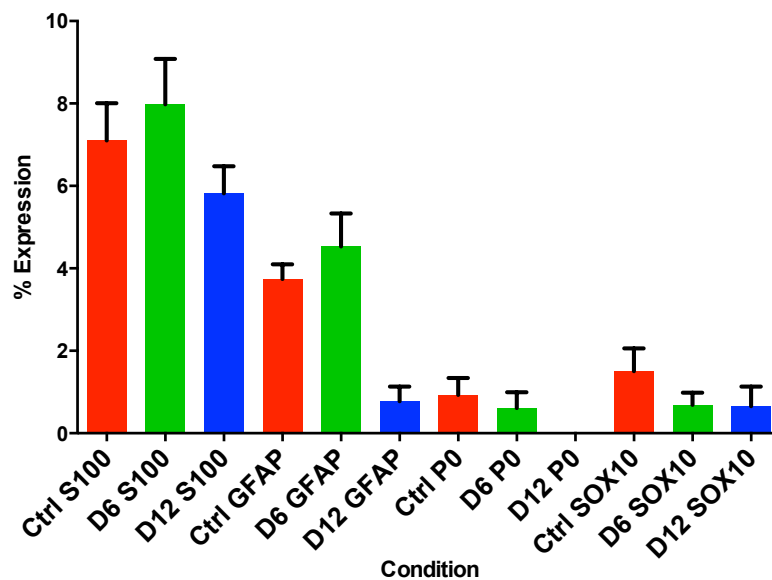


Fig 3.28 – Mean percentage expression of S100 with glial markers GFAP, SOX10 and P0 in early passage Shef-3.2 otic neural progenitors (P2). Statistical significance was determined using one-way ANOVA, with Tukey’s comparison of means post-test. Percentage expression was calculated against total cells staining with DAPI. Error bars denote standard error from mean. No significance difference in means was detected. (*Batch B*)

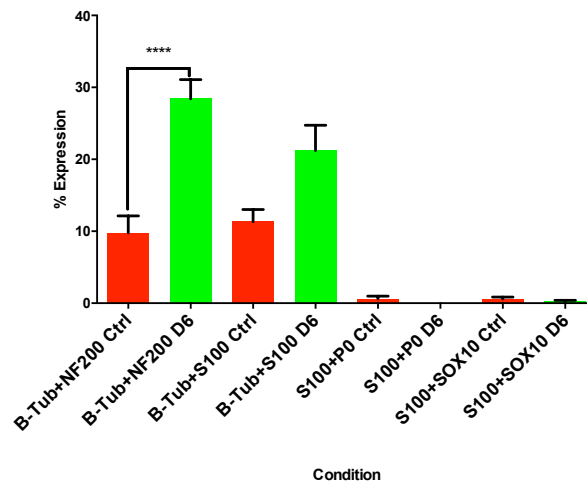


Fig 3.29 – Mean percentage co-expression of B-Tubulin with NF200, B-Tubulin with S100, S100 with SOX10 and S100 with P0 in early passage Shef-3.2 otic neural progenitors (P1+1) Cells were fixed at day 6 and compared to controls in OSCFM. Statistical significance was determined using one-way ANOVA, with Tukey’s comparison of means post-test. Percentage expression was calculated against total cells staining with DAPI. Error bars denote standard error from mean. ****P<0.0001, n=1 (Batch A)

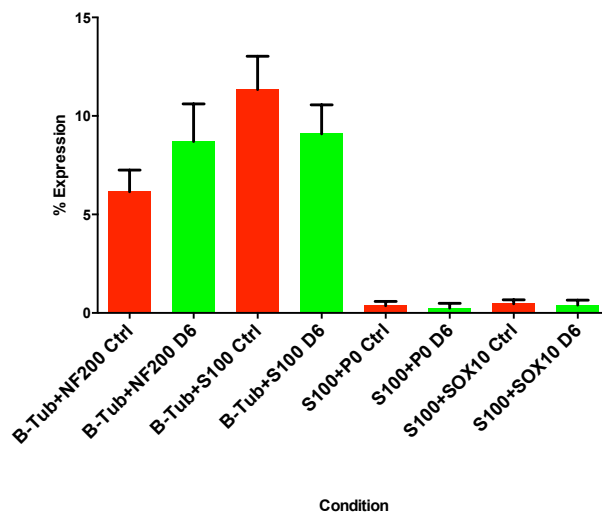


Fig 3.30 – Mean percentage co-expression of B-Tubulin with NF200, B-Tubulin with S100, S100 with SOX10 and S100 with P0 in early passage Shef-3.2 otic neural progenitors (P2) Cells were fixed at day 6 and compared to controls in OSCFM. Statistical significance was determined using one-way ANOVA, with Tukey’s comparison of means post-test. No significant difference between means was observed. Percentage expression was calculated against total cells staining with DAPI. Error bars denote standard error from mean. n=1 (Batch B)

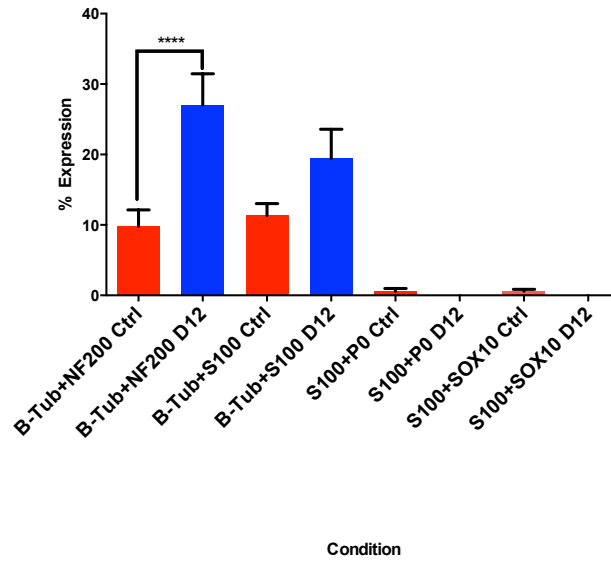


Fig 3.31 – Mean percentage co-expression of B-Tubulin with NF200, B-Tubulin with S100, S100 with SOX10 and S100 with P0 in early passage Shef-3.2 otic neural progenitors (P1+1) Cells were fixed at day 12 and compared to controls in OSCFM. Statistical significance was determined using one-way ANOVA, with Tukey’s comparison of means post-test. Percentage expression was calculated against total cells staining with DAPI. Error bars denote standard error from mean. ****P<0.0001, n=1

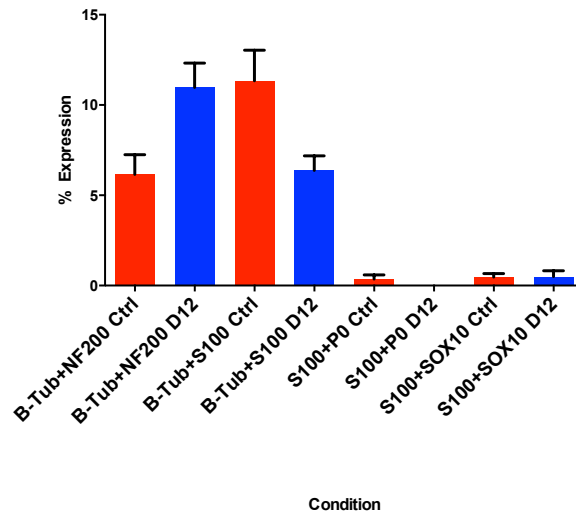


Fig 3.32 – Mean percentage co-expression of B-Tubulin with NF200, B-Tubulin with S100, S100 with SOX10 and S100 with P0 in early passage Shef-3.2 otic neural progenitors (P2) Cells were fixed at day 12 and compared to controls in OSCFM. Statistical significance was determined using one-way ANOVA, with Tukey’s comparison of means post-test. Percentage expression was calculated against total cells staining with DAPI. Error bars denote standard error from mean. n=1 (*Batch B*)

3.2.5 Otic Neural Progenitors do not produce significant amounts of glia in glial-driving conditions

Shf-1 otic neural progenitors appear to efficiently produce neuronal-like cells when placed into neuralising conditions, with hardly any production of glial-like cells. A possible explanation for this phenomenon centres around the neuron-glia switch hypothesis (Anderson, 1995); thus the neuralising protocol maintains the cells within the neurogenic phase, and as a result the cells do not produce much glia. If the otic neural progenitors do indeed possess a neuron-glia switch, then in theory it should be possible to produce glial-like cells from them by culturing them in conditions that shift the switch towards a gliogenic bias.

A protocol for generating Schwann-like cells from neural crest-like cells (derived from human embryonic stem cells) has been described by Lee and colleagues (Lee et al., 2007). In their protocol, neural crest-like cells were differentiated from human embryonic stem cells and continually passaged and maintained in a neural crest-like state until they were ready for differentiating into other cell types. To differentiate into Schwann-like cells, human embryonic stem cells were placed into N2 medium supplemented with ciliary neurotrophic factor, neuregulin-1 and dibutyryl cyclic AMP. The rationale for this protocol lies in the idea that cyclic AMP drives notch signaling, which is thought to be one of the principle signaling pathways in controlling the neuron-glia switch. Alongside this, the addition of neuregulin-1 also helps to push the switch towards a gliogenic phase. In their work, they found that whilst early passage neural crest-like cells lacked the capacity to produce significant quantities Schwann-like cells and instead

produced cells that appeared to be phenotypically neural, later passage cells did produce glial-like cells. They explained this phenomenon by suggesting that their cells go through the natural sequential progression from neurogenesis to gliogenesis, which occurs in neural progenitors of the central nervous system, and has also been suggested to occur in peripheral nervous system development.

Given the relationship that exists between the sensory placodes and the neural crest in utero, the protocol for generating Schwann cells from neural crest-like cells was attempted with Shf-1 otic neural progenitors. From the finding reported by Lee that later passage neural crest-like cells seemed to produce glia more readily, a comparison was made between early and late passage otic neural progenitors, in their ability to produce Schwann cell-like cells in glial-driving conditions.

Cells were cultured as previously described and a gentle trypsinisation step with 0.00625% trypsin was undertaken in order to negate the neuralising effects of a harsh trypsin treatment. Early (P1+1 to P1+3) and late (P1+6, P1+7) passage otic neural progenitors were then cultured in medium containing dibutyryl cyclic AMP, neuregulin-1 and ciliary neurotrophic factor. At the end of the protocol, cells were fixed for immunocytochemistry, while control cells were cultured in OSCFM and fixed at day 3-4.

Early passage otic neural progenitors appear to possess a strong neuronal phenotype when placed in glial conditions, with a markedly significant

upregulation of the markers NF200 and S100, as seen previously in neuralising conditions (Fig 3.33, 3.34 and 3.36). The cells also exhibited a convincing neuronal morphology, extending long processes, although interestingly the neuronal morphology of the cells did differ in glial conditions when compared to cells in neuronal conditions. There was also minimal expression of GFAP (Fig 3.34). This is similar to what was been reported with early neural crest-like cells.

The significant upregulation of S100 and NF200 was not seen in late passage otic neural progenitors, and the cells also did not appear to have neuronal morphology. However, the expression of GFAP remained low, suggesting that older otic neural progenitors still do not seem to differentiate into mature glial cells (Fig 3.35 and 3.37).

As with early otic neural progenitors in neuralising conditions, the upregulation of S100 alongside markers suggestive of a neuronal phenotype with a strong neuronal morphology, suggests yet again that S100 appears to be acting as a neuronal marker within this system (Fig 3.36). To ascertain if this was the case in glial driving conditions, early otic neural progenitors were placed into glial driving conditions, and immunocytochemistry was performed at the end of the protocol for P0 and SOX10 to detect the presence of any immature glial-like cells. One of these experiments was conducted using gelatin as a culture substrate, and another two repeats of this experiment were conducted using laminin/polyornithine as the substrate, which was the same substrate used by Lee et al. In all conditions, there was a significant upregulation in the expression of NF200 and S100 (Figs 3.38 and 3.39), with hardly any co-expression of S100

with P0 or SOX10 (Fig 3.40). Results from all three experiments were therefore analysed together, showing that the increased co-expression of S100 with NF200 and NF200 with B-Tubulin was statistically significant when compared to controls (Fig 3.41). These results suggest that when otic neural progenitors placed in conditions designed to drive glial differentiation, they still do not seem capable of producing significant populations of either immature or mature glial-like cells. Moreover, the upregulation of S100 continues to suggest that it seems to be a marker of neuronal phenotype within this paradigm.

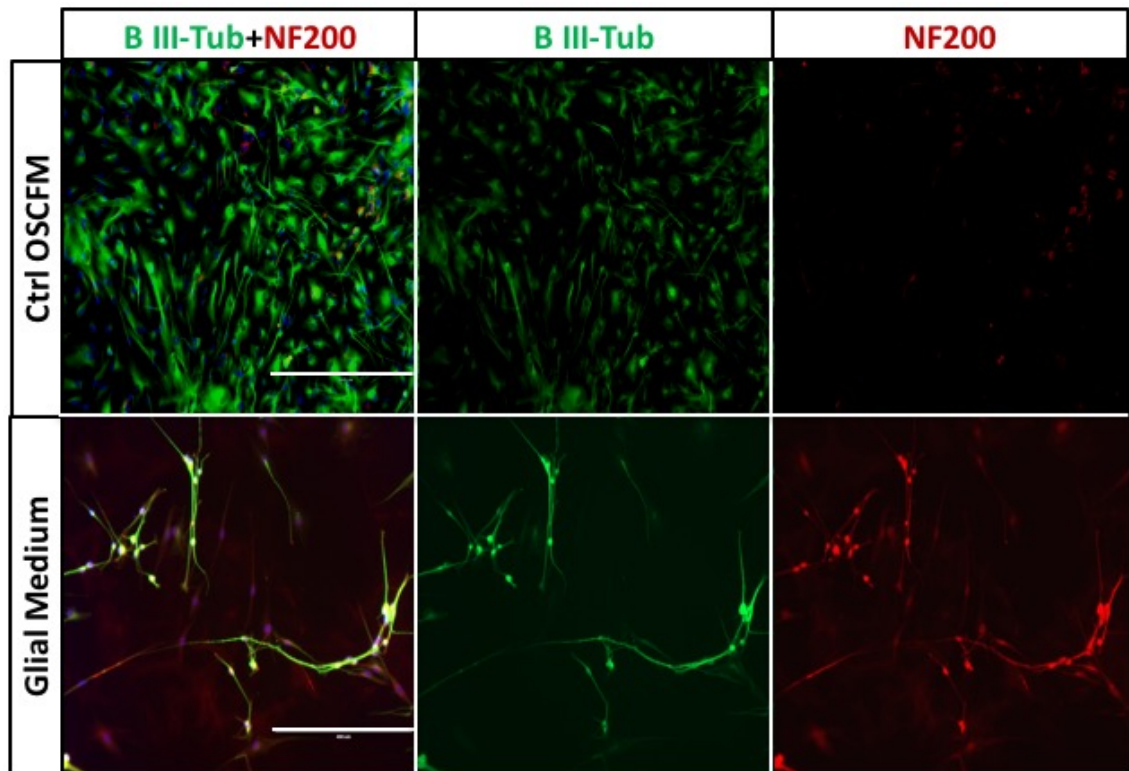


Fig 3.33– Representative images showing immunolabelling in early passage Shef-1 otic neural progenitors with B-Tubulin (green) and NF200 (red). Images are of cells in control conditions and at the culmination of the glial protocol. Scale bars represent 400µm

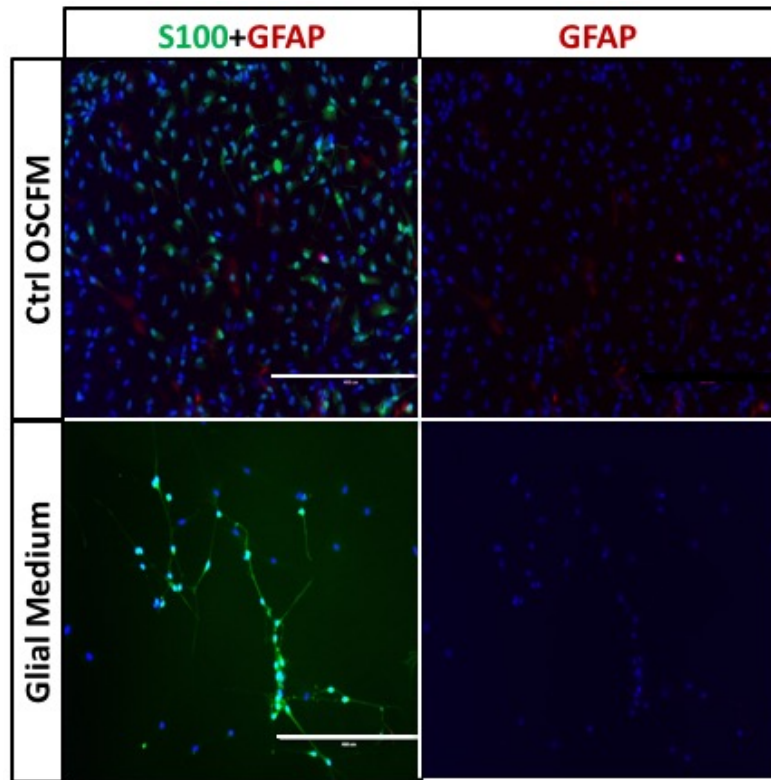


Fig 3.34– Representative images showing immunolabelling in early passage Shef-1 otic neural progenitors with S100 (green) and GFAP (red). Images are of cells in control conditions and at the culmination of the glial protocol. Scale bars represent 400µm

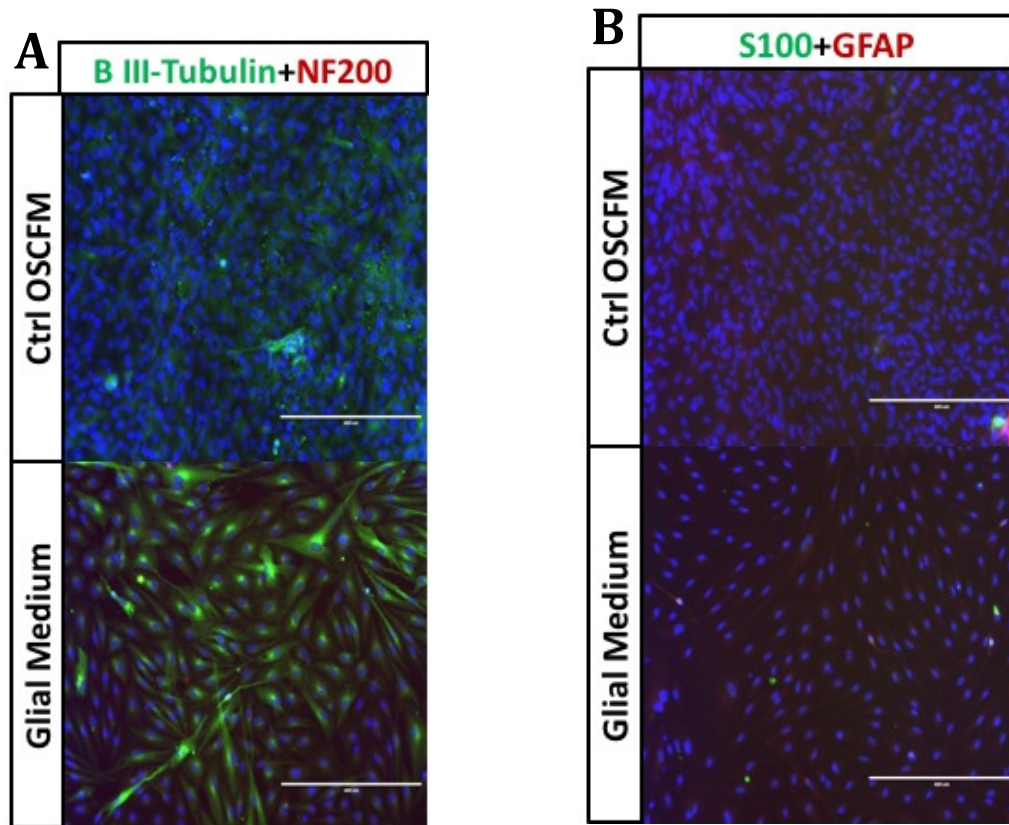


Fig 3.35 – Representative images showing immunolabelling in late passage Shef-1 otic neural progenitors in control conditions and at the culmination of the glial protocol. Panel A shows B-Tubulin (green) and NF200 (red) and panel B shows S100 (green) and GFAP (red). Scale bars represent 400µm.

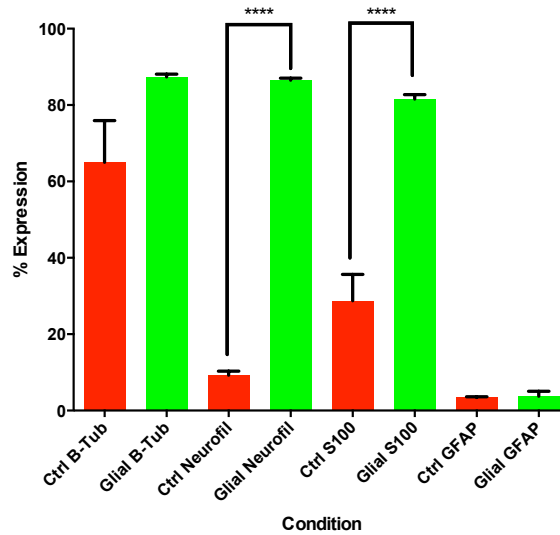


Fig 3.36 – Mean percentage expression of B-Tubulin, NF200, S100 and GFAP in early passage Shef-1 otic neural progenitors (P1+2, P1+3) Cells were fixed at day 12 and compared to controls in OSCFM. Statistical significance was determined using one-way ANOVA, with Tukey’s comparison of means post-test. Percentage expression was calculated against total cells staining with DAPI.. Error bars denote standard error

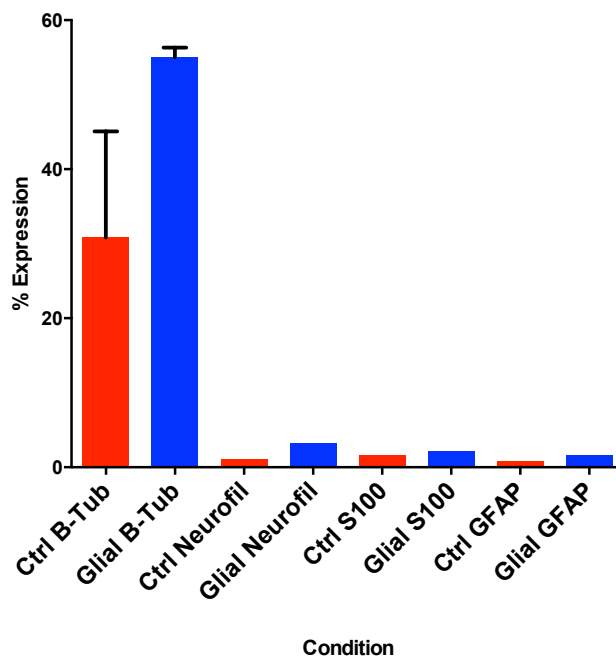


Fig 3.37 – Mean percentage expression of B-Tubulin, NF200, S100 and GFAP in late passage Shef-1 otic neural progenitors (P1+6, P1+7). Cells were fixed at day 12 and compared to controls in OSCFM. Statistical significance was determined using one-way ANOVA, with Tukey’s comparison of means post-test. There was no significant difference between means. Percentage expression was calculated against total cells staining with DAPI. Error bars denote standard error from mean. n=2

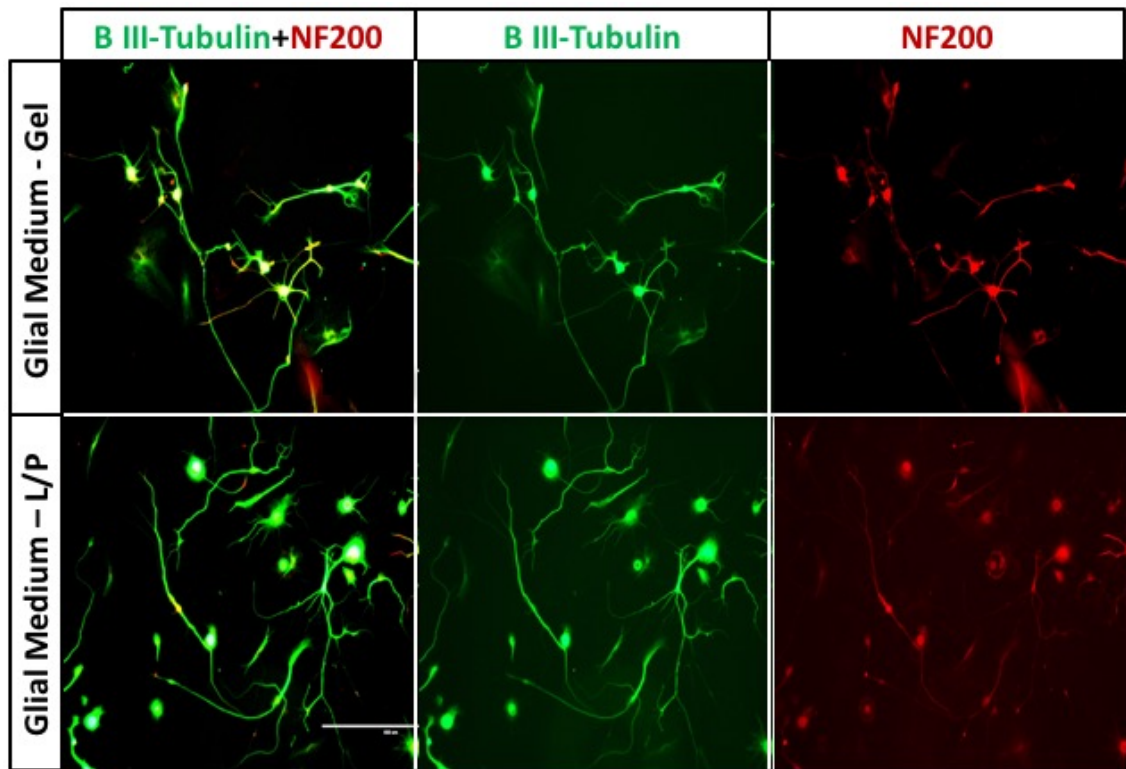


Fig 3.38– Representative images showing immunolabelling in early passage Shef-1 otic neural progenitors with B-Tubulin (green) and NF200 (red). Cells were in glial conditions on either gelatin or Laminin/Polyornithine and fixed at day 12. . Scale bars are 400µm

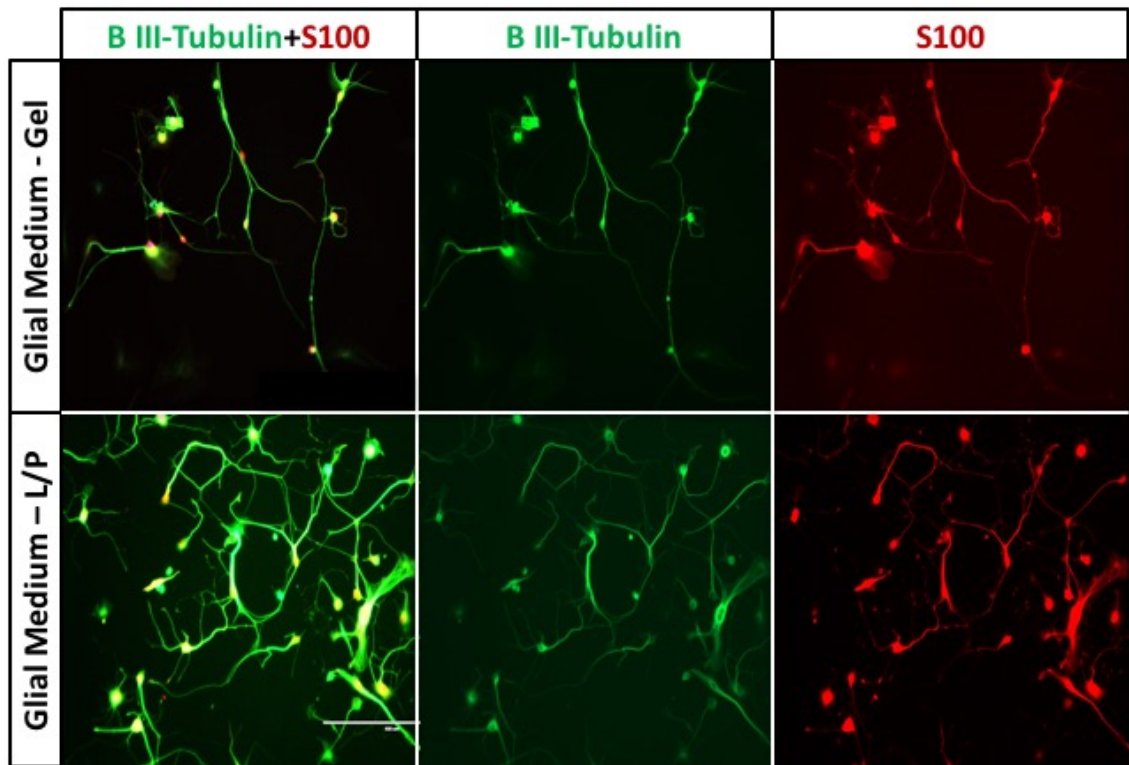


Fig 3.39– Representative images showing immunolabelling in early passage Shef-1 otic neural progenitors with B-Tubulin (green) and S100 (red). Cells were in glial conditions on either gelatin or laminin/polyornithine and fixed at day 12. Scale bars are 400µm

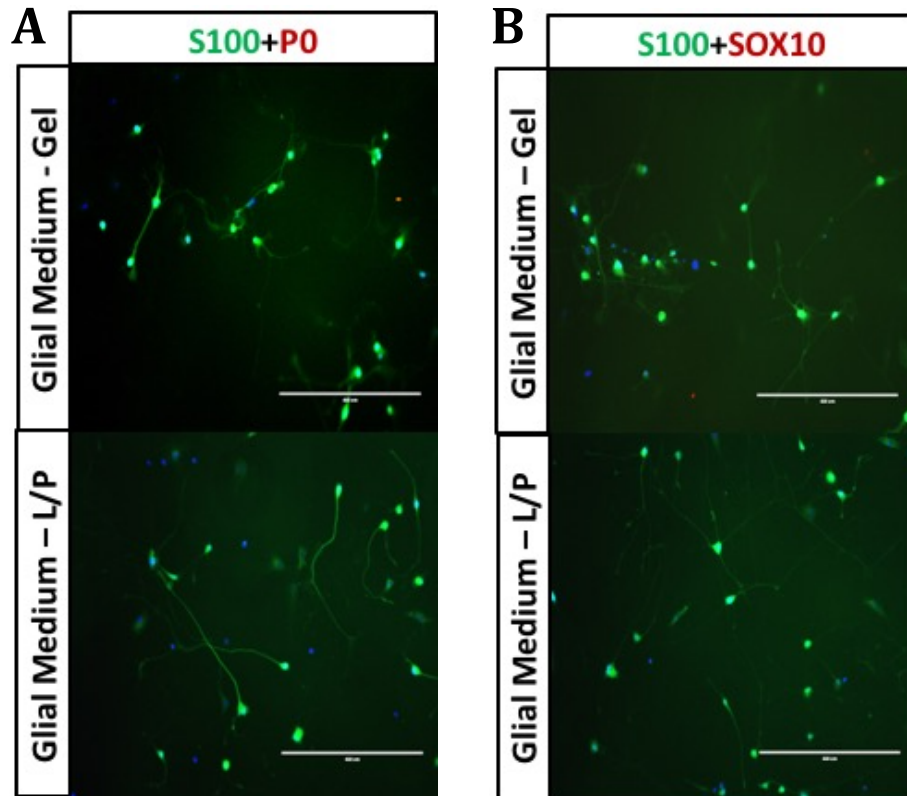


Fig 3.40 - Representative images showing immunolabelling in late passage Shef-1 otic neural progenitors in control conditions and at the culmination of the glial protocol. Cells were grown either on Gelatin or Laminin/Polyornithine. Panel A shows S100 (green) and P0 (red) and panel B shows S100 (green) and SOX10 (red). Scale bars represent 400µm.

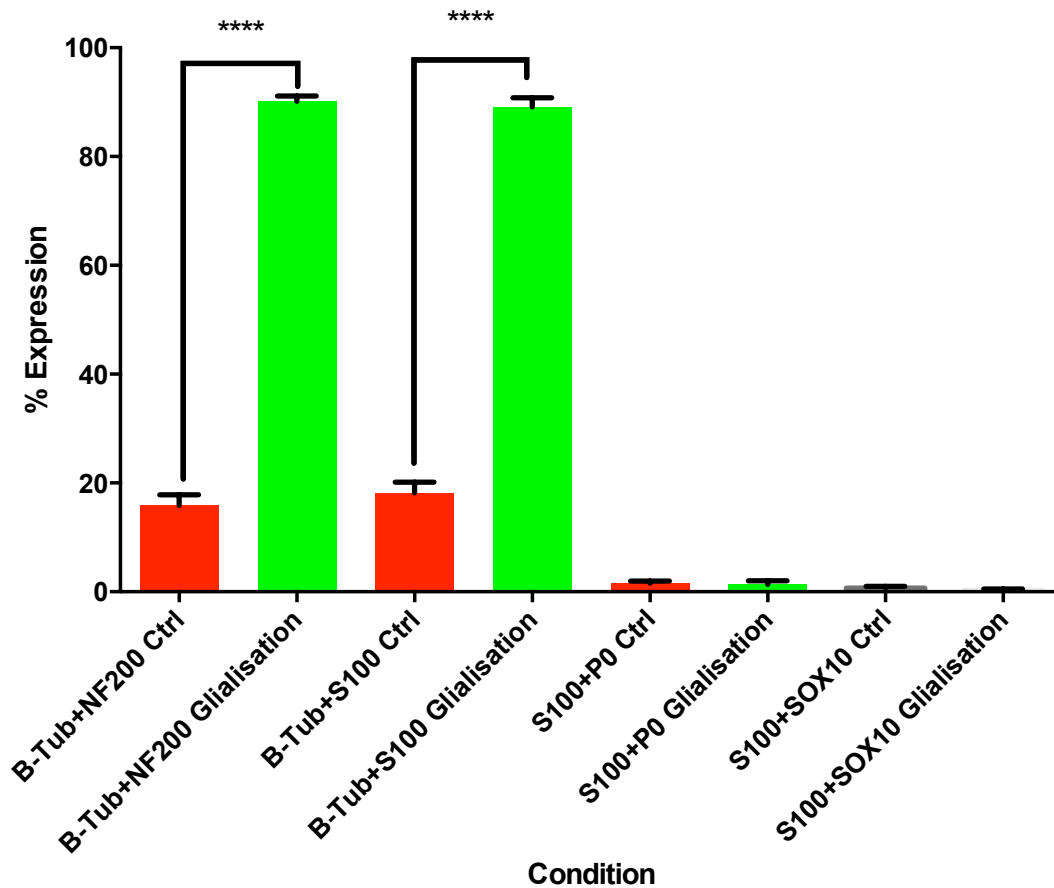


Fig 3.41 – Mean percentage co-expression of B-Tubulin with NF200, B-Tubulin with S100, S100 with SOX10 and S100 with P0 in early passage Shef-1 otic neural progenitors (P1+1) in glial conditions. Cells were fixed at day 12 and compared to controls in OSCFM. Statistical significance was determined using one-way ANOVA, with Tukey’s comparison of means post-test. Percentage expression was calculated against total cells staining with DAPI. Error bars denote standard error from mean. ****P<0.0001,

3.3 Discussion

3.3.1 Late passage ONPs lose the ability to differentiate into neurons

One of the most notable findings was that as ONPs are continually passaged and maintained in OSCFM, they appear to lose the ability to differentiate into neurons. Early passage Shes-1 otic neural progenitors that were placed in both neuralising conditions and conditions aimed at driving glial differentiation resulted in an extremely high quantity of neuronal-like cells, which displayed characteristic neuronal morphology, with upregulation of NF200 and S100, which appeared to be acting as a neuronal marker. In later passage cells, this upregulation was not seen, and cells lacked the typical neuronal morphology that was seen in younger cells.

It therefore seems apparent that the maintenance procedures which aim to keep otic neural progenitors within their progenitor state are inducing a gradual phenotypic change within the cells which make them less prone to differentiating into neurons. The effects of serial passaging in reducing the differentiation potential of stem cells is a well-known phenomenon, and has been reported within other systems. For example, Zhao et al. have observed that long term expansion of adipose derived stem cells has a negative impact on the adipogenic and chondrogenic differentiation potential of the cells (Zhao et al., 2012), whilst Kretlow and colleagues have reported similar decreases in the chondrogenic and osteogenic potential of bone marrow derived stem cells subject to serial passaging (Kretlow et al., 2008).

Within the context of otic neural progenitors, a possible explanation for this might be that as the cells age, they undergo an epithelial-mesenchymal transition. In development, neural crest cells take on mesenchymal morphology as they delaminate and migrate towards their eventual destinations in the periphery, which is controlled by the *snail* family of transcription factors (Nieto, 2002).

Given that the neural crest and otic placodes both originate from the ectoderm, and the similarities they share in producing migratory cells, it has been suggested that the mechanisms underlying this process may also be similar (McCabe et al., 2004). However, whilst developmental studies of the neurosensory placodes in the chick have suggested that migratory cells of the placodes do not undergo an epithelial-mesenchymal transition (Lassiter et al., 2014, Graham et al., 2007), the expression of *snail2* (an epithelial-mesenchymal transition marker) has been demonstrated in the neurogenic area of the otic placode within the developing zebrafish (Maier et al., 2014, Whitfield et al., 2002). Future experiments may therefore focus on whether the hESC derived otic neural progenitors undergo an epithelial-mesenchymal transition as they age, which not only would help to explain the diminished neurogenic potential of older otic neural progenitors, but would also yield some insight as to whether the phenomenon of mesenchymal transition occurs in developing human otic placodal cells.

Another possible explanation lies in the karyotypic changes that have been reported to occur in human embryonic stem cell cultures. The phenomenon of 'culture adaption' has been reported to occur within stem cell cultures, whereby genetically mutated cells with better growth and survival characteristics are able

to essentially take over the culture system (Baker et al., 2007, Enver et al., 2005). It has been postulated that the process of culture of culture adaption may mimic the process through which cancer cells acquire their malignant properties (Baker et al., 2007, Harrison et al., 2007). Interestingly, it has been reported that later passage cells are twice more likely to obtain karyotypic changes than earlier passage cells, and cells which undergo passaging with enzymatic methods also seem to be more prone to genetic abnormalities (International Stem Cell et al., 2011). Through such changes, cells may become 'nullipotent', whereby cells continue to renew but lose their ability to differentiate (Na et al., 2014).

Given that otic neural progenitors are essentially stem cells fate-restricted to an otic phenotype, it is possible that the processes of enzymatic passaging and maintenance in OSCFM induces karyotypic changes within the cells, which prevents them from differentiating into neuronal phenotypes. However, it must be remembered that the results presented in this chapter are from a limited set of experiments, and further work is required to ascertain whether 'culture adaption' occurs during the expansion phase of otic neural progenitor cultures.

3.3.2 S100 as a neuronal marker.

One of the unexpected findings was the expression of S100 with the neuronal markers NF200 and B-Tubulin, and the lack of co-expression with glial markers such as GFAP, P0 and SOX10.

S100 is a low molecular weight calcium binding protein, of which there are over 20 members (Donato et al., 2009). It has long been suggested that subtypes of the S100 protein are specific to particular cell types, based around observations from immunohistochemistry and PCR (Donato, 2003). However, the situation may be more complex than this; for example, S100B is not known to be expressed in normal cardiac myocytes, but is greatly upregulated in the rat myocardium following an ischaemic insult (Tsoporis et al., 1997). This raises the possibility that S100 expression isn't necessarily tissue specific, rather its expression is controlled by transcriptional regulation under the influence of environmental factors.

Classically, S100B is often cited in the literature as a 'glial marker', however S100B has been noted to be expressed in CNS neurons in both the rat and mouse (Friend et al., 1992, Rickmann and Wolff, 1995). Specifically, a widespread expression of S100B in the cortical, cerebellar and hippocampal neurons of both species has been reported (Vives et al., 2003), and S100B mRNA is reported to be present in the trigeminal nucleus of mice (Yang et al., 1996). S100B may also be expressed in proliferative neural progenitor cells that go on to produce neurons (Namba et al., 2005). Within the context of inner ear development, S100

expression has been noted to occur within the developing cochleovestibular ganglion of the mouse (Buckiova and Syka, 2009) and the human (Pechriggl et al., 2015), and within our otic differentiation model based upon signaling mechanisms in development, cells with a convincing neuronal morphology which co-expressed B-tubulin and NF200 also widely co-expressed S100.

Taking all these findings together, it should be apparent that the notion of S100B being a specific glial marker must be questioned, as it can be expressed by subtypes of neurons, both in the mammalian adult and also in development.

3.3.3 Otic Neural Progenitors Do Not Appear To Produce Significant Populations of Glia.

Early passage Shf-1 otic neural progenitors do not appear to generate significant populations of glia in neuralising conditions. In conditions aimed at driving glial differentiation, rather than witnessing glial differentiation, the cells continued to neuralise and although they retained a similar expression profile on immunocytochemistry to cells in neuralising conditions, the neuronal morphology was clearly different.

It is generally believed that unlike the other sensory placodes, putative vestibulocochlear neurons are exclusively placodal in origin, and their associated glial progenitors are chiefly derived from the neural crest. Freyer has contested this idea, using Wnt1-Cre, Pax3^{Cre/+} and Hoxb1^{Cre/+} to fate map cranial

neuroepithelial cells (Freyer et al., 2011). With respect to cochlear glial development, they showed that although SOX10 expressing cells within the developing cochleovestibular ganglion generally originate from the neural crest, there does seem to be some contribution from the otic placode, suggesting a dual embryological origin of glial progenitors within the cochleovestibular ganglion. To try and gain further insight into this, Mao and colleagues used the SOX10^{ff}, Tg(Wnt1-Cre) mouse to conditionally delete neural crest derived SOX10, allowing for otic SOX10 expression to persist. They found a total absence of putative Schwann cells within this model, with aberrant growth of spiral ganglion neurons (Mao et al., 2014). The finding from studies such as this, in conjunction with recent studies of human fetal cochlear development, all suggest that glial cells of the developing vestibulocochlear nerve originate chiefly from the neural crest.

The finding that otic neural progenitors do not appear to produce significant populations of glia therefore seems to mimic the situation *in utero*, where neural progenitors in the otic placode do not produce glia (Breuskin et al., 2010). This suggests that just like their *in utero* counterparts, otic neural progenitors are fate restricted to a neuronal lineage, and lack the plasticity to generate putative glial cells. The finding that later passage cells equally do not generate glia may indicate that these cells do not possess gliogenic properties.

The idea that neural progenitors in the peripheral nervous system sequentially progress from a neurogenic to gliogenic phase as seen in the central nervous system has been questioned. Whilst the effects of Notch signaling in promoting gliogenesis from neural crest stem cells has been demonstrated *in vitro* have

added strength to this hypothesis (Morrison et al., 2000), data from *in vivo* studies has suggested that rather than initiating a neuron-glia switch in the neural crest, Notch signaling acts further downstream in promoting the differentiation of Schwann cell precursors into immature Schwann cells (Woodhoo et al., 2009). Thus, a possible explanation for the observations by Lee et al. that their protocol generates Schwann-like cells from later passage neural crest-like cells (Lee et al., 2007), is that rather than the cells undergoing a sequential shift towards gliogenesis, the effect of the cells being maintained within a complex cell culture medium results in some of the cells differentiating into Schwann cell precursors, which are receptive to notch signaling and neuregulin signaling to stimulate these cells to produce populations of immature glia. If this is the case, then this would explain why we don't see glial-like cells being generated from later passage otic neural progenitors, as an upregulation of Schwann cell precursor markers such as P0 and SOX10 is not seen in later passage cells in OSCFM, suggesting that there isn't a population of precursor cells that might be responsive to the cues provided by the glial medium.

Whilst the data do indeed point towards a conclusion that otic neural progenitors do not produce glia, there are a number of points which must be considered before establishing this as a firm conclusion. Firstly, whilst the glial differentiation protocol produced cells with a neuronal phenotype, we were unable to demonstrate that the protocol can reliably and convincingly produce glial-like cells. Ideally, a set of experiments are required demonstrating a glial differentiation protocol that effectively produces glia within a neural crest-like cell line, prior to implementing the same protocol on the otic neural progenitors.

The rationale for using the protocol by Lee et al. to generate glia was on the basis of the similarities between the neural crest and the otic placode (both having an ectodermal origin), in conjunction with the fact that their protocol was based on work human embryonic stem cells. However, one of the weaknesses in their methodology is that they report the generation of glia solely on the basis of an upregulation of GFAP in older neural crest-like cells. GFAP is by no means a specific Schwann cell marker; it is commonly expressed in astrocytes and in neural progenitor cells, and thus it is difficult to conclude the presence of peripheral glial-like cells purely on the basis of this marker alone. Thus, in order to truly ascertain the gliogenic potential of otic neural progenitors, a number of glial differentiation protocols need to be employed upon the otic neural progenitors.

The finding that the glial protocol produced cells with neuronal morphology that was distinct from the neuronal morphology was also an interesting and unexpected finding, and it would be useful to further characterize the neuronal-like cells generated from this protocol, through real-time PCR and patch-clamping, to ascertain if they truly are spiral ganglion-like neurons, or if they are neurons with a differing phenotype.

CHAPTER 4: THE INTERACTION BETWEEN OTIC NEURAL PROGENITORS AND GLIA *IN VITRO*

4.1 Introduction

With the finding that otic neural progenitors do not readily produce glial-like cells when cultured *in vitro*, this raises the possibility that transplanted otic neural progenitors will be reliant upon the glial environment of the host for long term support, maintenance and survival. To gain further insight into how otic neural progenitors might interact with glia, co-cultures were set up *in vitro* to study the effect of peripheral and central glial cells on neurite extension from the otic neural progenitors.

4.1.1 Early interactions between axons and Schwann Cells

An intimate relationship is established between neural progenitors and Schwann cell precursors early on in development, where Schwann cells closely associate with developing axons and obtain survival cues through paracrine signaling. Neuregulin-1 in particular is a key molecular signal from immature neurons in helping to control the proliferation and maintenance of Schwann cell precursors (Jessen and Mirsky, 2005). The dependence of Schwann cell precursors upon paracrine signaling mechanisms from developing axons for their survival facilitates putative Schwann cells to be appropriately paired with neurons during their genesis. As Schwann cell precursors progress through their maturation pathway to become immature Schwann cells, they become less reliant on

paracrine signals for their survival and maintenance, as they establish in-house autocrine mechanisms for their survival. *In vitro* experimentation suggests that some of these autocrine factors include leukaemia inhibitory factor, insulin-like growth factor 2, lyophosphatidic acid, neurotrophin-3 and platelet derived growth factor-beta (Meier et al., 1999, Dowsing et al., 1999, Li et al., 2003c). In return for the neuregulin-1 support they receive from developing axons, Schwann cell precursors and immature Schwann cells support neuronal maturation through neurotrophin signaling (Newbern, 2015).

4.1.2 Radial Sorting

Radial sorting is the process whereby large axons for myelination are distinguished from axons with a smaller diameter, which generally remain unmyelinated within structures known as Remak Bundles.

Much of our understanding around the process of radial sorting came from work undertaken by Webster and colleagues, through examining serial sections of developing neurons in littermates by electron microscopy (Webster, 1971). In his work he described a common family of immature Schwann cells that arrange axons into bundles and secrete a common basal lamina between them. Schwann cells then send out cytoplasmic projections and through mitotic division of cells, larger diameter axons are segregated towards the periphery. As Schwann cells continue to divide, they eventually establish a 1:1 relationship with the larger diameter axons, and these Schwann cells will eventually go on to myelinate these axons (Feltri et al., 2016). The process continues until only smaller diameter

axons remain that go on to form Remak Bundles, whereby a single Schwann cell essentially ensheathes multiple small axons that remain unmyelinated; being separated from one another with a thin layer of cytoplasm (Grigoryan and Birchmeier, 2015).

4.1.3 The Role of Notch Signaling

As mentioned previously in Chapter 3, within the context of peripheral glia, Notch signaling seems to play an important role in the maturation of Schwann cell precursors into immature Schwann cells. Studies by Woodhoo and colleagues examined this idea by blocking Notch signaling through loss-of-function mutations, illustrating a marked reduction in the proliferation of Schwann cell precursors and a notable delay in the expression of characteristic markers associated with immature Schwann cells (Woodhoo et al., 2009).

Alongside its role in maturation, Notch signaling appears to make Schwann cells more receptive to Neuregulin signaling from associated axons, through the upregulation of the receptor protein ErbB2 (Woodhoo et al., 2009).

4.1.4 The Role of Neuregulin Signaling

Neuregulin signaling plays a fundamental role in the regulation of Schwann cell activity, both in development and in the mature state. Neuregulin is released from neighboring axons, and acts upon the tyrosine kinase receptors ErbB2 and ErbB3

on Schwann cells inducing its proliferative effects via the MAP-Kinase (Newbern and Birchmeier, 2010).

In mutant mouse models where neuregulin signaling is severely disrupted or absent, Schwann cell precursors and Schwann cells appear to be almost absent, suggesting that neureglins play a quintessential role in maintaining the survival of peripheral glia (Morris et al., 1999). Aside from its role in maintaining survival, neuregulin signaling is also involved in the transition of Schwann cell precursors into immature Schwann cells, and also plays a part in facilitating radial sorting (Meyer and Birchmeier, 1995).

Neuregulin signaling may also play a role in the fate determination from immature Schwann cell to either myelinating or non-myelinating mature phenotypes. It has been suggested that larger neurons express neuregulin-1 in larger quantities, thus resulting in Schwann cells adopting a myelinating phenotype capable of producing thick wrappings of myelin around large-diameter axons. Conversely, thinner neurons produce significantly less neuregulin, and thus they adopt a non-myelinating phenotype (Michailov et al., 2004).

4.1.5 Schwann Cell-Neuronal Co-culture systems

Understanding the mechanisms of interaction between Schwann cells and neurons during development, and subsequently in the mature state, is a fundamental ingredient in achieving the ultimate goal of peripheral nerve regeneration. *In vitro* co-culture systems of Schwann cells and neuronal cells

facilitate further study of cell interaction with a particular focus on cell-cell contacts, alongside providing models through which cell signaling mechanisms might be modulated to facilitate neuronal regeneration.

In earlier studies Seilheimer and Schachner cultured neurons from dorsal root ganglia on either Schwann cell or fibroblast monolayers. They showed that neurite outgrowth was more extensive on Schwann cell monolayers as compared to outgrowth on fibroblast monolayers. They also illustrated that Schwann cells established strong adhesion to adjacent neurites through the adhesion molecule L1, with N-CAM and J1 playing less of a role, and when antibodies to L1 were added to the culture system, neurite outgrowth was significantly inhibited (Seilheimer and Schachner, 1988). Others have similarly shown that L1 alongside N-CAM appear to play an important role in regulating the growth and guidance of neurite growth in *in vitro* co-culture systems (Bixby et al., 1988, Martini et al., 1994).

There is also some evidence to suggest that Schwann cells play a role in guiding neurite extension from a neuronal growth cone. Thompson and Buettner dissociated rat spinal neurons and grew them on orientated Schwann cell monolayers and showed that the orientation of neurite growth followed that of Schwann cell alignment by comparing the angle of growth between neurites and their adjacent Schwann cells (Thompson and Buettner, 2006). Similarly, Seggio et al have also shown that Schwann cell orientation is an important factor in directing neurite growth within an *in vitro* co-culture system, suggesting that the

mechanism of neurite guidance is likely to be as a result of cellular contact, as opposed to the secretion of soluble factors (Seggio et al., 2010).

Co-culture systems can also prove to be useful *in vitro* models through which the effects of modulating cell biology can be assessed to improve neurite growth, which can then subsequently be translated to *in vivo* experimentation. Koppes and colleagues examined the effect of subjecting a Schwann cell-neuronal co-culture system to a direct electrical current. Their results showed that neurite outgrowth was increased 1.2 fold when compared to co-cultures that were not electrically stimulated (Koppes et al., 2011). These results are interesting within the context of a neural regenerative strategy that aims to combine biological therapies alongside electrode neuroprostheses, and given that cochlear implants are without doubt the most successful neuroprosthesis in clinical use at present, the positive effects of electrical stimulation on neurite outgrowth observed in this study and others raises the possibility of a combined electrical/biological neural regeneration strategy for the cochlea (Koppes et al., 2014, Koppes et al., 2016, Song et al., 2016, Richardson et al., 2009).

4.1.6 Central Glial Development

In contrast to the peripheral nervous system, axons within the central nervous system are myelinated by oligodendrocytes. The developmental origin of oligodendrocytes has been a hotly debated topic in the past. Classically, it was thought that oligodendrocytes originated from a specific domain (known as the motor neuron progenitor, or pMN, domain) located in the ventral ventricular zone of the embryonic spinal cord (Rowitch, 2004). However it was later suggested

that oligodendrocytes may also originate from dorsal regions of the cord, implying multiple sites of origin (Richardson et al., 2006b). Within the pMN domain, Sonic Hedgehog signaling activates OLIG2, as OLIG2 progenitors subsequently give rise to motor neurons (Lu et al., 2000). Thereafter, the progenitors downregulate neurogenic transcription factors such as Neurogenin-2 and PAX6, and begin expressing oligodendrocyte transcription factors such as NKX2.2, and migratory oligodendrocyte precursor cells continue to express markers such as platelet derived growth factor alpha (PDGR-alpha) and membrane proteoglycan NG2 (Lee et al., 2005, Stolt et al., 2004, Breuskin et al., 2010).

Oligodendrocyte precursor cells continue to proliferate and migrate to the white matter, where they differentiate into mature oligodendrocytes (Noble et al., 1990, Fok-Seang and Miller, 1994, Richardson et al., 2006a). These cells then extend sheet like structures to axonal targets, providing a means for oligodendrocytes to deliver the components of myelin synthesis to axons (Pedraza et al., 2001, Kursula, 2008, Simons and Trajkovic, 2006). In contrast to the 'radial sorting' of myelinating Schwann cells in the peripheral nervous system, oligodendrocytes myelinate numerous axons simultaneously.

The stages of astrocyte development are not quite as clear as has been described for Schwann cells and oligodendrocytes (Molofsky et al., 2012). In mammalian development, neural stem cells (otherwise known as 'Radial Glia') initially produce neurons, and this is followed by gliogenesis, where they either differentiate directly into astrocytes, or into astrocyte progenitors. This switch is extremely important to ensure proper development of the central nervous system,

and is tightly controlled. Neurogenesis is initiated and maintained via signaling from basic loop-helix-loop transcription factors such as neurogenin-1, which promote neurogenesis whilst repressing gliogenesis (Kanski et al., 2014). During the neurogenic phase the JAK/STAT pathway, which closely interacts with Notch signaling, is also repressed, preventing the premature differentiation of radial glia into putative astrocytes (Wang et al., 2015). The switch from neurogenesis to gliogenesis has been well studied in the ventral spinal cord, where transcription factors such as SOX9 and NFIA have been implicated as regulators of a glial developmental cascade (Kang et al., 2012, Deneen et al., 2006). The Sonic Hedgehog and Notch pathways which are known to play a role in initiating astrocyte development (Garcia et al., 2010), both regulate SOX9 and NFIA respectively (Namihira et al., 2009).

A similar symbiotic relationship to the one that exists between neurons and Schwann cells in development may also be present between immature neurons and putative astrocytes. Developing neurons can release key cytokines that promote gliogenesis, an example being cardiotrophin-1 which, when depleted, results in significant disruptions in astroglial development (Barnabe-Heider et al., 2005). In addition, growth factors such as TGF-beta1 (Stipursky and Gomes, 2007) and BMPs (Nakashima et al., 1999) work in conjunction with these gliogenic cytokines in inducing the JAK/STAT pathway.

4.1.7 The Role of Astrocytes in the Central Nervous System

Astrocytes are the most populous glial cell type within the central nervous system that up until relatively recently were deemed to be merely structural components of the nervous system. Following Virchow's initial description of astrocyte function as 'nerve glue', we now know that astrocytes are an extremely heterogeneous genre of glial cells with multiple functions. It is now widely accepted that astrocytes are involved in the process of synaptic transmission and maintain extracellular homeostasis (Parpura and Zorec, 2010). It has also been postulated that astrocytes play a significant role in maintaining neuronal survival during situations of neuroinflammation (Saijo et al., 2009) and hypoxia (Vangeison and Rempe, 2009). Furthermore, and perhaps more interestingly from the perspective of regenerative medicine, within the SVZ, astrocyte-like cells that express GFAP have been illustrated to be a source of stem/progenitor cells, which can differentiate into neurons in the olfactory bulb of rodent models (Ihrie and Alvarez-Buylla, 2008). There are also some types of highly specialised glia found in specific regions of the CNS; for example Bergmann glia of the cerebellum and Muller glia in the retina may play a role in cell guidance in the developmental phase of their relevant systems (Reichenbach et al., 2010).

4.1.8 Reactive Astrocytes and In Vitro Co-Culture Models of Reactive Gliosis

Pathological insults to the central nervous system can cause significant losses of neurons and oligodendrocytes, with increased permeability of the Blood Brain Barrier. This results in the triggering of an acute inflammatory cascade, and in

the ensuing weeks following the initial insult, the microenvironment around the site of the initial pathology results in the remodeling of astrocytes, which undergo changes in morphology and primary function. The resulting 'reactive astrocytes' can be identified by the over-expression of the classic glial markers such as GFAP and Vimentin.

The traditional view that has prevailed regarding reactive astrocytes is that they are generally a hindrance to axonal regeneration. For example, astrocytes secrete extracellular matrix proteins which are inhibitory to neuronal regeneration by creating a physical barrier. The accumulation of reactive astrocytes with inflammatory cells around the site of neuronal injury is often referred to as the 'glial scar', and although this is thought to be a non-permissive environment for axonal repair, they do help to limit further neuronal damage. The pathogenesis of the glial scar and the debate that surrounds its precise role in neuronal damage and repair will be considered in further detail in chapter 5.

In vitro co-culture models of reactive astrocytes with neuronal cells are an important tool in understanding the mechanism behind the inhibitory effects of reactive astrocytes on neurite outgrowth, and also provide a means through which therapies can be developed to allow neurites to overcome the harsh environment of the reactive glial scar. In earlier studies, Rudge and Silver demonstrated the inhibitory effect of the glial scar on neurite outgrowth *in vitro* by removing the glial scar from an animal model of CNS trauma and placing it *in vitro* for culture. Hippocampal neurons were seeded onto the scar, and neurite outgrowth was compared to neurons that were seeded onto immature neural

tissue. Their results showed significant inhibition of neurite outgrowth when compared to cells grown on immature tissue, leading the authors to conclude that molecules on the surface of the glial scar are likely to be an important factor in preventing neural growth (Rudge and Silver, 1990). McKeon and colleagues later showed the inhibitory effects are due to extracellular matrix proteins such as chondroitin-6-sulfate proteoglycan and cytoacton/tenascin, which are known to inhibit neurite growth *in vitro*, are present around cells with intense GFAP activity (an indicating factor of reactive astrocytes) following CNS injury (McKeon et al., 1991).

Other attempts have been made to recreate the effects of reactive astrocytes *in vitro*. Wanner et al. developed a model of mechanical stretch injury *in vitro* by culturing primary astrocytes on a malleable substrate, and then adding meningeal fibroblasts to mimic the glial scar found in response to neuronal injury *in vivo* (Wanner et al., 2008). Cells exhibited the morphological characteristics of reactive astrocytosis with extension of long, fibrous processes and over-expression of GFAP, and co-culture with neural cells showed neurites showing avoidance behavior away from reactive astrocytes. Yu et al. used a different approach to induce reactive changes within astrocytes in culture, by treating them with transforming growth factor-beta which increases secretion of chondroitin sulfate proteoglycans, with treated cells being inhibitory to neurite outgrowth from co-cultured neurons (Yu et al., 2012). However, a criticism of this method lies in the authors concluding that their method produces reactive astrocytes purely on the basis of increased expression and secretion of chondroitin sulfate, with little

on the morphological and molecular changes that take place within cultured astrocytes as a result of transforming growth factor-beta treatment.

4.1.9 Aims and Objectives

Otic neural progenitors that are transplanted into the cochlear modiolus *in vivo* need to extend neurite projections to both the sensory epithelium in the periphery and the cochlear nucleus in the brainstem centrally. Thus, in order to maintain their survival in the long-term, neurites from transplanted cells will have to establish a supportive relationship with the glial environment of the auditory periphery, in addition to associating with the glial cells in the central portion of the nerve. On the basis of previous work with neuronal cells co-cultured with both peripheral and central glia *in vitro*, it is hypothesized that cells will interact with Schwann cells in a positive manner, whilst otic neural progenitors cultured with astrocytes will be comparatively less able to establish neurite projections in an *in vitro* environment. There are a couple of reasons for the importance of testing this hypothesis:

- 1) This will be a further means of confirming the neuronal identity of the neuronal-like cells generated from otic neural progenitors from the Rivolta lab protocol. A neuronal phenotype of the cells cultured *in vitro* has previously been reported on the basis of the molecular signature of the cells, alongside patch clamp recordings from the cells (Chen et al., 2012). A demonstration of the otic neural progenitors extending neurites in dynamic co-cultures with glial will be further confirmation of their neuronal

phenotype *in vitro*.

- 2) Co-cultures will provide a useful tool that can pave the way for future experiments in which the interaction between otic neural progenitors and glial cells can be modulated with the addition of pharmacological compounds, which may then be translated to *in vivo* testing.

4.2 Results

4.2.1 *The Effect of Neuralising Medium on Schwann Cells.*

Given that combined cultures of otic neural progenitors and cochlear Schwann cells were conducted in neuralising medium, in each of the co-culture experiments, a batch of spiral ganglion Schwann cells was cultured alone in either Schwann cell medium or neuralising medium, to control for any effects that a change in medium may induce upon the Schwann cells.

Schwann cells were extracted from the cochleae of P5 gerbil pups as previously described. At day 4-5 post plating, Schwann cells were either placed into neuralising conditions or were kept in Schwann cell medium. Cultures were allowed to continue for 3 days and were then fixed for analysis by immunocytochemistry. Schwann cells were identified as cells co-expressing S100 and SOX10, whilst cells with a neuronal phenotype were identified by co-expression of B-Tubulin and NF200. Figure 4.2 shows the expression data for individual markers and figure 4.3 shows the co-expression of Schwann cell markers and neuronal markers.

Results from cell counts showed that the methods used to obtain Schwann cells yielded a satisfactory quantity of cells, with mean co-expression for S100 and SOX10 at $70.5\% \pm 0.83$ for cells in Schwann cell medium. There was comparatively less expression of the neuronal markers B-Tubulin and NF200 ($13.3\% \pm 5.18$), suggesting that although there may have been some

contamination with cells of a neuronal phenotype, the absence of neurotrophins most probably suppressed their proliferation (Fig. 4.3).

When cells were placed into neuralising conditions, there was a decrease in the co-expression of S100 and SOX10 when compared to cells in Schwann cell conditions, although this difference was not statistically significant. There was an increase in the mean co-expression of B-Tubulin and NF200 in neuralising conditions by 15.7%, which was statistically significant ($P < 0.05$, Fig. 4.2).

The results from these experiments demonstrated that placing the cochlear Schwann cells into neuralising conditions generally didn't have a significant effect on their viability. Although there was a statistically significant increase in co-expression of NF200+B-Tubulin positive cells (Fig. 4.3), which may indicate that there was a slight proliferation of cells with a neuronal phenotype in neuralising conditions, this was not likely to interfere with co-culture experiments involving otic neural progenitors; neuron-like cells from otic neural progenitors in co-cultures could easily be identified by the co-expression of NF200 with Human Mitochondrial antibody (given the human source of the otic neural progenitors), and thus those cells staining solely for NF200 alone could be ignored from analysis in these experiments.

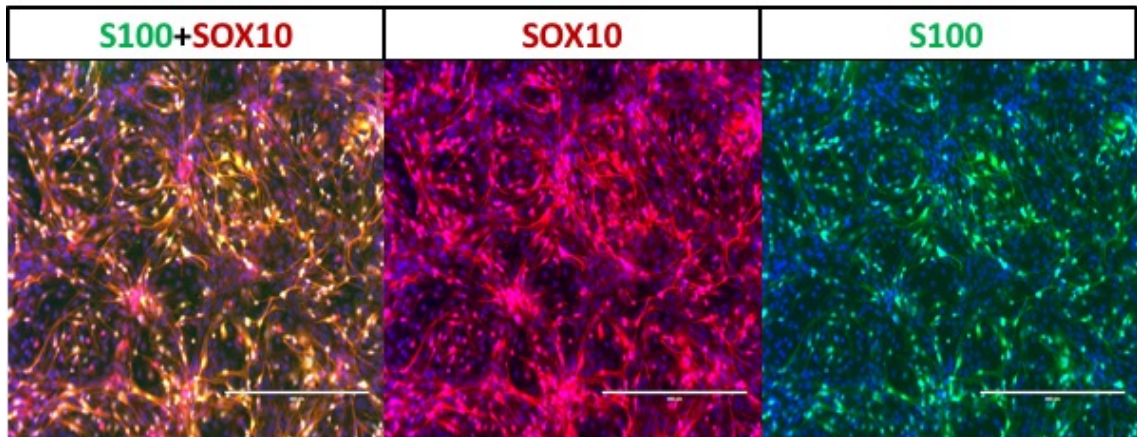


Fig 4.1- Representative images showing **immunolabelling** in cochlear Schwann cell cultures. SOX10 (red) and S100 (green) expression were used to ascertain the identity of Schwann cells. Scale bars represent 400 μ m

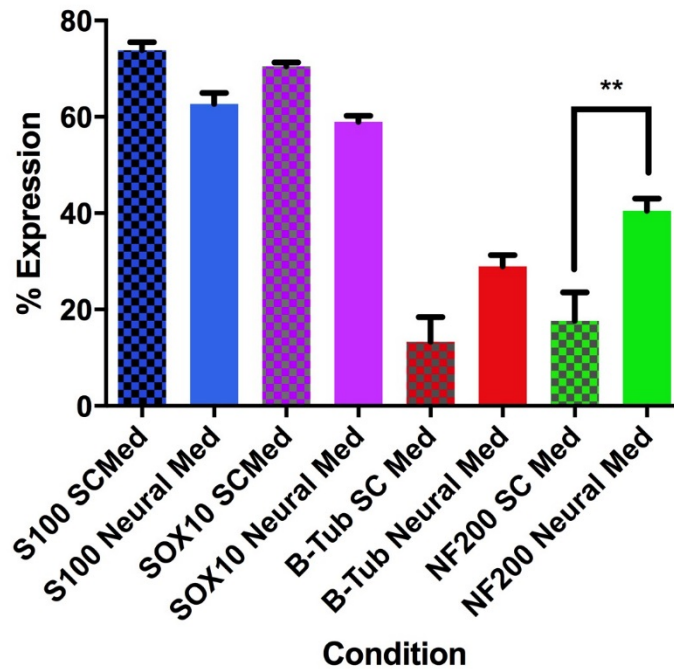


Fig 4.2 – Mean percentage expression of Schwann cell markers S100 and SOX10, alongside mean percentage expression of B-Tubulin and NF200 in Schwann cell cultures in Schwann cell culture medium versus neuralising medium. Error bars denote standard error from mean. Percentage expression was calculated against total cells staining with DAPI. Statistical significance was determined using a one-way ANOVA, with Tukey’s comparison of means performed post-test. **P<0.01. (n=3)

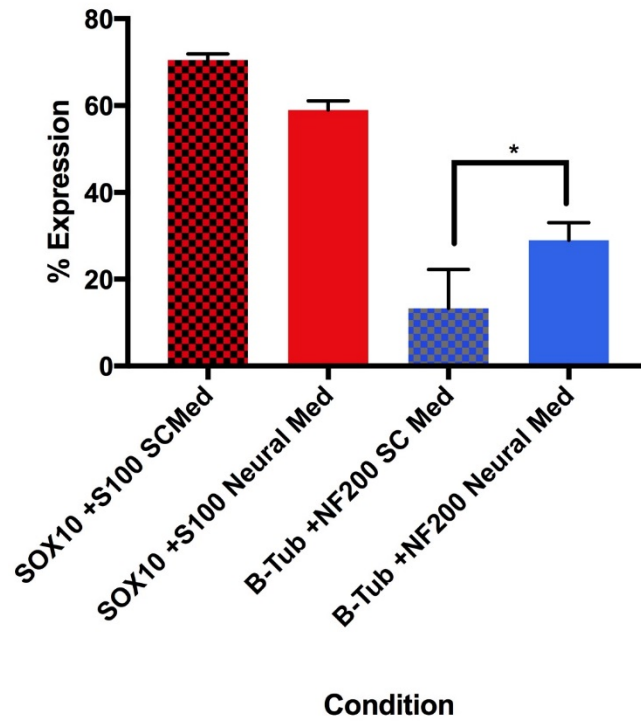


Fig 4.3 – Mean percentage of cells co-expressing Schwann cell markers S100 with SOX10, alongside mean percentage co-expression of neuronal markers B-Tubulin and NF200 in Schwann cell culture medium versus neuralising medium. Percentage expression was calculated against total cells staining with DAPI. Error bars denote standard error from mean. Statistical significance was determined using a one-way ANOVA, with Tukey’s comparison of means performed post-test. **P<0.05. (n=3)

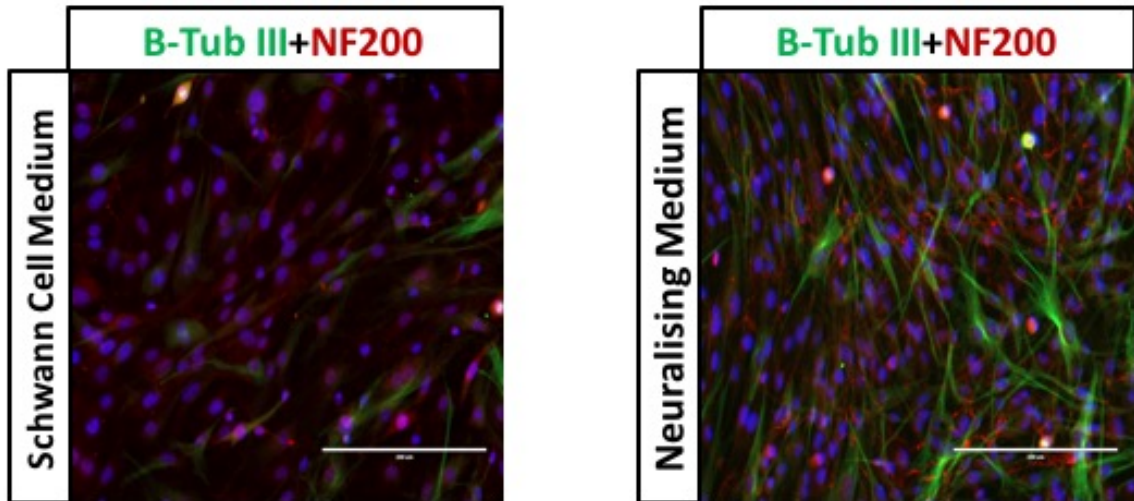


Fig 4.4 – Representative images showing immunolabelling from cochlear Schwann cell cultures for neuronal markers B-Tubulin (green) and NF200 (red), showing the difference in expression between cells in Schwann cell medium and neuralising medium. Scale bars represent 200µm

4.2.2 Schwann Cells promote and direct the growth of neurites from Otic Neural Progenitors *in vitro*

After 4 to 5 days post plating, otic neural progenitors were added to cochlear Schwann cell monolayers. The fundamental question that we were hoping to ascertain from these experiments was whether Schwann cells were supportive of neurite growth from otic neural progenitors, which may yield some insight into how transplanted otic neural progenitors might be interacting with Schwann cells in the auditory periphery *in vivo*. Three experiments were conducted with early otic neural progenitors derived from the Shef-1 cell line, whilst one was conducted with early otic neural progenitors derived from the H14 NOP/SOX2 reporter line, which was kindly provided by Darrell Barrott.

After 3 days, cells were fixed for immunocytochemistry and photographs were taken for image analysis, as described in chapter 2. Neurites derived from an otic neural progenitor were identified by the co-expression of human mitochondrial antibody and NF200. The course of co-labelled neurites was traced on the Image J software, which then gave a measurement of the neurite length. The length of neurites in co-culture were then compared to those of otic neural progenitors cultured in isolation.

Analysis revealed that cochlear Schwann cells have a positive effect on the growth of neurites from otic neural progenitors. The range of neurite lengths seen in co-culture was substantially larger than when cultured in isolation, and there was a positive shift in the median neurite length (125.8 μ m vs 42.5 μ m) and the

interquartile range of lengths when compared to neurites cultured alone (Fig 4.6a & 4.6b). This effect was seen in otic neural progenitors derived from the Shef-1 cell line (n=3), and also in a solitary experiment with cells derived from the H14 NOP/SOX2 line (Fig 4.8a & 4.8b). In addition, there was a statistically significant increase in the mean length of neurites in co-culture conditions compared to those cultured alone in both cell lines as shown in figures 4.7 and 4.9, indicating that spiral ganglion Schwann cells positively promoted neurite growth from otic neural progenitors when cultured in an *in vitro* environment, either by conditioning the cell culture medium to support growth, or through direct contact with the otic neural progenitors.

There was also a suggestion that neurites from otic neural progenitors were receiving directional cues from Schwann cell networks, as they seemed to be following their orientation of growth. To quantify this, a vertical line was drawn, and a line of best fit was drawn through a neurite and its adjacent Schwann cells, giving an estimation of the angle growth of a neurite and its adjacent Schwann cells. The difference between the two angles was then calculated, and plotted in a frequency distribution graph.

Most of the neurites analysed from the three experiments conducted with Shef-1 otic neural progenitors and the solitary experiment with H14 NOP/SOX2 cells appeared to be growing within 20 degrees of the adjacent Schwann cell network, suggesting that they were growing very close to parallel to them (Fig. 4.10). Thus, not only do the otic neural progenitors seem to be obtaining growth cues from the

spiral ganglion Schwann cells, but they seemed to be playing a role in guiding neurite growth as well.

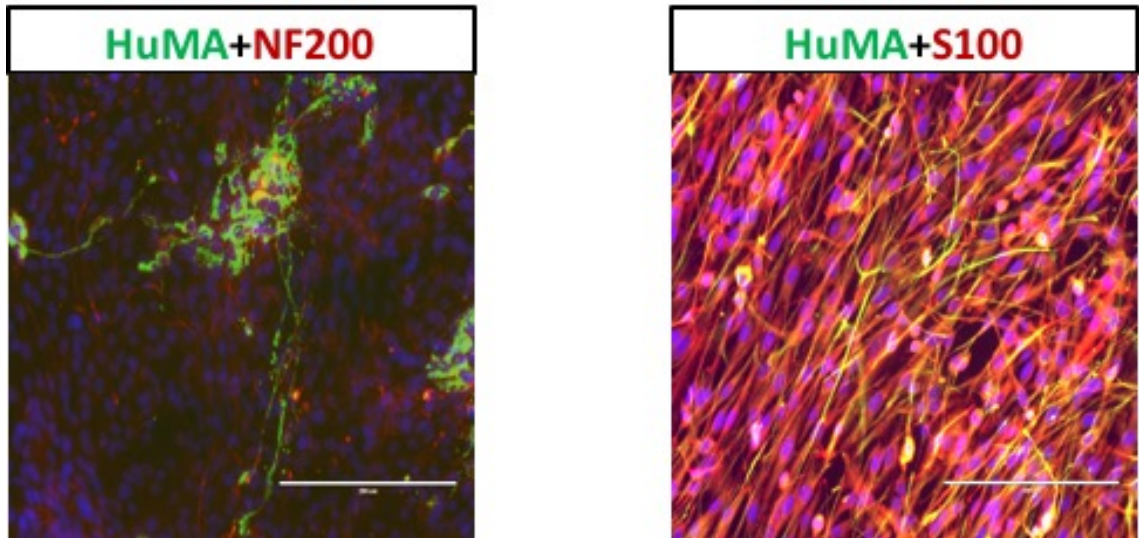


Fig 4.5 – Representative images showing immunolabelling from otic neural progenitors (P1+2+1) co-cultured with cochlear Schwann cells *in vitro*. The left hand image shows staining for NF200 (red) with human mitochondrial antibody (green) to distinguish the otic neural progenitors. The right hand image shows staining for S100 (red) to distinguish the cochlear Schwann cells with human mitochondrial antibody. Scale bars represent 200 μ m

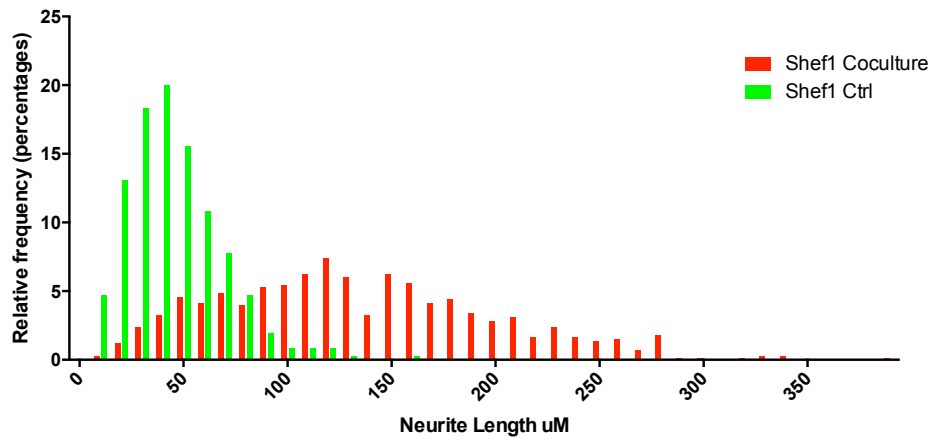


Fig 4.6 – Histogram showing combined frequency distribution data of neurite lengths from all experiments involving co-cultures of early Shef-1 otic neural progenitors (P1+2+1) with cochlear Schwann cells. (>500 neurites, n=3)

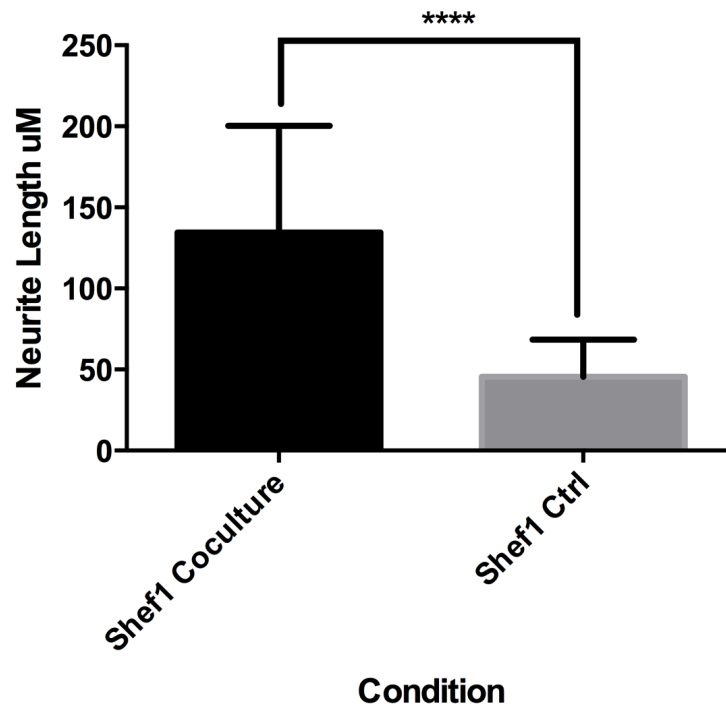


Fig 4.7 – Histogram showing a comparison of mean of neurite lengths from all experiments involving co-cultures of Shef-1 otic neural progenitors (P1+2+1) with cochlear Schwann cells. **** $P < 0.0001$. (>500 neurites, $n=3$)

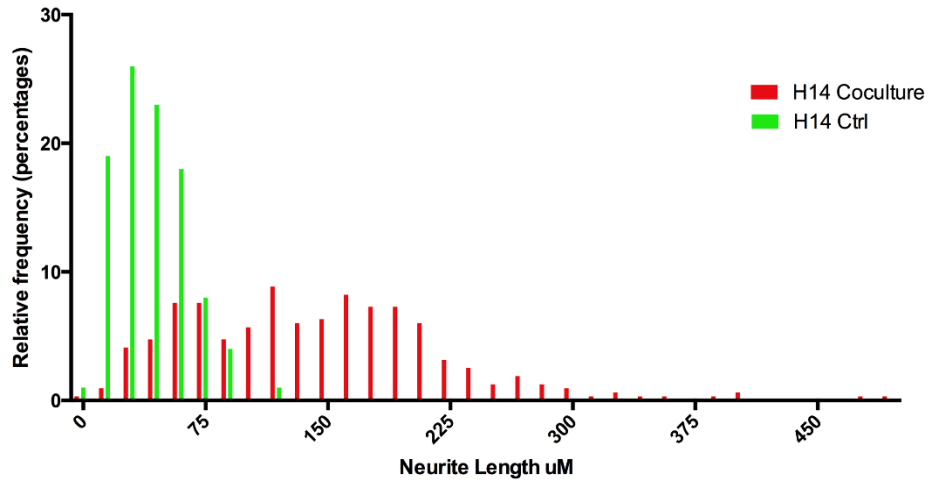


Fig 4.8 - Histogram showing frequency distribution data of neurite lengths from the solitary experiment involving co-cultures of H14 NOP/SOX2 otic neural progenitors (P1) with cochlear Schwann cells. (>200 neurites, n=1)

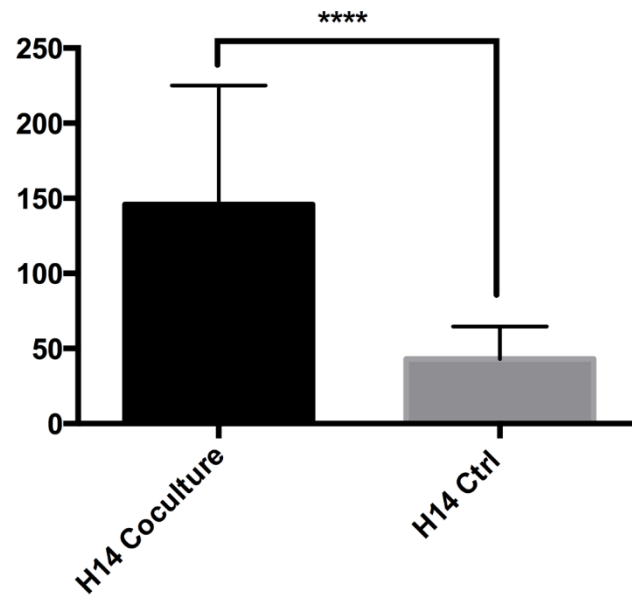


Fig 4.9 – Histogram showing a comparison of mean of neurite lengths from co-cultures of H14 NOP/SOX2 otic neural progenitors with cochlear Schwann cells. ****P<0.0001. (>200 neurites, n=1)

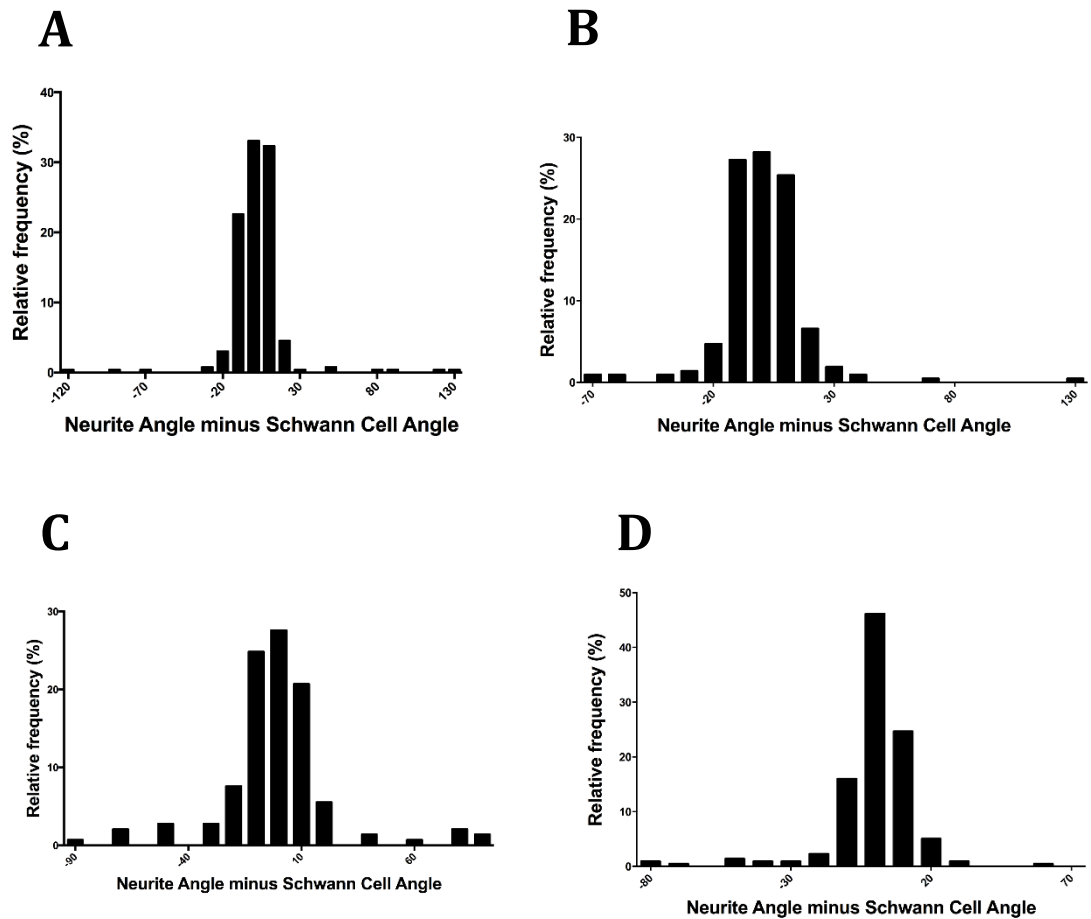


Fig 4.10 – Histograms showing frequency distribution data of neurite angle minus Schwann cell angle. Figs **a,b** and **c** show data from each of the Shef-1 otic neural progenitor co-cultures (P1+2+1), whilst fig **d** shows data from the co-culture experiment involving H14 NOP/SOX2 otic neural progenitors (P1).

4.2.3 Neuralising Medium Induces a Reactive Phenotype in Cultured Cortical Astrocytes

Prior to setting up co-cultures with astrocytes, a question arose as to the optimum time-point at which to add otic neural progenitors to the astrocytes cultures; should astrocytes be allowed to settle for a few days after passaging prior to setting up the co-cultures, or should co-cultures be set-up at the point when astrocytes are passaged? To determine an answer to this (and indeed whether it was a significant issue to be concerned about), the effects of allowing the cells to settle after passaging and then subsequently changing the medium after a few days were initially assessed.

Primary astrocyte cultures were prepared and maintained as previously described in chapter 2. Immediately after passaging, astrocytes were allowed to settle and placed in astrocyte medium for 2 days. Following this period, the medium was changed over to neuralising medium, and cultures were maintained for 6 days in these conditions. Cells were then fixed for immunocytochemistry, and cells were then counted for expression of GFAP, S100 and B-Tubulin. Cultures were compared to astrocytes that had been kept in astrocyte medium for the duration of the experiments.

When comparing marker expression of GFAP and S100, there was no significant difference between cells in astrocytic medium and cells in neuralising medium. Furthermore, although there was some weak staining for B-Tubulin, there was

also no significant difference between both conditions for its expression (Fig. 4.14).

However, it was clear from analyzing the micrographs of these images that the astrocytes had undergone some changes in neuralising medium. Firstly, the astrocytes had clearly undergone a morphological change; cells in astrocytic medium were generally flatter in their appearance, whilst astrocytes that had been placed in neuralising medium adopted a more 'fibrotic' appearance, extending multiple thin, long processes. Moreover, qualitative assessment of the images suggested the intensity of the GFAP signal appeared to be much brighter in cells that had been cultured in neuralising medium, when compared to cells that remained in astrocytic medium, indicating an over-expression of GFAP (figs 4.13a & b).

To quantify this effect, the experiments were repeated as described, and plates were then scanned in the Incell Analyser 1000 platform. The software was programmed to create a mask for the cells, allowing it to measure the signal intensity from each individual cell. There was a statistically significant increase in the mean fluorescence density of cells in neuralising medium (5062 ± 13.5) when compared to cells in astrocytic medium (2028 ± 3.95) as shown in figure 4.15.

Thus, although there is little difference in marker expression between the two conditions, the morphological changes within the cells alongside the overexpression of GFAP as indicated by the increase in signal intensity of the marker suggest that in neuralising medium the cells adopt a reactive phenotype.

If this is indeed the case, then one would expect that such an environment might not be supportive of neurite outgrowth from otic neural progenitors in co-culture conditions.

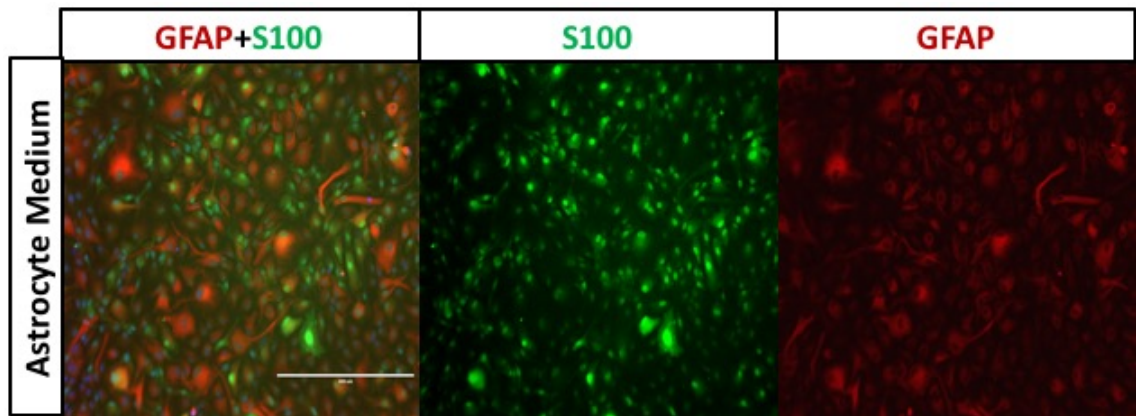


Fig 4.11- Representative images showing **immunolabelling** of cortical astrocytes in Astrocyte medium. GFAP (red) and S100 (green) expression were used to ascertain the identity of astrocytes. Scale bars represent 400µm

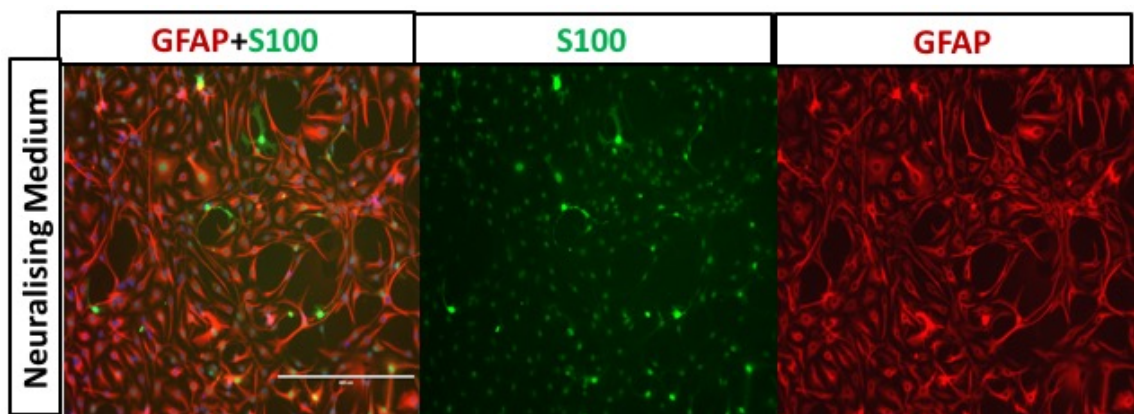


Fig 4.12- Representative images showing **immunolabelling** of cortical astrocytes in Neuralising medium. GFAP (red) and S100 (green) expression were used to ascertain the identity of astrocytes. Scale bars represent 400µm

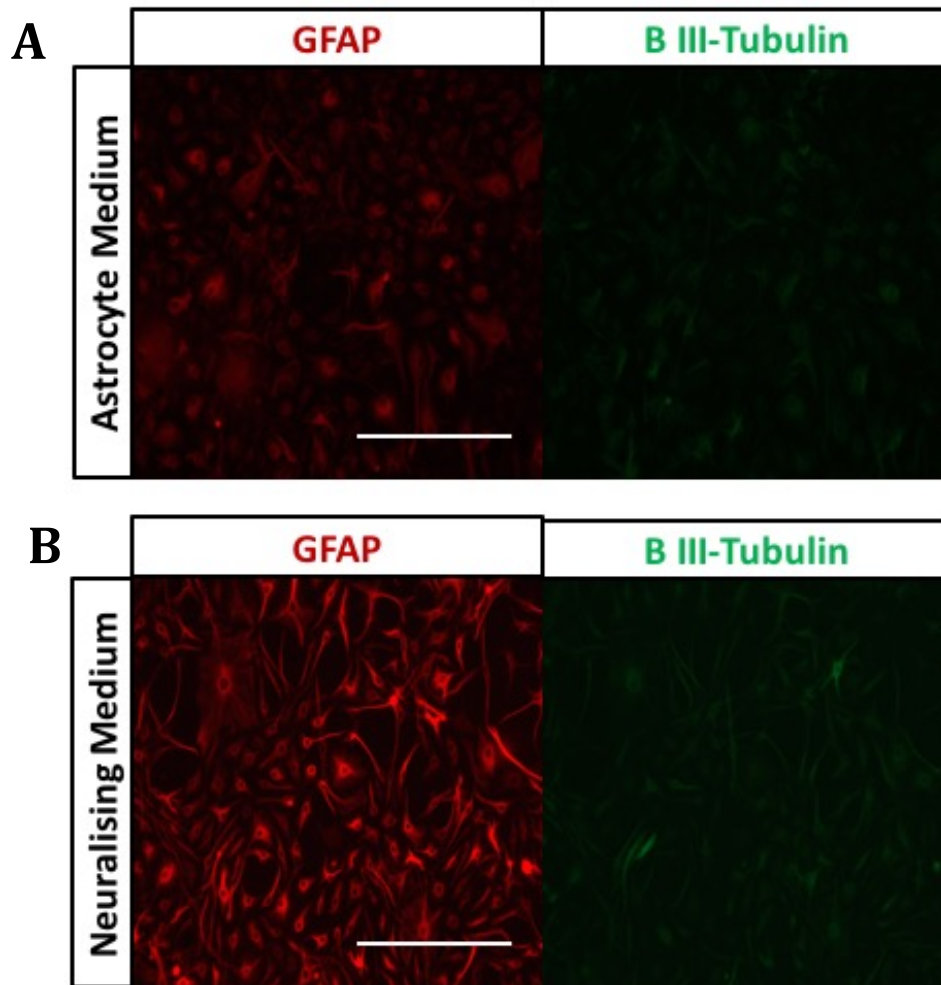


Fig 4.13a – Representative images showing immunolabelling of cortical astrocytes examining expression of GFAP (red) and B-Tubulin (green) in astrocyte medium. **Fig 4.13b** shows representative images of immunolabelling of cortical astrocytes in neuralising medium examining GFAP expression (red) and B-Tubulin (green). Scale bars are 400 μ m.

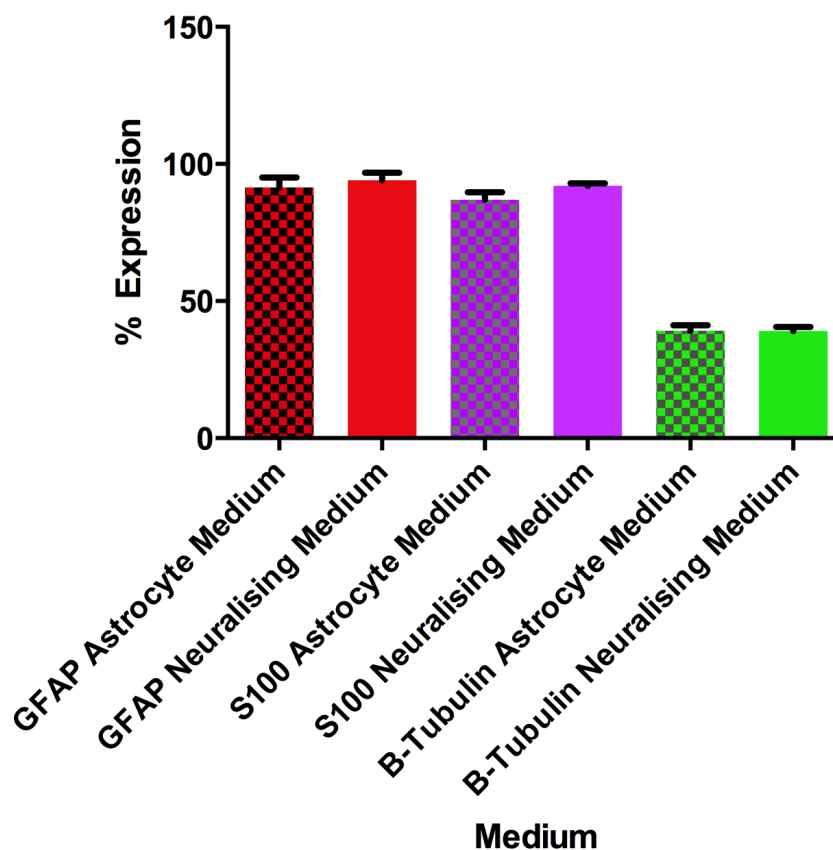


Fig 4.14 – Mean percentage expression of GFAP and S100, alongside mean percentage expression of B-Tubulin within Astrocytes in Astrocyte culture medium versus neutralising medium. Data combined from one experiment with P3 astrocytes and 2 experiments with P4 astrocytes. Percentage expression was calculated against total cells staining with DAPI. Error bars denote standard error from mean. Statistical significance was determined using a one-way ANOVA, with Tukey’s comparison of means performed post-test. (n=3)

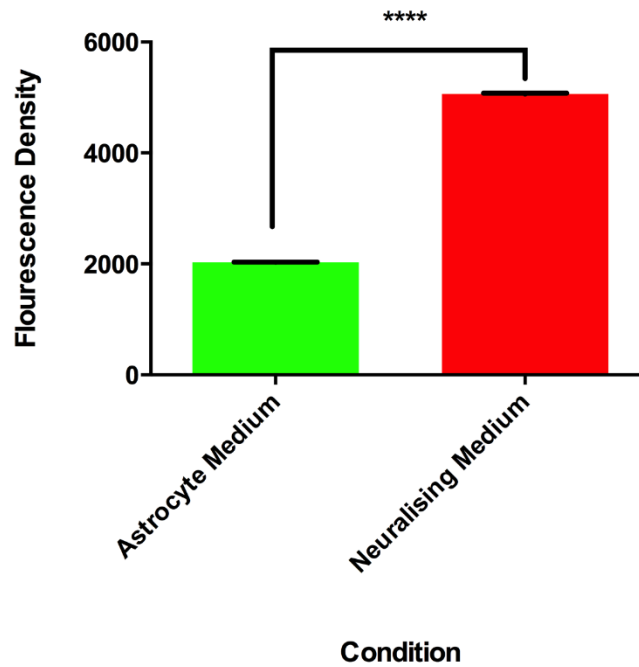


Fig 4.15 – Comparison of the mean fluorescence density of GFAP signal/cell in astrocytes within astrocyte medium versus neutralising medium, as measured on the Incell Analyser. Data combined from two experiments with P4 astrocytes and 1 experiment with P7 astrocytes. Error bars denote standard error from mean. Statistical significance was determined using an unpaired t-test. ****P<0.0001. (n=3)

4.2.4 Astrocytes appear to adopt a neuronal morphology in neuralising medium immediately after passaging

Given that astrocytes appear to adopt a reactive phenotype when they are placed in neuralising medium after being given a period of time to settle post passaging, we wanted to examine if this also was the case if cells were placed in neuralising medium immediately after passaging.

Experiments were set-up as described in chapter 2. Astrocytes were passaged, and immediately plated into culture dishes with neuralising medium. Cultures were allowed to continue for 6 days, and then cells were fixed for immunocytochemistry. Cells were compared to astrocytes that had remained in astrocytic medium for the duration of the experiment.

Results showed that there was no significant difference in the expression of S100 and GFAP in both conditions (Fig 4.17). There was however a stark difference in the morphology of the cells in neuralising conditions, in that cells appeared to adopt a strongly convincing neuronal morphology (Figs 4.16 a, b and c). Moreover, there was an obvious change in the staining for B-tubulin; the weak staining of B-Tubulin was again apparent in cells cultured in astrocytic medium, but there was a dramatic increase in the intensity of the signal in neuralising conditions.

Thus it is apparent that the timing of the medium change is an important factor to consider prior to setting up co-cultures with otic neural progenitors. Whilst in both

scenarios the astrocytes undergo some morphological changes, these changes are different in both situations; astrocytes placed in neuralising conditions immediately after passaging appear to possess neuronal morphology whereas cells that are placed in neuralising medium 2 days after passaging adopt a morphology associated with reactive astrocytes, extending short fibrous processes from their characteristic flattened appearance in control conditions.

Furthermore, alongside undergoing morphological changes, astrocytes that are placed immediately into neuralising medium after passaging also significantly upregulate their expression of B-Tubulin, whilst cells that allowed to settle prior to being placed in neuralising medium maintain the weak B-Tubulin expression seen in control conditions.

Thus it seems that neuralising medium does induce phenotypic changes in cultured cortical astrocytes *in vitro*. Given that our data seem to suggest that astrocytes adopt a neuronal phenotype immediately after passaging in neuralising conditions, it seems that it would be more appropriate to commence co-cultures with otic neural progenitors once astrocytes are given a period of time to settle after passaging.

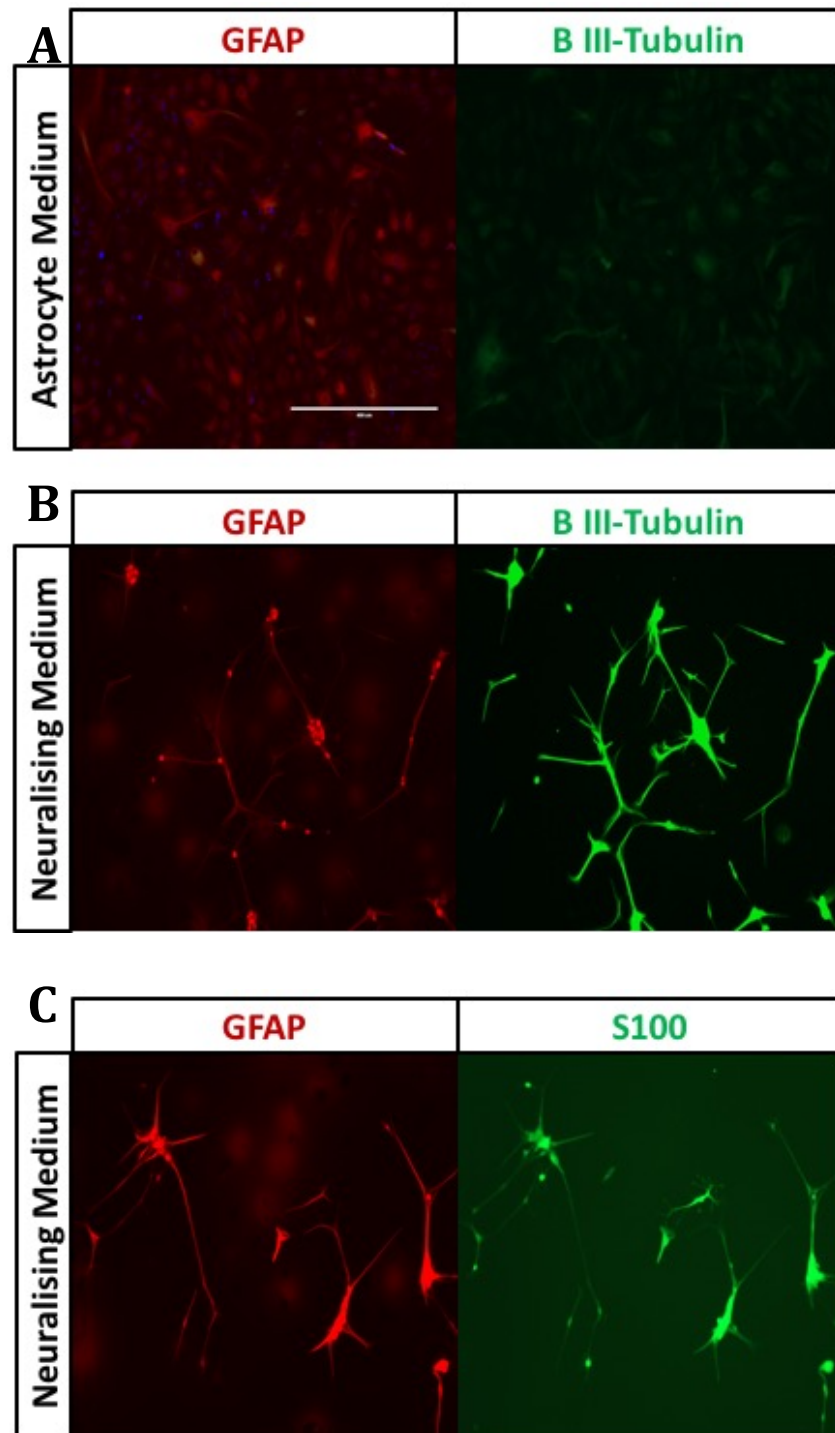


Fig 4.16a – Representative images showing immunolabelling of astrocytes in astrocyte medium. GFAP (red) and B-Tubulin (green) expression as previously seen. **Fig 4.16b** shows representative images of immunolabelling of astrocytes that were placed into neuralising medium immediately after passaging. GFAP expression is shown in red, B-Tubulin expression in green. **Fig 4.15c** shows GFAP expression (red) and S100 expression (green) in astrocytes placed immediately into neuralising medium after passaging. Scale bar represent 400µm.

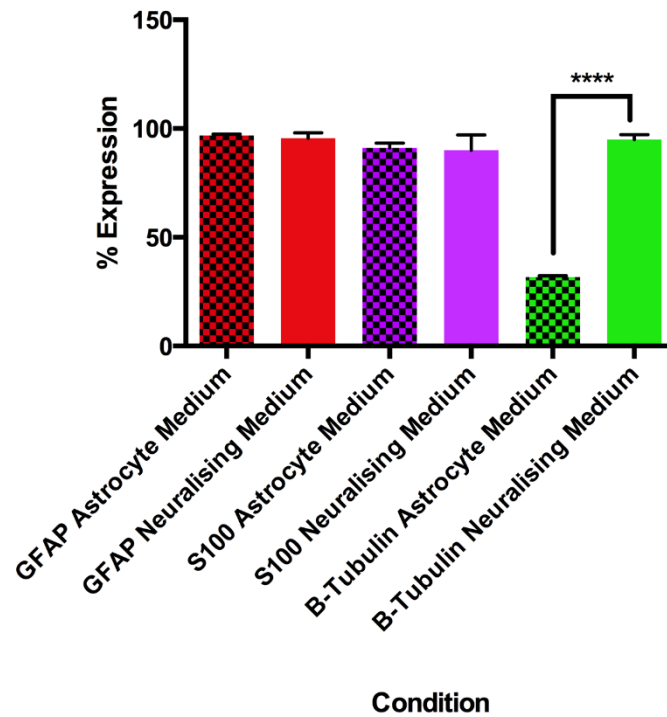


Fig 4.17 - Representative images showing immunolabelling of cortical astrocytes examining expression of GFAP and B-Tubulin in astrocyte medium and neuralising medium. Data combined from experiments with P3, P5 and P5+2 astrocytes. Percentage expression was calculated against total cells staining with DAPI. Error bars denote standard error from mean. Statistical significance was determined using a one-way ANOVA, with Tukey's comparison of means performed post-test. ****P<0.0001. (n=3)

4.2.5 Astrocytes are inhibitory to growth of neurites from otic neural progenitors in vitro.

On the basis of findings from the previous experiments, astrocytes were passaged and allowed to settle in astrocytic medium for 2 days prior to setting up co-cultures. Otic neural progenitors were then added to the astrocyte monolayer, and cultures were maintained for 6 days at which point cells were fixed for immunocytochemistry and subsequent image analysis. Neurites of cells co-expressing NF200 and human mitochondrial antibody were then traced on the image J software, giving an estimation of neurite length. The lengths of neurites grown in co-culture were then compared to those grown in isolation.

Experiments were initially conducted with the Shef-1 cell line. Examination of the micrographs from these experiments showed that otic neural progenitors seemed to congregate together (Fig 4.18), and generally did not grow on top of the astrocytic monolayer, possibly as a result of the astrocytes growing around the otic neural progenitor colonies and restricting their growth within a confined space. Moreover, and in stark contrast to co-cultures with Schwann cells, otic neural progenitors did not appear to be extending long neurites into the astrocytic regions.

When comparing the lengths of neurites in co-culture with those grown in isolation, there was a clear negative shift in the length of neurites in co-culture, with a lower median value and interquartile range of neurites in co-culture (Fig 4.19). Furthermore, there was a statistically significant decrease in the mean

length of neurites in co-culture, compared to those grown in isolation (Fig 4.20). This suggests that the astrocytes which undergo reactive changes are not supportive of neurite growth from otic neural progenitors within an *in vitro* environment.

Experiments were then repeated with otic neural progenitors derived from the Shef 3.2 cell line. As described in chapter 3, cells from two separate differentiations were characterized for their ability to neuralise and also for glial production, and these were the same cells used in co-culture experiments. Given that many of the cells did not convincingly express NF200, it was not possible to accurately calculate neurite lengths from these experiments. However, an interesting phenomenon was nevertheless observed; of the two separate Shef 3.2 otic neural progenitor lines, the cells which lacked any significant neuronal differentiation (Batch B, see fig 3.26 from Chapter 3) appeared to readily grow on top of the astrocytic monolayer, however the cells that had a partial differentiation into neuronal phenotypes (Batch A, see fig 3.25 from Chapter 3) in some fields displayed similar characteristics as seen with the Shef-1 cells in co-culture, where astrocytes appeared to be growing around colonies of otic neural progenitors and restricting their growth into the regions of astrocytes.

In an attempt to quantify this, the percentage of cells growing in astrocytic regions were counted from 10 fields, and the mean percentages of the three Shef-1 experiments were compared to the two experiments conducted with the Shef-3.2 cell lines. Results showed a lower percentage of Shef-1 otic neural progenitors that grew on top of astrocytes, with a higher percentage seen in the Shef-3.2 line

which demonstrated a partial neuronal differentiation, whilst the highest percentage was seen with the Shef-3.2 cells that demonstrated hardly any neuronal differentiation (Fig 4.22). This data seems to suggest a correlation between the inhibitory effect of the astrocytes in our culture system and the extent of the neuronal phenotype of the otic neural progenitors; raising the possibility that the inhibitory signals generated from reactive astrocytes principally affect cells with a neuronal phenotype.

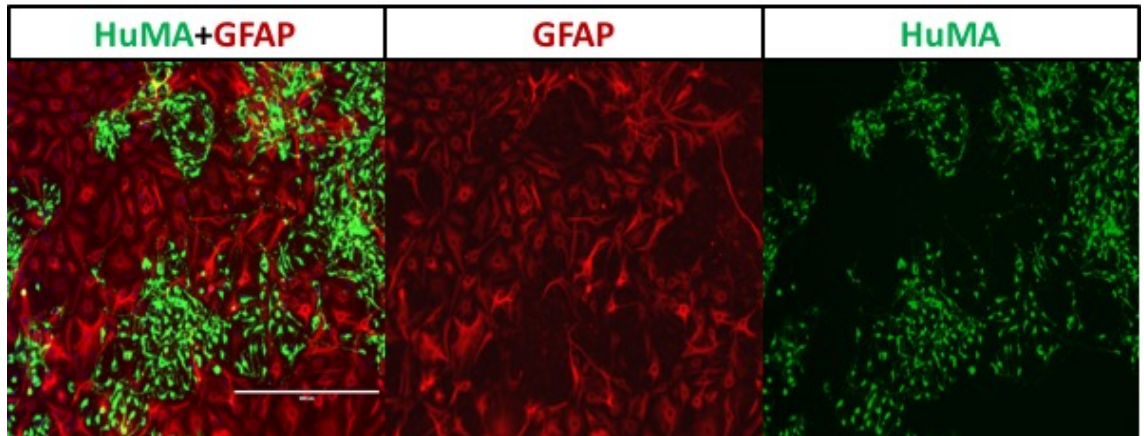


Fig 4.18 – Representative images showing immunolabelling from Shef-1 otic neural progenitors co-cultured with cortical astrocytes *in vitro*. Astrocytes are stained with GFAP (red) and otic neural progenitors are stained with human mitochondrial antibody (green). Scale bars represent 400 μ m

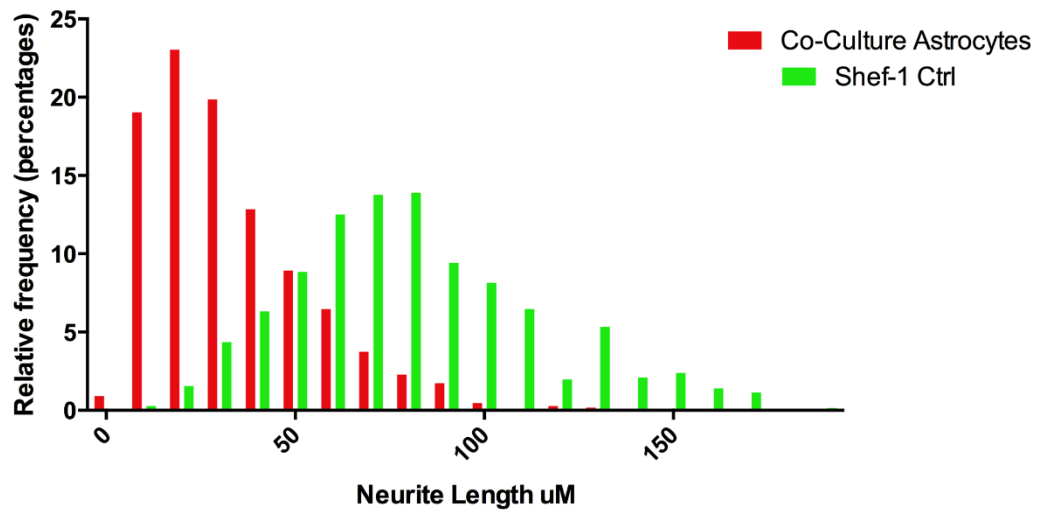


Fig 4.19 – Histogram showing combined frequency distribution data of neurite lengths from all experiments involving co-cultures of early Shef-1 otic neural progenitors with cortical astrocytes. Data were combined from 3 separate experiments using Shef-1 ONPs (P1+1+1) with P4 Astrocytes, and one experiment using Shef-1 ONPs (P1+1+2) with P7 astrocytes.. (>500 neurites, n=3)

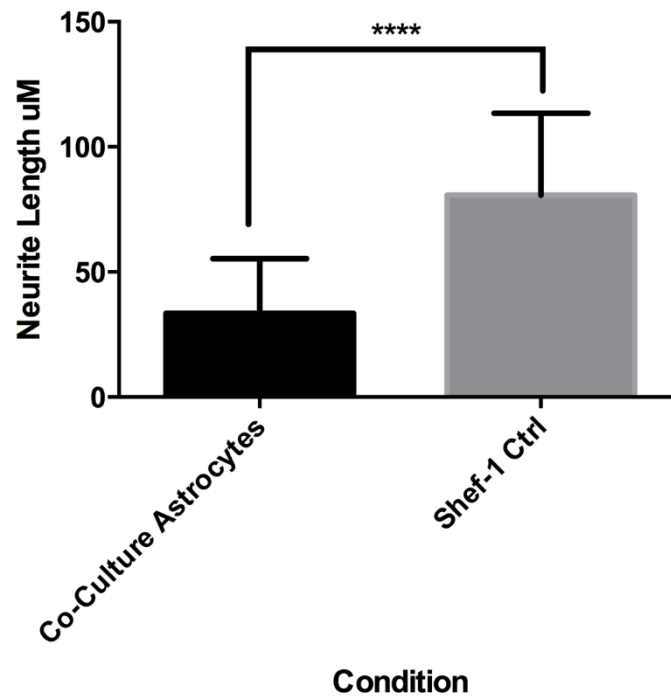


Fig 4.20 - Histogram comparing mean neurite length of shef-1 otic neural progenitors grown in co-culture with astrocytes vs in isolation. Data were combined from 3 separate experiments using Shef-1 ONPs (P1+1+1) with P4 Astrocytes, and one experiment using Shef-1 ONPs (P1+1+2) with P7 astrocytes. ****P<0.0001. (>500 neurites, n=3)

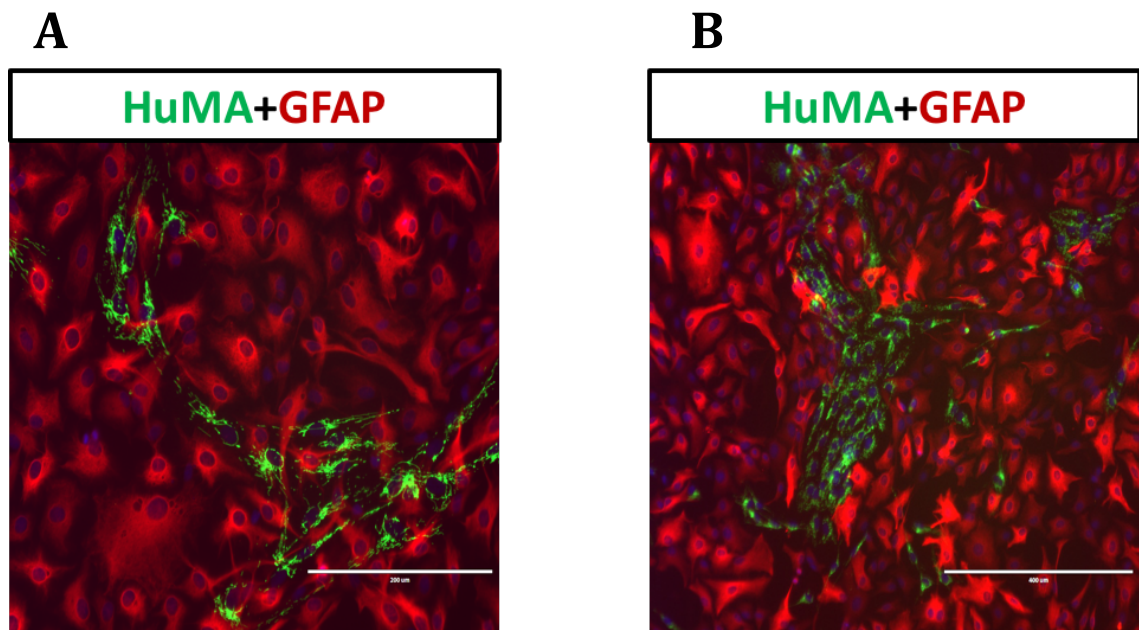


Fig 4.21a. – Representative images showing co-culture of Shef-3.2 Otic neural progenitors (P2, *Batch B*) with P7 astrocytes. GFAP expression is shown in red and human mitochondrial antibody is shown in green. Scale bar is 200µm **Fig 4.21b** shows representative images of immunolabelling of Shef-3.2 otic neural progenitors (P1+1, *Batch A*) with P7 astrocytes. GFAP expression is shown in red and human mitochondrial antibody expression is shown in green. Scale bars represent 400µm.

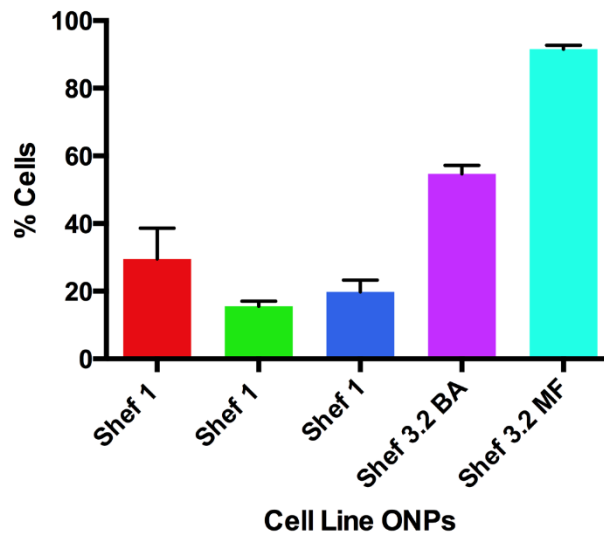


Fig 4.22 – Graph showing percentage of human mitochondrial positive cells growing on top of GFAP positive astrocytes from 5 experiments. Data were combined from 3 separate experiments with Shef-1 Otic neural progenitors (P1+1+1), and 2 experiments with Shef-3.2 otic neural progenitors (*with cells donated from Matthew Farr and Ben Allen*)

4.3 Discussion

4.3.1 *The plasticity of Schwann cells in vitro*

Prior to setting up co-cultures, we wished to ascertain the effects of neuralising medium on Schwann cells alone, given that co-cultures were set-up in neuralising medium. There was little change in the expression of Schwann cell markers S100 and SOX10 in neuralising conditions when compared to cells cultured in Schwann cell medium, and no obvious changes in cellular morphology either. There was however an increase in the mean percentage expression of the neuronal markers B-Tubulin and NF200 in neuralising medium, and although the increase was statistically significant in the case of NF200, this was not the case for B-Tubulin.

There are a couple of possible explanations for this observed result. Schwann cells are known to possess some intrinsic capability to de-differentiate in certain situations (Jessen and Mirsky, 2005) and change phenotype into a more immature cell type, which may have the plasticity to differentiate into cells of a neuronal lineage. Moreover, the idea that adult stem cell niches with a glial identity residing within the central nervous system is well established, and some have suggested a similar population of cells exists within the peripheral nervous system. Widera and colleagues have described the presence of neural crest stem cells within the palatal rugae of the palatal mucosa, which can be expanded to express markers such as Sox2, Oct4, c-myc and Klf4 (Widera et al., 2009). They later reported the presence of a nestin positive population in palatal

Schwann cells and Sciatic nerve Schwann cells, and that they could form neurospheres *in vitro*, with an overlapping of pluripotency markers with Schwann cell markers (Widera et al., 2009). Within the context of the ear, Lang and colleagues have also shown that auditory nerves that have been damaged following Ouabain injury appeared to possess the capability of producing neurospheres *in vitro* with upregulation of Sox2 and nestin. When these cells were then placed in neural differentiating conditions, and upregulation of TUJ1 and MAP2 was observed, suggesting that the neurospheres had differentiated into cells with a more mature neuronal phenotype (Lang et al., 2015). Our findings of an upregulation of B-Tubulin and NF200 may indeed fit with this hypothesis of a neural stem cell niche within the auditory nerve.

Another plausible explanation for our findings may lie in the possibility that although the cells were cultured in medium devoid of neurotrophins, which previously has been reported to cause death of the majority of spiral ganglion neurons *in vitro* and allowing Schwann cells proliferate (Hansen et al., 2001), it is possible that the increased expression in neuronal markers actually reflects the survival of some of these neurons, which are then able to proliferate when they are placed in neuralising conditions.

Whilst the principal purpose of this particular collection of experiments was to ensure that our neuralising medium didn't induce a significant change in the glial phenotype of cochlear Schwann cells *in vitro*, the subsequent finding of neuronal markers being upregulated is most certainly interesting, and if indeed there are a population of cells that have stem cell characteristics within the auditory nerve,

then this makes the reasons for lack of neuronal regenerative capacity within the cochlea an even greater conundrum to address.

4.3.2 Schwann cells are supportive of neurite growth from otic neural progenitors

Compared to when cultured in isolation, otic neural progenitors tended to extend longer neurites when co-cultured with cochlear Schwann cells. This is indicated by the positive shift in the interquartile range and the median values of the neurite lengths, alongside the statistically significant difference in the mean neurite lengths in the combined data from the three experiments involving the Shef-1 cell line, and the solitary experiment with the H14 NOP/SOX2 line. Furthermore, it appeared that neurites were receiving guidance cues from Schwann cells, most probably through physical contacts between the cells.

A similar relationship has also been reported in isolated spiral ganglia co-cultures with Schwann cells. Jeon and colleagues did a series of experiments to examine the effect of central glia and peripheral glia on the ability of spiral ganglion neurons to extend neurites *in vitro*. They reported that Schwann cells appear to gain directional cues from adjacent Schwann cells as most of the neurites they analysed followed Schwann cells, with only a small number showing features of growing away from them (Jeon et al., 2011). Similar experiments were also conducted by Whitlon et al, who showed that when spiral ganglia were co-cultured in a mixed glial environment, they preferentially associated with Schwann cells (Whitlon et al., 2009). Thus, the interaction we have seen with the

spiral ganglion-like neurites in co-culture with Schwann cells is similar to that which has previously been reported when isolated cochlear spiral ganglion neurons have been co-cultured *in vitro*. This group of experiments therefore adds further weight to the previous extensive work that has taken place in the Rivolta in characterising the spiral ganglion-like neurons from the otic neural progenitors (Chen et al., 2012); the similarities in behavior they exhibit to spiral ganglion like neurons in co-culture experiments with peripheral glia provides further evidence for their neuronal phenotype.

The striking appearance of long neurites from otic neural progenitors in co-culture conditions suggests that the cochlear Schwann cells must be providing some trophic cues that are supporting the growth and survival of spiral ganglion-like neurons. This is most probably due to the provision of the neurotrophins BDNF and NT-3 from cochlear Schwann cells which, along with the Sonic Hedgehog in the culture medium, facilitate the maturation of otic neural progenitors into spiral ganglion-like neurons and the subsequent neurite extension.

Although Jeon et al did report that cultured spiral ganglion cells appeared to be obtaining direction cues for growth from adjacent Schwann cells, their analysis of this phenomenon was somewhat crude, as they merely categorized neurites as either 'following', 'crossing' or 'avoiding' adjacent glial cells (Jeon et al., 2011). Our observations indicated that cultured monolayers of Schwann cells on a non-patterned culture surface naturally form areas of local orientation, and neurites from differentiating otic neural progenitors appear to follow the direction of growth of the Schwann cells in their immediate vicinity. This effect was quantified by

drawing a lines of best fit through the tortuous growth of a neurite and the direction of growth of neighboring Schwann cells, and the angles were subsequently compared and plotted. Seggio and colleagues have also reported a similar phenomenon in their work in cultured dorsal root ganglia on Schwann cell monolayers (Seggio et al., 2010). They too report the tendency of Schwann cells to form areas of local orientation, which dorsal root ganglia neurites appear to follow. Their analysis methods were similar to the ones used in this study, however they used the 'Farsight toolkit' software for image analysis, which has algorithms allowing for more accurate calculation of Schwann cell orientation. They also measured the angle of growth of neurites on a point by point basis, and used a Matlab program to compare the overlying neurite orientation per segment with the adjacent Schwann cells. Whilst their analysis methods were slightly more sophisticated than ours, they report similar results to the work presented here, that most neurites appear to grow in a direction between 0-20 degrees in relation to the neighboring Schwann cells.

4.3.3 Astrocytes adopt a reactive phenotype in neuralising conditions

As with Schwann cell co-cultures, it was important to ascertain the effects of neuralising medium on astrocytes prior to setting up co-cultures with otic neural progenitors. Initially we put cultured astrocytes in neuralising medium 2 days after passaging, and although there wasn't any significant difference in expression of glial markers in neuralising conditions when compared to cells remaining in astrocytic medium, there were some striking differences in the morphology of the

cells in neuralising conditions, with extension of processes and a marked increase in the intensity of the GFAP signal on immunocytochemistry, indicating an overexpression of this classic glial intermediate filament protein. To quantify the change in the intensity of the signal, cells were scanned on the InCell Analyser, which allowed for the intensity of each cell within the culture vessel to be measured, and a significant difference in the intensity of the GFAP signal was detected between cells in neuralising medium versus those that remained in astrocytic conditions. Furthermore, it appears that the time-point at which cells are put into neuralising medium also is an important factor; whilst cells that had been allowed some time to settle before being placed in neuralising medium adopted a phenotypic change highly suggestive of reactive astrocytes, those cells that had been placed into neuralising medium immediately after passaging appear to adopt a neuronal phenotype, with neuronal morphology and a significant upregulation of B-Tubulin.

Astrocytes are an extremely heterogeneous population of cells with complex cell biology, and there are significant differences in their behavior depending upon where they are located within the central nervous system. For example, subpopulations of cells within the subventricular zone and subgranular zone are actually neural stem cells which are proliferative, as opposed to cells within other regions which do not usually proliferate (Kriegstein and Alvarez-Buylla, 2009); however cells in these regions share in the electrophysiological properties that are characteristic of astrocytes (Fukuda et al., 2003). Astrocytes have also been shown to exhibit substantial differences in their gene expression profiles depending on their location within the brain (Doyle et al., 2008, Yeh et al., 2009).

In response to injury astrocytes undergo reactive changes with increased expression of filament proteins GFAP and Vimentin, cellular hypertrophy and outgrowth of cellular processes and proliferation (Sofroniew, 2009). However, there is even variation in reactive response of astrocytes depending upon the nature of the pathology affecting them. For example, whilst most cells exhibit morphological changes and upregulation of GFAP, differences have been reported in the proliferative response of specific subsets of astrocytes in chronic inflammation models versus acute insults (Sirko et al., 2013).

Evidence is also emerging that Sonic Hedgehog plays an important role in the modulation of the reactive response of astrocytes. In fact, reactive astrocytes have been shown to possess some stem cell characteristics, and in the presence of sonic hedgehog *in vitro* are able to proliferate and form multipotent neurospheres (Sirko et al., 2013). The same study also showed that sonic supplementation induced proliferation of reactive astrocytes *in vivo*. Levels of Sonic Hedgehog within the central nervous system have been shown to increase in response to neuronal damage from cerebral ischaemia and stab wounds to neural tissue (Sirko et al., 2013), and sonic hedgehog has been shown to generate astrocytes from NG2+ cells *in vitro*, and activation of hedgehog signaling *in vivo* caused a significant increase in the number of astrocytes derived from NG2+ cells within the glial scar in a model of cerebral ischaemia, indicating the importance of hedgehog signaling in the formation of the glial scar (Honsa et al., 2016).

Thus our findings of astrocytes undergoing reactive changes *in vitro* in neuralising medium which contain sonic hedgehog is in agreement with observations noted from others, and whilst our finding that astrocytes were capable of forming cells with a neuronal phenotype equally suggests that reactive astrocytes may possess multipotent stem cell characteristics, it is intriguing that the timing at which the cells are placed into neuralising medium after passaging can give such a profound difference in the cellular response to the medium change. This effect something that most certainly warrants further study, as it may hold clues to allow for the modulation of the reactive response of astrocytes.

4.3.4 Astrocytes are inhibitory to neurite outgrowth from otic neural progenitors.

In this collection of experiments, it was clearly apparent that astrocytes were inhibitory to neurite outgrowth from otic neural progenitors in our *in vitro* co-culture system. This has also been reported in cultures of spiral ganglion neurons with central glia (Jeon et al., 2011, Whitlon et al., 2009), as well as neurons from other parts of the nervous system in co-culture with astrocytes (Cua et al., 2013).

There are a couple of plausible explanations for this phenomenon. Firstly, as has been shown previously, the effect of placing the astrocytes in neuralising medium 2 days after setting up co-cultures elicits a reactive response from the cells. Given that co-cultures were set-up 48 hours after passaging, the reactive phenotype of the astrocytes in the presence of sonic hedgehog may be mimicking some of the mechanisms of glial scar formation *in vivo*, given the role that hedgehog signaling

plays in glial scar formation (Honsa et al., 2016). Reactive astrocytes are known to deposit a plethora of inhibitory extracellular matrix proteins, most notably chondroitin sulphate proteoglycans. It is likely that astrocytes in neuralising medium are producing these inhibitory extracellular matrix proteins, which subsequently hinder neurite outgrowth.

Interestingly, we observed a correlation between the avoidance behavior of otic neural progenitors from reactive astrocytes, and the degree of their neuronal phenotype; those cell batches that strongly expressed neuronal markers when differentiated in isolation tended to avoid regions of reactive astrocytes within culture dishes, whereas those cell lines that weakly expressed neuronal markers readily grew on top of reactive astrocytes. This suggests that the inhibitory effects of extracellular matrix proteins from reactive astrocytes may be specific to cells with a neuronal phenotype. In addition to the secretion of inhibitory extracellular matrix proteins, it is also feasible that astrocytes may also be preventing otic neural progenitors from differentiating into neurons, possibly by competing with otic neural progenitors for the sonic hedgehog within the neuralising medium.

This collection of experiments suggests that we have developed an *in vitro* model of reactive gliosis. This paves the way for future experiments in which we can test the efficacy of pharmacological agents to overcome the negative effects of reactive gliosis, which may subsequently be used with otic neural progenitors *in vivo* to obtain greater penetration of neurites into the central portion of the nerve.

A limitation of the work presented here with astrocytes is that cortical astrocytes were used for co-culture experiments, primarily due to their relative ease in culturing. However, given the heterogeneity of astrocytes from different portions of the brain, it is possible that there may be some subtle differences in the cell biology between astrocytes at the level of the cochlear nucleus and cortical astrocytes, including their responses to pathological insults. Thus, whilst our experiments have yielded a useful *in vitro* model of reactive astrogliosis, the model may not be totally representative of the glial changes that take place at the level of the brainstem *in vivo*.

CHAPTER 5: THE GLIAL COMPARTMENT IN THE OUABAIN MODEL OF AUDITORY NEUROPATHY AND CELL TRANSPLANTATION IN THE MURINE COCHLEA

5.1 Introduction

The Glia in Auditory Pathology

5.1.1 Disruption of peripheral glia on auditory function

There is now increasing evidence that glial cells within the auditory system are involved in hearing pathologies. In addition to the work of Morris et al. in which they illustrated that disrupted ErbB2 signaling resulted in aberrant innervation of the Organ of Corti (Morris et al., 2006), further work by Tang and colleague reports that Connexin 29 is strongly expressed in cochlear Schwann Cells and absence of the gene resulted in developmental delay in hearing sensitivities, early high frequency hearing loss in the mature cochlea, and distorted ABR responses (Tang et al., 2006).

More common pathologies such as presbycusis and noise induced hearing loss have also been shown to have an association with altered glial cell biology. A deficiency in fibroblast growth factor receptor signaling in myelinating glial cells has been shown to contribute to SGN degeneration and leads to age-related hearing loss (Wang et al., 2009). More recently, it has been shown that acoustic

overexposure elongates the nodes of Ranvier in the auditory nerve which results in decreased conduction velocities of action potentials, and a decreased number of release sites within the cochlear nucleus (Tagoe et al., 2014).

Schwann cells may also undergo changes in response to aminoglycoside injury. It has been shown that co-administration of gentamycin and furosemide can cause Schwann cells to stop expressing P0, suggesting that they phenotypically change into a non-myelinating cell in response to such an insult, and perhaps this phenotypic change explains the subsequent demyelination and SGN loss observed following ototoxic injury within the cochlea (Hurley et al., 2007). More recently, Corfas and Wang have investigated the role that Schwann cells play in the entity of 'Hidden Hearing Loss'; a condition in which people experience difficulties in speech discrimination despite normal audiometry. Whilst much of the work investigating this has focused on trying to understand the pathological changes that occur at the synapse between the auditory nerve and hair cells, Corfas and Wang have shown that loss of Schwann cells at the peripheral terminal of the auditory nerve can also result in a hidden hearing loss pattern (Wan and Corfas, 2017).

More relevant to the work presented in this chapter is the extensive study carried out by Hainan Lang on the effect of Ouabain administration on the peripheral glial cells of the cochlea. In response to the Ouabain induced spiral ganglion degeneration, hypertrophy and hyperplasia of glial-like cells was observed, which expressed classical glial markers such as SOX10 and S100 (Lang et al., 2011). Interestingly, these cells also switched on expression of SOX2 and increased

expression of BrdU, suggesting a phenotypic change from quiescence to actively re-entering the cell cycle. It has been suggested that this represents a de-differentiation of mature Schwann cells into a more immature state, which may foster an environment which facilitates the repair of SGNs in early deafness. The idea of Schwann cells within the auditory system de-differentiating in response to injury appears to agree with the observations from studies on sciatic nerve injury, where Schwann cell proliferation and de-differentiation has been a widely held view (Chen et al., 2007). However, very recently this idea has been questioned by Jessen and Mirsky in their most recent review article, where they assert that rather than de-differentiating into an immature state, Schwann cells trans-differentiate into a 'repair' Schwann cell, as these cells have a distinct molecular profile from immature, pre-myelinating Schwann cells (Jessen and Mirsky, 2016). For example, GDNF, Olig1, Shh and artemin are all upregulated in injured Schwann cells but are either absent or expressed in low quantities in immature Schwann cells (Arthur-Farraj et al., 2012, Fontana et al., 2012). Alongside this, repair cells are functionally different from immature Schwann cells, as they are involved in the innate immune response of activating macrophages and myelinophagy (Suzuki et al., 2015). Furthermore, repair cells form 'Bundles of Bungner', which essentially behave as a scaffold for regenerating neurites (Stoll and Muller, 1999), and whilst immature Schwann cells do play a role in pruning neurites in development, they are still able to find their targets in the absence of Schwann cells (Riethmacher et al., 1997). This suggests that more work is needed to understand the precise nature of the Schwann cell response to Ouabain injury within the cochlea, as to whether it represents a 'de-differentiation' into an immature phenotype or a 'trans-differentiation' into a repair cell.

5.1.2 Cochlear supporting cells – A specialised type of glia?

Traditionally, SNHL is thought to be commonly caused by an ototoxic insult to the inner hair cells of the cochlea, resulting in the inability of the cochlea to convert the mechanical energy from sound waves into electrical impulses. It has been postulated that hair cells are an important source of trophic support to SGNs, and thus loss of hair cells results in Wallerian degeneration and secondary loss of nerve fibres.

There is however some evidence to suggest that cochlear support cells also play a pivotal role in providing trophic support to SGN cells. Interestingly, loss of ErbB receptor signaling in cochlear support cells results in SGN loss whilst support cells and hair cells remain intact (Stankovic et al., 2004). Furthermore, support cells are also known to provide trophic support to SGNs, as neurotrophins such as NT-3 are known to be expressed by them (Sugawara et al., 2005). This symbiotic relationship between support cells and SGNs resembles the one that exists between Schwann Cells and neurons. Taking this into account alongside the fact that support cells express classic glial markers such as S100, PLP and GFAP (Rio et al., 2002, Gómez-Casati et al., 2010, Coppens et al., 2001) adds further weight to the theory that perhaps we should consider support cells as a specialised type of glial cell within the auditory system.

Whilst it is clear that support cells are an important trophic source, some have gone as far as suggesting that inner hair cells are actually not required for spiral ganglion survival, and that supporting cells are the principle cell type in

maintaining spiral ganglion survival. When mice lacking the high affinity thiamine transporter Slc19a2 are fed a thiamine depleted diet, a rapid loss of hair cells ensues, however the supporting cells remain intact. In these animals, spiral ganglion neurons survived for many months, despite the lack of hair cells (Zilberstein et al., 2012). Thus, given that support cells are equally susceptible to damage as hair cells from ototoxic agents (Sugawara et al., 2005), acoustic overstimulation and the processes of natural ageing (Kujawa and Liberman, 2015), coupled with the observation that inner hair cells are not necessary for neuronal survival, perhaps we ought to reconsider secondary Wallerian degeneration as a consequence of a pathological process within the specialised 'glial cells' of the cochlea?

5.1.3 Disruptions to central glia within the auditory system

Astrocytes can also undergo changes at the level of the cochlear nucleus. Following cochlear ablation, astrocytes undergo a proliferative response by increasing in size and density (Campos-Torres et al., 2005). Although astrocyte proliferation is typically thought to be inhibitory to neural regeneration, in the ablated cochlear nucleus, astrocyte proliferation occurs concomitantly with re-innervation of the cochlear nucleus by nerve fibres from the medial olivocochlear neurons, indicating that in certain circumstances astrocytes may be permissive to neuronal repair. In an attempt to understand these process within the cochlear nucleus further, Fredrich and colleagues (Fredrich et al., 2013) examined the astrocytic expression of matrix metalloproteases following ablation of the cochlear nucleus, and compared this with effects of ablating the cochlear nucleus

alongside inhibiting the re-innervating the medial olivocochlear neurons. They found that ezrin, polysialic acid, MMP-2 and MMP-9 were expressed in astrocytes during the first week of cochlear ablation, however when reinnervation of the CN was inhibited, astrocytic proliferation remained unchanged and ezrin and MMP-9 were normally expressed, however expression of polysialic acid and MMP-9 drastically decreased when neuronal re-innervation was inhibited. Thus, the authors conclude that axonal growth and synaptogenesis in the cochlear nucleus may result in astrocytes altering their molecular profile and facilitate the process of tissue re-organisation following neuronal damage.

It is possible that glial responses may vary at the level of the cochlear nucleus, depending upon the nature of the hearing loss. A recent study looked at glial cell response to an induced conductive hearing loss (Fuentes-Santamaria et al., 2014), in which the ossicles were surgically removed, resulting in decreased cochlear activity. Immunohistochemistry showed a marked proliferation of microglial cells 1-4 days post lesion, whereas astrocytic cells didn't change significantly. The authors conclude that astroglial reactions most probably accompany neuronal degeneration, like that seen following cochlear ablation, whereas microglial reactions may play a more important role in neuronal and synaptic re-organisation following conductive lesions.

Astrocyte proliferation has also been demonstrated in other models of auditory nerve pathology. Sekiya and co-workers (Sekiya et al., 2011) looked at glial responses to the application of mechanical pressure within the auditory nerve, in an attempt to simulate the pressure effects on the nerve by a tumour. They

illustrated a profound gliosis in the auditory nerve in response to nerve compression at the internal auditory meatus by a steel wire, whereby GFAP labeled central glia crossed the PCTZ into the peripheral auditory system. They later used this model to study the impact of this gliosis on cell transplantation within the cochlea, where they reported that cells transplanted onto the surface of gliotic nerves treated with chondroitinase ABC, they readily migrated within it to repair the neuronal circuit and recover some auditory function. Interestingly, they found that intraneural administration of cells into gliotic nerves treated with chondroitinase ABC was not effective (Sekiya et al., 2015).

Despite the fact that aminoglycoside injury is one of the most well studied models of sensorineural hearing loss, little is known about the effect it induces within the central glia of the auditory nerve. Astroglial reactions have recently been observed in mice following neomycin injury, with increased expression of GFAP being observed 3 weeks after injury, and GFAP labeled astrocytes crossing the glial transitional zone and migrating peripherally along the auditory nerve over a period of 6 weeks (Hu et al., 2014).

Methods of Stem Cell Delivery into the Cochlea

5.1.4 Methods of cochlear stem cell delivery – scala tympani approach

One of the fundamental factors needed for translating the concept of cochlear stem cell therapies from the bench to the bedside as a treatment for sensorineural hearing loss is a surgical technique that delivers the cells to their desired location without causing too much trauma to the existing structures within the cochlea.

Perhaps the simplest method through which to do this has been through the scala tympani approach, by infusing the cells through the round window of the cochlea. This approach has a number of benefits; the round window is easily accessible, thus making it the easiest to perform from a surgical point of view. Furthermore, of all the cell delivery approaches, it is the least traumatic to the cochlea and finally, a cell infusion through the round window provides easy access to all regions of the cochlea. Hu and colleagues were among the first to show the feasibility of this approach, in which they showed transplanted neural stem cells migrate in close proximity to their target of Rosenthal's canal (Hu et al., 2005). However, others who have tried this approach have found that cells remain within the perilymph, with little migration to their desired target areas (Coleman et al., 2006, Matsuoka et al., 2006, Matsuoka et al., 2007). This highlights one of the principle problems with this method of delivery, as one is reliant on the cells naturally migrating into their desired location within the cochlea, and of course cells are equally susceptible to unintended migration into areas of the cochlea where the cells are not required. Furthermore, whilst this technique is useful to

gain a cursory insight into the ability of cells to survive within the cochlea, significant recovery of auditory function is yet to be reported through this surgical approach.

5.1.5 Methods of cochlear stem cell delivery – Intraneural approach

To circumvent the problem of cellular spread, attempts have been made to inject cells into the specific regions of the cochlea where they are required. Attempts have been made to try and inject stem cells into the scala media for hair cell replacement, however thus far this has proven to be quite challenging surgically, causing cochlear damage and worsening of hearing thresholds as a result of surgical intervention, and containing the cells within the scala media remains to be a challenge (Iguchi et al., 2004, Hildebrand et al., 2005).

Intraneural surgical techniques have also been employed in an attempt to replace damaged spiral ganglion neurons within the cochlea. There are two principle ways in which this has been attempted. The first is through the internal auditory meatus approach, in which a craniotomy is made and the cells are carefully injected between the brainstem and the internal auditory meatus. Whilst this approach has been successful in showing cell survival and differentiation of cells into neuronal phenotypes, getting the cells to convincingly reach Rosenthal's canal still remains elusive (Palmgren et al., 2011, Sekiya et al., 2007, Sekiya et al., 2015). Moreover, this is quite an extensive surgical operation which would be quite technically challenging to replicate on humans, however, some functional

recovery of auditory function has been reported through this approach in a model of auditory nerve compression (Sekiya et al., 2015).

The other approach to the cochlear nerve would be through accessing the nerve through the cochlear modiolus through a 'modiolusostomy'. Hu and colleagues were one of the first groups to trial this method, showing cells to have migrated along the nerve towards the internal auditory meatus (Hu et al., 2004). Corrales et al have also used this approach, illustrating that although cells do not necessarily migrate into Rosenthal's canal, they form an ectopic ganglion at the injection site and extend projections towards to Organ of Corti (Corrales et al., 2006). The Rivolta lab has predominantly adopted the intramodiolar approach in its studies on otic neural progenitor transplantation within the deafened gerbil, showing that alongside extending projections both peripherally and centrally from an ectopic ganglion, a significant functional recovery of hearing can be achieved by delivering cells via this surgical approach (Chen et al., 2012). Moreover surgical access to the cochlear modiolus has recently been described in cadaveric human temporal bone studies through a trans-canal approach, which isn't too dissimilar to the surgical techniques used in otological surgery today (Kiumehr et al., 2013).

5.1.6 Aims and objectives

The Ouabain deafness model results in an auditory neuropathy in which Type I spiral ganglion nerves are damaged, and has been employed by the Rivolta lab in the gerbil to study the effects of otic neural progenitor transplantation into the cochlea. The effects observed by Lang and colleagues within the mouse raise interest in the glial responses to injury following Ouabain administration (Lang et al., 2011), in particular whether Lang's observations in the mouse are reproducible and whether they are also seen within the gerbil. This would require the establishment of a reliable surgical method to establish access to the round window for intracochlear administration of Ouabain within the mouse, which currently is not undertaken by any auditory research group within the United Kingdom. Furthermore, given the successes that have been seen in stem cell transplantation studies involving intramodiolar delivery of cells, the development of surgical access to the cochlear modious within the mouse, which is yet to be described, would open the field to the plethora of mouse models of deafness that have been described in the literature.

The aims of this chapter are as follows:

- 1) To establish a safe protocol for the administration of Ouabain in the mouse
- 2) To compare the responses of peripheral and central glia to Ouabain injury in both the mouse and the gerbil

- 3) To demonstrate the ability of transplanted otic neural progenitors to engraft in the base of the auditory nerve within the cochlear modiolus in the mouse.

5.2 Results

5.2.1 Surgical access to the murine cochlea for drug delivery and stem cell transplantation.

Unlike with the gerbil where auditory brainstem responses were measured immediately before surgery, for experiments involving mice, ABRs were typically measured 2-3 days prior to the day of surgery in order to reduce the duration of time that the animal is under general anaesthetic. Auditory brainstem responses were measured in mice prior to surgery as described in chapter 2. Animals aged 2-3 months were brought into the operating suite and were placed into the induction box of an anaesthetic machine. Isoflourane was used for induction and maintenance of anaesthesia (Isoflo, ABBOTT). After induction, mice were then placed onto the anaesthetic circuit with a heat-pad to prevent hypothermia. The post-aural skin on the left hand side was shaved to allow for adequate exposure of the surgical field. A subdermal injection with 0.25% Bupivacaine (Marcaine, ASTRA-ZENECA) was then performed. A curvilinear post-auricular incision was then made by retracting the skin gently with toothed forceps and sharp scissors.

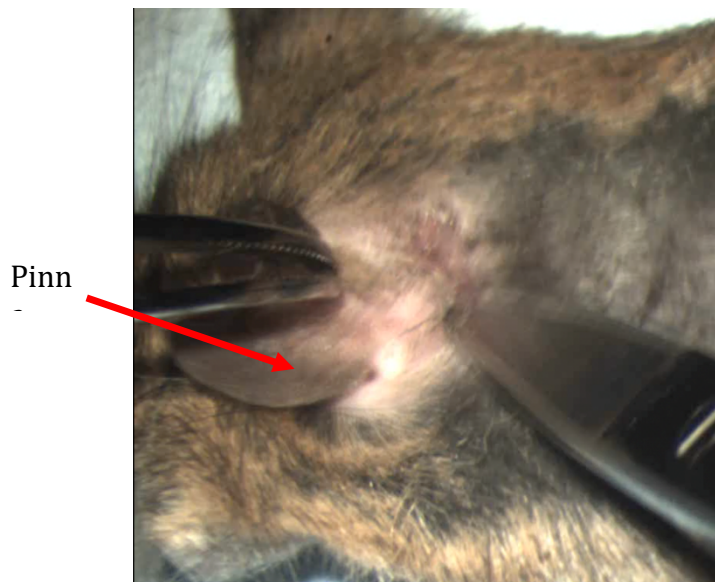


Fig 5.1 – Site of Post-aural incision

It is important to make an adequate sized incision to allow for identification of the underlying anatomical structures, thus facilitating a safe surgical procedure.

The underlying fascia was then grasped between two Dumont forceps and separated along the length of the incision to avoid ‘tunneling’. This was done until the belly of the sternocleidomastoid muscle and greater auricular nerve began to come into view. Performing the dissection in this manner avoids bleeding, and using a cutting method for this step risks damage to the underlying anatomical structures.

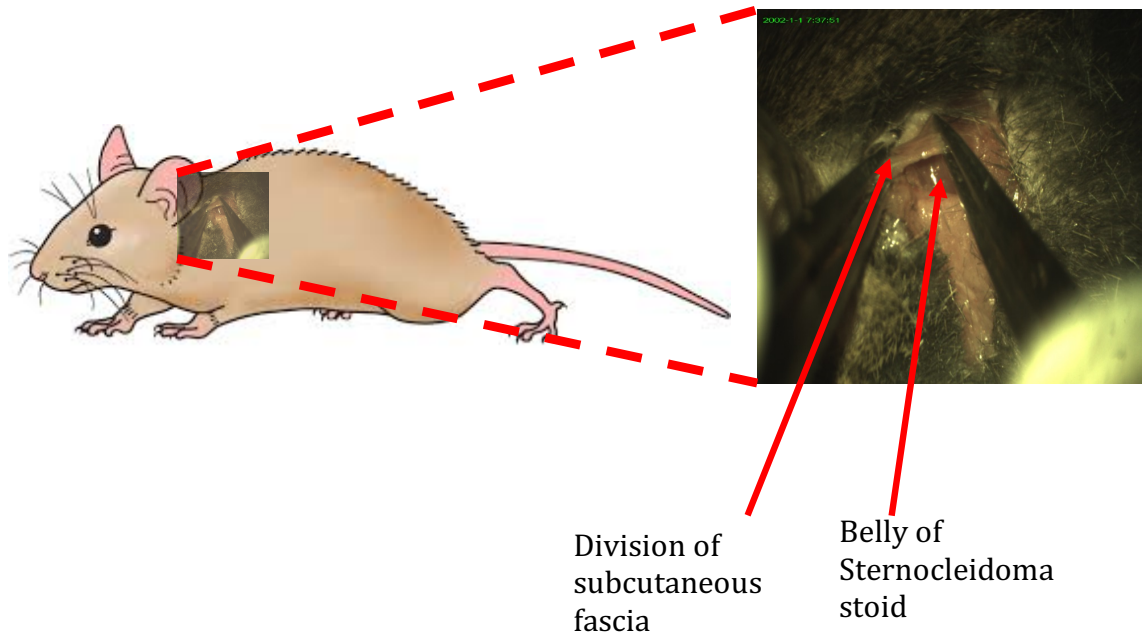


Fig 5.2 – Division of subcutaneous fat to expose the belly of Sternocleidomastoid.

The greater auricular nerve is an important anatomical landmark and must be clearly identified before progressing further with the dissection. It overlies the proximal third of the sternocleidomastoid muscle and runs in an oblique direction. The nerve was transected and a self-retaining retractor was then inserted into the surgical wound to allow the deeper anatomical structures to be visualized.

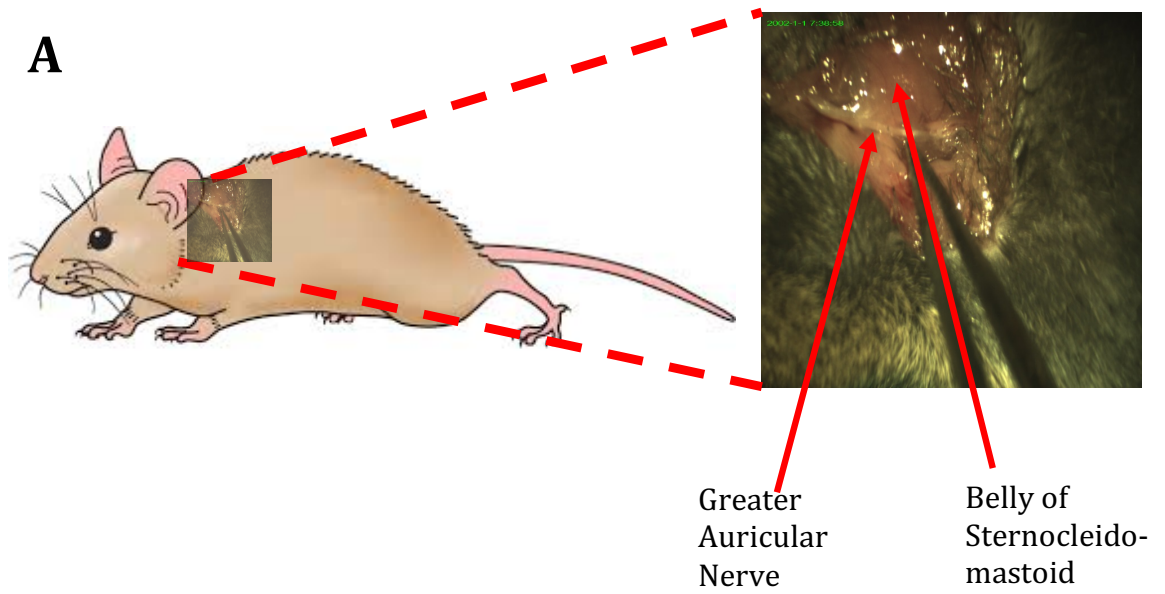


Fig 5.3a&b - Identification and transection of the Greater Auricular Nerve. Cartoon shows position of initial surgical incision and orientation of animal on the operating table

With the self-retaining retractor in situ, the sternocleidomastoid muscle should be clearly visible alongside the extracranial portion of the facial, which is the next key anatomical landmark. In order to fully visualize the extracranial exit-point of the facial nerve, the belly of the sternocleidomastoid muscle was grasped and divided.

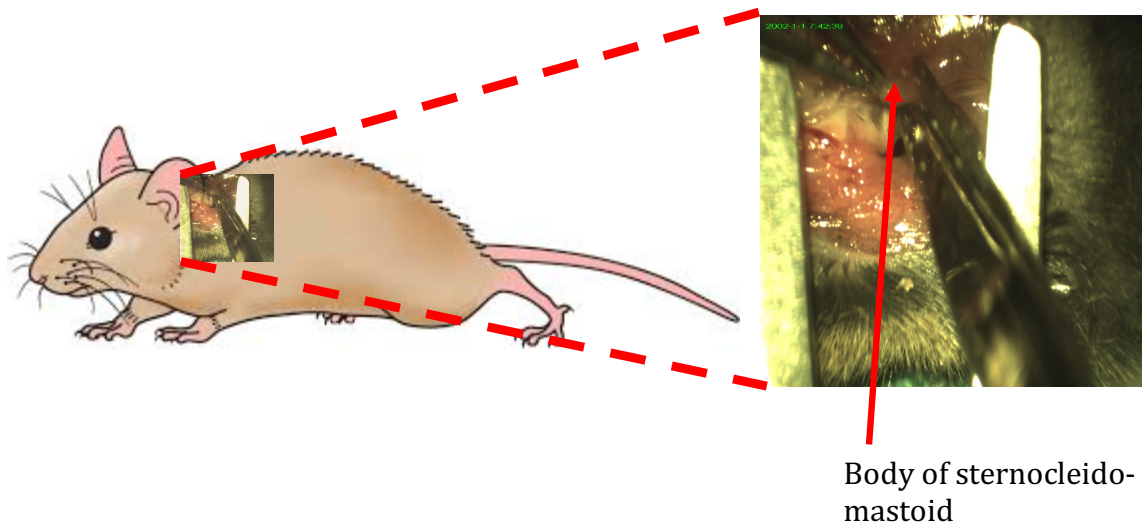
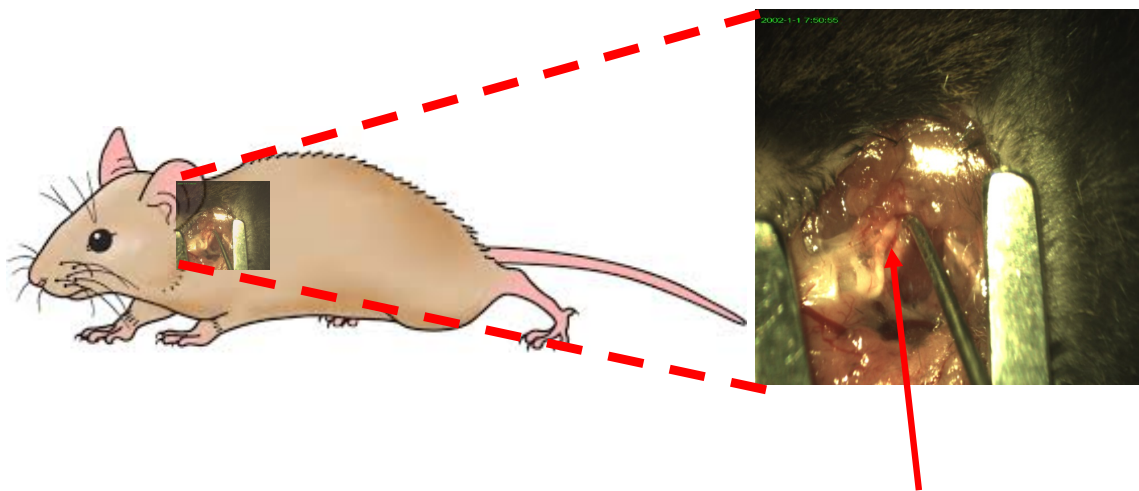


Fig 5.3c – Division of belly of Sternocleidomastoid
Cartoon shows position of initial surgical incision and orientation of animal on the operating table

The facial nerve should now be clearly exposed, and its extra-cranial exit point obviously apparent. A bullostomy just under this point should give a good view of the round window. However, this is a tight space and even a small amount of bleeding at this juncture could compromise the surgical view and severely hamper the remainder of the surgery. Care must therefore be taken to ensure adequate haemostasis and exposure of the bulla. This part of the operation must not be rushed.

In the first instance, the periosteal layer overlying the bulla should be cleared with a fine House-Rosen's needle.



Facial Nerve

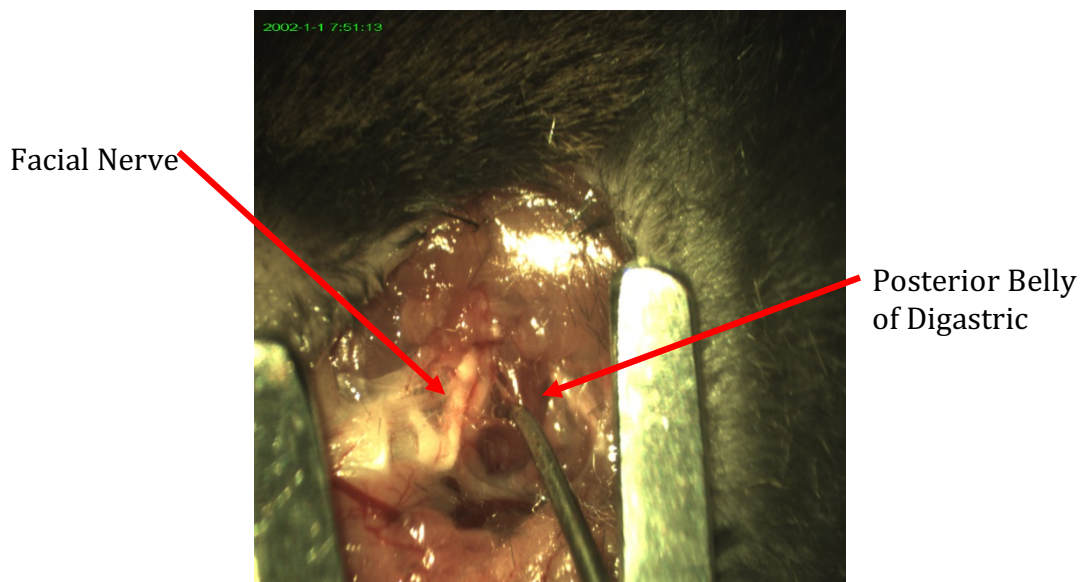


Fig 5.4 – Identification of Facial nerve and clearing of periosteum from bullostomy site **Fig 5.5** – Freeing posterior belly of digastric from inferior ridge of bulla..

The posterior belly of the digastric muscle is attached to the inferior border of the bulla, and this was freed from the bulla using the House-Rosen's needle to allow greater access to the bulla. This step can induce some bleeding, and to control this a small cotton wool patty soaked in 1:1000 adrenalin solution was packed into the space between the bulla and the muscle for a few minutes. In some animals, the trapezius muscle can also obscure the site of the bullostomy, and this can be scraped from the area gently away using the needle. To ensure a completely dry surgical field, haemostasis was achieved with a battery operated hand-held electro-cautery device (BOVIE).

Once the bullostomy site had been fully exposed, a handheld drill was used to make the bullostomy (Omnidrill35 WPI). A 0.5mm diamond cutting burr was attached to the hand-piece, and drilling was performed at 15,000rpm. Drilling was undertaken until only a thin sheet of translucent bone was present. This final piece of bone was gently swept away with the House-Rosen's needle. Drilling was performed in this fashion in order to avoid damage to structures within the inner ear, and specifically the stapedial artery which is at risk of injury.

The stapedial artery and round window should come into view. Access to the round window was improved with a combination of chipping away small amounts of bone with the House-Rosen's needle, and drilling the edges of the bullostomy to widen it.

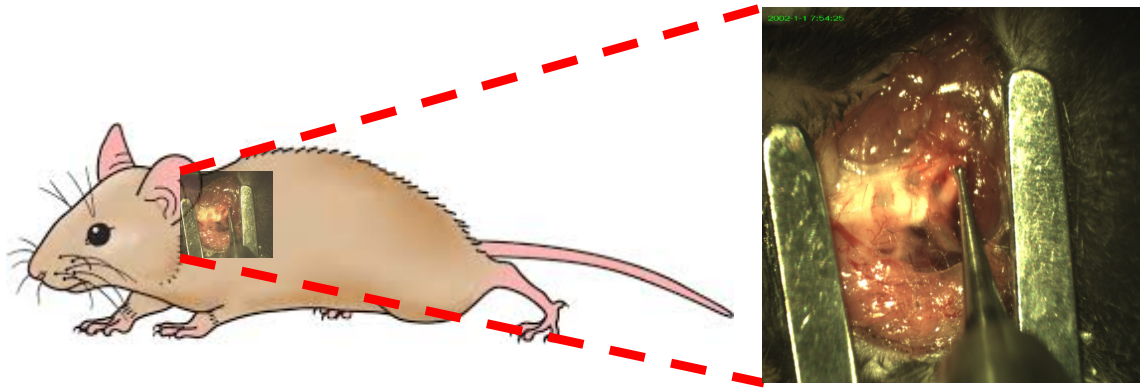


Fig 5.6 - Position of drill for Bullostomy.

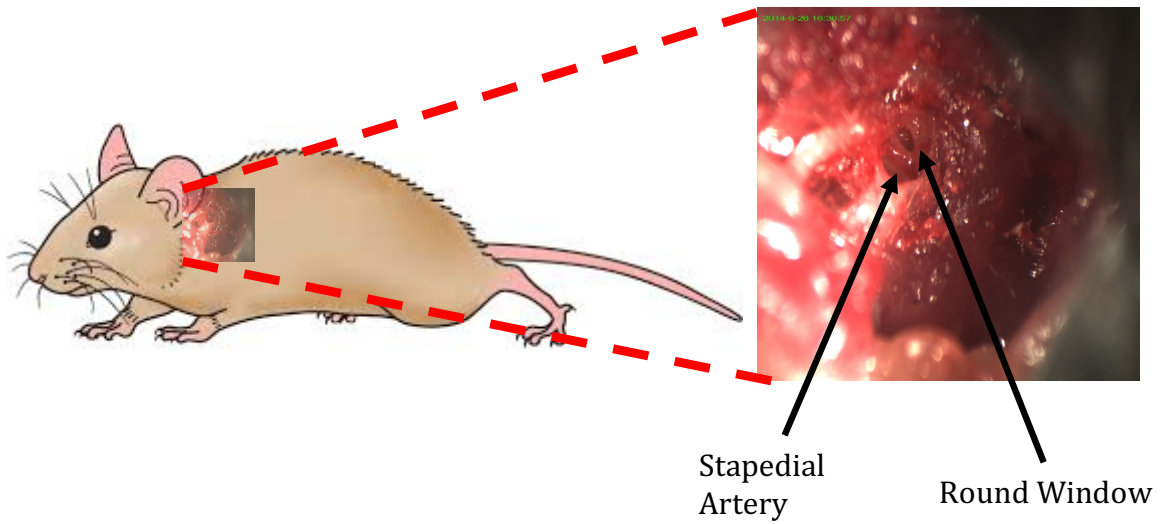


Fig 5.7 - Exposure of round window and stapedial artery.

With the round window clearly in view, Ouabain was then applied to the round window using a nanofil syringe (WPI). For the mouse, we used a concentration of 5mM of Ouabain, and 1-2 μ l was dropped carefully onto the round window, to avoid spread to the surrounding tissues. The Ouabain was left on the round window for 45 minutes after which the Ouabain was wicked off. A small piece of subcutaneous fat was cut away from the superficial fascia and applied onto the bullostomy site, and held secure with a drop of Vetbond tissue glue (3M). The wound was then closed in two layers with 4-0 vicryl, and a further injection of 0.25% Bupivacaine was applied to the edges of the surgical wound after closure.

Intramodiolar delivery of cells into the cochlea is yet to be described for the mouse, and so part of this work was to develop techniques for surgical access to the cochlear modiolus for cell delivery. For transplantation of cells into the cochlear modiolus, a small modiolusostomy was made with a fine dental file. With the operative microscope at the highest magnification and positioning the animal appropriately, the edge of the modiolus should become apparent through the round window, and this can be confirmed by gently palpating the bony surface of the modiolus with the tip of the dental file. Holding the file between the index finger and thumb, the dental file is gently advanced by rotating the file sequentially clockwise and anticlockwise between then finger and thumb. Minimal force should be applied to prevent cochlear damage. Eventually, a small sensation of a 'give' will indicate full penetration through the modiolar bone.

Otic neural progenitors derived from the H14 NOP/SOX2 line were used for transplantation studies. Cells were lifted with Trypsin as described in section

2.2.3 of chapter 2 and were resuspended in 10 μ l of DMEM, at a density of 50,000 cells/ μ l. A nanofil syringe dedicated for cell transplantation was used, which had been primed twice with 70% ethanol and then thrice with sterile PBS. 100,000 cells were then slowly injected into the cochlear modiolus, taking care to avoid overspill of cells. After injection, the bullostomy site was sealed with subcutaneous fat held in place in Vetbond, and a 2 layer wound closure was performed with 4-0 vicryl.

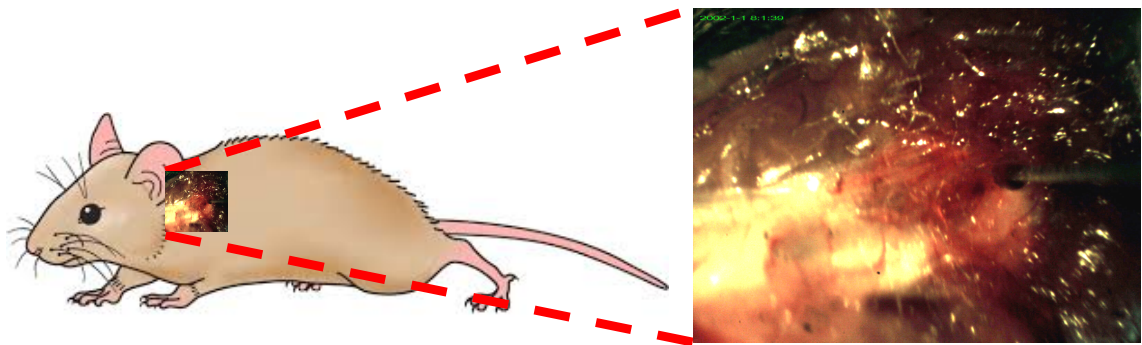


Fig 5.8 – Making the Modiolusostomy for stem cell delivery.

5.2.2 Effect of Ouabain on Spiral Ganglia within Mice and Gerbils

Prior to examining the effect of Ouabain on glial cells within the cochlea, it was important to confirm the known effect of Ouabain on spiral ganglion neurons. The round window was exposed in both mice and gerbils, and an identical deafness protocol was used in both the mouse and the gerbil, which entailed 5mM of Ouabain solution being dropped onto the round window for 45 minutes before being wicked off. Auditory brainstem responses were measured immediately prior to surgery in the case of the gerbil, and 2-3 days before surgery on mice, and in both species were measured 1 week postoperatively at which point experiments were terminated. Cochleae were then harvested from the animals and processed for immunohistochemistry.

Data were collated from experiments involving 5 mice and 3 gerbils. In order to demonstrate the loss of spiral ganglion neurons, staining with B-Tubulin was used to identify spiral ganglion neurons. In both mice and gerbils, immunohistochemistry demonstrated a substantial loss of spiral ganglion neurons, whilst hair cells remained intact (Figs 5.9, 5.11). Spiral ganglia loss was further quantified by counting cells in each turn of the cochlea from 5 sequential sections that were at least 36 μ m apart (to prevent over-counting). Cell counts showed that there was a <90% loss of spiral ganglia in cochleae treated with Ouabain when compared to the contralateral untreated ears in both species (Fig 5.10, Fig 5.12). In addition, Click ABR thresholds showed a significant shift in Ouabain treated ears of both species, with the untreated ear remaining unchanged (Fig. 5.14, 5.16). These results confirm that, in our hands, the

Ouabain protocol was effective in inducing a comparable auditory neuropathy lesion in both mice and gerbils. Also of note is the fact that there was no difference in the protocol employed. This facilitates a meaningful comparison of the glial responses to Ouabain injury in both species.

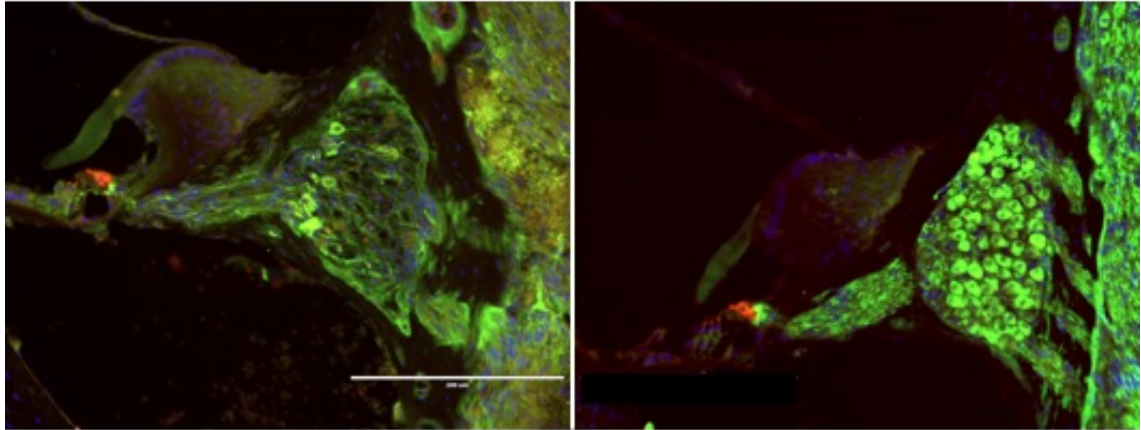


Fig 5.9 – Representative images showing immunolabelling from murine cochlear sections for B-Tubulin (green) and MYO 7A (red). The left- hand image is from the left ear treated with ouabain, and the right-hand image is from the right, untreated ear. Scale bars represent 200 μ m.

Density of TUJ1 Positive Cells In Mice

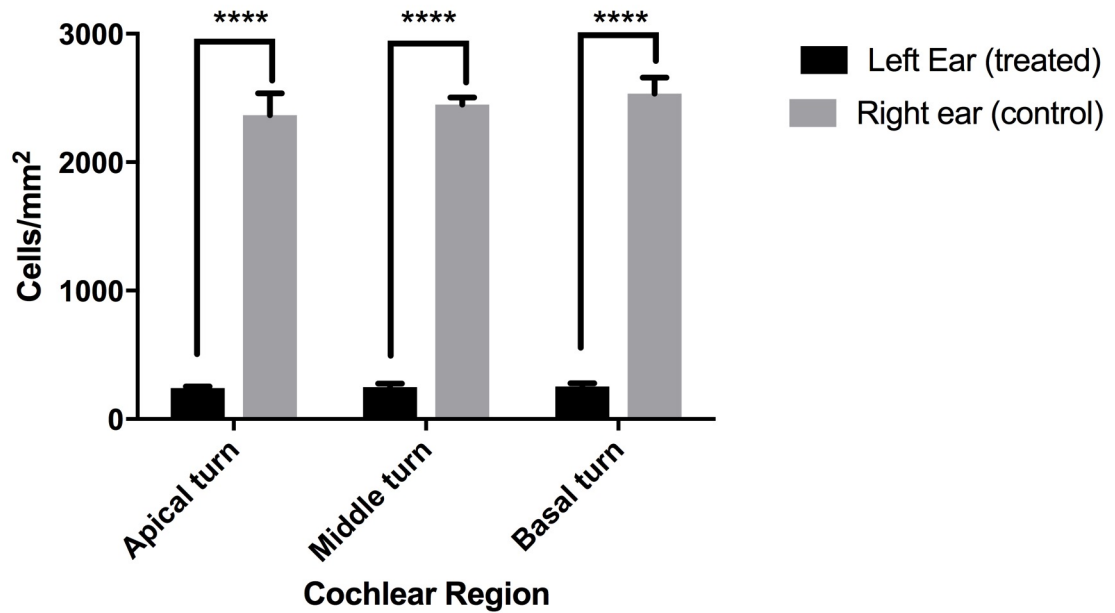


Fig 5.10 – Graph showing average counts for TUJ1 positive spiral ganglia in mice from the apical, mid and basal turns of the cochlea in left ears treated with ouabain versus counts from the right, untreated ear. Error bars denote standard error from the mean. Statistical significance was determined using 2-way ANOVA. ****P<0.0001. (n=5)

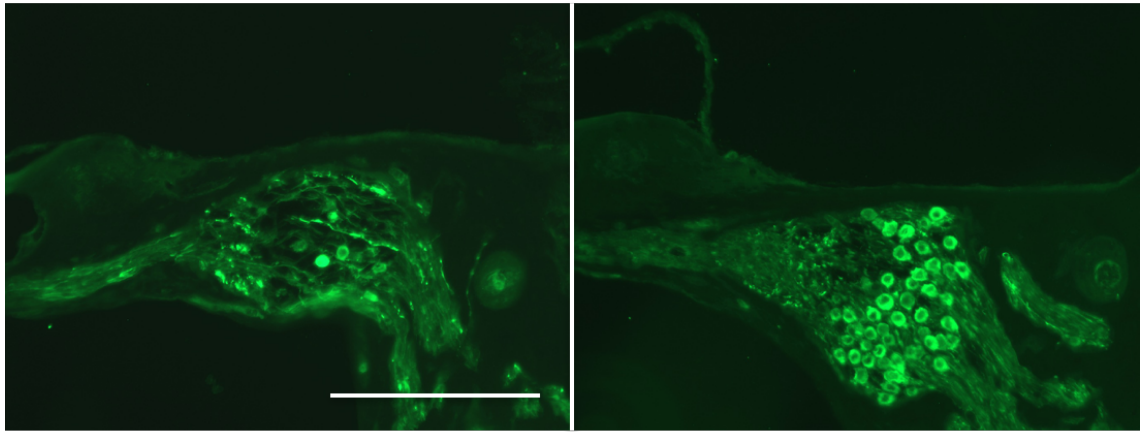


Fig 5.11 – Representative images showing immunolabelling from gerbil cochlear sections for B-Tubulin. The left-hand image is from the left ear treated with Ouabain and the right-hand image is from the right ear which was left untreated. Scale bar represents 200 μ m

Density of TUJ1 Positive Cells In Gerbils

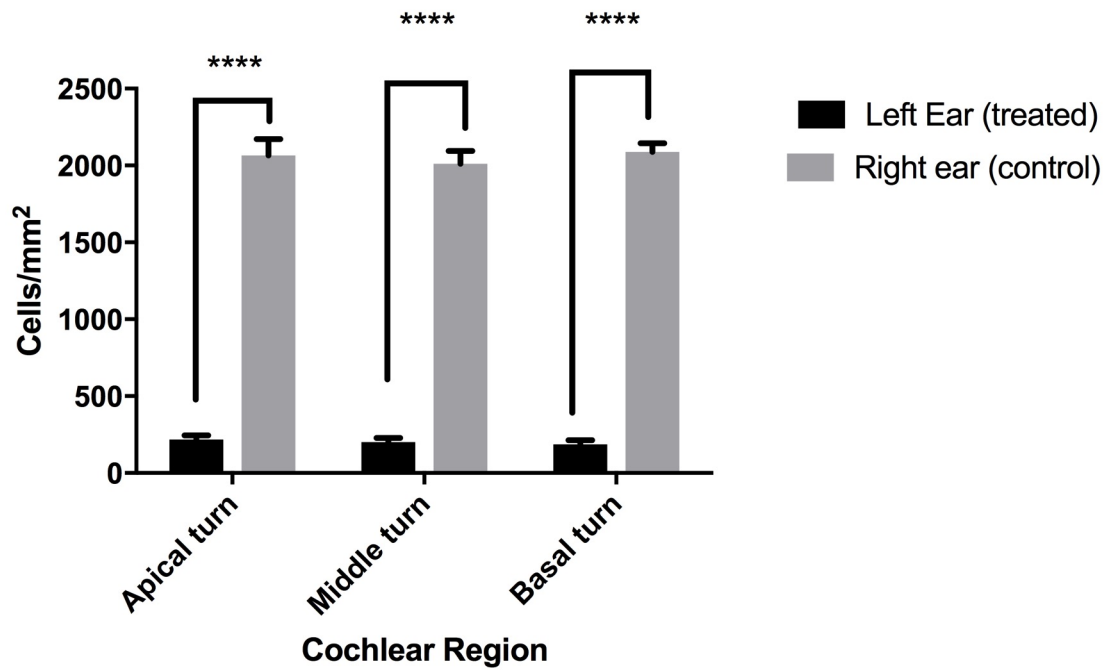


Fig 5.12 – Graph showing average counts for TUJ1 positive spiral ganglia in gerbils from the apical, mid and basal turns of the cochlea in left ears treated with ouabain versus counts from the right, untreated ear. Error bars denote standard error from the mean. Statistical significance was determined using 2-way ANOVA. ****P<0.0001. (n=3)

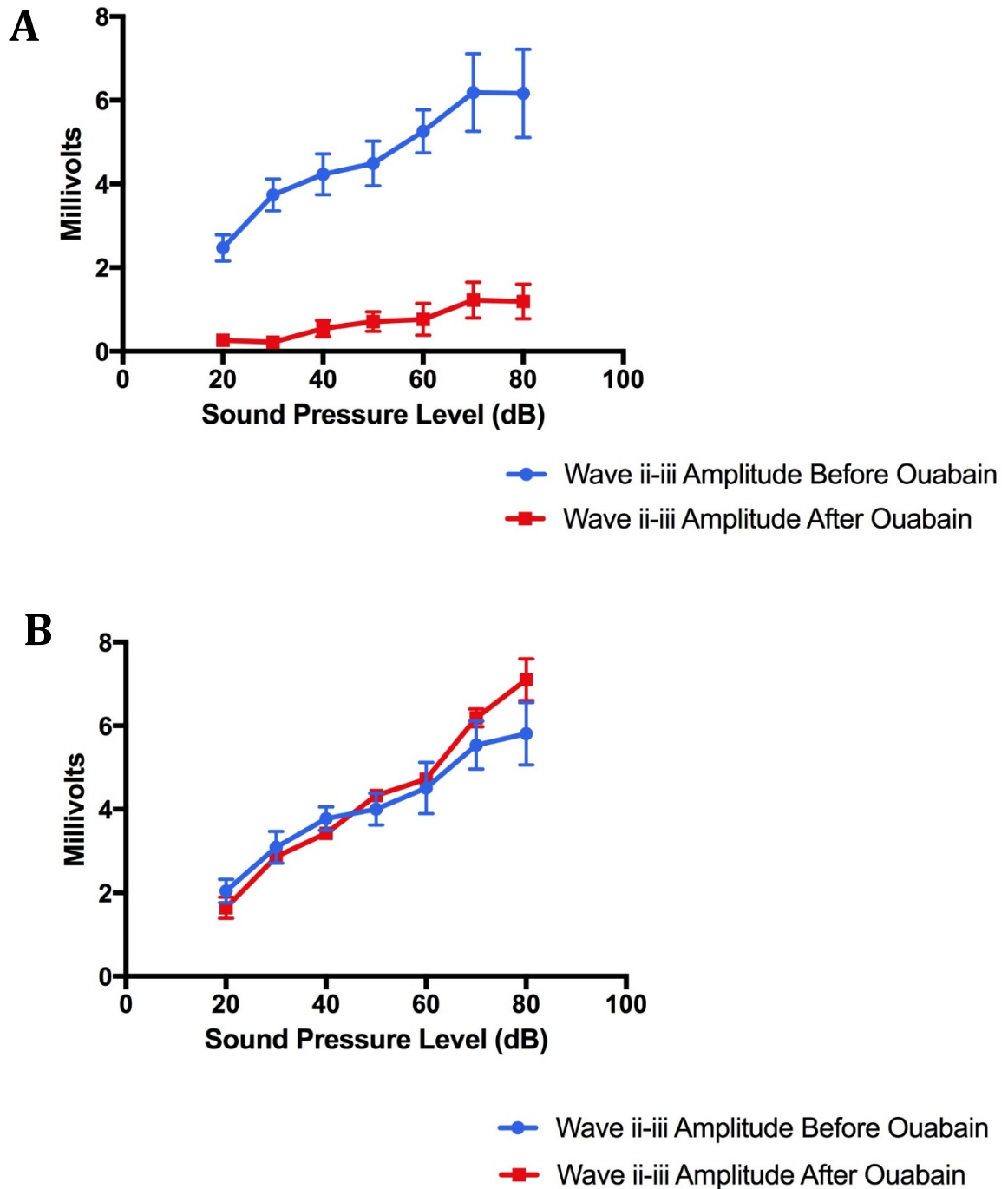


Fig 5.13 – Plot of difference between wave ii positive peak and wave iii negative peak at various Sound Pressure Levels (dB). Panel A shows the murine left ear before (blue) and after (red) Ouabain, and panel B shows the right ear. (n=5)

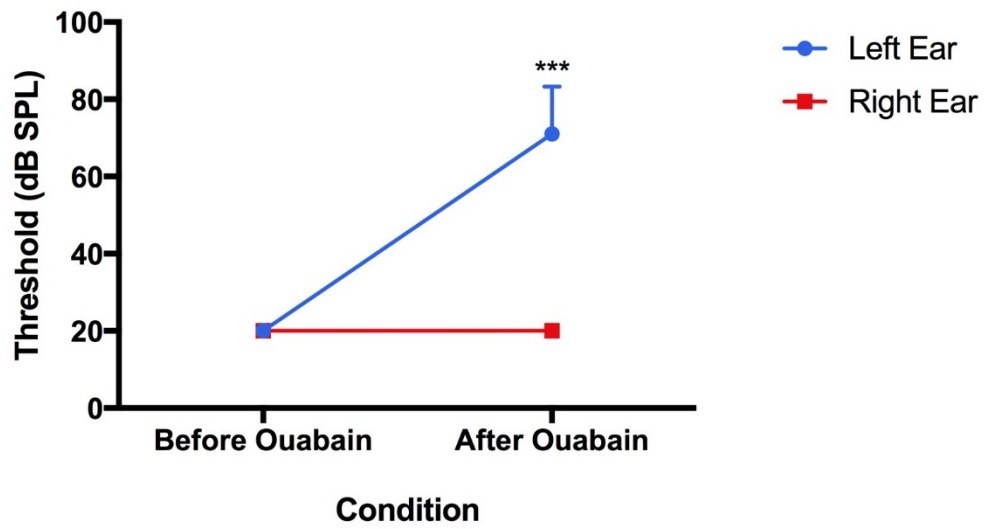


Fig 5.14 – Change in ABR threshold before and after Ouabain administration in the mouse. Blue denotes the left ear, whilst red denotes the right ear. *** $P < 0.001$. (n=5)

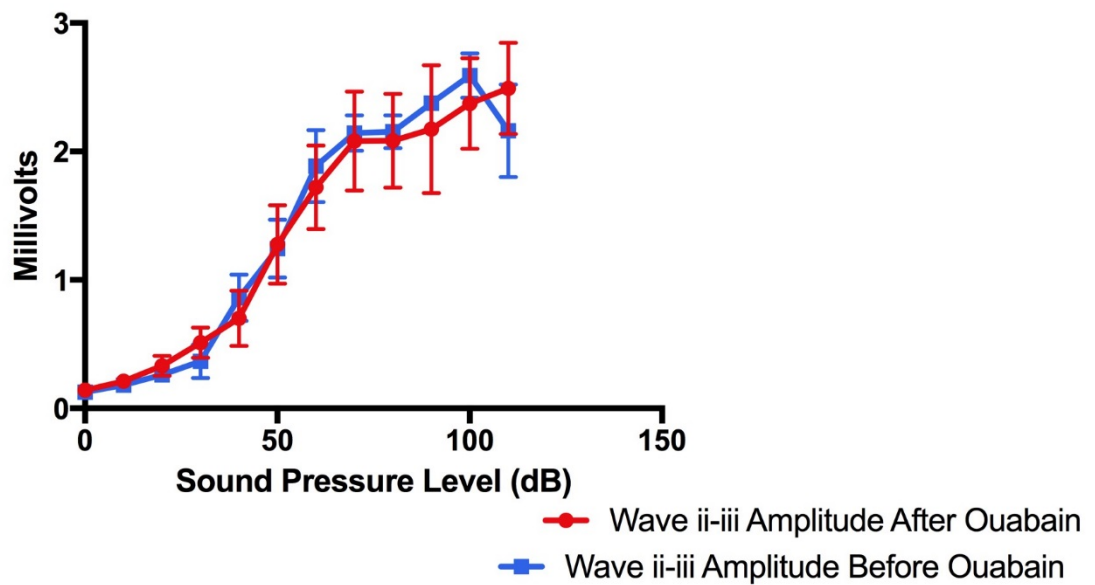
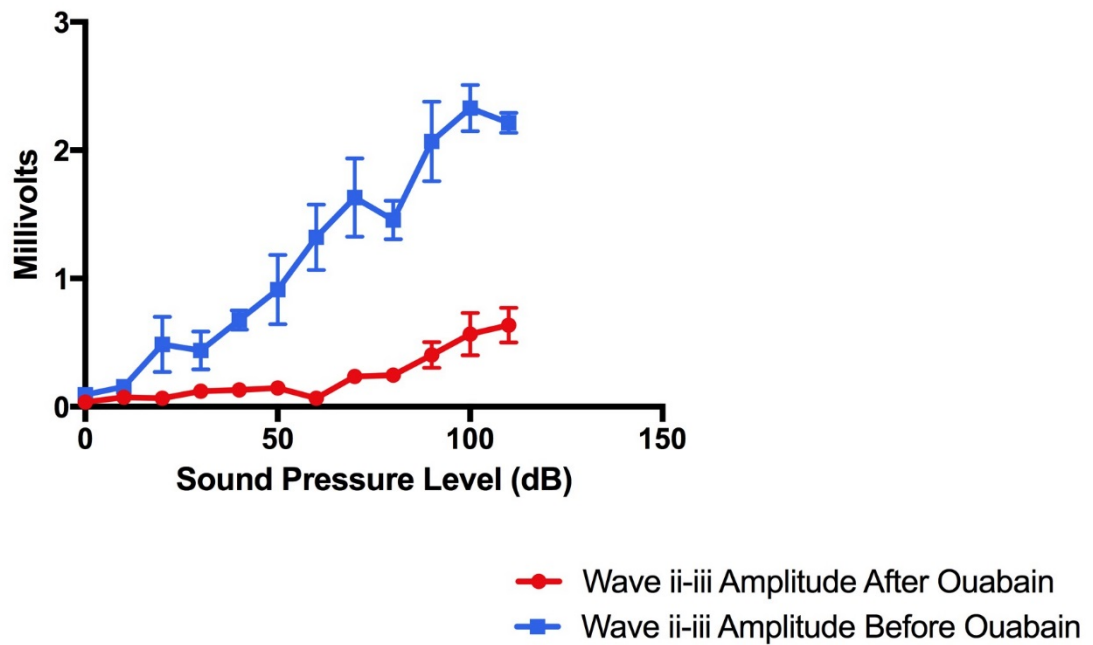


Fig 5.15 – Plot of difference between wave ii positive peak and wave iii negative peak at various Sound Pressure Levels (dB). Panel A shows the Gerbil left ear before (blue) and after (red) Ouabain, and panel B shows the right ear. (n=3)

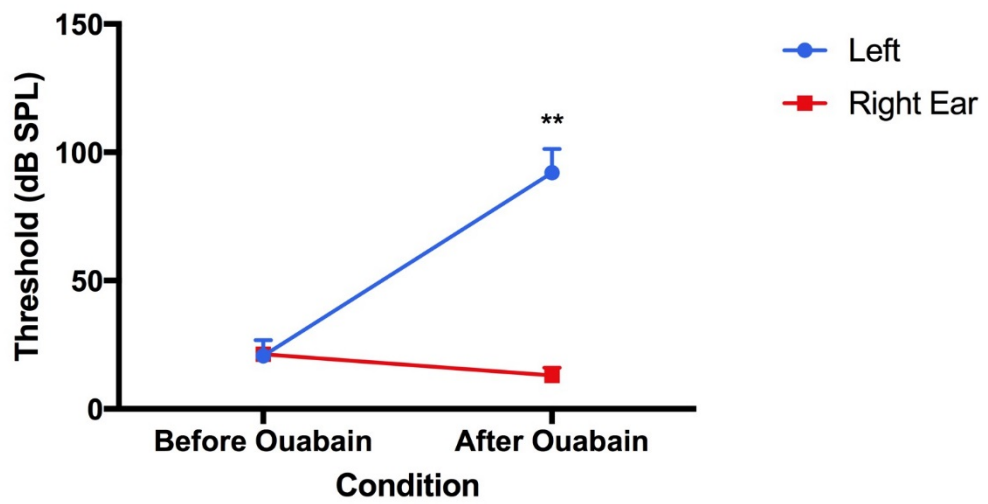


Fig 5.16 - Change in ABR threshold before and after Ouabain administration in the Gerbil. Blue denotes the left ear, whilst red denotes the right ear. ** $P < 0.01$. (n=3)

5.2.3 Effect of Ouabain on peripheral glia of the auditory system in gerbils and mice

After confirming the effectiveness of the Ouabain protocol within both species in inducing a substantial loss of spiral ganglion neurons without interfering with hair cells, the next step was to examine sections focusing initially on the effect of Ouabain administration on peripheral glial cells within the auditory system.

Previous work by Lang and colleagues in the mouse suggested that there is an upregulation of cells expressing SOX10 in response to an Ouabain induced injury (Lang et al., 2011, Lang et al., 2015), with the authors suggesting that peripheral glia become proliferative and de-differentiate into a more immature state. The aim from this set of experiments was to confirm this observation in the mouse with our Ouabain protocol, which differs slightly from that used by Lang, and also to compare this to the response in the gerbil. Data were collected from experiments in 5 mice and 3 gerbils. Immunostaining for SOX10 and P0 was undertaken, in order to further characterise the peripheral glial response.

In contrast to previous findings by Lang, results from these experiments showed a highly significant decrease in the expression of SOX10 in both the mouse and the gerbil (Fig 5.17, 5.19). To further quantify this, cell counts of SOX10 positive cells showed a >78% loss in treated ears of the mouse when compared to the control untreated ear (Fig 5.18), and a loss of >72% in the left ear of gerbils compared to the right ear control (Fig 5.20). In addition to testing for SOX10 staining, expression of P0 was also tested for in control and treated ears; in both species there was clear evidence of P0 staining the myelin sheaths around spiral

ganglion neurons, with a substantial disruption of this architecture in treated cochleae (Figs 5.21 and 5.22, Panel A). This loss of P0 expression isn't solely restricted to Rosenthal's canal, but appears to be widespread within the entire peripheral portion of the auditory nerve (Figs 5.21 and s.22, Panel B). These data suggest that rather than inducing a proliferative response, it appears that the Ouabain protocol used in these experiments is causing a substantial loss of peripheral glia within the auditory system. In keeping with the fact that the hair cells remain intact following Ouabain injury (Fig 5.9), we also noted that the cochlear support cells within the Organ of Corti also remain intact as illustrated on Hematoxylin and Eosin staining (Fig 5.23), and thus if one were to consider the Cochlear supporting cells to be a highly specialized type of peripheral glial cell, then it seems their response to Ouabain exposure is quite different to that of cochlear Schwann cells.

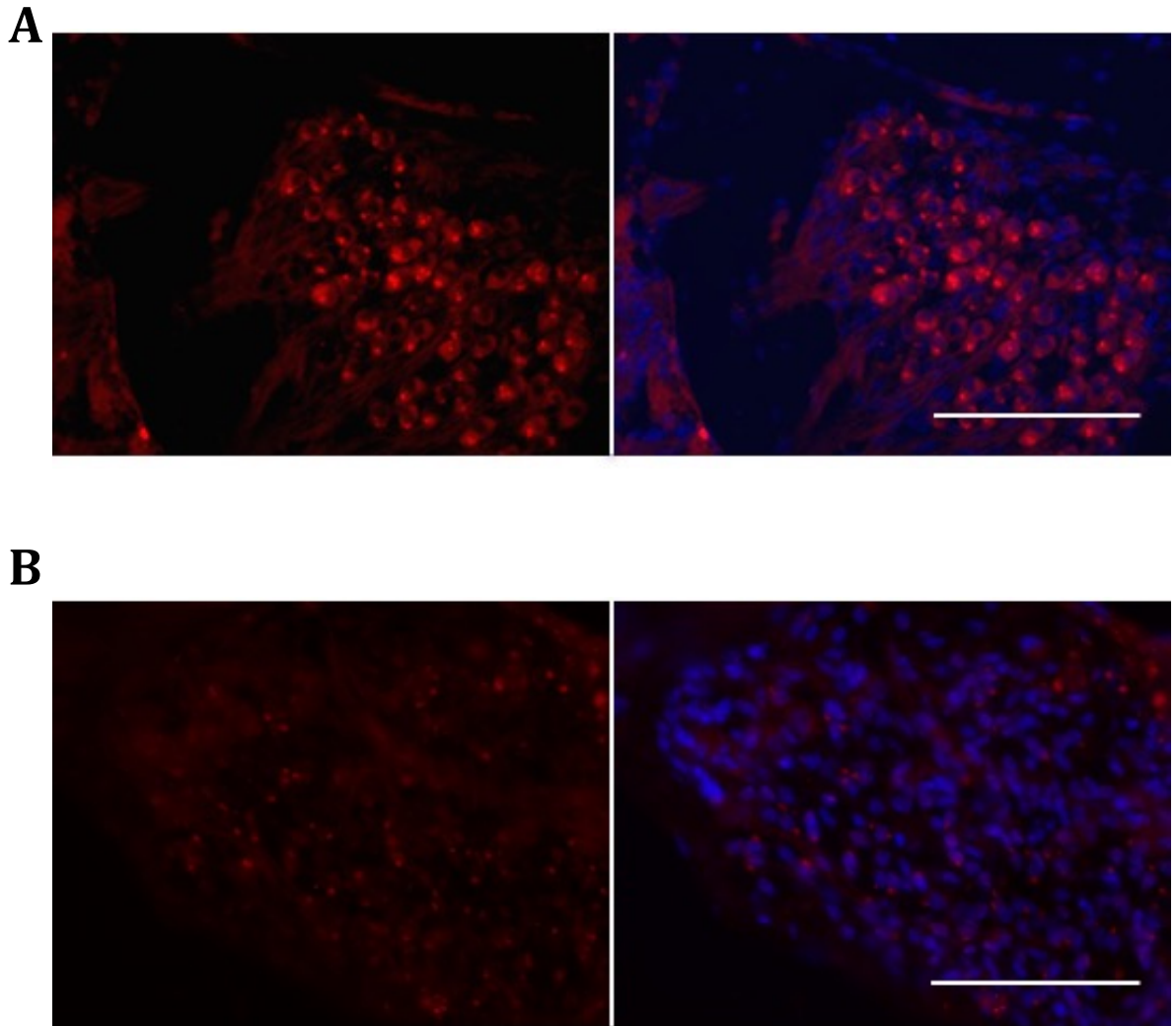


Fig 5.17 – Representative images showing immunolabelling from murine cochlear sections for SOX10 in Rosenthal's canal. Panel A is from the right, untreated ear and the lowermost image is from the left ear treated with ouabain. Nuclei have been counterstained with DAPI. Scale bars represent 100µm

Density of SOX10 Positive Cells In Mice

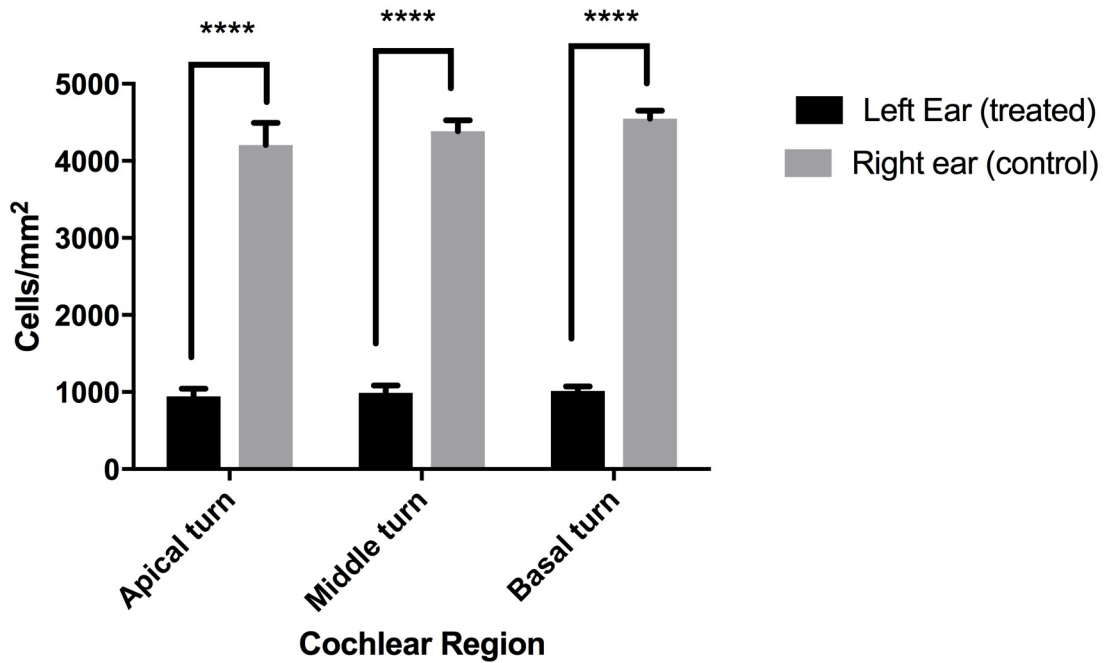
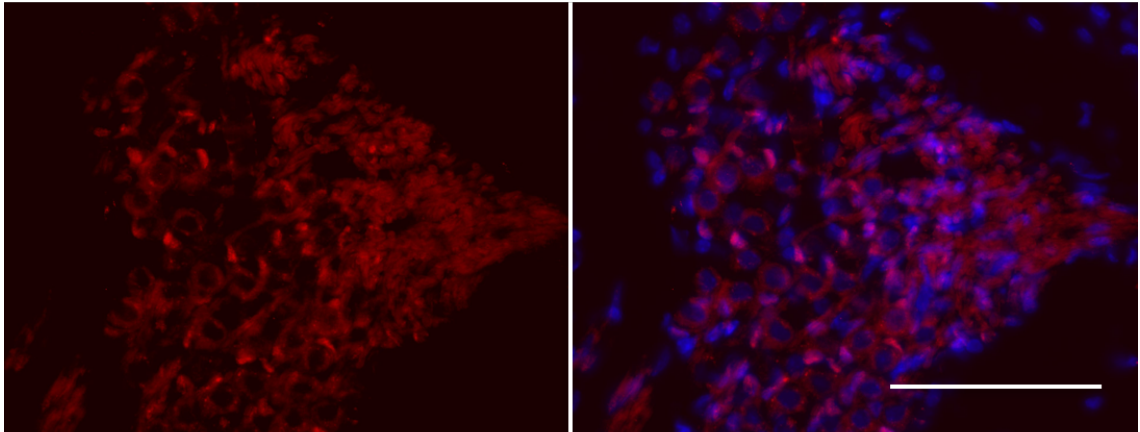


Fig 5.18 – Graph showing average counts for SOX10 positive cells in mice from the apical, mid and basal turns of the cochlea in left ears treated with ouabain versus counts from the right, untreated ear. Error bars denote standard error from the mean. Statistical significance was determined using 2-way ANOVA. ****P<0.0001. (n=5)

A



B

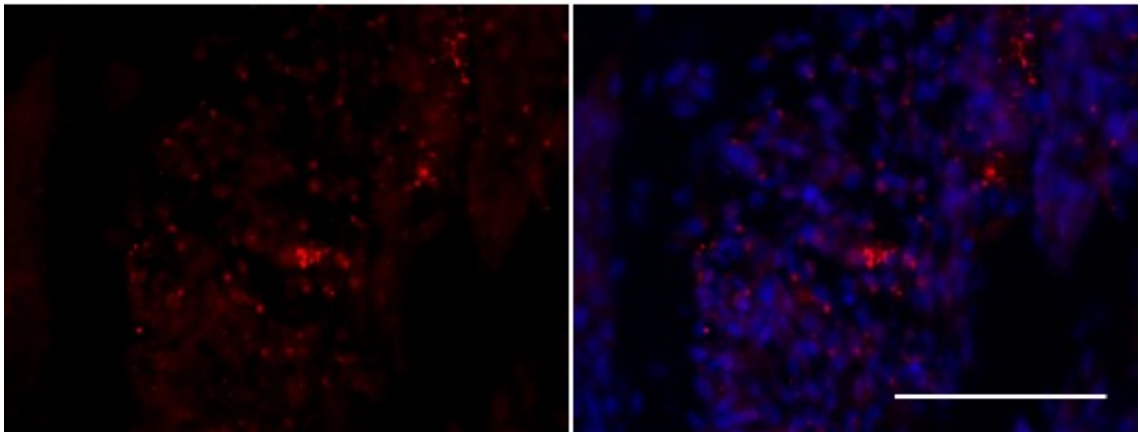


Fig 5.19 – Representative images showing immunolabelling from gerbil cochlear sections for SOX10 in Rosenthal’s canal. Panel A is from the right, untreated ear and the lowermost image is from the left ear treated with ouabain. Nuclei have been counterstained with DAPI. Scale bars represent 100µm

Density of SOX10 Positive Cells In Gerbils

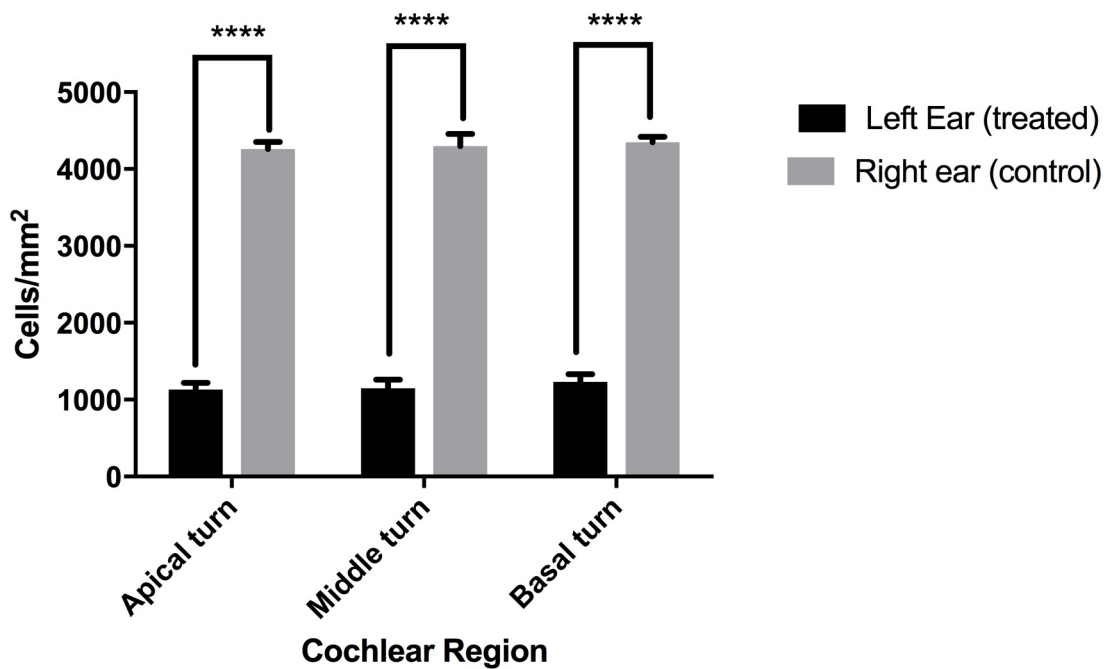
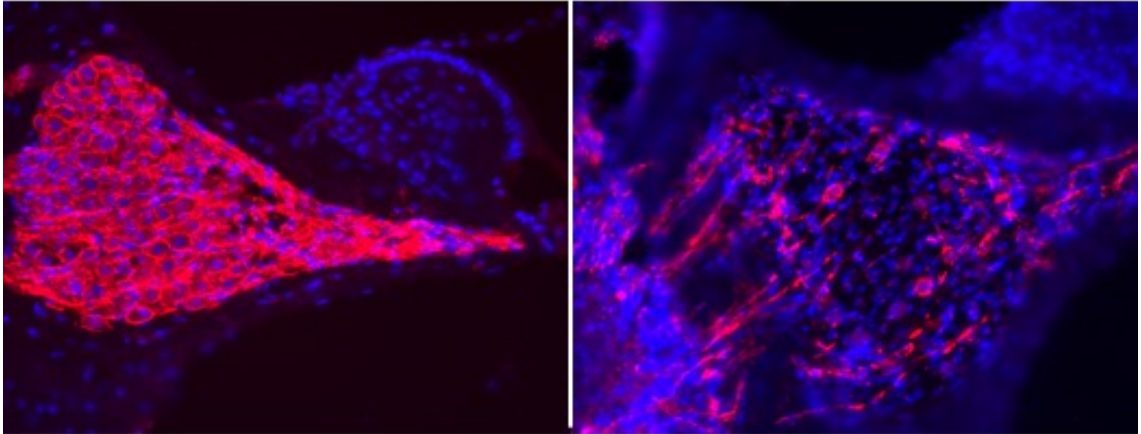


Fig 5.20 – Graph showing average counts for SOX10 positive cells in gerbils from the apical, mid and basal turns of the cochlea in left ears treated with ouabain versus counts from the right, untreated ear. Error bars denote standard error from the mean. Statistical significance was determined using 2-way ANOVA. ****P<0.0001. (n=5)

A



B

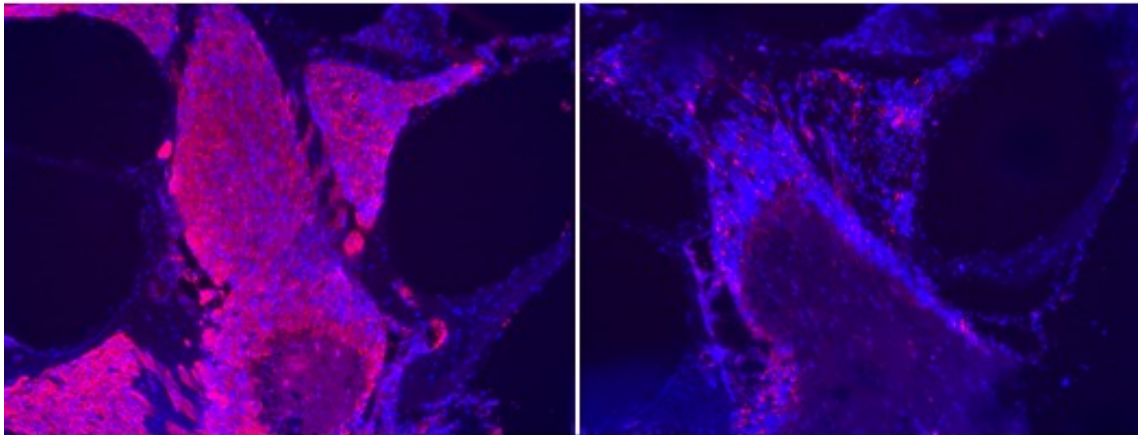
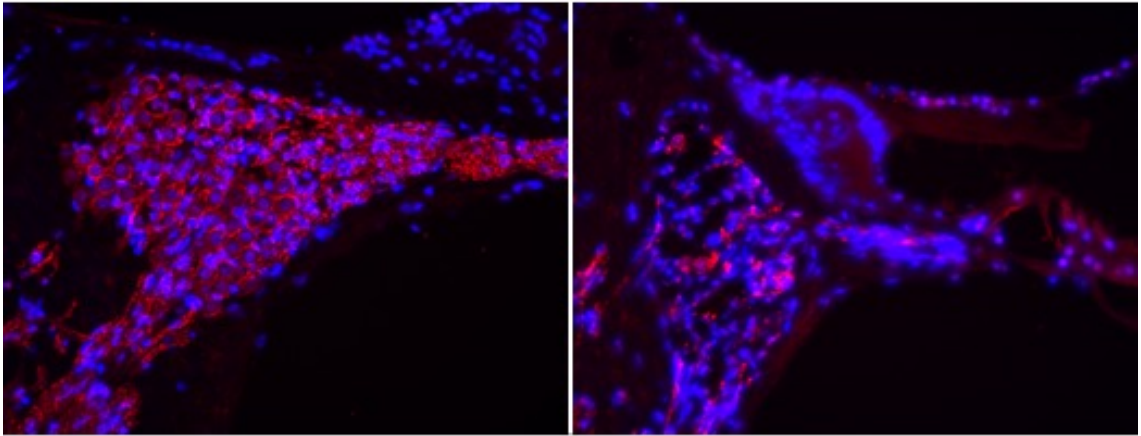


Fig 5.21 – Representative images showing immunolabelling from mouse cochlear sections for P0. Panel A shows P0 staining in Rosenthal's canal in the untreated ear (left-hand image) versus the treated ear (right-hand image). Panel b shows P0 staining in the modiolus in the untreated ear (left-hand image) versus the treated ear (right-hand image)

A



B

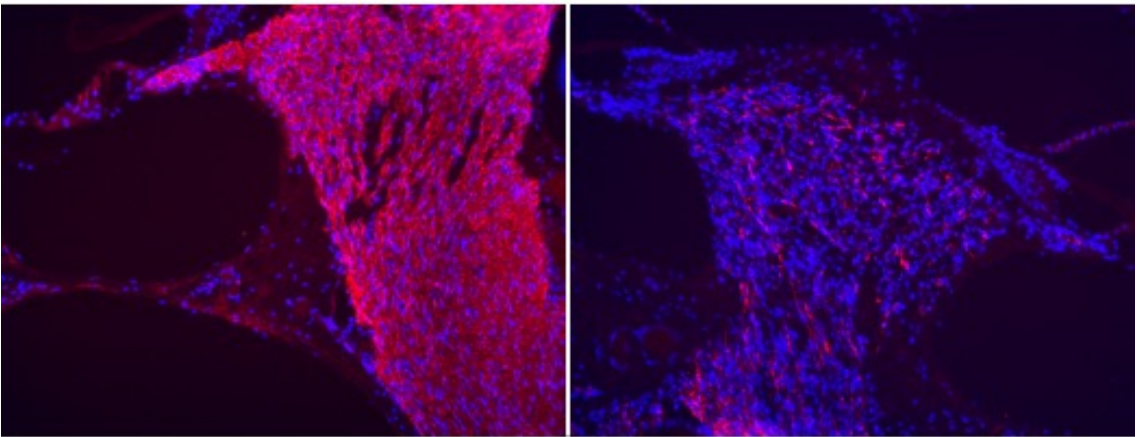


Fig 5.22 - Representative images showing immunolabelling from gerbil cochlear sections for P0. Panel A shows P0 staining in Rosenthal's canal in the untreated ear (left-hand image) versus the treated ear (right-hand image). Panel B shows P0 staining in the modiolus in the untreated ear (left-hand image) versus the treated ear (right-hand image)

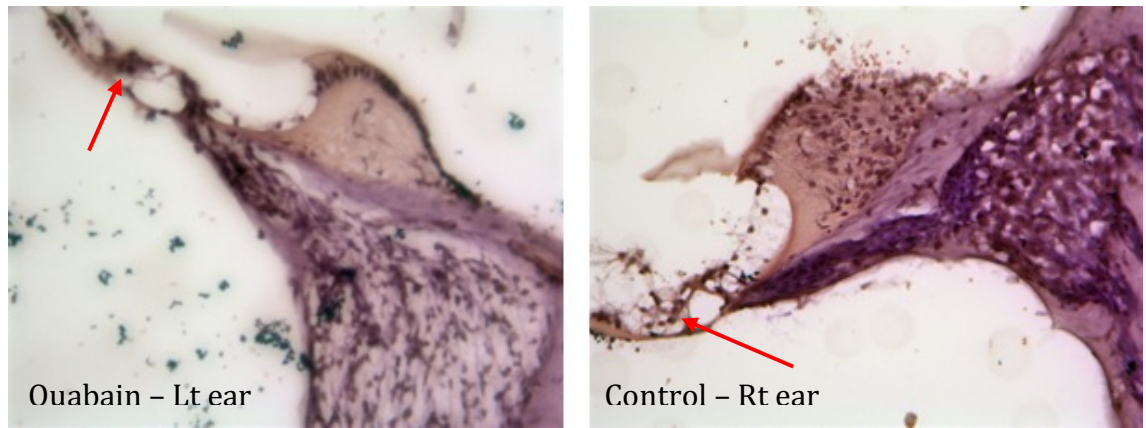


Fig 5.23 - Brightfield images of H and E staining from a mouse cochleae showing the left ear treated with Ouabain and the right ear which was the control untreated ear. The neuronal loss in Rosenthal's canal is clearly apparent. The red arrows point to the supporting cells within the organ of Corti, indicating that supporting cells remain intact despite Ouabain treatment.

5.2.4 Effect of ouabain on central glia of the auditory nerve in mice and gerbils.

In addition to examining the effects of Ouabain on peripheral glia, the central portion of the auditory nerve was also examined. Sections from 4 mice and 3 gerbils were examined and immunostaining for GFAP was undertaken to look for any changes at the glial transitional zone and within the central glia.

There was an obvious increase in the intensity of the GFAP signal from the processes of central glia in treated cochlea compared to controls (Fig 5.25, 5.27). To quantify this further, sections were scanned in the InCell Analyser, and through the processes of image segmentation and sieving, a mask was created which would allow the accompanying Developer Toolbox software to measure the GFAP signal intensity of each individual glial process within the central portion of the nerve (Fig 5.24). The dataset generated had a positive skew, and thus the Mann-Whitney test was used to compare mean fluorescence intensity values of the GFAP signal from each individual animal.

In each mouse and gerbil used for these experiments, there was a statistically significant increase in the mean fluorescence intensity of the GFAP signal in the auditory nerves treated with Ouabain versus the control, untreated ears (Figs. 5.26, 5.28). The increased intensity of the GFAP signal in treated ears suggests that there is an over-expression of GFAP, which raises the possibility that glia within the central portion of the nerve undergo reactive changes in response to Ouabain injury. There was no evidence of GFAP positive central glia migrating into the peripheral glial environment in these experiments.

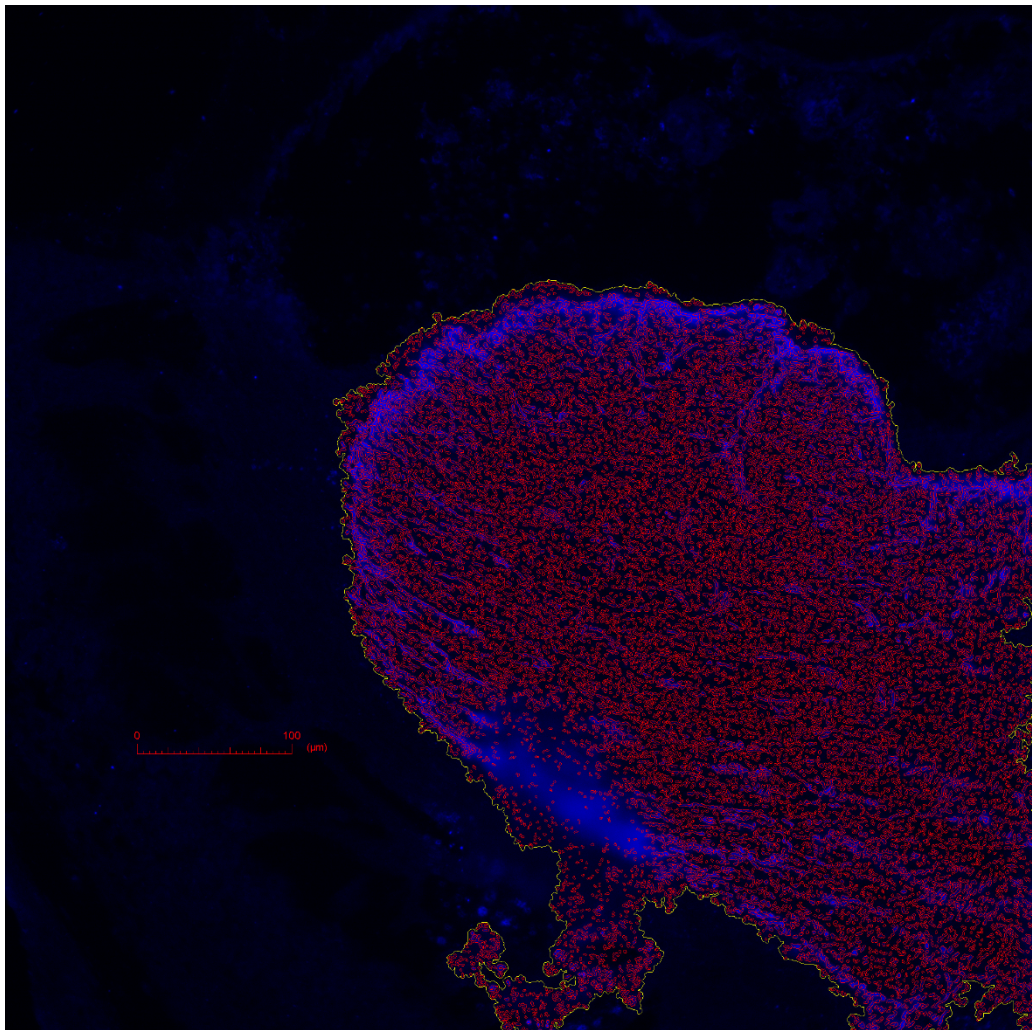


Fig 5.24 - Image showing the mask used by the Incell analyser to measure the intensity of glial fibres within the central portion of the auditory nerve.

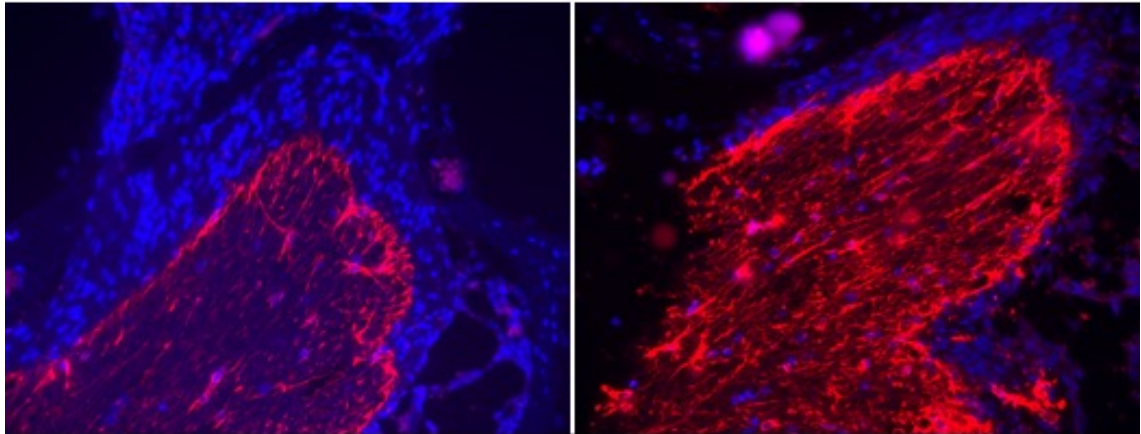


Fig 5.25– Representative images showing immunolabelling from mouse cochlear sections of the central portion of the auditory nerve for GFAP. The left-hand image is from the right, untreated ear and the right-hand image is from the left ear treated with ouabain. Nuclei have been counterstained with DAPI. Images were taken from the same animal.

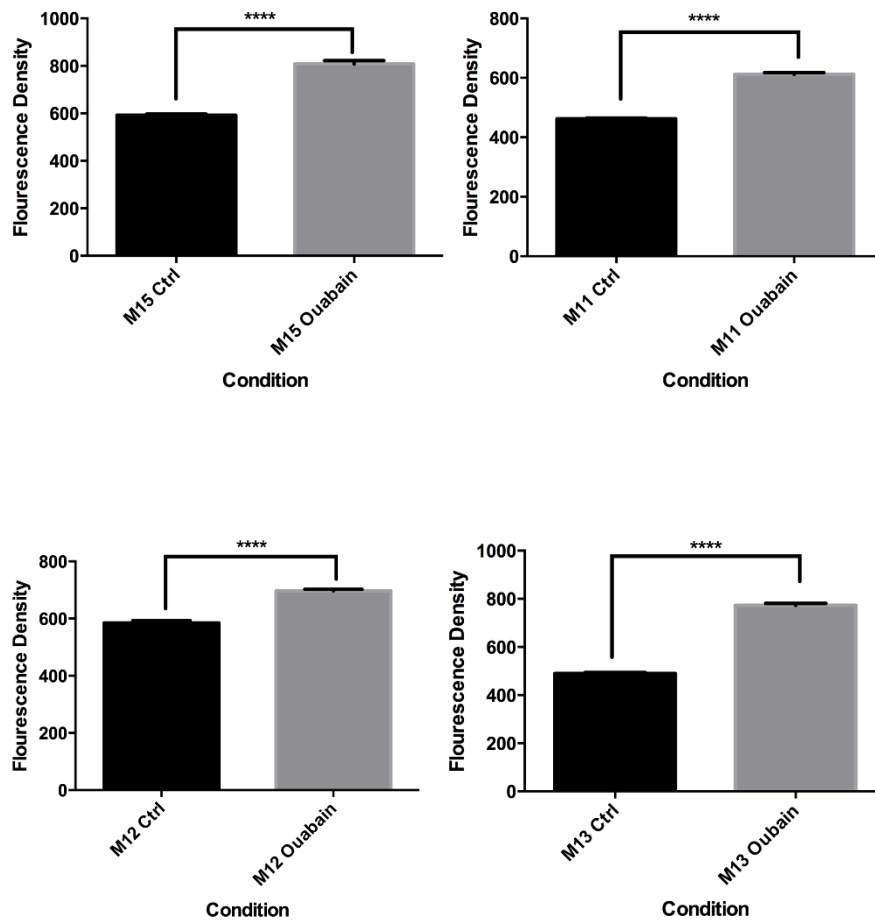


Fig 5.26 - Graphs showing mean fluorescence density of the GFAP signal from glial fibres in the central portion of the auditory nerve from individual mice. Statistical significance was determined using the Mann-Whitney test. ****P<0.0001. (n=4)

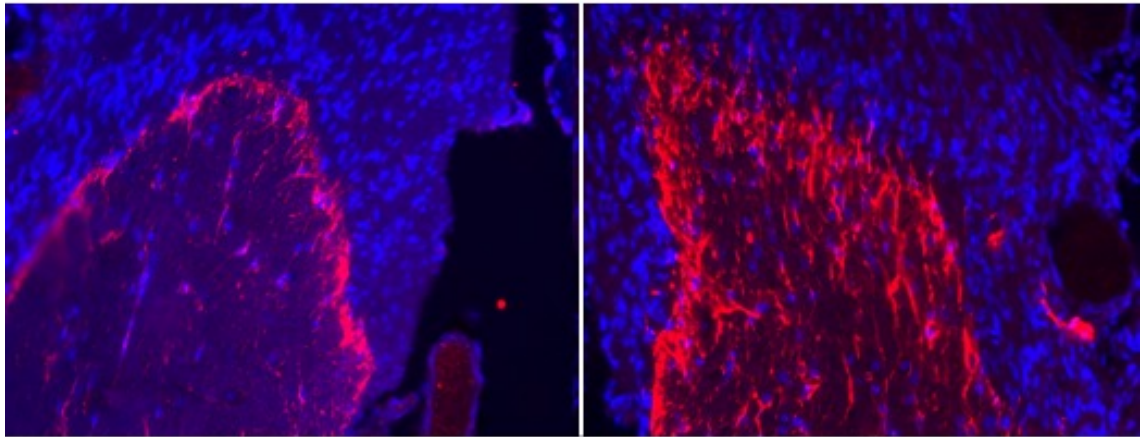


Fig 5.27 – Representative images showing immunolabelling from Gerbil cochlear sections of the central portion of the auditory nerve for GFAP. The left-hand image is from the right, untreated ear and the right-hand image is from the left ear treated with ouabain. Nuclei have been counterstained with DAPI. Images were taken from the same animal.

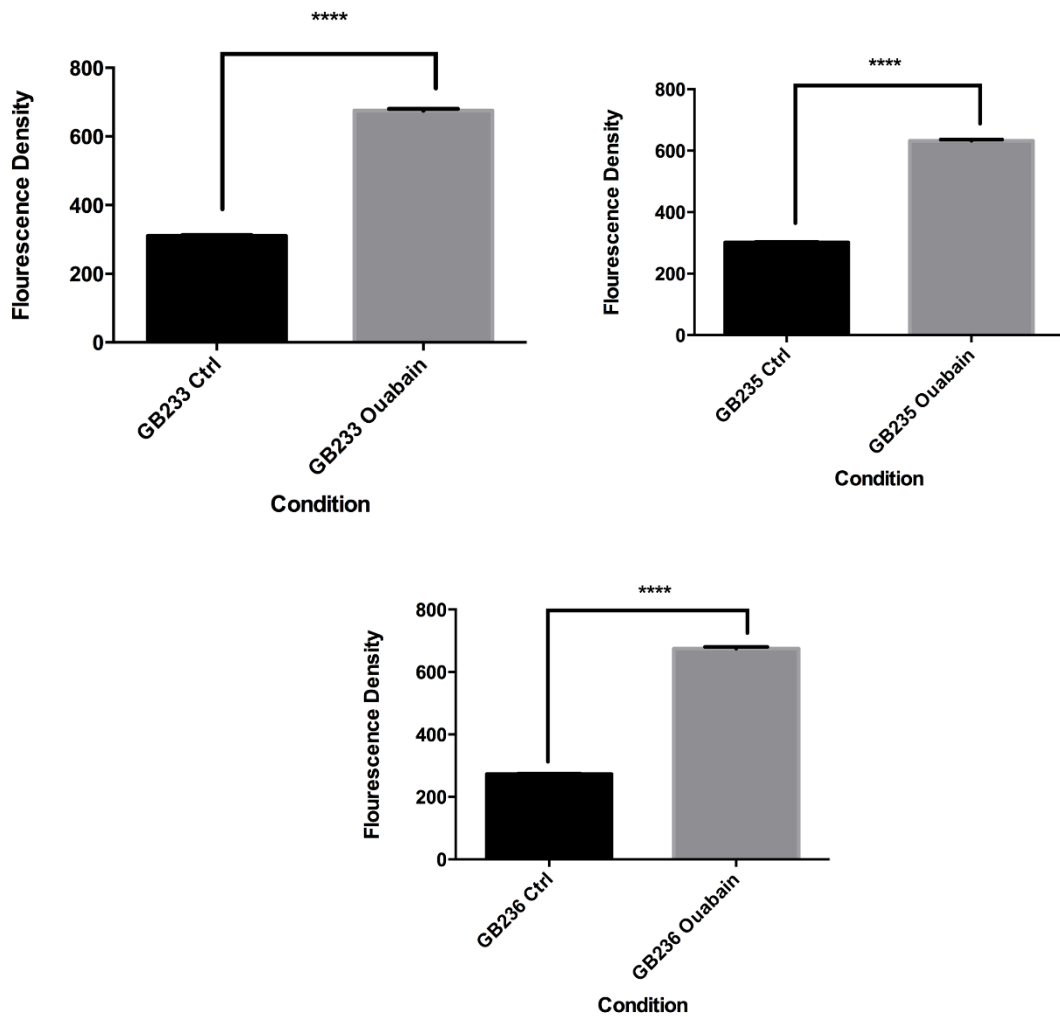


Fig 5.28 – Graphs showing mean fluorescence density of the GFAP signal from glial fibres in the central portion of the auditory nerve from individual gerbils. Statistical significance was determined using the Mann-Whitney test. ****P<0.0001. (n=3)

5.2.5 Transplantation of otic neural progenitors into the murine cochlea

The final set of experiments aimed to develop the surgical techniques for intramodiolar delivery of cells into the murine cochlea by making a modiolusostomy. Although Tamura and colleagues have previously demonstrated engraftment of cells into the modioli of murine cochleae, their surgical approach entailed injecting cells through the round window in the direction of the modiolus. Furthermore, their surgical method showed cells aberrant migration into many regions of the cochlea such as the scala tympani. Although the modiolostomy technique poses an extremely technical challenge within the mouse, a demonstration of its feasibility would open up the world of murine deafness models to cochlear stem cell transplantation studies.

The surgical approach was developed initially on cadaveric mice by injecting fluorescent beads into the modiolus and then harvesting the cochlea immediately after for cryosectioning. An indentation within the modiolus was apparent from where the dental file had penetrated the modiolus, with green fluorescent beads in its vicinity, suggesting that the beads had indeed reached their desired location (Fig 5.29).

Following on from this, 8 mice went on to be transplanted with otic neural progenitors derived from the H14 NOP/SOX2 cell line. 5 animals were given daily cyclosporin injections whilst 3 were not given any cyclosporine. The principle purpose of these experiments was to act as a proof of concept that cells can

delivered and go on to survive within the modiolus through the intramodiolar approach. Immunostaining was performed with GFP antibody, to enhance the GFP signal from transplanted cells.

Results from the transplantation studies are summarised in table 5.1. Of the 8 animals that were transplanted, one animal died on the operating table due to iatrogenic injury of the stapedial artery which ran a slightly unusual course in this animal. Another animal was culled 4 hours after transplantation due to anaesthetic complications. Two of the animals managed to survive 2 days post-transplant before they had to be terminated. These animals developed severe vestibular symptoms which did not resolve, and the animals lost a significant amount of body weight as a result.

Cells were present in 6 of the 8 animals that were transplanted. Of the animals in which cells were not identified, one of them had significant cochlear damage due to the modiolusostomy procedure, exemplifying the technical challenge that the procedure poses. Sections from the other animal were lost due to malfunction of the cryostat. The remaining animals all demonstrated the presence of cells within the base of the modiolus at 4 hours, 2 days and 1-week post-transplant. In one of the animals that survived 1-week post-transplant, the cells appeared to have migrated from the portion of the nerve adjacent to the basal turn of the nerve, towards the portion of the nerve in the apical region of the cochlea.

These experiments demonstrated that not only are transplanted cells able to survive within the murine cochlea for up to 1 week, but the intramodiolar delivery

method ensured that cells remained predominantly within the auditory nerve with little migration of cells into unwanted regions of the cochlea.

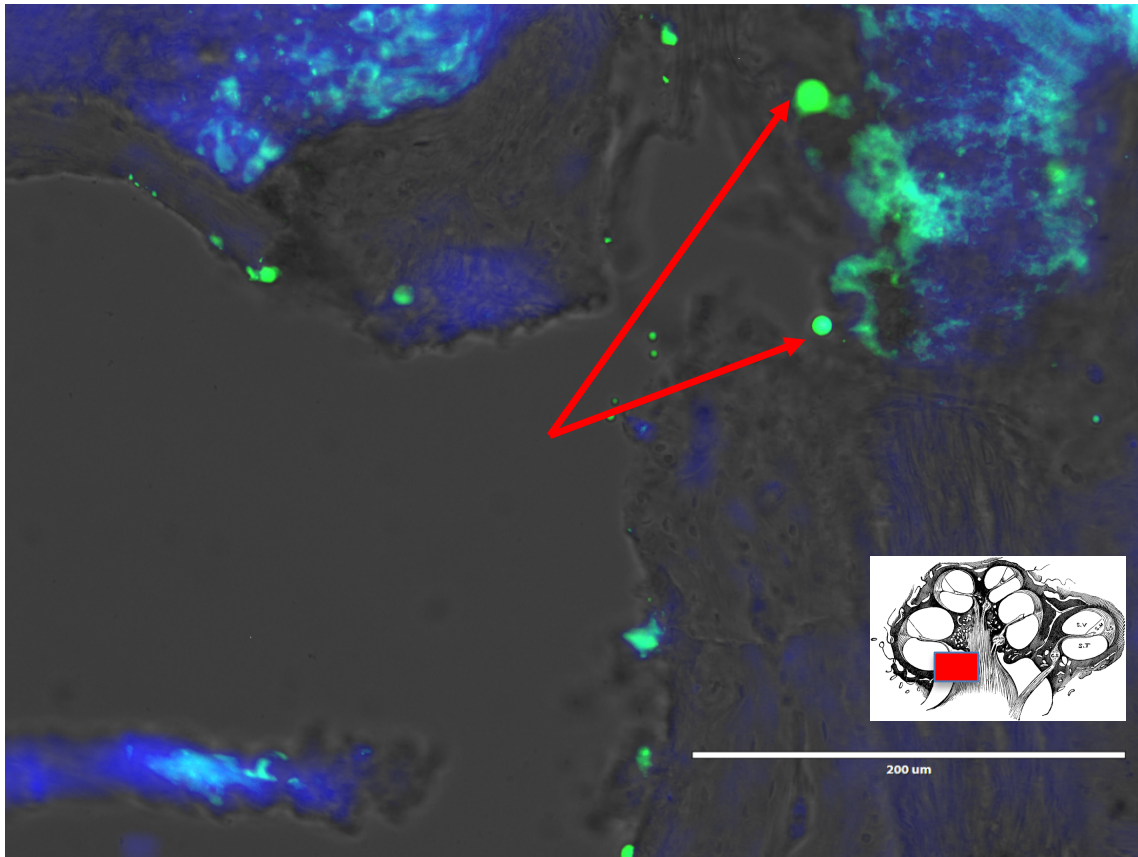


Fig 5.29– Micrographs of sections showing presence of beads within the Modiolus, as depicted by arrows.

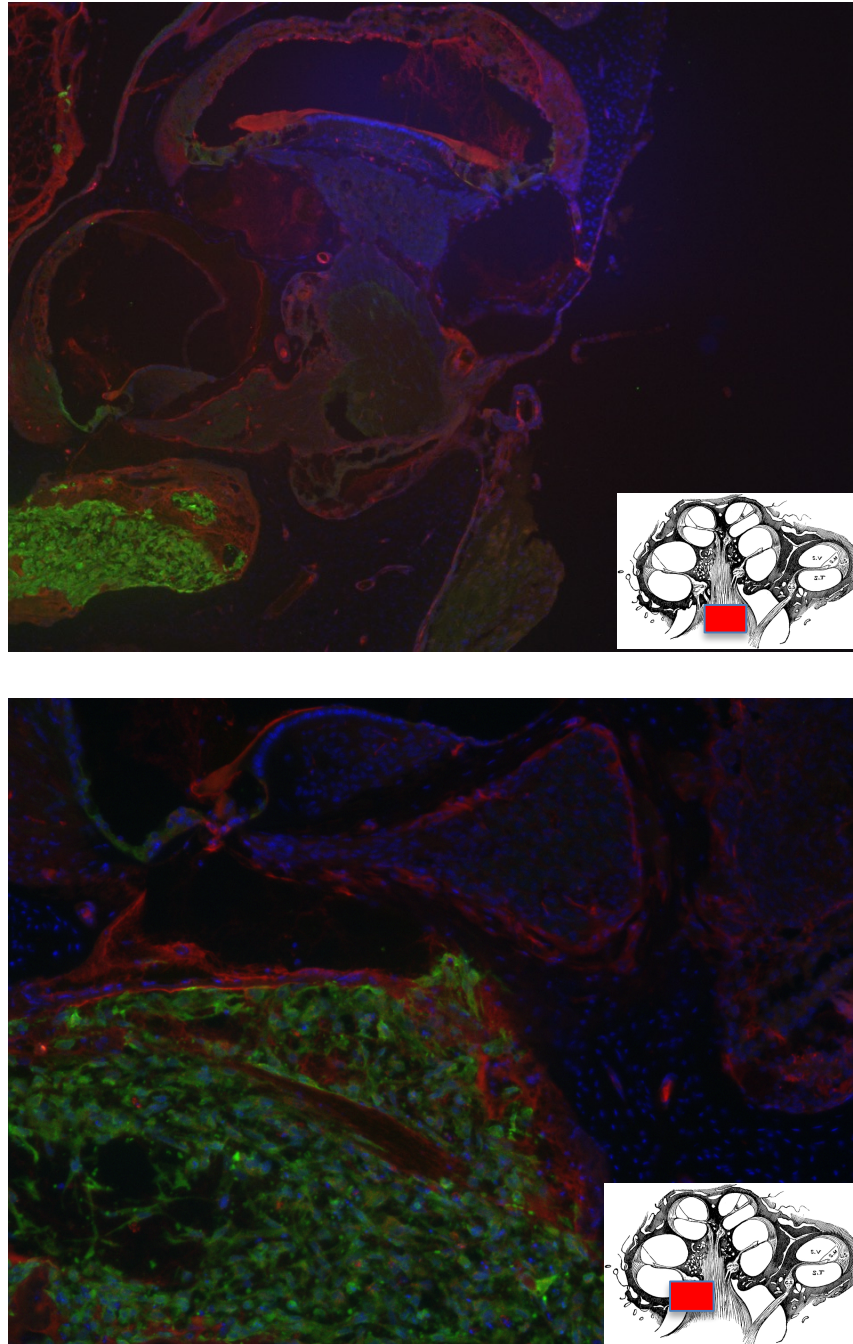


Fig 5.30 – Representative images showing immunolabelling cochlear sections of cochleae from M28 transplanted with H14 NOP/SOX2 cells (2 days' post -transplant). GFP was used to strengthen the intensity of the SOX2 reported to highlight the cells. Images show cells at the base of the modiolus. The uppermost image is taken at X4 magnification, whilst the lowermost is a section from the same animal taken at X10.

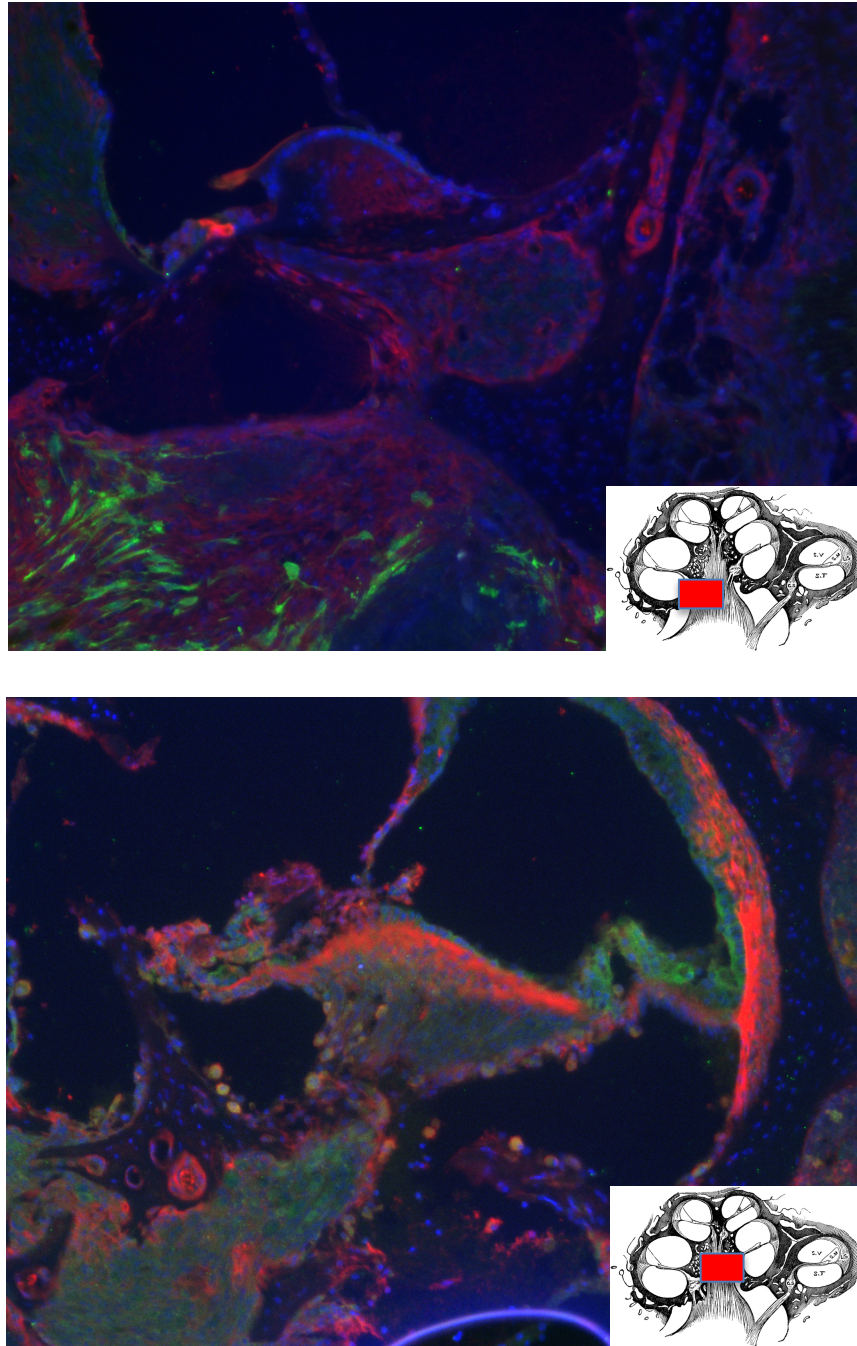


Fig 5.31 – Representative images showing immunolabelling from mouse cochlear sections of cochleae transplanted with H14 NOP/SOX2 cells. GFP was used to strengthen the intensity of the SOX2 reported to highlight the cells. Images show cells at the base of the modioli. The uppermost image is taken at X4 magnification of an animal M26, 7 days' post-transplant, whilst the lowermost is a section from M27 taken at X10, 17 days' post-transplant, where cells have migrated to the middle of the modioli.

ANIMAL ID	Sex	Age	Cell Line	Cyclosporin	Length of Survival	Immuno Summary
M22	F	4m	H14 Nop SOX2 (P7+1)	Y	8 days	Few cells in Modiolus
M23	M	3m	H14 Nop SOX2 (P7+1)	N	8 days	Poor sections due to cryostat malfunction
M24	M	3m	RIP	Y	Stapedial Artery Breached - No cells transplanted	
M25	M	3m	H14 Nop SOX2 (P7+1)	Y	Animal died after 4 hours post-transplant	Cells seen in base of nerve. GFP positive
M26	F	3m	H14 Nop SOX2 (P7+1)	Y	7 days	Cells seen in base of Nerve GFP Positive
M27	F	3m	H14 Nop SOX2 (P7+1)	N	7 days	Cells seen in base of nerve and also cells in apical portion of modiolus
M28	F	3m	H14 Nop SOX2 (P7+1)	N	2 days	Cells seen in base of nerve. GFP Positive
M29	F	3m	H14 Nop SOX2 (P6)	Y	2 days	Significant cochlear damage

Table 5.1 – Summary of all transplantation experiments involving mice

5.3 Discussion

5.3.1 Ouabain administration in the Mouse.

In addition to having techniques for Ouabain administration in the gerbil, our laboratory has now developed a reliable protocol for administering Ouabain in the mouse. We have demonstrated that through a single application of Ouabain at a concentration of 5mM leads to a significant sensorineural hearing loss, with an almost 90% wipeout of spiral ganglion neurons. A number of other groups have described methods in which they repetitively wick smaller concentrations of Ouabain every 10-15 minutes. The advantage of our method is that a satisfactory level of deafness is achieved, with less surgical handling of the structures within the inner ear.

One notable observation from experiments in mice was the significant vestibular symptoms they developed post-operatively. After a period of 24 hours post-operatively, all animals developed head tilt and circling symptoms, whilst a handful developed turning symptoms. The turning and circling gradually subsided at 72 hours post-operatively, and head tilt symptoms persisted until a week after the intervention. Thus, it was vital that within the first 72 hours, animals were kept well hydrated and fed, either through hand feeding them or even administering fluid boluses subcutaneously. In general, the gerbil tended to tolerate the procedure more readily than the mouse, and meticulous post-operative care and monitoring is necessary for the mouse.

5.3.2 Ouabain administration causes a loss of peripheral glial cells in murine and gerbil cochleae

One of the fundamental aims of this chapter was to compare and contrast the response of both peripheral and central glia to Ouabain injury. In contrast to the findings reported by Lang, the results presented here suggest a substantial loss of Schwann cells following Ouabain injury, which is similar in both the mouse and the gerbil.

Lang et al initially reported an increased expression of SOX2 within the peripheral auditory system based on cell counts, and micrographs indicated that many SOX2+ cells were also SOX10+ (Lang et al., 2011). Expanding on this work, they quantified an upregulation of SOX10, suggesting that SOX10+ nuclei undergo morphological changes in response to Ouabain, from a spindle shape in their normal state to a spherical shape akin to the nuclei of spiral ganglion nuclei (Lang et al., 2015). The thrust of their hypothesis lies in the idea that Schwann cells appear to de-differentiate in response to Ouabain injury. To explain the discrepancy between Cochlear neurons which do not regenerate following injury, and peripheral nerves where Schwann cells proliferate and play a key role in repair, the authors suggest that differences in Notch signaling may explain the differing response of Schwann cells within the auditory system, and those found in the peripheral nervous system; although some genes such as Dll1 and Hes1 were upregulated following Ouabain injury suggestive of a regenerative state, other patterns of expression were contrary to those seen in regeneration (supplementary figures, Lang et al., 2015)

There were a couple of methodological differences between the Ouabain protocol used in these experiments and that used by Lang. The protocol employed here was a single application of 1-2 μ l Ouabain at a concentration of 5mM applied to the round window for 45 minutes. Lang on the other hand applies 10 μ l of Ouabain at either 1mM (Lang et al., 2011) or at 3mM (Lang et al., 2015). Moreover, their method entailed wicking off the Ouabain solution from the round window every 10 minutes and replacing it with fresh solution, and a total of 6 applications were undertaken. As with all pharmacological agents, there is a narrow therapeutic window and a dose response effect of toxicity. It is therefore possible that at lower concentrations, Ouabain may induce a proliferation of Schwann cells with an altered phenotype, whilst at higher concentrations it induces an apoptosis of peripheral glial cells. To add further weight to this argument, an important point to note is the volume of Ouabain used. The round window of the murine cochlea is extremely small, and delivery of 10 μ l of Ouabain would inevitably result in leakage of ouabain into surrounding tissues, which may further dilute its concentration as it mixes with small quantities of fluid within the surgical field. The protocol used in these experiments involved a much smaller volume of Ouabain, which was precisely dropped onto the round window with a nanofil syringe.

The suggestion from Lang that cochlear Schwann cells de-differentiate in response to Ouabain injury is based upon observations of studies examining the response of glial cells to traumatic peripheral nerve injury (Chen et al., 2007). However, Jessen and Mirsky have recently questioned this notion, putting forward the view that rather than de-differentiating, Schwann cells trans-

differentiate into a 'repair-cell' phenotype, which has many differences to the immature Schwann cell, including increased expression of GDNF, Olig1 and Shh (Jessen and Mirsky, 2016). Gene expression data from Lang's work shows that whilst they do report an upregulation of GDNF within the auditory nerve following Ouabain injury, there was a significant down-regulation of Shh. Furthermore, neither Lang nor the data presented here illustrate the formation of 'bundles of Bungner', which are a key feature of the repair response of Schwann cells. This illustrates a couple of fundamental points that must be considered in the study of cochlear glial cells; firstly, much of the work studying the mechanisms of peripheral nerve injury and repair involves nerves that have been subjected to traumatic injury, either from a cut or a crush, which is a substantially different mechanism of injury to a pharmacological one, and it is quite likely that Schwann cell response will alter depending on the mechanism of injury. Secondly, it must be remembered that the cochlear nerve is fundamentally a specialized sensory cranial nerve which is developmentally and functionally unique from other peripheral nerves, and thus responses to injury are also likely to be different to other peripheral nerves.

5.3.3 Ouabain administration causes an upregulation of GFAP in the central segment of the auditory nerve

In both the mouse and the gerbil, experiments showed a significant increase in the intensity of the GFAP signal from glial fibres within the central segment of the auditory nerve 1 week after ouabain injury. This suggests an upregulation of GFAP expression within the central glia, indicating that they have undergone reactive changes in response to ouabain administration.

Given that the ultimate goal of auditory nerve regeneration is to establish a continuous neural connection between the cochlear epithelium and the auditory brainstem, understating the changes that take place within the microenvironment of the central portion of the nerve become extremely relevant. Sekiya and colleagues illustrated a remarkable glial response in their model of auditory nerve compression, suggesting that this may account for the deterioration in hearing that patients experience following microsurgery for vestibular Schwannoma (Sekiya et al., 2011). Changes have also been noted within the central glial segment following neomycin injury, with an increase in GFAP expression 3 weeks post injury, and migration of GFAP positive cells into the central portion of the nerve 6 weeks post injury (Hu et al., 2014). These studies have all described with changes within the central segment of the nerve in a qualitative fashion, whereas the experiments presented in this chapter have shown in a quantitative manner that ouabain administration also causes an increase in GFAP expression.

Interestingly, in their gene expression data Lang et al. have also shown a significant upregulation of GFAP, Vimentin and nestin in the auditory nerve following ouabain injury, and interpreted these results as indicating that peripheral glia upregulate genes that are commonly expressed in neural stem/progenitor cells (Lang et al., 2015). However, the upregulation of these markers may actually be reflecting the astrogliosis within the central portion of the nerve, given that upregulation of Vimentin, GFAP and nestin are also associated with astrocyte reactivity.

5.3.4 Changes in glia following ouabain injury – a supportive environment for neural regeneration?

Examining the changes within glia as a whole within the auditory nerve, the data presented here indicate a substantial loss of Schwann cells within the periphery, whilst astrocytes within the central portion of the nerve adopt a phenotype suggestive of reactive astrocytes. This would suggest that ouabain injury results in a microenvironment that is not conducive to neural regeneration. Yet, previous data from the laboratory has shown that following ouabain-induced deafness, functional hearing can be restored, with neural connection being re-established both peripherally and centrally (Chen et al., 2012).

Despite the significant loss of Schwann cells, we have found that support cells remain intact following ouabain injury. Zilberstein and colleagues have shown convincing data illustrating that spiral ganglia can survive for many months when

hair cells are lost and support cells remain intact, suggesting that it is in fact the support cells that are the principle trophic source within the cochlea (Zilberstein et al., 2012). If supporting cells are indeed the primary trophic source within the peripheral auditory system, then it is possible that transplanted otic neural progenitors differentiating into spiral-ganglion-like neurons maintain their survival as a result of the neurotrophic signals emanating from them.

Although the work presented by Chen et al. demonstrated functional recovery 4 weeks post-transplant, which gradually increased until week 7 before plateauing (Chen et al., 2012). It is possible that this plateau effect occurs as a result of the damage to the glia within the peripheral glia and the reactive changes within the central portion of the nerve, and ameliorating these pathological changes through pharmacotherapy alongside transplantation may result in better functional recovery.

5.3.5 Transplantation of otic neural progenitors within the murine cochlea

The transplantation experiments presented in this chapter illustrate the successful delivery of otic neural progenitors directly into the cochlear modiolus. There was hardly any ectopic spread of cells into unwanted regions of the cochlea, adding to work from previous groups showing intramodiolar delivery of cells to be the most efficient method of stem cell delivery (Corrales et al., 2006, Chen et al., 2012).

For the first time, it has been demonstrated here that this method of delivery is achievable within the mouse, despite the immense technical challenges it poses. Further refinement of the surgical technique will pave the way for transplantation studies to be undertaken within clinically relevant animal models of congenital deafness, which is a necessary step in taking this work from the bench to the bedside.

CHAPTER 6: CONCLUSIONS AND FUTURE IMPLICATIONS

6.1 Introduction

Regenerative medicine holds much promise as a therapy for sensorineural hearing loss. Although cochlear implants have been extremely effective as a neuroprosthetic therapy for deafness, their limitations are now becoming more apparent. Regenerative therapies could initially be used as an adjunct to cochlear implants in order to improve clinical outcomes for patients, and further refinement of regenerative strategies could pave the way for a wholly biological therapy for sensorineural hearing loss. Following on from the successes seen in transplantation of otic neural progenitors into a gerbil model of auditory neuropathy (Chen et al., 2012), efforts are already underway within the laboratory to determine the feasibility of concomitant stem cell transplantation with cochlear implantation.

In order for stem cell therapies to be translated from the bench to the clinic, there needs to be some clear scientific evidence that transplanted cells seamlessly integrate and interact with the host environment to establish mechanisms that maintain their long-term survival. This becomes even more relevant when one considers the pathological changes that take place within the cochlea in ageing, following noise exposure and iatrogenic injury with aminoglycosides and chemotherapeutics; essentially transplanted cells must be robust enough to survive within a potentially harsh intracochlear environment, after which they can instigate a repair process.

Given that transplantation of hair cell-like cells have a number of technical challenges that need to be overcome prior to translation, including the difficulties in developing a reproducible differentiation protocol that yields convincing cells with hair cell characteristics to the difficulties in surgically accessing the scala media, the focus of this work was to study otic neural progenitors, which have a greater likelihood of being translated as a cell based therapy in the shorter term. Thus, understanding how otic neural progenitors interact with glial cells of the auditory nerve is an important question that requires answering, as neuronal-glial interactions are fundamental for proper neural function and homeostasis.

6.2 The potency of otic neural progenitors to produce glia

The first question to answer was whether otic neural progenitors derived from the Rivolta lab protocol produced populations of glia, and if so, to quantify this. Not only would this give an indication of the efficiency of the neuralisation protocol, but also suggest that transplanted otic neural progenitors might not be wholly reliant on the host glial cells for support and maintenance. The data presented in this thesis strongly suggest that otic neural progenitors produced in vitro with this particular protocol hardly generate any cells with a glial phenotype when placed in a neuralisation protocol. This also seems to be the case in culture conditions designed to drive glial differentiation, suggesting that these otic neural progenitors behave similarly to neural progenitor cells derived from otic placodal cells during development.

A number of authors have reported the combined presence of cells with both neuronal and glial phenotypes from otic stem cells. This was done in a crude fashion using B-tubulin to identify neuronal cells, and GFAP to identify glia (Martinez-Monedero et al., 2008, Oshima et al., 2007b). The authors explain this phenomenon on the premise that developing neurons and glia have a common precursor. However, to-date there is no published data from groups investigating auditory stem cells which convincingly characterise this 'glial' population, for there are problems in concluding that these cells represent glia based purely on their morphological characteristics and GFAP expression, as they could equally represent undifferentiated neural stem cells. Moreover, whilst there is strong evidence to suggest that neurons and glia have a common precursor in the

central nervous system, the same cannot be said about the peripheral nervous system, where there is considerable debate on the matter. (Woodhoo and Sommer, 2008). Furthermore, even if a resident population of glial/progenitor cells present in the mature cochlea possess some ability to differentiate into neurons and glia does not indicate that these cells would be the natural progenitors giving origin to spiral ganglion neurons during otic development.

Using a range of peripheral glial markers which are present at different stages of Schwann cell development was employed to characterise any peripheral glial populations in differentiated cultures. The benefits of such an approach became apparent when a high level of S100 expression was observed; given that these cells did not co-label with markers associated with Schwann cell development and instead exhibited co-expression with neural markers suggested that S100 was probably acting as a neuronal marker within our system. Thus, future studies should adopt a similar approach in identifying peripheral glia on the basis of their gene expression at various stages of development.

An attempt was made to direct otic neural progenitors towards a glial lineage using the protocol developed in Studer's laboratory to generate glia from neural crest-like stem cells (Lee et al., 2007), and the cells did not produce significant populations of glia. Combining this with the findings that the neuralisation protocol yields minimal glia, leads to the strong possibility that the otic neural progenitors derived from the Rivolta lab FGF protocol are very similar to otic neural progenitors in development, which equally do not produce glia and are reliant upon the neural crest for glial populations. Whilst this may indeed be the case, a

firm conclusion cannot be drawn at this stage as the Studer protocol did not, in our hands, convincingly produce glia from in vitro generated neural-crest like cells. Thus, a collection of experiments in which otic neural progenitors and neural crest-like cells are placed into glial driving conditions side-by side are needed to allow for an adequate comparison. A number of protocols have been described for the differentiation of Schwann cells from stem cells (Fu et al., 2016, Al-Zer et al., 2015, Martens et al., 2014, Tong et al., 2010). Thus, a range of protocols should be employed in conjunction with that described by Studer's laboratory in order to add further evidence to the apparent lack of gliogenic potential in otic neural progenitors.

A further point of consideration is the observation that older otic neural progenitors lose their ability to produce neuronal-like cells in neuralising conditions. A possible explanation for this is the phenomenon of 'culture adaption' in which cells undergo karyotypic changes and outcompete stem cell populations. Recent studies have shown that aberrations most commonly occur in chromosome 17, with frequent aberrations also observed in chromosome 12, 1, 20 and X (Baker et al., 2016), and cells which are older and have been passaged with enzymatic methods also seem to be more susceptible to these changes (International Stem Cell et al., 2011). This is an important issue that needs to be addressed with respect to otic stem cell cultures, as the lack of neurogenesis from later passages may well be as a result of karyotypic changes within the cells. Further work needs to be done to karyotype otic neural progenitors in the OSCFM stage, as this may well present itself as a bottleneck for translation of these therapies from the bench to the bedside.

6.3 *The permissive effect of Schwann cells verses the inhibitory effect of reactive astrocytes on otic neural progenitors in vitro*

As otic neural progenitors do not produce significant quantities of glia when they differentiate in neuralising conditions, it is likely that they are going to be wholly reliant on the host glial environment for support and maintenance. Results from co-culture experiments showed that cochlear Schwann cells are supportive of neurite growth and provide directional cues to guide neurites from spiral ganglion-like cells. Contrary to this, cortical astrocytes appear to undergo reactive changes which seem inhibitory to neurite outgrowth.

Previous work examining interactions between spiral ganglion neurons and cochlear Schwann cells showed that within an *in vitro* environment, cochlear Schwann cells allow for neurite extension and facilitate directional growth (Jeon et al., 2011). Combining this with work from other groups showing the positive effects that Schwann cells have in facilitating neuronal differentiation from immature stem cells (Liao et al., 2010, Kingham et al., 2011), our work adds to the evidence obtained from work in peripheral nerve regeneration studies, that Schwann cells are supportive of growth from otic stem cells. Co-cultures of otic neural stem cells with peripheral glia is yet to be performed, and the data presented in this thesis indicate that alongside the molecular and electrophysiological data from these cells described previously (Chen et al., 2012), they also interact with peripheral glia as one would expect from peripheral sensory neurons.

The finding that astrocytes undergo reactive changes in neuralising medium, which restricts neurite growth from otic neural progenitors provides a foundational basis through which further work can be undertaken to identify the inhibitory mechanisms involved, and ways in which they can be overcome.

Overcoming the inhibitory signal from reactive astrocytes is an area of significant interest in neural regeneration within the central nervous system, particularly in relation to restoring function following spinal cord injury and following ischemic damage to the brain. A number of pharmacological agents have been tested *in vitro* to assess their potential applicability in repairing the central nervous system. For example, Brochier and colleagues have recently identified PARP1 as a crucial mediator of axonal growth inhibition, and showed that PARP inhibition allowed axonal growth on substrates of myelin associated glycoprotein, Nogo-A and chondroitin sulphate proteoglycan which are recognized components of the matrix secreted by reactive astrocytes (Brochier et al., 2015). EGFR blockade has also been shown to reduce reactive astrogliosis both *in vitro* and *in vivo* (Yang et al., 2011). In an alternative approach, Curcumin has been used as an agent to alter astrocyte phenotype in response to injury, thus reducing glial scar formation and fibrosis (Yuan et al., 2016). The co-culture system we have employed provides an assay through which future studies can be carried with such pharmacological agents, which could then be translated to *in vivo* transplantation studies with otic neural progenitors to improve penetration of cells within the central portion of the auditory nerve; thus improving neuronal contacts at the level of the cochlear nucleus.

6.4 Implications of Glial response to Ouabain for stem cell transplantation

Our data showed that ouabain administration to the cochlea caused a dramatic loss of Schwann cells in the peripheral cochlea, with an increase in GFAP expression in the central portion of the auditory nerve suggestive of reactive changes within astrocytes. The experiments were conducted in both mice and gerbils, and the data presented showed that the response was similar in both species. The glial response to ouabain injury in the gerbil is yet to be reported in the literature.

Our findings contrast those by Lang, who's data suggested that Schwann cells de-differentiate and proliferate in response to ouabain injury (Lang et al., 2011, Lang et al., 2015). The differences between the two studies may be as a result of the differing ouabain protocols employed, most notably the fact that Lang used repetitive applications of ouabain at 1mM, whilst we used a single application of ouabain at 5mM. This opens the possibility of a dose response effect of the toxicity of ouabain to peripheral glial cells, and thus further work should examine the effect of ouabain at a range of concentrations on the peripheral glia.

There is also little data on that changes the take place in glia following induction of deafness, either through aminoglycoside injury or loud noise exposure. Although it has previously been shown that Schwann cells change to a non-myelinating phenotype following aminoglycoside injury in the rat (Hurley et al., 2007) and GFAP is upregulated in the central portion of the nerve in the mouse

(Hu et al., 2014), further work needs to be undertaken to systematically characterise these changes.

Of course, the precise importance of Schwann cells within the cochlea remains elusive. Within the peripheral nervous system, Schwann cells are the principle source of neurotrophic support for the neurons they are associated with, however in the cochlea, it has long been thought that hair cells are the principle neurotrophic source (Richardson et al., 2009), with others later suggesting that support cells of the cochlear epithelium are the primary neurotrophic source (Zilberstein et al., 2012), which themselves are most probably a specialized type of glial cell. Our previous data indicates that support cells remain intact following Ouabain injury, and the fact that in previous observations in our laboratory, transplanted ONPs are able to survive for up to 12 weeks post-transplant following Ouabain injury (Chen et al., 2012) adds weight to the idea that the support cells are the principle source of neurotrophins for spiral ganglia. An alternative explanation for the survival of transplanted spiral ganglion-like cells in our Ouabain could be that the transplanted cells trigger a gliogenic response within the host cochlea, resulting in de novo Schwann cells associating with transplanted spiral ganglion-like neurites.

The upregulation of GFAP in both mice and gerbils following ouabain injury is a novel finding, and is of particular relevance to auditory stem cell transplantation. Further work must build on attempting to understand the precise nature of the reactive changes that take place within the auditory nerve following ouabain injury. It is now well known that reactive astrocytes are quite heterogeneous, and

the term 'reactivity' actually reflects a continuum of changes that take place within cells following injury, some of which may be beneficial, whilst others may be detrimental. This is in addition to the fact that reactive changes within astrocytes can vary depending on their precise location within the central nervous system (Anderson et al., 2014). Although there is limited data of astrocyte behavior in response to injury within the auditory system, already there is a suggestion that there are likely to be differences with respect to the mechanism of injury. For example, compression of the nerve leads to a marked astroglial reaction in which fibres from astrocytes extend long, fibrotic processes into the peripheral auditory system (Sekiya et al., 2011), which is in contrast to the reactive changes seen in this study, where an upregulation of GFAP was seen without any extension into the peripheral system. It is therefore likely that the phenotypic changes within astrocytes is likely to be dependent upon the mechanism of injury, and further understanding of this is going to be of benefit, particularly in understanding the applicability of auditory stem cells to repair the damaged auditory nerve following various paradigms of injury. Future experiments should compare the astrocytic response to various forms of injury, including traumatic, loud noise exposure and hypoxia.

The transplantation of otic neural progenitors into the murine cochlear modiolus is yet to be reported in the literature, and we have demonstrated that this can be achieved successfully, with cells occupying the base of the modiolus with hardly any spread to unwanted areas of the cochlea. This is a particularly intriguing finding from this work, as it opens up the prospect of studying auditory stem cell transplantation to a vast array of mouse models of genetic deafness, including

those of auditory neuropathy, which will be especially relevant in elucidating the clinical applicability of otic stem cell transplantation in congenital deafness.

6.5 Summary

To summarise, otic neural progenitors have been cultured *in vitro* in neuralising and glial driving conditions, with minimal differentiation of glia, suggesting that otic neural progenitors are restricted in their fate to a neuronal phenotype. This indicates that otic neural progenitors are likely to be dependent upon their host environment for long term support and survival. When co-cultured with peripheral and central glia within an *in vitro* environment, it was shown that cochlear Schwann cells were supportive of neuronal growth from otic neural progenitors, whilst reactive cortical astrocytes were inhibitory. In studying the glial response in both the mouse and gerbil, the data presented here indicate that Ouabain induces a substantial loss of Schwann cells within the auditory periphery, whilst astrocytes in the central portion of the nerve undergo reactive changes. The impact of this work will be crucial in further understanding the role of glia within the auditory system, particularly their response to pathological insults to the cochlea, which will be extremely relevant in the long-term goal of re-establishing neuronal connections between the auditory periphery and the cochlear nucleus.

REFERENCES

- ABBAS, L. & RIVOLTA, M. N. 2015. Aminoglycoside ototoxicity and hair cell ablation in the adult gerbil: A simple model to study hair cell loss and regeneration. *Hear Res*, 325, 12-26.
- ACTIONONHEARINGLOSS. 2015. *Statistics on Hearing Loss* [Online]. Available: <https://www.actiononhearingloss.org.uk/your-hearing/about-deafness-and-hearing-loss/statistics.aspx> [Accessed 7th July 2016].
- AGTERBERG, M. J., VERSNEL, H., VAN DIJK, L. M., DE GROOT, J. C. & KLIS, S. F. 2009. Enhanced survival of spiral ganglion cells after cessation of treatment with brain-derived neurotrophic factor in deafened guinea pigs. *J Assoc Res Otolaryngol*, 10, 355-67.
- AL-ZER, H., APEL, C., HEILAND, M., FRIEDRICH, R. E., JUNG, O., KROEGER, N., EICHHORN, W. & SMEETS, R. 2015. Enrichment and Schwann Cell Differentiation of Neural Crest-derived Dental Pulp Stem Cells. *In Vivo*, 29, 319-26.
- ALZHEIMERSOCIETY. 2015. Available: <https://www.alzheimers.org.uk/statistics> [Accessed 7th July 2016].
- AMATUZZI, M. G., NORTHROP, C., LIBERMAN, M. C., THORNTON, A., HALPIN, C., HERRMANN, B., PINTO, L. E., SAENZ, A., CARRANZA, A. & EAVEY, R. D. 2001. Selective inner hair cell loss in premature infants and cochlea pathological patterns from neonatal intensive care unit autopsies. *Arch Otolaryngol Head Neck Surg*, 127, 629-36.
- ANDERSON, D. J. 1995. A molecular switch for the neuron-glia developmental decision. *Neuron*, 15, 1219-22.
- ANDERSON, M. A., AO, Y. & SOFRONIEW, M. V. 2014. Heterogeneity of reactive astrocytes. *Neurosci Lett*, 565, 23-9.
- APPLER, J. M., LU, C. C., DRUCKENBROD, N. R., YU, W. M., KOUNDAKJIAN, E. J. & GOODRICH, L. V. 2013. Gata3 is a critical regulator of cochlear wiring. *J Neurosci*, 33, 3679-91.
- ARTHUR-FARRAJ, P. J., LATOUCHE, M., WILTON, D. K., QUINTES, S., CHABROL, E., BANERJEE, A., WOODHOO, A., JENKINS, B., RAHMAN, M., TURMAINE, M., WICHER, G. K., MITTER, R., GREENSMITH, L., BEHRENS, A., RAIVICH, G., MIRSKY, R. & JESSEN, K. R. 2012. c-Jun reprograms Schwann cells of injured nerves to generate a repair cell essential for regeneration. *Neuron*, 75, 633-47.
- ATKINSON, P. J., WISE, A. K., FLYNN, B. O., NAYAGAM, B. A. & RICHARDSON, R. T. 2014. Hair cell regeneration after ATOH1 gene therapy in the cochlea of profoundly deaf adult guinea pigs. *PLoS One*, 9, e102077.
- ATTWELL, D., BUCHAN, A. M., CHARPAK, S., LAURITZEN, M., MACVICAR, B. A. & NEWMAN, E. A. 2010. Glial and neuronal control of brain blood flow. *Nature*, 468, 232-43.
- BAGGER-SJOBACK, D., STROMBACK, K., HAKIZIMANA, P., PLUE, J., LARSSON, C., HULTCRANTZ, M., PAPANZAMOS, G., SMEDS, H., DANCKWARDT-LILLIESTROM, N., HELLSTROM, S., JOHANSSON, A., TIDEHOLM, B. & FRIDBERGER, A. 2015. A randomised, double blind trial of N-Acetylcysteine for hearing protection during stapes surgery. *PLoS One*, 10, e0115657.

- BAGULEY, D. R., E. MCCOMBE, A. 2008. Age-related Sensorineural Hearing Impairment. . In: GLEESON, M. (ed.) *Scott Brown's Otorhinolaryngology, Head And Neck Surgery* London: Edward Arnold.
- BAILEY, A. P., BHATTACHARYYA, S., BRONNER-FRASER, M. & STREIT, A. 2006. Lens specification is the ground state of all sensory placodes, from which FGF promotes olfactory identity. *Dev Cell*, 11, 505-17.
- BAKER, C. V. & BRONNER-FRASER, M. 2001. Vertebrate cranial placodes I. Embryonic induction. *Dev Biol*, 232, 1-61.
- BAKER, D., HIRST, A. J., GOKHALE, P. J., JUAREZ, M. A., WILLIAMS, S., WHEELER, M., BEAN, K., ALLISON, T. F., MOORE, H. D., ANDREWS, P. W. & BARBARIC, I. 2016. Detecting Genetic Mosaicism in Cultures of Human Pluripotent Stem Cells. *Stem Cell Reports*, 7, 998-1012.
- BAKER, D. E., HARRISON, N. J., MALTBY, E., SMITH, K., MOORE, H. D., SHAW, P. J., HEATH, P. R., HOLDEN, H. & ANDREWS, P. W. 2007. Adaptation to culture of human embryonic stem cells and oncogenesis in vivo. *Nat Biotechnol*, 25, 207-15.
- BALTES, P. B. & LINDENBERGER, U. 1997. Emergence of a powerful connection between sensory and cognitive functions across the adult life span: a new window to the study of cognitive aging? *Psychol Aging*, 12, 12-21.
- BARCLAY, M., RYAN, A. F. & HOUSLEY, G. D. 2011. Type I vs type II spiral ganglion neurons exhibit differential survival and neuritogenesis during cochlear development. *Neural Dev*, 6, 33.
- BARNABE-HEIDER, F., WASYLKA, J. A., FERNANDES, K. J., PORSCHE, C., SENDTNER, M., KAPLAN, D. R. & MILLER, F. D. 2005. Evidence that embryonic neurons regulate the onset of cortical gliogenesis via cardiotrophin-1. *Neuron*, 48, 253-65.
- BELL, D., STREIT, A., GOROSPE, I., VARELA-NIETO, I., ALSINA, B. & GIRALDEZ, F. 2008. Spatial and temporal segregation of auditory and vestibular neurons in the otic placode. *Dev Biol*, 322, 109-20.
- BERTHOLD, C. H. & CARLSTEDT, T. 1977. Observations on the morphology at the transition between the peripheral and the central nervous system in the cat. III. Myelinated fibres in S1 dorsal rootlets. *Acta Physiol Scand Suppl*, 446, 43-60.
- BERTOLI, S., STAEHELIN, K., ZEMP, E., SCHINDLER, C., BODMER, D. & PROBST, R. 2009. Survey on hearing aid use and satisfaction in Switzerland and their determinants. *Int J Audiol*, 48, 183-95.
- BHUTANI, V. K., STARK, A. R., LAZZERONI, L. C., POLAND, R., GOURLEY, G. R., KAZMIERCZAK, S., MELOY, L., BURGOS, A. E., HALL, J. Y., STEVENSON, D. K., INITIAL CLINICAL TESTING, E. & RISK ASSESSMENT FOR UNIVERSAL SCREENING FOR HYPERBILIRUBINEMIA STUDY, G. 2013. Pre-discharge screening for severe neonatal hyperbilirubinemia identifies infants who need phototherapy. *J Pediatr*, 162, 477-482 e1.
- BIXBY, J. L., LILIEN, J. & REICHARDT, L. F. 1988. Identification of the major proteins that promote neuronal process outgrowth on Schwann cells in vitro. *J Cell Biol*, 107, 353-61.
- BODDY, S. L., CHEN, W., ROMERO-GUEVARA, R., KOTTAM, L., BELLANTUONO, I. & RIVOLTA, M. N. 2012. Inner ear progenitor cells can be generated in vitro from human bone marrow mesenchymal stem cells. *Regen Med*, 7, 757-67.

- BOK, J., RAFT, S., KONG, K. A., KOO, S. K., DRAGER, U. C. & WU, D. K. 2011. Transient retinoic acid signaling confers anterior-posterior polarity to the inner ear. *Proc Natl Acad Sci U S A*, 108, 161-6.
- BOWL, M. R., SIMON, M. M., INGHAM, N. J., GREENAWAY, S., SANTOS, L., CATER, H., TAYLOR, S., MASON, J., KURBATOVA, N., PEARSON, S., BOWER, L. R., CLARY, D. A., MEZIANE, H., REILLY, P., MINOWA, O., KELSEY, L., INTERNATIONAL MOUSE PHENOTYPING, C., TOCCHINI-VALENTINI, G. P., GAO, X., BRADLEY, A., SKARNES, W. C., MOORE, M., BEAUDET, A. L., JUSTICE, M. J., SEAVITT, J., DICKINSON, M. E., WURST, W., DE ANGELIS, M. H., HERAULT, Y., WAKANA, S., NUTTER, L. M. J., FLENNIKEN, A. M., MCKERLIE, C., MURRAY, S. A., SVENSON, K. L., BRAUN, R. E., WEST, D. B., LLOYD, K. C. K., ADAMS, D. J., WHITE, J., KARP, N., FLICEK, P., SMEDLEY, D., MEEHAN, T. F., PARKINSON, H. E., TEBOUL, L. M., WELLS, S., STEEL, K. P., MALLON, A. M. & BROWN, S. D. M. 2017. A large scale hearing loss screen reveals an extensive unexplored genetic landscape for auditory dysfunction. *Nat Commun*, 8, 886.
- BREUSKIN, I., BODSON, M., THELEN, N., THIRY, M., BORGS, L., NGUYEN, L., STOLT, C., WEGNER, M., LEFEBVRE, P. P. & MALGRANGE, B. 2010. Glial but not neuronal development in the cochleo-vestibular ganglion requires Sox10. *J Neurochem*, 114, 1827-39.
- BRITO, M. A., LIMA, S., FERNANDES, A., FALCAO, A. S., SILVA, R. F., BUTTERFIELD, D. A. & BRITES, D. 2008. Bilirubin injury to neurons: contribution of oxidative stress and rescue by glycooursodeoxycholic acid. *Neurotoxicology*, 29, 259-69.
- BRITSCH, S., GOERICH, D. E., RIETHMACHER, D., PEIRANO, R. I., ROSSNER, M., NAVE, K. A., BIRCHMEIER, C. & WEGNER, M. 2001. The transcription factor Sox10 is a key regulator of peripheral glial development. *Genes Dev*, 15, 66-78.
- BROCHIER, C., JONES, J. I., WILLIS, D. E. & LANGLEY, B. 2015. Poly(ADP-ribose) polymerase 1 is a novel target to promote axonal regeneration. *Proc Natl Acad Sci U S A*, 112, 15220-5.
- BROOKS, D. N. 1985. Factors relating to the under-use of postaural hearing aids. *Br J Audiol*, 19, 211-7.
- BROWN, A. S. & EPSTEIN, D. J. 2011. Otic ablation of smoothed reveals direct and indirect requirements for Hedgehog signaling in inner ear development. *Development*, 138, 3967-76.
- BUCHMAN, C. A., ROUSH, P. A., TEAGLE, H. F., BROWN, C. J., ZDANSKI, C. J. & GROSE, J. H. 2006. Auditory neuropathy characteristics in children with cochlear nerve deficiency. *Ear Hear*, 27, 399-408.
- BUCKIOVA, D. & SYKA, J. 2009. Calbindin and S100 protein expression in the developing inner ear in mice. *J Comp Neurol*, 513, 469-82.
- CAMPOS-TORRES, A., TOURET, M., VIDAL, P. P., BARNUM, S. & DE WAELE, C. 2005. The differential response of astrocytes within the vestibular and cochlear nuclei following unilateral labyrinthectomy or vestibular afferent activity blockade by transtympanic tetrodotoxin injection in the rat. *Neuroscience*, 130, 853-65.
- CHEN, M. A., WEBSTER, P., YANG, E. & LINTHICUM, F. H., JR. 2006. Presbycusis neuritic degeneration within the osseous spiral lamina. *Otol Neurotol*, 27, 316-22.

- CHEN, W., JOHNSON, S. L., MARCOTTI, W., ANDREWS, P. W., MOORE, H. D. & RIVOLTA, M. N. 2009. Human fetal auditory stem cells can be expanded in vitro and differentiate into functional auditory neurons and hair cell-like cells. *Stem Cells*, 27, 1196-204.
- CHEN, W., JONGKAMONWIWAT, N., ABBAS, L., ESHTAN, S. J., JOHNSON, S. L., KUHN, S., MILO, M., THURLOW, J. K., ANDREWS, P. W., MARCOTTI, W., MOORE, H. D. & RIVOLTA, M. N. 2012. Restoration of auditory evoked responses by human ES-cell-derived otic progenitors. *Nature*, 490, 278-82.
- CHEN, Z. L., YU, W. M. & STRICKLAND, S. 2007. Peripheral regeneration. *Annu Rev Neurosci*, 30, 209-33.
- CHIEN, W. & LIN, F. R. 2012. Prevalence of hearing aid use among older adults in the United States. *Arch Intern Med*, 172, 292-3.
- CHOW, C., TRIVEDI, P., PYLE, M., MATULLE, J., FETTIPLACE, R. & GUBBELS, S. P. 2016. Evaluation of Nestin Expression in the Developing and Adult Mouse Inner Ear. *Stem Cells Dev*.
- CLARK, G. M., PYMAN, B. C. & BAILEY, Q. R. 1979. The surgery for multiple-electrode cochlear implantations. *J Laryngol Otol*, 93, 215-23
- CLARKE, L. E. & BARRES, B. A. 2013. Emerging roles of astrocytes in neural circuit development. *Nat Rev Neurosci*, 14, 311-21.
- COHEN-MANSFIELD, J. & TAYLOR, J. W. 2004. Hearing aid use in nursing homes. Part 2: Barriers to effective utilization of hearing AIDS. *J Am Med Dir Assoc*, 5, 289-96.
- COLEMAN, B., HARDMAN, J., COCO, A., EPP, S., DE SILVA, M., CROOK, J. & SHEPHERD, R. 2006. Fate of embryonic stem cells transplanted into the deafened mammalian cochlea. *Cell Transplant*, 15, 369-80.
- COLLETTI, V., FIORINO, F. G., CARNER, M., MIORELLI, V., GUIDA, M. & COLLETTI, L. 2004. Auditory brainstem implant as a salvage treatment after unsuccessful cochlear implantation. *Otol Neurotol*, 25, 485-96; discussion 496.
- COPPENS, A. G., KISS, R., HEIZMANN, C. W., SCHÄFER, B. W. & PONCELET, L. 2001. Immunolocalization of the calcium binding S100A1, S100A5 and S100A6 proteins in the dog cochlea during postnatal development. *Brain Res Dev Brain Res*, 126, 191-9.
- CORFAS, G., VELARDEZ, M. O., KO, C. P., RATNER, N. & PELES, E. 2004. Mechanisms and roles of axon-Schwann cell interactions. *J Neurosci*, 24, 9250-60.
- CORRALES, C. E., PAN, L., LI, H., LIBERMAN, M. C., HELLER, S. & EDGE, A. S. 2006. Engraftment and differentiation of embryonic stem cell-derived neural progenitor cells in the cochlear nerve trunk: growth of processes into the organ of Corti. *J Neurobiol*, 66, 1489-500.
- CORWIN, J. T. 1985. Perpetual production of hair cells and maturational changes in hair cell ultrastructure accompany postembryonic growth in an amphibian ear. *Proc Natl Acad Sci U S A*, 82, 3911-5.
- CORWIN, J. T. & COTANCHE, D. A. 1988. Regeneration of sensory hair cells after acoustic trauma. *Science*, 240, 1772-4.
- CRISPINO, G., DI PASQUALE, G., SCIMEMI, P., RODRIGUEZ, L., GALINDO RAMIREZ, F., DE SIATI, R. D., SANTARELLI, R. M., ARSLAN, E., BORTOLOZZI, M., CHIORINI, J. A. & MAMMANO, F. 2011. BAAV mediated GJB2 gene transfer restores gap junction coupling in cochlear organotypic cultures from deaf Cx26Sox10Cre mice. *PLoS One*, 6, e23279.

- CUA, R. C., LAU, L. W., KEOUGH, M. B., MIDHA, R., APTE, S. S. & YONG, V. W. 2013. Overcoming neurite-inhibitory chondroitin sulfate proteoglycans in the astrocyte matrix. *Glia*, 61, 972-84.
- D'AMICO-MARTEL, A. & NODEN, D. M. 1983. Contributions of placodal and neural crest cells to avian cranial peripheral ganglia. *Am J Anat*, 166, 445-68.
- DAWES, P., EMSLEY, R., CRUICKSHANKS, K. J., MOORE, D. R., FORTNUM, H., EDMONDSON-JONES, M., MCCORMACK, A. & MUNRO, K. J. 2015. Hearing loss and cognition: the role of hearing AIDS, social isolation and depression. *PLoS One*, 10, e0119616.
- DELACROIX, L. & MALGRANGE, B. 2015. Cochlear afferent innervation development. *Hear Res*, 330, 157-69.
- DENEEN, B., HO, R., LUKASZEWICZ, A., HOCHSTIM, C. J., GRONOSTAJSKI, R. M. & ANDERSON, D. J. 2006. The transcription factor NFIA controls the onset of gliogenesis in the developing spinal cord. *Neuron*, 52, 953-68.
- DJOURNO, A. & EYRIES, C. 1957. [Auditory prosthesis by means of a distant electrical stimulation of the sensory nerve with the use of an indwelt coiling]. *Presse Med*, 65, 1417.
- DO CARMO CUNHA, J., DE FREITAS AZEVEDO LEVY, B., DE LUCA, B. A., DE ANDRADE, M. S., GOMIDE, V. C. & CHADI, G. 2007. Responses of reactive astrocytes containing S100beta protein and fibroblast growth factor-2 in the border and in the adjacent preserved tissue after a contusion injury of the spinal cord in rats: implications for wound repair and neuroregeneration. *Wound Repair Regen*, 15, 134-46.
- DODSON, H. C. 1997. Loss and survival of spiral ganglion neurons in the guinea pig after intracochlear perfusion with aminoglycosides. *J Neurocytol*, 26, 541-56.
- DOETSCH, F. 2003. The glial identity of neural stem cells. *Nat Neurosci*, 6, 1127-34.
- DONATO, R. 2003. Intracellular and extracellular roles of S100 proteins. *Microsc Res Tech*, 60, 540-51.
- DONATO, R., SORCI, G., RIUZZI, F., ARCURI, C., BIANCHI, R., BROZZI, F., TUBARO, C. & GIAMBANCO, I. 2009. S100B's double life: intracellular regulator and extracellular signal. *Biochim Biophys Acta*, 1793, 1008-22.
- DONG, Z., BRENNAN, A., LIU, N., YARDEN, Y., LEFKOWITZ, G., MIRSKY, R. & JESSEN, K. R. 1995. Neu differentiation factor is a neuron-glia signal and regulates survival, proliferation, and maturation of rat Schwann cell precursors. *Neuron*, 15, 585-96.
- DOWSING, B. J., MORRISON, W. A., NICOLA, N. A., STARKEY, G. P., BUCCI, T. & KILPATRICK, T. J. 1999. Leukemia inhibitory factor is an autocrine survival factor for Schwann cells. *J Neurochem*, 73, 96-104.
- DOYLE, J. B., JR., DOYLE, J. H., TURNBULL, F. M., ABBEY, J. & HOUSE, L. 1963. Electrical Stimulation in Eighth Nerve Deafness. A Preliminary Report. *Bull Los Angel Neuro Soc*, 28, 148-50.
- DOYLE, J. P., DOUGHERTY, J. D., HEIMAN, M., SCHMIDT, E. F., STEVENS, T. R., MA, G., BUPP, S., SHRESTHA, P., SHAH, R. D., DOUGHTY, M. L., GONG, S., GREENGARD, P. & HEINTZ, N. 2008. Application of a translational profiling approach for the comparative analysis of CNS cell types. *Cell*, 135, 749-62.
- DUAN, M., QIU, J., LAURELL, G., OLOFSSON, A., COUNTER, S. A. & BORG, E. 2004. Dose and time-dependent protection of the antioxidant N-L-acetylcysteine against impulse noise trauma. *Hear Res*, 192, 1-9.

- DUMAN, D. & TEKIN, M. 2012. Autosomal recessive nonsyndromic deafness genes: a review. *Front Biosci (Landmark Ed)*, 17, 2213-36.
- DUNCAN, J. S. & FRITZSCH, B. 2013. Continued expression of GATA3 is necessary for cochlear neurosensory development. *PLoS One*, 8, e62046.
- EISENBERG, L. S., MALTAN, A. A., PORTILLO, F., MOBLEY, J. P. & HOUSE, W. F. 1987. Electrical stimulation of the auditory brain stem structure in deafened adults. *J Rehabil Res Dev*, 24, 9-22.
- ELKABETZ, Y., PANAGIOTAKOS, G., AL SHAMY, G., SOCCI, N. D., TABAR, V. & STUDER, L. 2008. Human ES cell-derived neural rosettes reveal a functionally distinct early neural stem cell stage. *Genes Dev*, 22, 152-65.
- ENVER, T., SONEJI, S., JOSHI, C., BROWN, J., IBORRA, F., ORNTOFT, T., THYKJAER, T., MALTBY, E., SMITH, K., ABU DAWUD, R., JONES, M., MATIN, M., GOKHALE, P., DRAPER, J. & ANDREWS, P. W. 2005. Cellular differentiation hierarchies in normal and culture-adapted human embryonic stem cells. *Hum Mol Genet*, 14, 3129-40.
- FARINAS, I., JONES, K. R., TESSAROLLO, L., VIGERS, A. J., HUANG, E., KIRSTEIN, M., DE CAPRONA, D. C., COPPOLA, V., BACKUS, C., REICHARDT, L. F. & FRITZSCH, B. 2001. Spatial shaping of cochlear innervation by temporally regulated neurotrophin expression. *J Neurosci*, 21, 6170-80.
- FAYAD, J., LINTHICUM, F. H., JR., OTTO, S. R., GALEY, F. R. & HOUSE, W. F. 1991. Cochlear implants: histopathologic findings related to performance in 16 human temporal bones. *Ann Otol Rhinol Laryngol*, 100, 807-11.
- FELTRI, M. L., POITELON, Y. & PREVITALI, S. C. 2016. How Schwann Cells Sort Axons: New Concepts. *Neuroscientist*, 22, 252-65.
- FETONI, A. R., RALLI, M., SERGI, B., PARRILLA, C., TROIANI, D. & PALUDETTI, G. 2009. Protective effects of N-acetylcysteine on noise-induced hearing loss in guinea pigs. *Acta Otorhinolaryngol Ital*, 29, 70-5.
- FITCH, M. T. & SILVER, J. 1997. Activated macrophages and the blood-brain barrier: inflammation after CNS injury leads to increases in putative inhibitory molecules. *Exp Neurol*, 148, 587-603.
- FOK-SEANG, J. & MILLER, R. H. 1994. Distribution and differentiation of A2B5+ glial precursors in the developing rat spinal cord. *J Neurosci Res*, 37, 219-35.
- FONTANA, X., HRISTOVA, M., DA COSTA, C., PATODIA, S., THEI, L., MAKWANA, M., SPENCER-DENE, B., LATOUCHE, M., MIRSKY, R., JESSEN, K. R., KLEIN, R., RAIVICH, G. & BEHRENS, A. 2012. c-Jun in Schwann cells promotes axonal regeneration and motoneuron survival via paracrine signaling. *J Cell Biol*, 198, 127-41.
- FRAHER, J. P. 1992. The CNS-PNS transitional zone of the rat. Morphometric studies at cranial and spinal levels. *Prog Neurobiol*, 38, 261-316.
- FREDRICH, M., ZEBER, A. C., HILDEBRANDT, H. & ILLING, R. B. 2013. Differential molecular profiles of astrocytes in degeneration and re-innervation after sensory deafferentation of the adult rat cochlear nucleus. *Eur J Neurosci*, 38, 2041-56.
- FREYER, L., AGGARWAL, V. & MORROW, B. E. 2011. Dual embryonic origin of the mammalian otic vesicle forming the inner ear. *Development*, 138, 5403-14.
- FRIEND, W. C., CLAPOFF, S., LANDRY, C., BECKER, L. E., O'HANLON, D., ALLORE, R. J., BROWN, I. R., MARKS, A., RODER, J. & DUNN, R. J. 1992. Cell-specific expression of high levels of human S100 beta in transgenic mouse brain is dependent on gene dosage. *J Neurosci*, 12, 4337-46.

- FU, X., TONG, Z., LI, Q., NIU, Q., ZHANG, Z., TONG, X., TONG, L. & ZHANG, X. 2016. Induction of adipose-derived stem cells into Schwann-like cells and observation of Schwann-like cell proliferation. *Mol Med Rep*, 14, 1187-93.
- FUCHS, P. A. 2010. *The Oxford Handbook Of Auditory Neuroscience*, Oxford, Oxford University Press.
- FUENTES-SANTAMARIA, V., ALVARADO, J. C., LOPEZ-MUNOZ, D. F., MELGAR-ROJAS, P., GABALDON-ULL, M. C. & JUIZ, J. M. 2014. Glia-related mechanisms in the anteroventral cochlear nucleus of the adult rat in response to unilateral conductive hearing loss. *Front Neurosci*, 8, 319.
- FUKUDA, S., KATO, F., TOZUKA, Y., YAMAGUCHI, M., MIYAMOTO, Y. & HISATSUNE, T. 2003. Two distinct subpopulations of nestin-positive cells in adult mouse dentate gyrus. *J Neurosci*, 23, 9357-66.
- GANEK, H., MCCONKEY ROBBINS, A. & NIPARKO, J. K. 2012. Language outcomes after cochlear implantation. *Otolaryngol Clin North Am*, 45, 173-85.
- GARCIA, A. D., PETROVA, R., ENG, L. & JOYNER, A. L. 2010. Sonic hedgehog regulates discrete populations of astrocytes in the adult mouse forebrain. *J Neurosci*, 30, 13597-608.
- GARRATT, A. N., BRITSCH, S. & BIRCHMEIER, C. 2000. Neuregulin, a factor with many functions in the life of a schwann cell. *Bioessays*, 22, 987-96.
- GIFFORD, R. H., DORMAN, M. F., SKARZYNSKI, H., LORENS, A., POLAK, M., DRISCOLL, C. L., ROLAND, P. & BUCHMAN, C. A. 2013. Cochlear implantation with hearing preservation yields significant benefit for speech recognition in complex listening environments. *Ear Hear*, 34, 413-25.
- GILLESPIE, L. N., CLARK, G. M., BARTLETT, P. F. & MARZELLA, P. L. 2003. BDNF-induced survival of auditory neurons in vivo: Cessation of treatment leads to accelerated loss of survival effects. *J Neurosci Res*, 71, 785-90.
- GÓMEZ-CASATI, M. E., MURTIE, J., TAYLOR, B. & CORFAS, G. 2010. Cell-specific inducible gene recombination in postnatal inner ear supporting cells and glia. *J Assoc Res Otolaryngol*, 11, 19-26.
- GOTZ, M. 2003. Glial cells generate neurons--master control within CNS regions: developmental perspectives on neural stem cells. *Neuroscientist*, 9, 379-97.
- GRAHAM, A., BLENIC, A., DUQUE, S. & BEGBIE, J. 2007. Delamination of cells from neurogenic placodes does not involve an epithelial-to-mesenchymal transition. *Development*, 134, 4141-5.
- GREENWOOD, G. J. 1959. Neomycin ototoxicity; report of a case. *AMA Arch Otolaryngol*, 69, 390-7.
- GRIGORYAN, T. & BIRCHMEIER, W. 2015. Molecular signaling mechanisms of axon-glia communication in the peripheral nervous system. *Bioessays*, 37, 502-13.
- GRIM, M., HALATA, Z. & FRANZ, T. 1992. Schwann cells are not required for guidance of motor nerves in the hindlimb in Splotch mutant mouse embryos. *Anat Embryol (Berl)*, 186, 311-8.
- GUNewardENE, N., BERGEN, N. V., CROMBIE, D., NEEDHAM, K., DOTTORI, M. & NAYAGAM, B. A. 2014. Directing human induced pluripotent stem cells into a neurosensory lineage for auditory neuron replacement. *Biores Open Access*, 3, 162-75.
- GURGEL, R. K., WARD, P. D., SCHWARTZ, S., NORTON, M. C., FOSTER, N. L. & TSCHANZ, J. T. 2014. Relationship of hearing loss and dementia: a prospective, population-based study. *Otol Neurotol*, 35, 775-81.

- HAMERNIK, R. P. & HENDERSON, D. 1974. Impulse noise trauma. A study of histological susceptibility. *Arch Otolaryngol*, 99, 118-21.
- HAN, C. & SOMEYA, S. 2013. Mouse models of age-related mitochondrial neurosensory hearing loss. *Mol Cell Neurosci*, 55, 95-100.
- HANSEN, M. R., VIJAPURKAR, U., KOLAND, J. G. & GREEN, S. H. 2001. Reciprocal signaling between spiral ganglion neurons and Schwann cells involves neuregulin and neurotrophins. *Hear Res*, 161, 87-98.
- HARRISON, N. J., BAKER, D. & ANDREWS, P. W. 2007. Culture adaptation of embryonic stem cells echoes germ cell malignancy. *Int J Androl*, 30, 275-81; discussion 281.
- HASHINO, E. & SHERO, M. 1995. Endocytosis of aminoglycoside antibiotics in sensory hair cells. *Brain Res*, 704, 135-40.
- HAUSTEIN, M. D., READ, D. J., STEINERT, J. R., PILATI, N., DINSDALE, D. & FORSYTHE, I. D. 2010. Acute hyperbilirubinaemia induces presynaptic neurodegeneration at a central glutamatergic synapse. *J Physiol*, 588, 4683-93.
- HEALTH&SAFETYEXEC. 2015. *Noise Induced Hearing Loss in Great Britain* [Online]. Available: <http://www.hse.gov.uk/Statistics/causdis/deafness/index.htm> [Accessed 18th July 2016].
- HEIL, P. & PETERSON, A. J. 2016. Spike timing in auditory-nerve fibers during spontaneous activity and phase locking. *Synapse*.
- HENDERSON, D., BIELEFELD, E. C., HARRIS, K. C. & HU, B. H. 2006. The role of oxidative stress in noise-induced hearing loss. *Ear Hear*, 27, 1-19.
- HILDEBRAND, M. S., DAHL, H. H., HARDMAN, J., COLEMAN, B., SHEPHERD, R. K. & DE SILVA, M. G. 2005. Survival of partially differentiated mouse embryonic stem cells in the scala media of the guinea pig cochlea. *J Assoc Res Otolaryngol*, 6, 341-54.
- HOCK, R. & ANDERSON, R. J. 1995. Prevention of drug-induced nephrotoxicity in the intensive care unit. *J Crit Care*, 10, 33-43.
- HONSA, P., VALNY, M., KRISKA, J., MATUSKOVA, H., HARANTOVA, L., KIRDAJOVA, D., VALIHRACH, L., ANDROVIC, P., KUBISTA, M. & ANDEROVA, M. 2016. Generation of reactive astrocytes from NG2 cells is regulated by sonic hedgehog. *Glia*, 64, 1518-31.
- HOWARD, J., ROBERTS, W. M. & HUDSPETH, A. J. 1988. Mechanoelectrical transduction by hair cells. *Annu Rev Biophys Biophys Chem*, 17, 99-124.
- HU, Z. 2013. Formation of the peripheral-central transitional zone in the postnatal mouse cochlear nerve. *Otolaryngol Head Neck Surg*, 149, 296-300.
- HU, Z., ULFENDAHL, M. & OLIVIVUS, N. P. 2004. Central migration of neuronal tissue and embryonic stem cells following transplantation along the adult auditory nerve. *Brain Res*, 1026, 68-73.
- HU, Z., WEI, D., JOHANSSON, C. B., HOLMSTROM, N., DUAN, M., FRISEN, J. & ULFENDAHL, M. 2005. Survival and neural differentiation of adult neural stem cells transplanted into the mature inner ear. *Exp Cell Res*, 302, 40-7.
- HU, Z., ZHANG, B., LUO, X., ZHANG, L., WANG, J., BOJRAB, D. & JIANG, H. 2014. The Astroglial Reaction along the Mouse Cochlear Nerve following Inner Ear Damage. *Otolaryngol Head Neck Surg*, 150, 121-5.
- HUDSPETH, A. J. 2001. How the ear's works work: mechanoelectrical transduction and amplification by hair cells of the internal ear. *Harvey Lect*, 97, 41-54.

- HUNTER-DUVAR, I. M. & BREDBERG, G. 1974. Effects of intense auditory stimulation: hearing losses and inner ear changes in the chinchilla. *J Acoust Soc Am*, 55, 795-801.
- HURLEY, P. A., CROOK, J. M. & SHEPHERD, R. K. 2007. Schwann cells revert to non-myelinating phenotypes in the deafened rat cochlea. *Eur J Neurosci*, 26, 1813-21.
- IGUCHI, F., NAKAGAWA, T., TATEYA, I., ENDO, T., KIM, T. S., DONG, Y., KITA, T., KOJIMA, K., NAITO, Y., OMORI, K. & ITO, J. 2004. Surgical techniques for cell transplantation into the mouse cochlea. *Acta Otolaryngol Suppl*, 43-7.
- IHRIE, R. A. & ALVAREZ-BUYLLA, A. 2008. Cells in the astroglial lineage are neural stem cells. *Cell Tissue Res*, 331, 179-91.
- IKEDA, K., OSHIMA, T., HIDAKA, H. & TAKASAKA, T. 1997. Molecular and clinical implications of loop diuretic ototoxicity. *Hear Res*, 107, 1-8.
- INGHAM, N. J., PEARSON, S. & STEEL, K. P. 2011. Using the Auditory Brainstem Response (ABR) to Determine Sensitivity of Hearing in Mutant Mice. *Curr Protoc Mouse Biol*, 1, 279-87.
- INTERNATIONAL STEM CELL, I., AMPS, K., ANDREWS, P. W., ANYFANTIS, G., ARMSTRONG, L., AVERY, S., BAHARVAND, H., BAKER, J., BAKER, D., MUNOZ, M. B., BEIL, S., BENVENISTY, N., BEN-YOSEF, D., BIANCOTTI, J. C., BOSMAN, A., BRENA, R. M., BRISON, D., CAISANDER, G., CAMARASA, M. V., CHEN, J., CHIAO, E., CHOI, Y. M., CHOO, A. B., COLLINS, D., COLMAN, A., CROOK, J. M., DALEY, G. Q., DALTON, A., DE SOUSA, P. A., DENNING, C., DOWNIE, J., DVORAK, P., MONTGOMERY, K. D., FEKI, A., FORD, A., FOX, V., FRAGA, A. M., FRUMKIN, T., GE, L., GOKHALE, P. J., GOLAN-LEV, T., GOURABI, H., GROPP, M., LU, G., HAMPL, A., HARRON, K., HEALY, L., HERATH, W., HOLM, F., HOVATTA, O., HYLLNER, J., INAMDAR, M. S., IRWANTO, A. K., ISHII, T., JACONI, M., JIN, Y., KIMBER, S., KISELEV, S., KNOWLES, B. B., KOPPER, O., KUKHARENKO, V., KULIEV, A., LAGARKOVA, M. A., LAIRD, P. W., LAKO, M., LASLETT, A. L., LAVON, N., LEE, D. R., LEE, J. E., LI, C., LIM, L. S., LUDWIG, T. E., MA, Y., MALTBY, E., MATEIZEL, I., MAYSHAR, Y., MILEIKOVSKY, M., MINGER, S. L., MIYAZAKI, T., MOON, S. Y., MOORE, H., MUMMERY, C., NAGY, A., NAKATSUJI, N., NARWANI, K., OH, S. K., OH, S. K., OLSON, C., OTONKOSKI, T., PAN, F., PARK, I. H., PELLIS, S., PERA, M. F., PEREIRA, L. V., QI, O., RAJ, G. S., REUBINOFF, B., ROBINS, A., ROBSON, P., ROSSANT, J., et al. 2011. Screening ethnically diverse human embryonic stem cells identifies a chromosome 20 minimal amplicon conferring growth advantage. *Nat Biotechnol*, 29, 1132-44.
- IZUMIKAWA, M., MINODA, R., KAWAMOTO, K., ABRASHKIN, K. A., SWIDERSKI, D. L., DOLAN, D. F., BROUGH, D. E. & RAPHAEL, Y. 2005. Auditory hair cell replacement and hearing improvement by Atoh1 gene therapy in deaf mammals. *Nat Med*, 11, 271-6.
- JEON, E. J., XU, N., XU, L. & HANSEN, M. R. 2011. Influence of central glia on spiral ganglion neuron neurite growth. *Neuroscience*, 177, 321-34.
- JESSEN, K. R. 2004. Glial cells. *Int J Biochem Cell Biol*, 36, 1861-7.
- JESSEN, K. R. & MIRSKY, R. 1999. Why do Schwann cells survive in the absence of axons? *Ann N Y Acad Sci*, 883, 109-15.
- JESSEN, K. R. & MIRSKY, R. 2005. The origin and development of glial cells in peripheral nerves. *Nat Rev Neurosci*, 6, 671-82.

- JESSEN, K. R. & MIRSKY, R. 2016. The repair Schwann cell and its function in regenerating nerves. *J Physiol*, 594, 3521-31.
- JIANG, H., TALASKA, A. E., SCHACHT, J. & SHA, S. H. 2007. Oxidative imbalance in the aging inner ear. *Neurobiol Aging*, 28, 1605-12.
- JINEK, M., JIANG, F., TAYLOR, D. W., STERNBERG, S. H., KAYA, E., MA, E., ANDERS, C., HAUER, M., ZHOU, K., LIN, S., KAPLAN, M., IAVARONE, A. T., CHARPENTIER, E., NOGALES, E. & DOUDNA, J. A. 2014. Structures of Cas9 endonucleases reveal RNA-mediated conformational activation. *Science*, 343, 1247997.
- JUNG, T. T., RHEE, C. K., LEE, C. S., PARK, Y. S. & CHOI, D. C. 1993. Ototoxicity of salicylate, nonsteroidal antiinflammatory drugs, and quinine. *Otolaryngol Clin North Am*, 26, 791-810.
- KAEWKHAW, R., SCUTT, A. M. & HAYCOCK, J. W. 2012. Integrated culture and purification of rat Schwann cells from freshly isolated adult tissue. *Nat Protoc*, 7, 1996-2004.
- KANG, P., LEE, H. K., GLASGOW, S. M., FINLEY, M., DONTI, T., GABER, Z. B., GRAHAM, B. H., FOSTER, A. E., NOVITCH, B. G., GRONOSTAJSKI, R. M. & DENEEN, B. 2012. Sox9 and NFIA coordinate a transcriptional regulatory cascade during the initiation of gliogenesis. *Neuron*, 74, 79-94.
- KANSKI, R., VAN STRIEN, M. E., VAN TIJN, P. & HOL, E. M. 2014. A star is born: new insights into the mechanism of astrogenesis. *Cell Mol Life Sci*, 71, 433-47.
- KAWAMOTO, K., ISHIMOTO, S., MINODA, R., BROUGH, D. E. & RAPHAEL, Y. 2003. Math1 gene transfer generates new cochlear hair cells in mature guinea pigs in vivo. *J Neurosci*, 23, 4395-400.
- KELSELL, D. P., DUNLOP, J., STEVENS, H. P., LENCH, N. J., LIANG, J. N., PARRY, G., MUELLER, R. F. & LEIGH, I. M. 1997. Connexin 26 mutations in hereditary non-syndromic sensorineural deafness. *Nature*, 387, 80-3.
- KHAN, A. M., HANDZEL, O., BURGESS, B. J., DAMIAN, D., EDDINGTON, D. K. & NADOL, J. B., JR. 2005. Is word recognition correlated with the number of surviving spiral ganglion cells and electrode insertion depth in human subjects with cochlear implants? *Laryngoscope*, 115, 672-7.
- KHYNRIAM, D. & PRASAD, S. B. 2002. Changes in glutathione-related enzymes in tumor-bearing mice after cisplatin treatment. *Cell Biol Toxicol*, 18, 349-58.
- KIERNAN, A. E., PELLING, A. L., LEUNG, K. K., TANG, A. S., BELL, D. M., TEASE, C., LOVELL-BADGE, R., STEEL, K. P. & CHEAH, K. S. 2005. Sox2 is required for sensory organ development in the mammalian inner ear. *Nature*, 434, 1031-5.
- KIL, K., CHOI, M. Y. & PARK, K. H. 2016. In Vitro Differentiation of Human Wharton's Jelly-Derived Mesenchymal Stem Cells into Auditory Hair Cells and Neurons. *J Int Adv Otol*, 12, 37-42.
- KIM, E. & CHO, S. 2016. Microglia and Monocyte-Derived Macrophages in Stroke. *Neurotherapeutics*.
- KINGHAM, P. J., MANTOVANI, C. & TERENCE, G. 2011. Stem cell and neuron cocultures for the study of nerve regeneration. *Methods Mol Biol*, 695, 115-27.
- KIUMEHR, S., MAHBOUBI, H., MIDDLEBROOKS, J. C. & DJALILIAN, H. R. 2013. Transcanal approach for implantation of a cochlear nerve electrode array. *Laryngoscope*, 123, 1261-5.

- KOEHLER, K. R., MIKOSZ, A. M., MOLOSH, A. I., PATEL, D. & HASHINO, E. 2013. Generation of inner ear sensory epithelia from pluripotent stem cells in 3D culture. *Nature*, 500, 217-21.
- KOO, S. K., HILL, J. K., HWANG, C. H., LIN, Z. S., MILLEN, K. J. & WU, D. K. 2009. *Lmx1a* maintains proper neurogenic, sensory, and non-sensory domains in the mammalian inner ear. *Dev Biol*, 333, 14-25.
- KOPKE, R. D., WEISSKOPF, P. A., BOONE, J. L., JACKSON, R. L., WESTER, D. C., HOFFER, M. E., LAMBERT, D. C., CHARON, C. C., DING, D. L. & MCBRIDE, D. 2000. Reduction of noise-induced hearing loss using L-NAC and salicylate in the chinchilla. *Hear Res*, 149, 138-46.
- KOPPE, A. N., KEATING, K. W., MCGREGOR, A. L., KOPPE, R. A., KEARNS, K. R., ZIEMBA, A. M., MCKAY, C. A., ZUIDEMA, J. M., RIVET, C. J., GILBERT, R. J. & THOMPSON, D. M. 2016. Robust neurite extension following exogenous electrical stimulation within single walled carbon nanotube-composite hydrogels. *Acta Biomater*, 39, 34-43.
- KOPPE, A. N., NORDBERG, A. L., PAOLILLO, G. M., GOODSELL, N. M., DARWISH, H. A., ZHANG, L. & THOMPSON, D. M. 2014. Electrical stimulation of schwann cells promotes sustained increases in neurite outgrowth. *Tissue Eng Part A*, 20, 494-506.
- KOPPE, A. N., SEGGIO, A. M. & THOMPSON, D. M. 2011. Neurite outgrowth is significantly increased by the simultaneous presentation of Schwann cells and moderate exogenous electric fields. *J Neural Eng*, 8, 046023.
- KRETLOW, J. D., JIN, Y. Q., LIU, W., ZHANG, W. J., HONG, T. H., ZHOU, G., BAGGETT, L. S., MIKOS, A. G. & CAO, Y. 2008. Donor age and cell passage affects differentiation potential of murine bone marrow-derived stem cells. *BMC Cell Biol*, 9, 60.
- KRIEGSTEIN, A. & ALVAREZ-BUYLLA, A. 2009. The glial nature of embryonic and adult neural stem cells. *Annu Rev Neurosci*, 32, 149-84.
- KUJAWA, S. G. & LIBERMAN, M. C. 2009. Adding insult to injury: cochlear nerve degeneration after "temporary" noise-induced hearing loss. *J Neurosci*, 29, 14077-85.
- KUJAWA, S. G. & LIBERMAN, M. C. 2015. Synaptopathy in the noise-exposed and aging cochlea: Primary neural degeneration in acquired sensorineural hearing loss. *Hear Res*, 330, 191-9.
- KURSULA, P. 2008. Structural properties of proteins specific to the myelin sheath. *Amino Acids*, 34, 175-85.
- LAMMERS, M. J., VENEKAMP, R. P., GROLMAN, W. & VAN DER HEIJDEN, G. J. 2014. Bilateral cochlear implantation in children and the impact of the inter-implant interval. *Laryngoscope*, 124, 993-9.
- LANDRY, T. G., WISE, A. K., FALLON, J. B. & SHEPHERD, R. K. 2011. Spiral ganglion neuron survival and function in the deafened cochlea following chronic neurotrophic treatment. *Hear Res*, 282, 303-13.
- LANG, H., LI, M., KILPATRICK, L. A., ZHU, J., SAMUVEL, D. J., KRUG, E. L. & GODDARD, J. C. 2011. Sox2 up-regulation and glial cell proliferation following degeneration of spiral ganglion neurons in the adult mouse inner ear. *J Assoc Res Otolaryngol*, 12, 151-71.
- LANG, H., XING, Y., BROWN, L. N., SAMUVEL, D. J., PANGANIBAN, C. H., HAVENS, L. T., BALASUBRAMANIAN, S., WEGNER, M., KRUG, E. L. & BARTH, J. L. 2015.

- Neural stem/progenitor cell properties of glial cells in the adult mouse auditory nerve. *Sci Rep*, 5, 13383.
- LASSITER, R. N., STARK, M. R., ZHAO, T. & ZHOU, C. J. 2014. Signaling mechanisms controlling cranial placode neurogenesis and delamination. *Dev Biol*, 389, 39-49.
- LAVIGNE-REBILLARD, M. & PUJOL, R. 1988. Hair cell innervation in the fetal human cochlea. *Acta Otolaryngol*, 105, 398-402.
- LAWOKO-KERALI, G., RIVOLTA, M. N., LAWLOR, P., CACCIABUE-RIVOLTA, D. I., LANGTON-HEWER, C., VAN DOORNINCK, J. H. & HOLLEY, M. C. 2004. GATA3 and NeuroD distinguish auditory and vestibular neurons during development of the mammalian inner ear. *Mech Dev*, 121, 287-99.
- LEAKE, P. A., HRADEK, G. T., HETHERINGTON, A. M. & STAKHOVSKAYA, O. 2011. Brain-derived neurotrophic factor promotes cochlear spiral ganglion cell survival and function in deafened, developing cats. *J Comp Neurol*, 519, 1526-45.
- LEAKE, P. A., STAKHOVSKAYA, O., HETHERINGTON, A., REBSCHER, S. J. & BONHAM, B. 2013. Effects of brain-derived neurotrophic factor (BDNF) and electrical stimulation on survival and function of cochlear spiral ganglion neurons in deafened, developing cats. *J Assoc Res Otolaryngol*, 14, 187-211.
- LEE, G., KIM, H., ELKABETZ, Y., AL SHAMY, G., PANAGIOTAKOS, G., BARBERI, T., TABAR, V. & STUDER, L. 2007. Isolation and directed differentiation of neural crest stem cells derived from human embryonic stem cells. *Nat Biotechnol*, 25, 1468-75.
- LEE, S. K., LEE, B., RUIZ, E. C. & PFAFF, S. L. 2005. Olig2 and Ngn2 function in opposition to modulate gene expression in motor neuron progenitor cells. *Genes Dev*, 19, 282-94.
- LEMASURIER, M. & GILLESPIE, P. G. 2005. Hair-cell mechanotransduction and cochlear amplification. *Neuron*, 48, 403-15.
- LI, H., LIU, H. & HELLER, S. 2003a. Pluripotent stem cells from the adult mouse inner ear. *Nat Med*, 9, 1293-9.
- LI, H., ROBLIN, G., LIU, H. & HELLER, S. 2003b. Generation of hair cells by stepwise differentiation of embryonic stem cells. *Proc Natl Acad Sci U S A*, 100, 13495-500.
- LI, J., ZHANG, L., CHU, Y., NAMAKA, M., DENG, B., KONG, J. & BI, X. 2016. Astrocytes in Oligodendrocyte Lineage Development and White Matter Pathology. *Front Cell Neurosci*, 10, 119.
- LI, Y., GONZALEZ, M. I., MEINKOTH, J. L., FIELD, J., KAZANIETZ, M. G. & TENNEKOON, G. I. 2003c. Lysophosphatidic acid promotes survival and differentiation of rat Schwann cells. *J Biol Chem*, 278, 9585-91.
- LIAO, D., GONG, P., LI, X., TAN, Z. & YUAN, Q. 2010. Co-culture with Schwann cells is an effective way for adipose-derived stem cells neural transdifferentiation. *Arch Med Sci*, 6, 145-51.
- LIM, D. J. & MELNICK, W. 1971. Acoustic damage of the cochlea. A scanning and transmission electron microscopic observation. *Arch Otolaryngol*, 94, 294-305.
- LIMB, C. J. & ROY, A. T. 2014. Technological, biological, and acoustical constraints to music perception in cochlear implant users. *Hear Res*, 308, 13-26.

- LIN, F. R., METTER, E. J., O'BRIEN, R. J., RESNICK, S. M., ZONDERMAN, A. B. & FERRUCCI, L. 2011. Hearing loss and incident dementia. *Arch Neurol*, 68, 214-20.
- LIN, F. R., YAFFE, K., XIA, J., XUE, Q. L., HARRIS, T. B., PURCHASE-HELZNER, E., SATTERFIELD, S., AYONAYON, H. N., FERRUCCI, L., SIMONSICK, E. M. & HEALTH, A. B. C. S. G. 2013. Hearing loss and cognitive decline in older adults. *JAMA Intern Med*, 173, 293-9.
- LINDENBERGER, U. & BALTES, P. B. 1994. Sensory functioning and intelligence in old age: a strong connection. *Psychol Aging*, 9, 339-55.
- LITSIOU, A., HANSON, S. & STREIT, A. 2005. A balance of FGF, BMP and WNT signalling positions the future placode territory in the head. *Development*, 132, 4051-62.
- LIU, X. Z., WALSH, J., MBURU, P., KENDRICK-JONES, J., COPE, M. J., STEEL, K. P. & BROWN, S. D. 1997. Mutations in the myosin VIIA gene cause non-syndromic recessive deafness. *Nat Genet*, 16, 188-90.
- LOCHER, H., DE GROOT, J. C., VAN IPEREN, L., HUISMAN, M. A., FRIJNS, J. H. & CHUVA DE SOUSA LOPES, S. M. 2014. Distribution and development of peripheral glial cells in the human fetal cochlea. *PLoS One*, 9, e88066.
- LOEB, J. A., KHURANA, T. S., ROBBINS, J. T., YEE, A. G. & FISCHBACH, G. D. 1999. Expression patterns of transmembrane and released forms of neuregulin during spinal cord and neuromuscular synapse development. *Development*, 126, 781-91.
- LONGART, M., LIU, Y., KARAVANOVA, I. & BUONANNO, A. 2004. Neuregulin-2 is developmentally regulated and targeted to dendrites of central neurons. *J Comp Neurol*, 472, 156-72.
- LU, Q. R., YUK, D., ALBERTA, J. A., ZHU, Z., PAWLITZKY, I., CHAN, J., MCMAHON, A. P., STILES, C. D. & ROWITCH, D. H. 2000. Sonic hedgehog--regulated oligodendrocyte lineage genes encoding bHLH proteins in the mammalian central nervous system. *Neuron*, 25, 317-29.
- LUSTIG, L. R. & AKIL, O. 2012. Cochlear gene therapy. *Curr Opin Neurol*, 25, 57-60.
- MAIER, E. C., SAXENA, A., ALSINA, B., BRONNER, M. E. & WHITFIELD, T. T. 2014. Sensational placodes: neurogenesis in the otic and olfactory systems. *Dev Biol*, 389, 50-67.
- MAO, Y., REIPRICH, S., WEGNER, M. & FRITZSCH, B. 2014. Targeted deletion of Sox10 by Wnt1-cre defects neuronal migration and projection in the mouse inner ear. *PLoS One*, 9, e94580.
- MARCHIONNI, M. A., GOODEARL, A. D., CHEN, M. S., BIRMINGHAM-MCDONOGH, O., KIRK, C., HENDRICKS, M., DANEHY, F., MISUMI, D., SUDHALTER, J. & KOBAYASHI, K. 1993. Glial growth factors are alternatively spliced erbB2 ligands expressed in the nervous system. *Nature*, 362, 312-8.
- MARCOTTI, W., VAN NETTEN, S. M. & KROS, C. J. 2005. The aminoglycoside antibiotic dihydrostreptomycin rapidly enters mouse outer hair cells through the mechano-electrical transducer channels. *J Physiol*, 567, 505-21.
- MARTENS, W., SANEN, K., GEORGIU, M., STRUYS, T., BRONCKAERS, A., AMELOOT, M., PHILLIPS, J. & LAMBRICHTS, I. 2014. Human dental pulp stem cells can differentiate into Schwann cells and promote and guide neurite outgrowth in an aligned tissue-engineered collagen construct in vitro. *FASEB J*, 28, 1634-43.

- MARTIN, K. & GROVES, A. K. 2006. Competence of cranial ectoderm to respond to Fgf signaling suggests a two-step model of otic placode induction. *Development*, 133, 877-87.
- MARTINEZ-MONEDERO, R., YI, E., OSHIMA, K., GLOWATZKI, E. & EDGE, A. S. 2008. Differentiation of inner ear stem cells to functional sensory neurons. *Dev Neurobiol*, 68, 669-84.
- MARTINI, R., XIN, Y. & SCHACHNER, M. 1994. Restricted localization of L1 and N-CAM at sites of contact between Schwann cells and neurites in culture. *Glia*, 10, 70-4.
- MATSUOKA, A. J., KONDO, T., MIYAMOTO, R. T. & HASHINO, E. 2006. In vivo and in vitro characterization of bone marrow-derived stem cells in the cochlea. *Laryngoscope*, 116, 1363-7.
- MATSUOKA, A. J., KONDO, T., MIYAMOTO, R. T. & HASHINO, E. 2007. Enhanced survival of bone-marrow-derived pluripotent stem cells in an animal model of auditory neuropathy. *Laryngoscope*, 117, 1629-35.
- MATZ, G. J. 1993. Aminoglycoside cochlear ototoxicity. *Otolaryngol Clin North Am*, 26, 705-12.
- MCCABE, K. L., MANZO, A., GAMMILL, L. S. & BRONNER-FRASER, M. 2004. Discovery of genes implicated in placode formation. *Dev Biol*, 274, 462-77.
- MCCORMACK, A. & FORTNUM, H. 2013. Why do people fitted with hearing aids not wear them? *Int J Audiol*, 52, 360-8.
- MCKEON, R. J., SCHREIBER, R. C., RUDGE, J. S. & SILVER, J. 1991. Reduction of neurite outgrowth in a model of glial scarring following CNS injury is correlated with the expression of inhibitory molecules on reactive astrocytes. *J Neurosci*, 11, 3398-411.
- MCLARREN, K. W., LITSIU, A. & STREIT, A. 2003. DLX5 positions the neural crest and preplacode region at the border of the neural plate. *Dev Biol*, 259, 34-47.
- MEIER, C., PARMANTIER, E., BRENNAN, A., MIRSKY, R. & JESSEN, K. R. 1999. Developing Schwann cells acquire the ability to survive without axons by establishing an autocrine circuit involving insulin-like growth factor, neurotrophin-3, and platelet-derived growth factor-BB. *J Neurosci*, 19, 3847-59.
- MENARDO, J., TANG, Y., LADRECH, S., LENOIR, M., CASAS, F., MICHEL, C., BOURIEN, J., RUEL, J., REBILLARD, G., MAURICE, T., PUEL, J. L. & WANG, J. 2012. Oxidative stress, inflammation, and autophagic stress as the key mechanisms of premature age-related hearing loss in SAMP8 mouse Cochlea. *Antioxid Redox Signal*, 16, 263-74.
- MERZENICH, M. M., MICHELSON, R. P., PETTIT, C. R., SCHINDLER, R. A. & REID, M. 1973. Neural encoding of sound sensation evoked by electrical stimulation of the acoustic nerve. *Ann Otol Rhinol Laryngol*, 82, 486-503.
- MERZENICH, M. M., SCHINDLER, D. N. & WHITE, M. W. 1974. Feasibility of multichannel scala tympani stimulation. *Laryngoscope*, 84, 1887-93.
- MEYER, D. & BIRCHMEIER, C. 1995. Multiple essential functions of neuregulin in development. *Nature*, 378, 386-90.
- MICHAÏLOV, G. V., SEREDA, M. W., BRINKMANN, B. G., FISCHER, T. M., HAUG, B., BIRCHMEIER, C., ROLE, L., LAI, C., SCHWAB, M. H. & NAVE, K. A. 2004. Axonal neuregulin-1 regulates myelin sheath thickness. *Science*, 304, 700-3.

- MIRANDA, P. C., SAMPAIO, A. L., LOPES, R. A., RAMOS VENOSA, A. & DE OLIVEIRA, C. A. 2014. Hearing preservation in cochlear implant surgery. *Int J Otolaryngol*, 2014, 468515.
- MOLOFSKY, A. V., KRENCIK, R., ULLIAN, E. M., TSAI, H. H., DENEEN, B., RICHARDSON, W. D., BARRES, B. A. & ROWITCH, D. H. 2012. Astrocytes and disease: a neurodevelopmental perspective. *Genes Dev*, 26, 891-907.
- MORRIS, J. K., LIN, W., HAUSER, C., MARCHUK, Y., GETMAN, D. & LEE, K. F. 1999. Rescue of the cardiac defect in ErbB2 mutant mice reveals essential roles of ErbB2 in peripheral nervous system development. *Neuron*, 23, 273-83.
- MORRIS, J. K., MAKLAD, A., HANSEN, L. A., FENG, F., SORENSEN, C., LEE, K. F., MACKLIN, W. B. & FRITZSCH, B. 2006. A disorganized innervation of the inner ear persists in the absence of ErbB2. *Brain Res*, 1091, 186-99.
- MORRISON, S. J., PEREZ, S. E., QIAO, Z., VERDI, J. M., HICKS, C., WEINMASTER, G. & ANDERSON, D. J. 2000. Transient Notch activation initiates an irreversible switch from neurogenesis to gliogenesis by neural crest stem cells. *Cell*, 101, 499-510.
- MORTON, C. C. & NANCE, W. E. 2006. Newborn hearing screening--a silent revolution. *N Engl J Med*, 354, 2151-64.
- MOSER, T. & STARR, A. 2016. Auditory neuropathy--neural and synaptic mechanisms. *Nat Rev Neurol*, 12, 135-49.
- NA, J., BAKER, D., ZHANG, J., ANDREWS, P. W. & BARBARIC, I. 2014. Aneuploidy in pluripotent stem cells and implications for cancerous transformation. *Protein Cell*, 5, 569-79.
- NADOL, J. B., JR., SHIAO, J. Y., BURGESS, B. J., KETTEN, D. R., EDDINGTON, D. K., GANTZ, B. J., KOS, I., MONTANDON, P., COKER, N. J., ROLAND, J. T., JR. & SHALLOP, J. K. 2001. Histopathology of cochlear implants in humans. *Ann Otol Rhinol Laryngol*, 110, 883-91.
- NAKASHIMA, K., YANAGISAWA, M., ARAKAWA, H. & TAGA, T. 1999. Astrocyte differentiation mediated by LIF in cooperation with BMP2. *FEBS Lett*, 457, 43-6.
- NAMBA, T., MOCHIZUKI, H., ONODERA, M., MIZUNO, Y., NAMIKI, H. & SEKI, T. 2005. The fate of neural progenitor cells expressing astrocytic and radial glial markers in the postnatal rat dentate gyrus. *Eur J Neurosci*, 22, 1928-41.
- NAMIHIRA, M., KOHYAMA, J., SEMI, K., SANOSAKA, T., DENEEN, B., TAGA, T. & NAKASHIMA, K. 2009. Committed neuronal precursors confer astrocytic potential on residual neural precursor cells. *Dev Cell*, 16, 245-55.
- NAWAZ, S., MCNEILL, C. & GREENBERG, S. L. 2014. Improving sound localization after cochlear implantation and auditory training for the management of single-sided deafness. *Otol Neurotol*, 35, 271-6.
- NEWBERN, J. & BIRCHMEIER, C. 2010. Nrg1/ErbB signaling networks in Schwann cell development and myelination. *Semin Cell Dev Biol*, 21, 922-8.
- NEWBERN, J. M. 2015. Molecular control of the neural crest and peripheral nervous system development. *Curr Top Dev Biol*, 111, 201-31.
- NIETO, M. A. 2002. The snail superfamily of zinc-finger transcription factors. *Nat Rev Mol Cell Biol*, 3, 155-66.
- NOBLE, M., FOK-SEANG, J., WOLSWIJK, G. & WREN, D. 1990. Development and regeneration in the central nervous system. *Philos Trans R Soc Lond B Biol Sci*, 327, 127-43.

- O'LEARY, S. J. 2008. Ototoxicity. In: GLEESON, M. (ed.) *Scott-Brown's Otorhinolaryngology, Head and Neck Surgery*. London: Edward Arnold.
- OHLEMILLER, K. K., WRIGHT, J. S. & DUGAN, L. L. 1999. Early elevation of cochlear reactive oxygen species following noise exposure. *Audiol Neurootol*, 4, 229-36.
- OHNISHI, H., SKERLEVA, D., KITAJIRI, S., SAKAMOTO, T., YAMAMOTO, N., ITO, J. & NAKAGAWA, T. 2015. Limited hair cell induction from human induced pluripotent stem cells using a simple stepwise method. *Neurosci Lett*, 599, 49-54.
- OSHIMA, K., GRIMM, C. M., CORRALES, C. E., SENN, P., MARTINEZ MONEDERO, R., GELEOC, G. S., EDGE, A., HOLT, J. R. & HELLER, S. 2007a. Differential distribution of stem cells in the auditory and vestibular organs of the inner ear. *J Assoc Res Otolaryngol*, 8, 18-31.
- OSHIMA, K., SHIN, K., DIENSTHUBER, M., PENG, A. W., RICCI, A. J. & HELLER, S. 2010. Mechanosensitive hair cell-like cells from embryonic and induced pluripotent stem cells. *Cell*, 141, 704-16.
- OSHIMA, K., TEO, D. T., SENN, P., STARLINGER, V. & HELLER, S. 2007b. LIF promotes neurogenesis and maintains neural precursors in cell populations derived from spiral ganglion stem cells. *BMC Dev Biol*, 7, 112.
- PALMGREN, B., JIN, Z., JIAO, Y., KOSTYSZYN, B. & OLIVIVUS, P. 2011. Horseradish peroxidase dye tracing and embryonic statoacoustic ganglion cell transplantation in the rat auditory nerve trunk. *Brain Res*, 1377, 41-9.
- PAN, N., JAHAN, I., KERSIGO, J., KOPECKY, B., SANTI, P., JOHNSON, S., SCHMITZ, H. & FRITZSCH, B. 2011. Conditional deletion of *Atoh1* using *Pax2-Cre* results in viable mice without differentiated cochlear hair cells that have lost most of the organ of Corti. *Hear Res*, 275, 66-80.
- PARPURA, V. & ZOREC, R. 2010. Gliotransmission: Exocytotic release from astrocytes. *Brain Res Rev*, 63, 83-92.
- PECHRIGGL, E. J., BITSCHKE, M., GLUECKERT, R., RASK-ANDERSEN, H., BLUMER, M. J., SCHROTT-FISCHER, A. & FRITZSCH, H. 2015. Development of the innervation of the human inner ear. *Dev Neurobiol*, 75, 683-702.
- PEDRAZA, L., HUANG, J. K. & COLMAN, D. R. 2001. Organizing principles of the axoglial apparatus. *Neuron*, 30, 335-44.
- PICKLES, J. O. 2008. *An Introduction To The Physiology Of Hearing*, Bingley, Emerald.
- PLACK, C. J., BARKER, D. & PRENDERGAST, G. 2014. Perceptual consequences of "hidden" hearing loss. *Trends Hear*, 18.
- PRIUSKA, E. M. & SCHACHT, J. 1995. Formation of free radicals by gentamicin and iron and evidence for an iron/gentamicin complex. *Biochem Pharmacol*, 50, 1749-52.
- PUJOL R, L.-R. M., LENOIR M. 1998. *Development of sensory and neural structures in the mammalian cochlea*, New York, Springer.
- RANCE, G. 2005. Auditory neuropathy/dys-synchrony and its perceptual consequences. *Trends Amplif*, 9, 1-43.
- RANCE, G., CORBEN, L., BARKER, E., CAREW, P., CHISARI, D., ROGERS, M., DOWELL, R., JAMALUDDIN, S., BRYSON, R. & DELATYCKI, M. B. 2010. Auditory perception in individuals with Friedreich's ataxia. *Audiol Neurootol*, 15, 229-40.

- RANCE, G., RYAN, M. M., BAYLISS, K., GILL, K., O'SULLIVAN, C. & WHITECHURCH, M. 2012. Auditory function in children with Charcot-Marie-Tooth disease. *Brain*, 135, 1412-22.
- RAY, B., ROY, T. S., WADHWA, S. & ROY, K. K. 2005. Development of the human fetal cochlear nerve: a morphometric study. *Hear Res*, 202, 74-86.
- REEDER, R. M., FIRSZT, J. B., HOLDEN, L. K. & STRUBE, M. J. 2014. A longitudinal study in adults with sequential bilateral cochlear implants: time course for individual ear and bilateral performance. *J Speech Lang Hear Res*, 57, 1108-26.
- REICHENBACH, A., DEROUICHE, A. & KIRCHHOFF, F. 2010. Morphology and dynamics of perisynaptic glia. *Brain Res Rev*, 63, 11-25.
- REJALI, D., LEE, V. A., ABRASHKIN, K. A., HUMAYUN, N., SWIDERSKI, D. L. & RAPHAEL, Y. 2007. Cochlear implants and ex vivo BDNF gene therapy protect spiral ganglion neurons. *Hear Res*, 228, 180-7.
- RICHARDSON, R. M., HOLLOWAY, K. L., BULLOCK, M. R., BROADDUS, W. C. & FILLMORE, H. L. 2006a. Isolation of neuronal progenitor cells from the adult human neocortex. *Acta Neurochir (Wien)*, 148, 773-7.
- RICHARDSON, R. T., WISE, A. K., THOMPSON, B. C., FLYNN, B. O., ATKINSON, P. J., FRETWELL, N. J., FALLON, J. B., WALLACE, G. G., SHEPHERD, R. K., CLARK, G. M. & O'LEARY, S. J. 2009. Polypyrrole-coated electrodes for the delivery of charge and neurotrophins to cochlear neurons. *Biomaterials*, 30, 2614-24.
- RICHARDSON, W. D., KESSARIS, N. & PRINGLE, N. 2006b. Oligodendrocyte wars. *Nat Rev Neurosci*, 7, 11-8.
- RICKMANN, M. & WOLFF, J. R. 1995. S100 protein expression in subpopulations of neurons of rat brain. *Neuroscience*, 67, 977-91.
- RIETHMACHER, D., SONNENBERG-RIETHMACHER, E., BRINKMANN, V., YAMAAI, T., LEWIN, G. R. & BIRCHMEIER, C. 1997. Severe neuropathies in mice with targeted mutations in the ErbB3 receptor. *Nature*, 389, 725-30.
- RIO, C., DIKES, P., LIBERMAN, M. C. & CORFAS, G. 2002. Glial fibrillary acidic protein expression and promoter activity in the inner ear of developing and adult mice. *J Comp Neurol*, 442, 156-62.
- RIZZI, M. D. & HIROSE, K. 2007. Aminoglycoside ototoxicity. *Curr Opin Otolaryngol Head Neck Surg*, 15, 352-7.
- ROBLES, L. & RUGGERO, M. A. 2001. Mechanics of the mammalian cochlea. *Physiol Rev*, 81, 1305-52.
- RODRIGUEZ-BALLESTEROS, M., REYNOSO, R., OLARTE, M., VILLAMAR, M., MORERA, C., SANTARELLI, R., ARSLAN, E., MEDA, C., CURET, C., VOLTER, C., SAINZ-QUEVEDO, M., CASTORINA, P., AMBROSETTI, U., BERRETTINI, S., FREI, K., TEDIN, S., SMITH, J., CRUZ TAPIA, M., CAVALLE, L., GELVEZ, N., PRIMIGNANI, P., GOMEZ-ROSAS, E., MARTIN, M., MORENO-PELAYO, M. A., TAMAYO, M., MORENO-BARRAL, J., MORENO, F. & DEL CASTILLO, I. 2008. A multicenter study on the prevalence and spectrum of mutations in the otoferlin gene (OTOF) in subjects with nonsyndromic hearing impairment and auditory neuropathy. *Hum Mutat*, 29, 823-31.
- RONAGHI, M., NASR, M., EALY, M., DURRUTHY-DURRUTHY, R., WALDHAUS, J., DIAZ, G. H., JOUBERT, L. M., OSHIMA, K. & HELLER, S. 2014. Inner ear hair cell-like cells from human embryonic stem cells. *Stem Cells Dev*, 23, 1275-84.

- ROUX, I., SAFIEDDINE, S., NOUVIAN, R., GRATI, M., SIMMLER, M. C., BAHLOUL, A., PERFETTINI, I., LE GALL, M., ROSTAING, P., HAMARD, G., TRILLER, A., AVAN, P., MOSER, T. & PETIT, C. 2006. Otoferlin, defective in a human deafness form, is essential for exocytosis at the auditory ribbon synapse. *Cell*, 127, 277-89.
- ROWITCH, D. H. 2004. Glial specification in the vertebrate neural tube. *Nat Rev Neurosci*, 5, 409-19.
- RUDGE, J. S. & SILVER, J. 1990. Inhibition of neurite outgrowth on astroglial scars in vitro. *J Neurosci*, 10, 3594-603.
- RYALS, B. M. & RUBEL, E. W. 1988. Hair cell regeneration after acoustic trauma in adult Coturnix quail. *Science*, 240, 1774-6.
- SADZUKA, Y., SHOJI, T. & TAKINO, Y. 1992. Mechanism of the increase in lipid peroxide induced by cisplatin in the kidneys of rats. *Toxicol Lett*, 62, 293-300.
- SAIJO, K., WINNER, B., CARSON, C. T., COLLIER, J. G., BOYER, L., ROSENFELD, M. G., GAGE, F. H. & GLASS, C. K. 2009. A Nurr1/CoREST pathway in microglia and astrocytes protects dopaminergic neurons from inflammation-induced death. *Cell*, 137, 47-59.
- SANDELL, L. L., BUTLER TJADEN, N. E., BARLOW, A. J. & TRAINOR, P. A. 2014. Cochleovestibular nerve development is integrated with migratory neural crest cells. *Dev Biol*, 385, 200-10.
- SCHECTERSON, L. C. & BOTHWELL, M. 1994. Neurotrophin and neurotrophin receptor mRNA expression in developing inner ear. *Hear Res*, 73, 92-100.
- SCHILDGE, S., BOHRER, C., BECK, K. & SCHACHTRUP, C. 2013. Isolation and culture of mouse cortical astrocytes. *J Vis Exp*.
- SCHUKNECHT, H. F. 1964. Further Observations on the Pathology of Presbycusis. *Arch Otolaryngol*, 80, 369-82.
- SEGGIO, A. M., NARAYANASWAMY, A., ROYSAM, B. & THOMPSON, D. M. 2010. Self-aligned Schwann cell monolayers demonstrate an inherent ability to direct neurite outgrowth. *J Neural Eng*, 7, 046001.
- SEILHEIMER, B. & SCHACHNER, M. 1988. Studies of adhesion molecules mediating interactions between cells of peripheral nervous system indicate a major role for L1 in mediating sensory neuron growth on Schwann cells in culture. *J Cell Biol*, 107, 341-51.
- SEKIYA, T., HOLLEY, M. C., HASHIDO, K., ONO, K., SHIMOMURA, K., HORIE, R. T., HAMAGUCHI, K., YOSHIDA, A., SAKAMOTO, T. & ITO, J. 2015. Cells transplanted onto the surface of the glial scar reveal hidden potential for functional neural regeneration. *Proc Natl Acad Sci U S A*, 112, E3431-40.
- SEKIYA, T., HOLLEY, M. C., KOJIMA, K., MATSUMOTO, M., HELYER, R. & ITO, J. 2007. Transplantation of conditionally immortal auditory neuroblasts to the auditory nerve. *Eur J Neurosci*, 25, 2307-18.
- SEKIYA, T., MATSUMOTO, M., KOJIMA, K., ONO, K., KIKKAWA, Y. S., KADA, S., OGITA, H., HORIE, R. T., VIOLA, A., HOLLEY, M. C. & ITO, J. 2011. Mechanical stress-induced reactive gliosis in the auditory nerve and cochlear nucleus. *J Neurosurg*, 114, 414-25.
- SENNAROGLU, L., ZİYAL, I., ATAS, A., SENNAROGLU, G., YUCEL, E., SEVINC, S., EKIN, M. C., SARAC, S., ATAY, G., OZGEN, B., OZCAN, O. E., BELGIN, E., COLLETTI, V. & TURAN, E. 2009. Preliminary results of auditory brainstem implantation in prelingually deaf children with inner ear malformations including severe

- stenosis of the cochlear aperture and aplasia of the cochlear nerve. *Otol Neurotol*, 30, 708-15.
- SHAH, N. M., MARCHIONNI, M. A., ISAACS, I., STROOBANT, P. & ANDERSON, D. J. 1994. Glial growth factor restricts mammalian neural crest stem cells to a glial fate. *Cell*, 77, 349-60.
- SHEPHERD, R. K., COCO, A., EPP, S. B. & CROOK, J. M. 2005. Chronic depolarization enhances the trophic effects of brain-derived neurotrophic factor in rescuing auditory neurons following a sensorineural hearing loss. *J Comp Neurol*, 486, 145-58.
- SHI, F., CORRALES, C. E., LIBERMAN, M. C. & EDGE, A. S. 2007. BMP4 induction of sensory neurons from human embryonic stem cells and reinnervation of sensory epithelium. *Eur J Neurosci*, 26, 3016-23.
- SIMONS, M. & TRAJKOVIC, K. 2006. Neuron-glia communication in the control of oligodendrocyte function and myelin biogenesis. *J Cell Sci*, 119, 4381-9.
- SIRKO, S., BEHRENDT, G., JOHANSSON, P. A., TRIPATHI, P., COSTA, M., BEK, S., HEINRICH, C., TIEDT, S., COLAK, D., DICHGANS, M., FISCHER, I. R., PLESNILA, N., STAUFENBIEL, M., HAASS, C., SNAPYAN, M., SAGHATELYAN, A., TSAI, L. H., FISCHER, A., GROBE, K., DIMOU, L. & GOTZ, M. 2013. Reactive glia in the injured brain acquire stem cell properties in response to sonic hedgehog. [corrected]. *Cell Stem Cell*, 12, 426-39.
- SKINNER, A. H. 1931. SOME HISTOLOGIC FEATURES OF THE CRANIAL NERVES. *Arch Neurol Psychiat*, 25, 356-72.
- SLACK, R. W., WRIGHT, A., MICHAELS, L. & FROHLICH, S. A. 1986. Inner hair cell loss and intracochlear clot in the preterm infant. *Clin Otolaryngol Allied Sci*, 11, 443-6.
- SLEPECKY, N. 1996. *Structure Of The Mammalian Cochlea*, New York, Springer-Verlag.
- SMITH, C. M., BARNES, G. P., JACOBSON, C. A. & OELBERG, D. G. 2004. Auditory brainstem response detects early bilirubin neurotoxicity at low indirect bilirubin values. *J Perinatol*, 24, 730-2.
- SOFRONIEW, M. V. 2009. Molecular dissection of reactive astrogliosis and glial scar formation. *Trends Neurosci*, 32, 638-47.
- SOFRONIEW, M. V. & VINTERS, H. V. 2010. Astrocytes: biology and pathology. *Acta Neuropathol*, 119, 7-35.
- SONG, J., SUN, B., LIU, S., CHEN, W., ZHANG, Y., WANG, C., MO, X., CHE, J., OUYANG, Y., YUAN, W. & FAN, C. 2016. Polymerizing Pyrrole Coated Poly (l-lactic acid-co-epsilon-caprolactone) (PLCL) Conductive Nanofibrous Conduit Combined with Electric Stimulation for Long-Range Peripheral Nerve Regeneration. *Front Mol Neurosci*, 9, 117.
- SPOENDLIN, H. 1971. Primary structural changes in the organ of Corti after acoustic overstimulation. *Acta Otolaryngol*, 71, 166-76.
- STANKOVIC, K., RIO, C., XIA, A., SUGAWARA, M., ADAMS, J. C., LIBERMAN, M. C. & CORFAS, G. 2004. Survival of adult spiral ganglion neurons requires erbB receptor signaling in the inner ear. *J Neurosci*, 24, 8651-61.
- STARR, A., PICTON, T. W., SININGER, Y., HOOD, L. J. & BERLIN, C. I. 1996. Auditory neuropathy. *Brain*, 119 (Pt 3), 741-53.
- STIPURSKY, J. & GOMES, F. C. 2007. TGF-beta1/SMAD signaling induces astrocyte fate commitment in vitro: implications for radial glia development. *Glia*, 55, 1023-33.

- STOLL, G. & MULLER, H. W. 1999. Nerve injury, axonal degeneration and neural regeneration: basic insights. *Brain Pathol*, 9, 313-25.
- STOLT, C. C., LOMMES, P., FRIEDRICH, R. P. & WEGNER, M. 2004. Transcription factors Sox8 and Sox10 perform non-equivalent roles during oligodendrocyte development despite functional redundancy. *Development*, 131, 2349-58.
- STREIT, A. 2004. Early development of the cranial sensory nervous system: from a common field to individual placodes. *Dev Biol*, 276, 1-15.
- SUGAWARA, M., CORFAS, G. & LIBERMAN, M. C. 2005. Influence of supporting cells on neuronal degeneration after hair cell loss. *J Assoc Res Otolaryngol*, 6, 136-47.
- SUZUKI, K., LOVERA, M., SCHMACHTENBERG, O. & COUVE, E. 2015. Axonal Degeneration in Dental Pulp Precedes Human Primary Teeth Exfoliation. *J Dent Res*, 94, 1446-53.
- TAGOE, T., BARKER, M., JONES, A., ALLCOCK, N. & HAMANN, M. 2014. Auditory nerve perinodal dysmyelination in noise-induced hearing loss. *J Neurosci*, 34, 2684-8.
- TAKAHASHI, K., TANABE, K., OHNUKI, M., NARITA, M., ICHISAKA, T., TOMODA, K. & YAMANAKA, S. 2007. Induction of pluripotent stem cells from adult human fibroblasts by defined factors. *Cell*, 131, 861-72.
- TAKAHASHI, K. & YAMANAKA, S. 2006. Induction of pluripotent stem cells from mouse embryonic and adult fibroblast cultures by defined factors. *Cell*, 126, 663-76.
- TANG, W., ZHANG, Y., CHANG, Q., AHMAD, S., DAHLKE, I., YI, H., CHEN, P., PAUL, D. L. & LIN, X. 2006. Connexin29 is highly expressed in cochlear Schwann cells, and it is required for the normal development and function of the auditory nerve of mice. *J Neurosci*, 26, 1991-9.
- TARLOV, I. M. 1937a. Structure of the nerve root. I. Nature of the junction between the central and peripheral nervous system. *Arch Neurol Psychiat*, 37, 555-583.
- TARLOV, I. M. 1937b. Structure of the nerve root. II. Differentiation of sensory from motor roots; observations on identification of function in roots of mixed cranial nerves. *Arch Neurol Psychiat*, 37, 1338-1355.
- THIRLWALL, A. S., BROWN, D. J., MCMILLAN, P. M., BARKER, S. E. & LESPERANCE, M. M. 2003. Phenotypic characterization of hereditary hearing impairment linked to DFNA25. *Arch Otolaryngol Head Neck Surg*, 129, 830-5.
- THOMPSON, D. M. & BUETTNER, H. M. 2006. Neurite outgrowth is directed by schwann cell alignment in the absence of other guidance cues. *Ann Biomed Eng*, 34, 161-8.
- TONG, L., JI, L., WANG, Z., TONG, X., ZHANG, L. & SUN, X. 2010. Differentiation of neural stem cells into Schwann-like cells in vitro. *Biochem Biophys Res Commun*, 401, 592-7.
- TRACHOO, O. 2010. *Extracellular serine proteases as triggers of neuronal differentiation in human foetal auditory stem cells*. PhD, University of Sheffield.
- TSOPORIS, J. N., MARKS, A., KAHN, H. J., BUTANY, J. W., LIU, P. P., O'HANLON, D. & PARKER, T. G. 1997. S100beta inhibits alpha1-adrenergic induction of the hypertrophic phenotype in cardiac myocytes. *J Biol Chem*, 272, 31915-21.

- VANGEISON, G. & REMPE, D. A. 2009. The Janus-faced effects of hypoxia on astrocyte function. *Neuroscientist*, 15, 579-88.
- VENAIL, F., SICARD, M., PIRON, J. P., LEVI, A., ARTIERES, F., UZIEL, A. & MONDAIN, M. 2008. Reliability and complications of 500 consecutive cochlear implantations. *Arch Otolaryngol Head Neck Surg*, 134, 1276-81.
- VIVES, V., ALONSO, G., SOLAL, A. C., JOUBERT, D. & LEGRAVEREND, C. 2003. Visualization of S100B-positive neurons and glia in the central nervous system of EGFP transgenic mice. *J Comp Neurol*, 457, 404-19.
- VOLTA, A. 1800. On the electricity excited by the mere contact of conducting substances of different kinds. *Philos Trans R Soc Lond B Biol Sci*, 90, 403-431.
- VON BEKESY, G. 1960. *Experiments In Hearing*, New York, McGraw-Hill.
- WAN, G. & CORFAS, G. 2017. Transient auditory nerve demyelination as a new mechanism for hidden hearing loss. *Nat Commun*, 8, 14487.
- WANG, Q. & STEYGER, P. S. 2009. Trafficking of systemic fluorescent gentamicin into the cochlea and hair cells. *J Assoc Res Otolaryngol*, 10, 205-19.
- WANG, S. J., FURUSHO, M., D'SA, C., KUWADA, S., CONTI, L., MOREST, D. K. & BANSAL, R. 2009. Inactivation of fibroblast growth factor receptor signaling in myelinating glial cells results in significant loss of adult spiral ganglion neurons accompanied by age-related hearing impairment. *J Neurosci Res*, 87, 3428-37.
- WANG, T., YUAN, W., LIU, Y., ZHANG, Y., WANG, Z., ZHOU, X., NING, G., ZHANG, L., YAO, L., FENG, S. & KONG, X. 2015. The role of the JAK-STAT pathway in neural stem cells, neural progenitor cells and reactive astrocytes after spinal cord injury. *Biomed Rep*, 3, 141-146.
- WANG, Y., CHENG, X., HE, Q., ZHENG, Y., KIM, D. H., WHITTEMORE, S. R. & CAO, Q. L. 2011. Astrocytes from the contused spinal cord inhibit oligodendrocyte differentiation of adult oligodendrocyte precursor cells by increasing the expression of bone morphogenetic proteins. *J Neurosci*, 31, 6053-8.
- WANGEMANN, P. 2002. K⁺ cycling and the endocochlear potential. *Hear Res*, 165, 1-9.
- WANNER, I. B., DEIK, A., TORRES, M., ROSENDAHL, A., NEARY, J. T., LEMMON, V. P. & BIXBY, J. L. 2008. A new in vitro model of the glial scar inhibits axon growth. *Glia*, 56, 1691-709.
- WEBSTER, H. D. 1971. The geometry of peripheral myelin sheaths during their formation and growth in rat sciatic nerves. *J Cell Biol*, 48, 348-67.
- WEIL, D., KUSSEL, P., BLANCHARD, S., LEVY, G., LEVI-ACOBAS, F., DRIRA, M., AYADI, H. & PETIT, C. 1997. The autosomal recessive isolated deafness, DFNB2, and the Usher 1B syndrome are allelic defects of the myosin-VIIA gene. *Nat Genet*, 16, 191-3.
- WHITFIELD, T. T., RILEY, B. B., CHIANG, M. Y. & PHILLIPS, B. 2002. Development of the zebrafish inner ear. *Dev Dyn*, 223, 427-58.
- WHITLON, D. S., TIEU, D., GROVER, M., REILLY, B. & COULSON, M. T. 2009. Spontaneous association of glial cells with regrowing neurites in mixed cultures of dissociated spiral ganglia. *Neuroscience*, 161, 227-35.
- WIDERA, D., ZANDER, C., HEIDBREDER, M., KASPEREK, Y., NOLL, T., SEITZ, O., SALDAMLI, B., SUDHOFF, H., SADER, R., KALTSCHMIDT, C. & KALTSCHMIDT, B. 2009. Adult palatum as a novel source of neural crest-related stem cells. *Stem Cells*, 27, 1899-910.

- WILCOX, E. R., BURTON, Q. L., NAZ, S., RIAZUDDIN, S., SMITH, T. N., PLOPLIS, B., BELYANTSEVA, I., BEN-YOSEF, T., LIBURD, N. A., MORELL, R. J., KACHAR, B., WU, D. K., GRIFFITH, A. J., RIAZUDDIN, S. & FRIEDMAN, T. B. 2001. Mutations in the gene encoding tight junction claudin-14 cause autosomal recessive deafness DFNB29. *Cell*, 104, 165-72.
- WINSECK, A. K., CALDERO, J., CIUTAT, D., PREVETTE, D., SCOTT, S. A., WANG, G., ESQUERDA, J. E. & OPPENHEIM, R. W. 2002. In vivo analysis of Schwann cell programmed cell death in the embryonic chick: regulation by axons and glial growth factor. *J Neurosci*, 22, 4509-21.
- WOLDEYESUS, M. T., BRITSCH, S., RIETHMACHER, D., XU, L., SONNENBERG-RIETHMACHER, E., ABOU-REBYEH, F., HARVEY, R., CARONI, P. & BIRCHMEIER, C. 1999. Peripheral nervous system defects in erbB2 mutants following genetic rescue of heart development. *Genes Dev*, 13, 2538-48.
- WOODHOO, A., ALONSO, M. B., DROGGITI, A., TURMAINE, M., D'ANTONIO, M., PARKINSON, D. B., WILTON, D. K., AL-SHAWI, R., SIMONS, P., SHEN, J., GUILLEMOT, F., RADTKE, F., MEIJER, D., FELTRI, M. L., WRABETZ, L., MIRSKY, R. & JESSEN, K. R. 2009. Notch controls embryonic Schwann cell differentiation, postnatal myelination and adult plasticity. *Nat Neurosci*, 12, 839-47.
- WOODHOO, A. & SOMMER, L. 2008. Development of the Schwann cell lineage: from the neural crest to the myelinated nerve. *Glia*, 56, 1481-90.
- XU, H., VIOLA, A., ZHANG, Z., GERKEN, C. P., LINDSAY-ILLINGWORTH, E. A. & BALDINI, A. 2007. Tbx1 regulates population, proliferation and cell fate determination of otic epithelial cells. *Dev Biol*, 302, 670-82.
- XU, P. X., ADAMS, J., PETERS, H., BROWN, M. C., HEANEY, S. & MAAS, R. 1999. Eya1-deficient mice lack ears and kidneys and show abnormal apoptosis of organ primordia. *Nat Genet*, 23, 113-7.
- XU, Y. P., SHAN, X. D., LIU, Y. Y., PU, Y., WANG, C. Y., TAO, Q. L., DENG, Y., CHENG, Y. & FAN, J. P. 2016. Olfactory epithelium neural stem cell implantation restores noise-induced hearing loss in rats. *Neurosci Lett*, 616, 19-25.
- YAMANE, H., NAKAI, Y., TAKAYAMA, M., IGUCHI, H., NAKAGAWA, T. & KOJIMA, A. 1995. Appearance of free radicals in the guinea pig inner ear after noise-induced acoustic trauma. *Eur Arch Otorhinolaryngol*, 252, 504-8.
- YANG, Q., HAMBERGER, A., WANG, S. & HAGLID, K. G. 1996. Appearance of neuronal S-100 beta during development of the rat brain. *Brain Res Dev Brain Res*, 91, 181-9.
- YANG, Q., WANG, E. Y., HUANG, X. J., QU, W. S., ZHANG, L., XU, J. Z., WANG, W. & TIAN, D. S. 2011. Blocking epidermal growth factor receptor attenuates reactive astrogliosis through inhibiting cell cycle progression and protects against ischemic brain injury in rats. *J Neurochem*, 119, 644-53.
- YEH, T. H., LEE, D. Y., GIANINO, S. M. & GUTMANN, D. H. 2009. Microarray analyses reveal regional astrocyte heterogeneity with implications for neurofibromatosis type 1 (NF1)-regulated glial proliferation. *Glia*, 57, 1239-49.
- YOON, J. Y., YANG, K. J., KIM DA, E., LEE, K. Y., PARK, S. N., KIM, D. K. & KIM, J. D. 2015. Intratympanic delivery of oligoarginine-conjugated nanoparticles as a gene (or drug) carrier to the inner ear. *Biomaterials*, 73, 243-53.

- YU, P., WANG, H., KATAGIRI, Y. & GELLER, H. M. 2012. An in vitro model of reactive astrogliosis and its effect on neuronal growth. *Methods Mol Biol*, 814, 327-40.
- YU, Q., WANG, Y., CHANG, Q., WANG, J., GONG, S., LI, H. & LIN, X. 2014. Virally expressed connexin26 restores gap junction function in the cochlea of conditional Gjb2 knockout mice. *Gene Ther*, 21, 71-80.
- YUAN, J., LIU, W., ZHU, H., CHEN, Y., ZHANG, X., LI, L., CHU, W., WEN, Z., FENG, H. & LIN, J. 2016. Curcumin inhibits glial scar formation by suppressing astrocyte-induced inflammation and fibrosis in vitro and in vivo. *Brain Res*.
- ZHANG, L.I., ZHOU, Y. & TAO, W. 2011. Inhibitory Synaptic Mechanisms Underlying Functional Diversity In Auditory Cortex. *JGP* 138(3): 311
- ZHANG, S. C. 2006. Neural subtype specification from embryonic stem cells. *Brain Pathol*, 16, 132-42.
- ZHANG, W., ZHANG, Y., LOBLER, M., SCHMITZ, K. P., AHMAD, A., PYYKKO, I. & ZOU, J. 2011. Nuclear entry of hyperbranched polylysine nanoparticles into cochlear cells. *Int J Nanomedicine*, 6, 535-46.
- ZHAO, Y., WALDMAN, S. D. & FLYNN, L. E. 2012. The effect of serial passaging on the proliferation and differentiation of bovine adipose-derived stem cells. *Cells Tissues Organs*, 195, 414-27.
- ZHENG, W., HUANG, L., WEI, Z. B., SILVIUS, D., TANG, B. & XU, P. X. 2003. The role of Six1 in mammalian auditory system development. *Development*, 130, 3989-4000.
- ZILBERSTEIN, Y., LIBERMAN, M. C. & CORFAS, G. 2012. Inner hair cells are not required for survival of spiral ganglion neurons in the adult cochlea. *J Neurosci*, 32, 405-10.
- ZURIS, J. A., THOMPSON, D. B., SHU, Y., GUILINGER, J. P., BESSEN, J. L., HU, J. H., MAEDER, M. L., JOUNG, J. K., CHEN, Z. Y. & LIU, D. R. 2015. Cationic lipid-mediated delivery of proteins enables efficient protein-based genome editing in vitro and in vivo. *Nat Biotechnol*, 33, 73-80